Abstract

Title of Thesis:	The Influence of Variable Flow Velocity on Unsteady Airfoil Behavior
Name of degree candidate:	Berend G. van der Wall
Degree and year:	Master of Science, 1991
Thesis directed by:	Dr. J. Gordon Leishman Assistant Professor Department of Aerospace Engineering

The importance of unsteady aerodynamics for prediction of rotor dynamics is unquestioned today. The purpose of unsteady aerodynamic models is to represent the effect of unsteady airfoil motion on the lift, moment and drag characteristics of a blade section. This includes unsteady motion (arbitrary motion) of the airfoil in angle of attack (pitch) and vertical movement (plunge), as well as the effects of an airfoil travelling through a vertical gust field. However, the additional degrees of freedom, namely the fore-aft motion and the unsteady freestream variations commonly are acknowledged, but neglected in virtually all analyses.

Since the effect of unsteady freestream results in a stretching and compressing of the shed wake vorticity distribution behind an airfoil, it will have an effect on the airfoil characteristics. The subject of this thesis is to provide a review of the analytic and experimental work done in the area of unsteady freestream and unsteady fore-aft motion, to clarify the limits of the various theories, and to show the differences between them. This will be limited to the attached flow regime since all theories are based on the small disturbance

assumption in incompressible flow. As far as possible the theories are compared with experimental data, however most of the available experimental data are confined to stalled flow conditions and are not useful here.

In addition to the theories, a semiempirical mathematical model will be used based on the aerodynamics of indicial functions. The purpose is to show the differences of using the theories of unsteady airfoil motion in a constant flow, and those accounting for unsteady freestream flow. This will help to justify whether it is necessary to include the unsteady freestream effect in comprehensive rotor codes.

Finally, a generalisation of Isaacs unsteady aerodynamic theory for an airfoil undergoing a frequency spectra in pitch and plunge in a freestream oscillating with the fundamental frequency is presented here for the first time. Therein the axis of rotation of the airfoil is a free parameter.

The Influence of Variable Flow Velocity on Unsteady Airfoil Behavior

by

Berend G. van der Wall

Thesis submitted to the Faculty of The Graduate School
of The University of Maryland in partial fulfillment
of the requirements for the degree of
Master of Science
1991

Advisory Committee:

Assistant Professor J. Gordon Leishman, Chairman and Advisor
Professor Inderjit Chopra
Assistant Professor Roberto Celi

Contents

List of Figures

List of Tables

Nomenclature

Symbol	Meaning
a	Pitch axis
A_i, b_i	Coefficients of the approximation of the Wagner function
c	Airfoil chord
C_L, C_M	Aerodynamic lift and moment coefficient
$C = F + iG$	Theodorsen function
$\hat{C} = \hat{F} + i\hat{G}$	Approximation of the Theodorsen function
$h = \alpha_0 \frac{c}{2}(\bar{h}_{1S} \sin \omega_h t + \bar{h}_{1C} \cos \omega_h t)$	Vertical (plunge) motion of the airfoil
$k = \frac{\omega c}{2V_0}$	Reduced frequency
L, M	Aerodynamic lift and moment, M also Mach number
r, R	Rotor radial coordinate and radius
$\bar{s} = \frac{2V_0}{c}t$	Mean value of distance travelled by the airfoil
$s = \bar{s} - \frac{\lambda}{k} \cos k\bar{s}$	Actual distance travelled by the airfoil
t	Time
$V = V_0(1 + \lambda \sin \omega_V t)$	Velocity at the airfoil
w	Normal velocity at the airfoil
X	Deficiency functions
x, y, z	Airfoil coordinate system

$\alpha = \alpha_0 \ (\bar{\alpha}_0 + \bar{\alpha}_{1S} \sin \omega_\alpha t + \bar{\alpha}_{1C} \cos \omega_\alpha t)$	Angle of attack
$\beta = \sqrt{1 - M^2}$	Glauert's compressibility factor
Γ	Airfoil circulation
γ	Vorticity
$\lambda = \dfrac{\Delta V}{V_0}$	Nondimensional freestream oscillation amplitude
μ	Rotor advance ratio
ρ	Air density
$\phi(s)$	Wagner function
$\psi = \omega_V t$	Rotor azimuth
ω	Frequency of oscillation

Indices

b	Airfoil bound contribution
c, nc	circulatory, noncirculatory
dyn	dynamic
qs	quasisteady
w	Wake contribution
$0, S, C$	Mean value, sine-comonent, cosine-component
$1/4, 3/4$	Quarter chord, threequarter chord
α, h, V	Related to angle of attack, plunge motion or velocity

Chapter 1

Introduction

A helicopter rotor blade in forward flight encounters a highly nonuniform flowfield. In order to predict the aeroelastic behavior of the rotor, it is necessary to accurately calculate the aerodynamic loads acting on the blades. These consist of both steady as well as unsteady components. One source of aerodynamic loads is the varying oncoming flow velocity at each blade station. This leads to a dynamic pressure variation containing steady, $1/rev$ and $2/rev$ components. Additional degrees of freedom result from the blade motion in flap, lag and torsion, and the nonuniform inflow.

In forward flight, an unsteady aerodynamic theory must be used to predict the aerodynamic loads. This has been discussed by various authors, for example by Johnson and Kaza [1, 2]. Both state that the lift deficiency function $C(k)$ must be generalized to account for the unsteady freestream effects. This generalisation was given by Johnson [3], but in most analysis the Theodorsen lift deficiency function for constant freestream flow [4] is used instead. However, the direct application of Theodorsen's theory to rotorcraft in forward flight is questionable. A theory including the effect of

periodically stretching and compressing the shed wake vorticity distribution behind the oscillating and/or plunging airfoil should be used in order to include the effects of varying freestream on the unsteady aerodynamic forces and moments.

In addition to this, one has to differentiate between two kinds of velocity changes that a rotor blade encounters in forward flight. First there will be a fore-aft (lead-lag) motion of the rotor blade, and second, an oscillating freestream velocity resulting from the superposition of the rotational velocity and the forward speed of the helicopter. The first case (lead-lag) leads to a uniform velocity distribution across the airfoil chord, while the second produces a velocity gradient across the chord. For of very high frequencies, lead-lag motion will result in very high noncirculatory forces, while in the oscillating freestream the noncirculatory lift will reduce to zero again since several modes along the chord cancel each other. For the form of the wake behind the airfoil, however, there is no difference to be seen between both cases because the positioning and velocity of vorticity in the shed wake relative to the airfoil is the same in both cases.

A complicating factor, is the fact that helicopter blade sections operate over the whole range of subsonic Mach numbers and at different Reynolds numbers; both are periodically changing at a given radial station. Additionally, some flow separation regimes can occur, especially at high forward speeds. It is also of interest, what the impact of decelleration and acceleration of flow velocity on the separated flow characteristics of the airfoil will be.

The following sections give an overview of the theoretical and experimental work previously done in the past concerning the problem of freestream velocity changes, and its impact on the unsteady aerodynamic loads.

1.1 Short Historical Review, Analytical Approaches

The general solution for an airfoil undergoing harmonic motion in angle of attack about an arbitrary axis and plunge motion at constant freestream velocity was given by Theodorsen in 1935 [4], and in 1940 in operational form by Sears [5]. Probably the first attempt to derive a solution for the case of unsteady freestream velocity variations was given by Isaacs ten years later, and then only for the case of constant angle of attack [6]. This reflects the increasing complexity of the solution when the varying freestream velocity is taken into account. In 1946, Isaacs gave a solution to this problem, including a periodic change in angle of attack, in order to fulfill the needs of helicopter aerodynamicists [7]. His solution, however, was confined to a pitch axis at half chord, and therefore it was not very appropriate for helicopter calculations since nearly all helicopter blades have a feathering axis at the quarter chord.

It must be noted here that both publications [6, 7] claim to handle the effect of freestream velocity fluctuations, however the instantaneous value of the oncoming flow velocity is taken as *constant along the chord.* This means that the problem is modelled as a fore-aft motion of the airfoil instead as an unsteady freestream flow problem. This latter case would cause a velocity gradient along chord, and therefore is a different physical problem. For small frequencies, however, the gradients are small and both types of unsteady

motion are very similar. In the second report Isaacs [7] gave solutions for lift and moment development, and the latter can be reduced to the case of constant angle of attack. No graphical presentation of the results were given in [6, 7], but a numerical example for the Fourier coefficients of the lift response at constant angle of attack at a moderate freestream oscillation amplitude and a small reduced ferquency was given in [6].

In the same year Greenberg [8] published his extension of Theodorsen's theory to include harmonic variations of the freestream velocity; also in view of the needs of helicopter engineers. Even today, his results are thought to be the most reliable for application to rotorcraft aeroelastic problems; for example, by Diniavari and Friedmann [9]. However, Greenberg made some additional assumptions about the shed wake behind the airfoil to obtain a solution in terms of the Theodorsen function only. Also, Greenberg's theory claims to handle the unsteady freestream effect, but this theory has assumed that the instantaneous value of the velocity along the chord is a constant. In an appendix to [8] Greenberg explicitly writes: *"Consider an airfoil moving back and forth harmonically in a uniform stream having a velocity* V_0*"*. Greenberg gave equations for lift and moment, but no graphical presentation. The only comparison with Isaacs' theory was done by examining the Fourier coefficients of the lift response for the same conditions as used by Isaacs in [6]. The agreement for the $1/rev$ response was found to be good.

In 1952 Ashley *et. al* developed two methods for predicting the unsteady lift of an airfoil in accelerated motion [10]. Examples were given for an airfoil undergoing a sudden change in speed in a stationary atmosphere (i.e., Wagner's problem [11], which is for a step change in angle of attack in a uniform

flow field). A case of constant airfoil acceleration was presented in [10] with respect to the case of an airplane launched via a catapult, for example on a ship. It was found that the unsteady lift build-up lags significantly the quasisteady lift, leading to longer runway requirements for the airplane to become airborne. An example was given for the Helioplane[1], see Fig. 1.1. Ashley *et. al* [10] gave no solution for a periodically varying velocity, and therefore the result for a helicopter blade will be of qualitative nature; in the accelerating region (rear part of the rotor disk) the lift buildup will lag the quasisteady lift.

The influence of horizontal gusts on the aerodynamic coefficients was the subject of interest in Drischler and Diederich's work in 1957 [12]. Indicial functions for the lift and moment response penetrating gusts having both vertical as well as horizontal speed were given in integral form, and must be integrated numerically. Therefore, they are not of direct use in rotor calculations, but the results show significant effects in the time history of lift buildup after the gust hits the airfoil, Fig. 1.2. In case of the horizontal velocity being infinitely greater than the vertical velocity, the result of Wagner [11] is obtained. In the case of zero horizontal velocity, the Küssner function [13] is the result. A positive gust (approaching the wing) leads to a peak in the lift for the first instant of time, while a negative gust (travelling away from the wing, but is overtaken by it) leads to very slow lift build-up.

Strand's study of 1972 [14] is related to the maximum lift of an airplane in decelerating flight with a simulataneously increasing angle of attack. He

[1]This is a light airplane designed at MIT, see *"New Slow-Flying Plane Developed,"* Aviation Week, Vol. 50, No. 20, pp. 51-52, 1949

found an increase in lift (compared to the quasisteady lift) proportional to the time rate of change in velocity and angle of attack, but in comparison to flight and wind tunnel measurements this increase was of minor importance. Strand concludes that the measured lift increases were the result of viscous effects, both for the airplane and the helicopter case. No results for the aerodynamic pitching moment was given.

After Greenberg's results were published [8], it took more than 30 years to develop a new theory directly related to rotorcraft. This was in 1977 by Kottapalli [15], and again in 1985 [17] where the main subject of consideration was the development of the unsteady drag under unsteady freestream conditions. His derivation also gives results for the lift and moment development (published in 1985 for airfoils with inplane motions), however he developed his theory explicitly by applying the boundary condition of small lead-lag oscillation amplitudes with respect to the mean velocity. Consequently, Kottapalli limits the validity of his approach to the case of blade flutter in the hover condition. Consequently, Kottapalli's results seem to be of limited help for helicopter applications in forward flight, since the assumption of small flow oscillation amplitudes holds only for very small advance ratios. In 1979 there was another publication by Kottapalli and Pierce [16] regarding the computation of drag on an airfoil in a fluctuating free stream, but here too the amplitudes were confined to small values. Comparisons were not made with Isaacs' or Greenberg's theory, and no graphical presentation of lift or moment development was made.

Ando and Ichikawa presented a study concerning the lift development during the acceleration of an airplane [18]. The conclusions are basically the

same as those of Ashley *et. al*; an acceleration leads to a lag in unsteady lift buildup, see Fig. 1.3. No comparisons were made, and there were no results presented for the pitching moment.

Johnson published some discussion regarding the problem of a varying velocity in his famous book *Helicopter Theory* [3]. Using the same assumptions made by Isaacs [6, 7], Johnson basically followed Isaacs' theory to give expressions for lift and moment of an airfoil having plunge as well as pitch motion about an arbitrary pitch axis. This approach is very interesting, but the final result is given in form of integrals without giving the appropriate solution of these in terms of Bessel functions. No comparisons were made with the other existing theories, but a result is given for the second harmonic component of the resulting lift deficiency function, see Fig. 1.4, for flow oscillation amplitudes from zero to 90% of the mean velocity and a reduced frequency of $k = 0.04$, based upon the mean velocity.

The effect of varying velocity is described by Johnson as:

"On the advancing side, the increased velocity lowers the reduced frequency and hence the lift deficiency function is nearer unity. On the retreating side there is the greatest accumulation of shed vorticity in the wake near the trailing edge, and thus the greatest reduction in lift.

In summary ... all these effects basically produce 1/rev variations of the loads."

Johnson's conclusion is that the approximation using the Theodorsen function with the local reduced frequency will work for flow oscillation amplitudes of up to 70% of the mean velocity. For small flow oscillation amplitudes, the Theodorsen function calculated using the mean velocity will be

accurate enough, which effectively means neglecting the unsteady freestream fluctuations. However, this statement seems to be based only on one presented result, and it is doubtful whether or not it will hold for other mean reduced freuencies and other harmonics of the response.

Until now, there is no other theory available. It must be kept in mind, that all the theoretical approaches were made with certain assumptions. In summary, these are:

1. Two-dimensional flow (i.e., no spanwise effects or curved wake forms included)
2. Incompressible flow (i.e., infinite speed of sound)
3. Small desturbances (i.e., thin airfoil, small angles, small frequencies)
4. No friction forces (i.e., infinite Reynolds number = nonviscous flow)
5. Planar, infinite wake (i.e., no distortion, no diffusion)

Therefore, the results can be valid only in the attached flow regime. In case of comparisons with experimental data, these have to be taken at a very low wind tunnel speed. Especially, the assumption of an infinite planar wake is questionable when it comes to the application to rotorcraft since the wake there is more of a helical form. However for unsteady aerodynamics, the part of the wake closest to the airfoil generating it (some chord lengths behind it) is of primary importance, since in view of the Biot-Savart law the more distantly positioned elements of the wake have only a minor effect. Therefore, the results of a planar wake should also be representative for rotorcraft wake geometries.

Another approximation is the assumption of incompressible flow. Even in hover a rotor blade tip operates at Mach numbers of typically 0.64, and in fast forward flight can increase to values very close to 1.0. Keeping in mind that the incompressible theory is applicable only to Mach numbers of up to about 0.3, only a small range of rotorcraft aerodynamics can be handled with an incompressible flow theory. However, there are no theories capable of handling the compressible subsonic case of unsteady motion of airfoil *and* freestream velocity, therefore one has no choice but to start with the available incompressible theories.

In the following chapter, the theories of Isaacs, Greenberg and Kottapalli are examined in order to clarify their implicit assumptions and restrictions in application. This will be done, not by rederiving them, but by presenting the final results and the basis of the derivations. This will be accompanied by graphical presentation of these results. The graphical presentation is the most satisfactory method to compare the different results obtained by the different theories.

1.2 Experimental Approaches

Most of the experimental work done in this area of research is the measurement of the aerodynamic coefficients in a wind tunnel. Because wind tunnels were build to provide a steady freestream velocity and as turbulence-free as possible, it is a very difficult task to produce harmonic flow oscillations at various frequencies and with amplitudes of up to the mean velocity itself. Therefore one has to apply certain modifications to obtain harmonically varying velocities in the test section. A number of experiments with airfoils

oscillating in a constant freestream velocity have been conducted, for example [19, 20]. Only few experiments have been done in an oscillating freestream velocity environment, which is of interest here.

Probably the first experiments on this problem were done by Fejer, Saxena and Morkovin at Illinois Institute of Technology in 1976 [21, 22]. A $1ft$-chord NACA 0012 model with pressure transducers was mounted in a low speed wind tunnel providing flow oscillations amplitudes of 18% of the freestream by means of periodically opening and closing shutters behind the test section. The aspect ratio of the model was only 2.0, so that three dimensional effects could be expected. The Reynolds numbers were about 2.5×10^5, and therefore relatively small compared to helicopters. However, a trip was mounted to force the boundary layer to be turbulent. With this facility, reduced frequencies of 0.18 and 0.9 could be achieved. It was found in [21, 22] that at these moderate flow oscillation amplitudes, the influence of frequency is an important parameter affecting the pressure distribution and the boundary layer behavior. This was especially true when the angle of attack was above the static stall angle; large oscillations in the normal force coefficient occured and the average value of the normal force coefficient was about 60% higher than in the steady case. In case of angles below the stall angle, there was an increasing unsteady behavior of the leading edge separation bubble. An example of pressure distributions at a fixed angle of attack of $\alpha = 14.2^o$ is shown in Fig. 1.5 for different times during one flow oscillation cycle. In addition, there is a region of separated flow over the airfoil, indicating significant dependency of the instantaneous velocity.

In later tests, angle of attack variations in an oscillating flow were made

[23, 24]. It has been found that in periodically changing flows, dynamic stall of airfoils can assume a variety of forms depending on the frequency and amplitude of the oscillations. The airfoil coefficients do not behave in a quasisteady manner anymore, and it was concluded that for the case of helicopter dynamic stall the freestream flow fluctuations must be taken into account and cannot be neglected.

Parallel to the analytical work of Kottapalli at Georgia Institute of Technology, some experiments were also conducted there by Pierce, Kunz and Malone [25] in 1976. The exit of a low speed wind tunnel was provided with a system of periodically opening and closing vanes to produce flow oscillations. The mean velocity in the test section was at $42.5 ft/s$ ($\approx 13 m/s$) with a normalized amplitude of $\lambda = 0.177$ at a flow oscillation frequency in most cases set to $1 Hz$, while the pitch frequency was set to 6 times of that value. The reason for this was mainly to have one airfoil oscillation during the more or less linear regime of accelerating flow, and one in the appropriate regime of decelerating flow. The instrumentation used in this experiment was limited, and consisted of an accelerometer for angle of attack determination, and a strain gage bridge on the drive arm outside the test section to measure the total moment on the entire model. Therefore wind tunnel interference effects and 3-D flow effects are included in the measurements, and cannot be eliminated. Additionally there is no possibility of measuring lift or drag using this equipment.

Steady tests showed thin airfoil stall characteristics on the NACA 0012 airfoil. This is not surprising, since the Reynolds number was only $Re = 2.02 \times 10^5$. The Mach number was about $M \approx 0.04$, so the flow can be

considered as incompressible. Dynamic tests showed a large effect of flow oscillations on the dynamic stall behavior, and some moment hysteresis loops were given; an example is shown here in Fig. 1.6. However, all experiments included separated flow, so they are not useful for comparing with attached flow theories. Additionally, there are some results which are questionable since in steady flow, for example, the break in pitching moment appears at the lowest angles of attack, and not at the highest as one would expect.

At about the same time, the French team of Maresca, Favier and Rebont at IMFM Marseille started a series of experiments with an airfoil undergoing fore-aft motions, plunge motions and pitch motions in a steady stream [26, 27]. In order to obtain high velocity amplitudes at the airfoil, the mean velocity of the flow was very small. Therefore, the basic concern in all these experiments will be the low Reynolds number, here 2.5×10^5. Flow and plunge oscillations took place at the same frequency by moving the airfoil model in the test section along an inclined path, and the model itself was fixed with a certain angle relative to this path. The tunnel speed remained constant, and all variations in freestream velocity were produced by the model drive mechanism. There was also no possibility to have different phase angles between the flow and plunge oscillations, other than the in-phase or out-of-phase condition. Because of a very low aspect ratio of 1.65, there are also serious three dimensional effects to be expected. Aerodynamic forces and moments were measured by torsional dynamometers. Additionally there were pressure transducers for measurement of steady pressures, and some hotfilm gauges for skin friction measurement.

The measurements performed were first pure fore-aft motion at a fixed

angle of attack (that could be a good comparison with Isaacs' theory, but the angle of attack was set to 20^o, so there is entirely separated flow on the airfoil, and therefore this prohibits any kind of comparison). As a result of the combined fore-aft and plunge motion, the flow oscillations were nearly pure sinusoids, but the resulting angle of attack oscillation also contained several higher harmonics. As an example, the influence of the flow oscillations on the lift and drag development is given here in Fig. 1.7. The differences in the unsteady lift and drag development as compared to quasisteady theory are obvious; namely a lag in the force development, as well as a change in the amplitude in comparison to the quasisteady values.

In 1982 the same authors presented some additional measurements of combined motion for oscillations below the static stall angle, as well as for those going beyond stall, and compared the results for lift, drag and moment with the appropriate plunge oscillations in a constant freestream flow [29]. The hysteresis loops were found to be entirely different, and for oscillations below stall, the moment coefficient clearly indicated flow separation, with a significant peak at high angle of attack, see Fig. 1.8. The Reynolds number was $Re = 1.44 \times 10^5$, and therefore one must be careful to assume the flow below the static stall angle as attached since the airfoil is very likely to experience thin airfoil stall.

After having redesigned the drive mechanism to be able to oscillate the airfoil about its pitch axis, additional measurements were conducted and presented in 1988 [30]. Now any phase angle between the flow and the angle of attack oscillations could be achieved. For pure fore-aft motion, the flow frequency was varied at two different angles of attack; one below static stall

and the other at the static stall angle. Results were given as time histories, as well as in the form of lift amplitude and phase so they could be compared with unsteady theories. Additionally lift hysteresis loops were given, showing even at the smallest reduced frequency of $k = 0.1$ a clockwise sense of rotation (phase lead) that normally would appear only at higher reduced frequencies. Therefore, the statement of attached flow conditions cannot hold even at the angles lower than the static stall angle, since the airfoil underwent thin airfoil stall with flow separation regimes beginning to form at very small angles. This leads to serious questions whether or not these results can be compared with any of the attached flow theories. It was shown, however, that the phase of the flow velocity and the angle of attack oscillations is an important parameter and changes the lift coefficient hysteresis in a significant manner, see Fig. 1.9.

Recently a transonic wind tunnel at the University of the Bundeswehr in Munich, Germany, was made operational. This tunnel has been constructed to produce periodically changes of velocity in the test section by means of a shutter at the end of the test section itself. Up to now no results have been published, but this facility seems to be the only one in the moment to be able to handle freestream fluctuations at Mach numbers and Reynolds numbers typical of helicopter rotors.

As a result of the foregoing, it can be stated that there is only limited airfoil data for freestream fluctuations available to compare with theory, and the data already published are mostly confined to the dynamic stall phenomenon, not to the case of attached flow. In case of the tests having angles of attack smaller than the static stall angle, the flow will also not be attached

because of the small Reynolds numbers, leading to thin airfoil stall characteristics with separation regimes beginning at very small angles of attack. Therefore it will be very difficult, if not impossible, to compare the theories with experimental data. The reason is that the theories are developed for attached incompressible flow at high Reynolds number, but experiments were done at high angles of attack at very low Reynolds numbers, where stall effects are starting to show up even at very small angles of attack.

1.3 Problem Statement

From all of the unsteady aerodynamic theories, there are only three direcly related to rotorcraft application in hover and forward flight: Isaacs', Greenberg's and Kottapalli's theories. None of these authors have presented results either numerically or graphically to show the differences between these theories. Furthermore, the limitations and simplifications in these theories are not clear, especially for the Isaacs' and Greenberg's. The effect of periodically accelerating and decelerating flow with superimposed oscillations in angle of attack on the lift and moment coefficient is not compared or even shown. A conclusion as to whether the inclusion of these effects is really necessary for the helicopter rotor is still lacking.

1.4 Present Work

In this study, the theories of Isaacs, Greenberg and Kottapalli will be analysed and compared. There will be strong emphasis on a graphical presentation of the results in order to compare the theories with each other, and with quasisteady theory. Also, predictions made using Theodorsen's theory will

be compared, since this is widely used. The limitations and assumptions will be clearly shown and, as far as possible, the results will be compared with available experimental measurements.

The objective is first to find an answer to whether or not it is necessary to model the effects of unsteady freestream fluctuations in a rotor loads or aeroelastic analysis in forward flight. The second objective, is to show whether or not it is possible to simulate the attached flow behavior using an arbitrary motion theory, comprizing of Duhamel's integral and indicial functions for step changes in angle of attack, pitch rate and plunge velocity.

Chapter 2

Review of Theories for Unsteady Freestream and Unsteady Inplane Motion

Before describing the airfoil theories for modeling the unsteady airloads in an unsteady freestream, it is worthwhile to examine the basic assumption of small angles. Since the flow velocity appears in the denominator when determining the angle of attack in plunge motion (or pitch rate), it is questionable whether or not the small angle assumption is violated by the theory. Also the limits of applying this assumption are unclear, and it is necessary to be aware of this. The airfoil theory results for a constant freestream velocity (Theodorsen's theory) will be presented first since this gives a good physical insight into unsteady aerodynamics, and the results also form the basis of the unsteady aerodynamics in an unsteady freestream. Furthermore, the principle of arbitrary motion will be first shown for the case of constant freestream velocity, and is also applied later to the case of an unsteady freestream.

2.1 Introduction

2.1.1 Definition of an Unsteady Freestream

Before any unsteady aerodynamic theory due to unsteady freestream effects can be derived, it must be defined what an unsteady freestream physically means. This sounds trivial, but there are mainly two possibilities, as in the case of vertical gusts. In the first case, the freestream can be viewed as a mass of fluid changing velocity with time as a whole, e.g., the fluid particles at every location change their velocity at the same time by the same amount. This is identical to an airfoil having a pure lead-lag type of motion in a constant freestream velocity, since both produce a normal velocity distribution along the airfoil that is constant in space, but varying in time. The other possibility (let us call it the second case), that is more real for a helicopter, is to view the unsteady freestream as a system of longitudinally propagating gusts. This leads to a nonlinear (sinusoidal) gradient in the normal velocity distribution across the airfoil, and therefore, it is much more difficult to handle in a general analytical approach. The relative velocity of the wake behind the airfoil to the airfoil trailing edge, however, is the same in both cases.

Another issue, is that large differences are to be found in the noncirculatory parts of the loading that contribute to the airfoil characteristics. Also, there is an effect on the circulatory part of the bound vortex sheet when the reduced frequency is high. The reason is that in the first case the noncirculatory lift, for example, becomes infinite because of the constant normal velocity distribution along chord, while in the second case several waves are found to act on the chord at the same time, and therefore effectively cancel

each other out. Therefore, the final value of noncirculatory lift for very high reduced frequency in the second case will be zero, as in constant freestream flow. For small reduced frequencies however, the gradient of the normal velocity across chord will be small. Therefore, the gradient may be handled as zero with a constant normal velocity distribution in a first approximation, even for the case of large freestream velocity oscillation amplitudes. Therefore, the first case (lead-lag) can be viewed only as an *approximation* for the second case (longitudinal gusts) for small reduced frequencies.

In a helicopter rotor environment, it is the second case that is of interest. In Fig. 2.1 a rotor blade in a forward flight condition is shown. Since the aerodynamic problem is viewed as two dimensional, this amounts to a projection of the rotating environment onto a two dimensional plane. For a rotating blade like that shown, we must look at the velocities at a constant radius (lower part of the figure). It is obvious that the leading edge has a different normal velocity than the trailing edge, simply because they are not at the same azimuth and are separated by the chord in distance. Thus, a velocity gradient exists along the chord. A special case is the position of zero azimuth, where the leading edge has a small component of forward flight velocity that adds to the rotational velocity, while at the trailing edge there is a small amount subtracted from it (and vice versa at 180^o azimuth). Therefore, the projection of the rotating blade element onto a two dimensional plane leads to an unsteady freestream problem with a velocity gradient across the chord; and any angle of attack produces a gradient in normal velocity. However, the classical view is that the airfoil (upper part of Fig. 2.1) is not taken from the rotating coordinate system, but from the cartesian blade coordinate system.

Therefore, the tangential velocities are defined to be the same at the leading edge and the trailing edge. In this case, no velocity gradient exists across the chord and the previous case (lead-lag) of the two possibilities comes into account. The advantage is a much easier derivation of aerodynamic theory, that is already complicated enough. Yet, it must be kept in mind that this is a small frequency approximation for the real case of a system of longitudinally propagating gusts and is only exact, when the motion of the airfoil itself is under investigation.

2.1.2 The Small Perturbations Assumption

Since all the theories are built up on the assumption of small perturbations, say small geometric angles and small accelerations, it is necessary to prove whether or not this assumption can be made in a helicopter rotor environment. In an incompressible flow, the angle of attack at 3/4 chord is of interest for the circulatory part of the lift since the multplication with the oncoming flow velocity gives the normal velocity at 3/4 chord. This is

$$\alpha_{3/4} = \alpha_{geo} + \tan \frac{\dot{\alpha} c \left(\frac{1-2a}{2}\right)}{2V} + \tan \frac{\dot{h}}{V} \tag{2.1}$$

For the small angle assumption, the tangent can be replaced by its argument. Now, when the freestream velocity V is varying, it is questionable whether or not the argument still remains small to justify this assumption.

Consider a rotor blade undergoing flap motion in a simple case of a rigid blade hinged at the axis of rotation, and with an amplitude at the tip of 10% of the radius (see Fig. 2.2). In forward flight the flap motion is upwards on the advancing side and downwards on the retreating side, with maximum

λ	0	0.2	0.4	0.6	0.8	0.9	0.95	0.99
$\frac{\dot{h}}{V}\Big\|_{270^o}$	0.1	0.125	0.167	0.25	0.5	1.0	2.0	10.0

Table 2.1: Relation between flow oscillation amplitude and angle of attack at $\psi = 270^o$

velocities at $\psi = 90^o$ and $\psi = 270^o$. Now the argument of the tangent in Eq. 2.1 takes the following form

$$\begin{aligned} h(r) &= (0.1R\cos\psi)\frac{r}{R} \\ V(r) &= \omega_V R\left(\frac{r}{R} + \mu\sin\psi\right) \\ \rightarrow \frac{\dot{h}}{V} &= -0.1\frac{\sin\psi}{1+(\mu/y)\sin\psi} \qquad \text{with} \quad y = \frac{r}{R} \end{aligned} \tag{2.2}$$

The worst case occurs at the retreating side at $\psi = 270^o$ and so

$$\left.\frac{\dot{h}}{V}\right|_{270^o} = \frac{0.1}{1-\mu/y} = \frac{0.1}{1-\lambda} \tag{2.3}$$

At high forward speed, the flow oscillation amplitude λ increases, and small radial positions y also cause an increase in λ. Since the available theories are not adequate in the reversed flow region, the parameter λ must be limited to a maximum of 1. Some values for the ratio λ are listed in Table 2.1. None of these values $\alpha_{eff} = \dot{h}/V$ fulfills the requirement that it be small (say about 0.05 or less) compared to 1. When λ is equal to one, then the velocity is zero at $\psi = 270^o$ and therefore an angle of attack of 90^o is produced by any flap motion.

The reduced frequencies at which the blade sections are operating are also of interest. These are defined by the mean velocity, that is the velocity

normal to the blade in hover. Taking a typical value of $R/c = 20$, the distribution of reduced frequencies depends on the geometry only

$$k_V = \frac{\omega_V c}{2V} = \frac{\omega_V c}{2\omega_V r} \approx \frac{0.025}{y} \tag{2.4}$$

So the reduced frequencies at a typical rotor blade section range from 0.025 at the tip, to 0.125 at the beginning of the profiled section that starts at about 20% radius. The reduced frequencies are not very high, since only the $1/rev$ motion was taken into account, but high enough to justify the need of unsteady aerodynamic theory in rotor calculations. When considering torsional motion of the rotor blade, the reduced frequencies are considerably higher.

As an example, Table 2.2 gives an idea for the values of λ encountered at different blade sections at different forward speed of the helicopter. A value of $\lambda = 0.9$ will be encountered at 55% radius, when the advance ratio is $\mu = 0.5$, or, when $\mu = 0.3$, at 33% radius. Also, a value of $\lambda = 0.6$ will be found at 83% radius, when $\mu = 0.5$. This shows, that in fast forward flight even the blade sections with high lift encounter significant changes in velocity. So these combinations occur in normal flight conditions at high speed. In addition, the values at the blade tip on the retreating side are of interest since a lot of lift is produced by the tip region on the retreating side. Here, at a reduced frequency of $k = 0.025$ the following ratios are typical for different advance ratios (Table 2.3). So even for the tip, none of these values is small, and therefore the small perturbation assumption, here more a small angle assumption, in general is violated when the flow fluctuation amplitude is of medium ($\lambda = 0.5$) or higher value.

$\lambda = 0.6$				$\lambda = 0.9$		
$\mu = 0.3$	$y = 0.5$	$k = 0.05$	and	$\mu = 0.3$	$y = 0.3335$	$k = 0.075$
	or:				or:	
$\mu = 0.5$	$y = 0.83$	$k = 0.03$		$\mu = 0.5$	$y = 0.55$	$k = 0.045$

Table 2.2: Relation between advance ratio, radial station and reduced frequency for different flow oscillation amplitudes. Basis is a $1/rev$ plunge motion with amplitude of $10\%R$.

$\mu = 0.2$	$\rightarrow$	$\lambda = 0.2$	$\left.\frac{\dot{h}}{V}\right\|_{270^o} = 0.125$
$\mu = 0.3$	$\rightarrow$	$\lambda = 0.3$	$\left.\frac{\dot{h}}{V}\right\|_{270^o} = 0.143$
$\mu = 0.5$	$\rightarrow$	$\lambda = 0.5$	$\left.\frac{\dot{h}}{V}\right\|_{270^o} = 0.200$

Table 2.3: Proof of small angle assumption at $\psi = 270^o$ for the blade tip, $k = 0.025$

This is not the case when the angle of attack stays constant, and only flow oscillations (or lead-lag motion) are taken into account. In this case, the angle of attack at 3/4 chord is constant and small. The small perturbations assumption is only limited by the resulting accelerations, here represented by the reduced frequency.

2.1.3 Theodorsen's Theory of Unsteady Airfoil Motion in a Constant Freestream Flow

Before the unsteady freestream is taken into account, it is worthwhile to examine the well-known result of Theodorsen [4] for unsteady airfoil motion in pitch and plunge in a constant freestream. The lift and moment is split into circulatory and noncirculatory parts,

$$\begin{aligned} L_{nc} &= \pi\rho\frac{c^2}{4}[\ddot{h} + V\dot{\alpha} - a\frac{c}{2}\ddot{\alpha}] \\ L_c &= 2\pi\frac{\rho}{2}Vc\left[V\alpha_0 + \left(\frac{c}{2}\left(\frac{1-2a}{2}\right)\dot{\alpha} + V\alpha_{dyn} + \dot{h}\right)C(k)\right] \end{aligned} \tag{2.5}$$

Here the parameter a accounts for the position of the axis of rotation. It is positive for an offset of the rotational axis behind the midchord position. In most cases is $a = -0.5$, that is the rotational axis is at the quarter chord.

For the noncirculatory part, all accelerations normal to the chord are involved and integrated over the chord, so the distribution of acceleration across the chord is of interest here.

$C(k)$ is the well known Theodorden function that represents the influence of the unsteady wake on the circulatory lift. From the $\dot{\alpha}$-term in the circulatory lift it can be seen that for a rotation axis at 3/4 chord, there is no

influence of $\dot{\alpha}$ on the circulatory part of the lift. Therefore, in incompressible flow under the assumptions made by Theodorsen, only the velocity normal to the chord at the 3/4 chord point is of importance for the circulatory lift response. This leads to a simple superposition of angle of attack and plunge motion, and so the pitch and plunge effects can be handled separately and the frequencies of angle of attack and plunge motion are not necessarily the same.

Since only the time derivatives of h are involved, it is more physical to take the normal velocity produced by plunge motion $w_h = \dot{h}$ into the equation. In the case of different frequencies, one can generally write for simple harmonic motions

$$\begin{aligned} \alpha = &\quad \alpha_0[\bar{\alpha}_0 + \bar{\alpha}_{1S}\sin\omega_\alpha t + \bar{\alpha}_{1C}\cos\omega_\alpha t] \\ w_h = &\quad \alpha_0 V_0[\bar{w}_{1S}\sin\omega_\alpha t + \bar{w}_{1C}\cos\omega_\alpha t] \end{aligned} \tag{2.6}$$

wherein the nondimensional amplitudes are defined as

$$\bar{\alpha}_0 = \frac{\alpha_{mean}}{\alpha_0} \qquad \bar{\alpha}_{1S} = \frac{\alpha_{1S}}{\alpha_0} \qquad \bar{\alpha}_{1C} = \frac{\alpha_{1C}}{\alpha_0}$$

$$\bar{w}_{1S} = \frac{-k_h h_{1C}}{\alpha_0 c/2} \qquad \bar{w}_{1C} = \frac{k_h h_{1S}}{\alpha_0 c/2}$$

For convenience, Theodorsen's result can be written in nondimensional form by dividing by the lift at mean angle of attack,

$$L_0 = 2\pi\frac{\rho}{2}V^2 c\alpha_0 \tag{2.7}$$

to obtain the nondimensional lift response, including different reduced frequencies for pitch and plunge oscillations, i.e.,

$$\frac{L_{nc}}{L_0} = \frac{1}{2}\{k_h[\bar{w}_{1S}\cos\omega_h t - \bar{w}_{1C}\sin\omega_h t]$$

$$+k_\alpha[\bar{\alpha}_{1S}\cos\omega_\alpha t - \bar{\alpha}_{1C}\sin\omega_\alpha t + ak_\alpha(\bar{\alpha}_{1S}\sin\omega_\alpha t + \bar{\alpha}_{1C}\cos\omega_\alpha t)]\}$$

$$\begin{aligned}\frac{L_c}{L_0} &= \bar{\alpha}_0 + \left[\left(\bar{\alpha}_{1S} - k_\alpha\left(\frac{1-2a}{2}\right)\bar{\alpha}_{1C}\right)\sin\omega_\alpha t\right. \\ &\quad \left. + \left(\bar{\alpha}_{1C} + k_\alpha\left(\frac{1-2a}{2}\right)\bar{\alpha}_{1S}\right)\cos\omega_\alpha t\right] C(k_\alpha) \\ &\quad + (\bar{w}_{1S}\sin\omega_h t + \bar{w}_{1C}\cos\omega_h t)\, C(k_h) \qquad (2.8)\end{aligned}$$

The reduced frequency k is introduced for both of the motions,

$$k_\alpha = \frac{\omega_\alpha c}{2V} \qquad k_h = \frac{\omega_h c}{2V} \qquad (2.9)$$

It is important to notice, that with help of this parameter the product of frequency and time can be transformed into

$$\omega_V t = k_V s \qquad (2.10)$$

This result will be helpful when Duhamel's integral is applied to arbitrary motion of the airfoil in a later section of this thesis.

The lift transfer function of the circulatory part and of the total lift (including the noncirculatory part) with respect to the reduced frequency is shown in Fig. 2.3 for plunge and pitch oscillations about the quarter chord, and for pitch oscillations about the midchord and 3/4 chord in Fig. 2.4. For small reduced frequencies, the amplitude of lift decreases while there is a phase lag. For higher frequencies, due to the noncirculatory parts of the lift, the phase lag changes to a lead, and the normalized lift amplitude begins to increase above unity.

Considering only the circulatory lift transfer function for plunge motion, (that is identically to the Theodorsen function $C(k)$ itself), the influence of

the unsteady wake reduces the lift amplitude for high reduced frequencies to 1/2 of its value at $k = 0$; the phase lag reaches its maximum at about $k = 0.3$. In case of pitch oscillation about the quarter chord, the range of phase lag is decreased to values of k from 0 to about 0.25, while at higher frequencies a phase lead and lift amplitude increase occurs. This is due to the position of the rotation axis being a half chord ahead the 3/4 chord point, introducing a factor $k_\alpha(1 - 2a)/2$ into the circulatory lift transfer function. The inclusion of the noncirculatory terms leads to a change in phase from lag to lead at $k = 0.35$ in plunge, and an increase of amplitude proportional to k. Basically the same effect can be seen in pitch motion; the range of phase lag appears only at $0 < k < 0.14$ and at higher frequencies a phase lead due to the noncirculatory parts becomes important. Since the noncirculatory lift also affects the real part of the lift by $k_\alpha^2 a/2$, the phase lead becomes more than 90^o.

2.1.4 Arbitrary Motion Theory in a Constant Freestream Flow

In general, the operational environment of a helicopter blade section can be considered as an airfoil in an arbitrary varying freestream with perturbations in pitch, plunge and lead-lag. This general case will be covered in a later chapter, but for a background understanding it is worthwhile to look to the case of a pitching and plunging airfoil in a constant incompressible freestream velocity. Basically, this is the same starting point as for Theodorsen's theory.

The basic idea is to handle the arbitrary motion response as the superposition of small increments of step responses, the so called indicial functions.

These functions represent the lift (and moment) development after a sudden step change in angle of attack or plunge velocity; there are different indicial functions for step changes in $\alpha, \dot{\alpha}$ and for the gust problem. All basics of the theory of arbitrary motion and its applications have been published several times, for example [31, 32, 33].

The indicial functions ϕ are generally expressed in the form of a series of exponential functions with different coefficients representing the response in the time domain

$$\phi(s) = \sum_{i=1}^{N} A_i e^{b_i s} \tag{2.11}$$

The noncirculatory part of the lift (or moment) depends on the instantaneous motion only (for incompressible flow), and therefore the lift development is obtained by the use of Duhamel's integral applied only to the circulatory part

$$L = \pi\rho\frac{c^2}{4}[\ddot{h} + V\dot{\alpha} - ba\ddot{\alpha}] + 2\pi\rho V\frac{c}{2}\left[w_{3/4}(0)\phi(s) + \int_0^s \frac{\partial w_{3/4}}{\partial\sigma}\phi(s-\sigma)d\sigma\right] \tag{2.12}$$

The velocity at 3/4 chord is composed of the vertical motion of the airfoil, and the instantaneous angle of attack, as well as the pitch rate term

$$w_{3/4} = V\alpha + \dot{h} + \frac{c}{2}\left(\frac{1-2a}{2}\right)\dot{\alpha} \tag{2.13}$$

The variable s (in semichords) is the distance travelled by the airfoil, i.e.,

$$s = \frac{2}{c}\int_0^t V dt \tag{2.14}$$

Here V is constant, so $s = 2Vt/c$. For harmonic motion, α and h may be defined as

$$\alpha \;=\; \alpha_0[\bar{\alpha}_0 + \bar{\alpha}_{1S}\sin ks + \bar{\alpha}_{1C}\cos ks]$$

$$h = \alpha_0 \frac{c}{2}[\bar{h}_{1S} \sin ks + \bar{h}_{1C} \cos ks] \tag{2.15}$$

The frequencies in pitch and plunge are kept the same here for simplicity, but this is not the general case and can be changed as required. As shown in Appendix A, the final result for the lift is

$$\begin{aligned} L = {} & \pi\rho\frac{c^2}{4}[\ddot{h} + V\dot{\alpha} - ba\ddot{\alpha}] + 2\pi\rho V^2 \frac{c}{2}\alpha_0 \Bigg\{ \bar{\alpha}_0 \\ & + \left[\left(\bar{w}_{1S} + \bar{\alpha}_{1S} - k\left(\frac{1-2a}{2}\right)\bar{\alpha}_{1C} \right) \sin \omega t \right. \\ & \left. + \left(\bar{w}_{1C} + \bar{\alpha}_{1C} + k\left(\frac{1-2a}{2}\right)\bar{\alpha}_{1S} \right) \cos \omega t \right] \sum_{i=1}^{N} \frac{A_i k^2}{b_i^2 + k^2} \\ & + \left[\left(\bar{w}_{1S} + \bar{\alpha}_{1S} - k\left(\frac{1-2a}{2}\right)\bar{\alpha}_{1C} \right) \cos \omega t \right. \\ & \left. - \left(\bar{w}_{1C} + \bar{\alpha}_{1C} + k\left(\frac{1-2a}{2}\right)\bar{\alpha}_{1S} \right) \sin \omega t \right] \sum_{i=1}^{N} \frac{A_i k b_i}{b_i^2 + k^2} \end{aligned} \tag{2.16}$$

Comparing this with the result obtained by Theodorsen, one immediately obtains the identity $C(k) = F(k) + iG(k)$ for an infinite number of exponential terms, and in the practical case where the series is truncated after N terms one obtains the approximation, denoted by $\hat{F}$ and $\hat{G}$.

$$\begin{aligned} F(k) &\approx \sum_{i=1}^{N} \frac{A_i k^2}{b_i^2 + k^2} = \hat{F}(k) \\ G(k) &\approx -\sum_{i=1}^{N} \frac{A_i k b_i}{b_i^2 + k^2} = \hat{G}(k) \end{aligned} \tag{2.17}$$

In most cases, the above approximation is very close to the exact Theodorsen function. A very commonly used approximation is the one obtained by Jones [34], using the coefficients listed in Table 2.4. This approximation leads to the correct values for zero as well as for infinite reduced frequency, while

i	1	2	3
A_i	1	-0.165	-0.335
b_i	0	-0.0455	-0.3

Table 2.4: Coefficients of Jones' approximation of the Theodorsen function

i	1	2	3	4
A_i	1	-0.1058	-0.2876	-0.1011
b_i	0	-0.0367	-0.1853	-0.5912

Table 2.5: Coefficients of Petersen and Crawley's approximation of the Theodorsen function

for any frequencies in between it is an approximation. To obtain a better approximation, one can use a set of coefficients recently evaluated by Peterson and Crawley [35] (Table 2.5) or Eversmann and Tewari [36] (Table 2.6) who claim that their two element approximation is closer to the Theodorsen function than the three element series of Peterson and Crawley. It is noteworthy, that the final value for infinite reduced frequency of both approximations is not identical to that of the Theodorsen function, because only the range of reduced frequencies up to $k = 1$ was approximated. The approximation of Eversmann and Tewari even does not give the exact value for zero reduced frequency in order to obtain a better *overall* agreement in the range of reduced frequencies from zero to one. However, the differences to Jones classical approximation are not significant enough to justify one term more in the exponential series, since this means more computing time for the aerodynamic subroutine in a rotor analysis.

i	1	2	3
A_i	0.9962	-0.1667	-0.3119
b_i	0	-0.0553	-0.2861

Table 2.6: Coefficients of Eversmann and Tewari's approximation of the Theodorsen function

2.1.5 Theodorsen's Theory and Unsteady Freestream

To apply Theodorsen's result to unsteady freestream, it is necessary to include the freestream variations into the noncirculatory and circulatory parts. This may be referred to as the direct effect of velocity changes on the lift development; the additional phase lags and amplifications to be expected by an unsteady freestream are not included. Starting from

$$\begin{aligned} L_{nc} &= \pi\rho\frac{c^2}{4}[\ddot{h} + (V\alpha)^{\cdot} - a\frac{c}{2}\ddot{\alpha}] \\ L_c &= 2\pi\frac{\rho}{2}Vc\left\{V\alpha_0 + \left[\frac{c}{2}\left(\frac{1-2a}{2}\right)\dot{\alpha} + V\alpha_{dyn} + \dot{h}\right]C(k)\right\} \end{aligned} \tag{2.18}$$

and defining a freestream variation and airfoil motion of the form

$$\begin{aligned} V(t) &= V_0(1 + \lambda\sin\omega_V t) \\ \alpha(t) &= \alpha_0\left(\bar{\alpha}_0 + \bar{\alpha}_{1S}\sin\omega_V t + \bar{\alpha}_{1C}\cos\omega_V t\right) \\ h(t) &= \frac{c}{2}\alpha_0\left(\bar{h}_{1S}\sin\omega_V t + \bar{h}_{1C}\cos\omega_V t\right) \end{aligned} \tag{2.19}$$

this leads to the following result for the lift in the form of a Fourier series

$$\begin{aligned} \frac{L_{nc}}{L_0} = \frac{k_V}{2}\Big\{&\left[\lambda\bar{\alpha}_0 + \bar{\alpha}_{1S} + k_V(a\bar{\alpha}_{1C} - \bar{h}_{1C})\right]\cos\omega_V t + \lambda\bar{\alpha}_{1C}\cos 2\omega_V t \\ &+ \left[-\bar{\alpha}_{1C} + k_V(a\bar{\alpha}_{1S} - \bar{h}_{1S})\right]\sin\omega_V t + \lambda\bar{\alpha}_{1S}\sin 2\omega_V t\Big\} \end{aligned} \tag{2.20}$$

$$
\begin{aligned}
\frac{L_c}{L_0} = \; & \bar{\alpha}_0 \left(1 + \frac{\lambda^2}{2}\right) + \frac{\lambda}{2}\left[f_{1S} + F(k_V)\bar{\alpha}_{1S} - G(k_V)\bar{\alpha}_{1C}\right] \\
& + \left\{ f_{1C} + \frac{\lambda^2}{4}\left[F(k_V)\bar{\alpha}_{1C} + G(k_V)\bar{\alpha}_{1S}\right] \right\} \cos\omega_V t \\
& + \left\{ 2\lambda\bar{\alpha}_0 + f_{1S} + \frac{3\lambda^2}{4}\left[F(k_V)\bar{\alpha}_{1S} - G(k_V)\bar{\alpha}_{1C}\right] \right\} \sin\omega_V t \\
& - \frac{\lambda}{2}\left[\lambda\bar{\alpha}_0 + f_{1S} + F(k_V)\bar{\alpha}_{1S} - G(k_V)\bar{\alpha}_{1C}\right] \cos 2\omega_V t \\
& + \frac{\lambda}{2}\left[f_{1C} + F(k_V)\bar{\alpha}_{1C} + G(k_V)\bar{\alpha}_{1S}\right] \sin 2\omega_V t \\
& - \frac{\lambda^2}{4}\left[F(k_V)\bar{\alpha}_{1C} + G(k_V)\bar{\alpha}_{1S}\right] \cos 3\omega_V t \\
& - \frac{\lambda^2}{4}\left[F(k_V)\bar{\alpha}_{1S} - G(k_V)\bar{\alpha}_{1C}\right] \sin 3\omega_V t
\end{aligned}
\tag{2.21}
$$

with the coefficients

$$
\begin{aligned}
f_{1S} = \; & F(k_V)\left[\bar{\alpha}_{1S} - k_V\left(\left(\frac{1-2a}{2}\right)\bar{\alpha}_{1C} + \bar{h}_{1C}\right)\right] \\
& - G(k_V)\left[\bar{\alpha}_{1C} + k_V\left(\left(\frac{1-2a}{2}\right)\bar{\alpha}_{1S} + \bar{h}_{1S}\right)\right] \\
f_{1C} = \; & F(k_V)\left[\bar{\alpha}_{1C} + k_V\left(\left(\frac{1-2a}{2}\right)\bar{\alpha}_{1S} + \bar{h}_{1S}\right)\right] \\
& + G(k_V)\left[\bar{\alpha}_{1S} - k_V\left(\left(\frac{1-2a}{2}\right)\bar{\alpha}_{1C} + \bar{h}_{1C}\right)\right]
\end{aligned}
\tag{2.22}
$$

From these equations, the quasisteady theory result follows as a special case. This assumes very small frequencies, and therefore the noncirculatory part becomes zero while the Theodorsen function takes the values $F(k_V) = 1$ and

$G(k_V) = 0$. Therefore

$$\begin{aligned}
\frac{L_{c,qs}}{L_0} &= \bar{\alpha}_0\left(1+\frac{\lambda^2}{2}\right)+\lambda\left[\bar{\alpha}_{1S}-\frac{k_V}{2}\left(\left(\frac{1-2a}{2}\right)\bar{\alpha}_{1C}+\bar{h}_{1C}\right)\right] \\
&+\left[\bar{\alpha}_{1C}\left(1+\frac{\lambda^2}{4}\right)+k_V\left(\left(\frac{1-2a}{2}\right)\bar{\alpha}_{1S}+\bar{h}_{1S}\right)\right]\cos\omega_V t \\
&+\left[2\lambda\bar{\alpha}_0+\bar{\alpha}_{1S}\left(1+\frac{3\lambda^2}{4}\right)-k_V\left(\left(\frac{1-2a}{2}\right)\bar{\alpha}_{1C}+\bar{h}_{1C}\right)\right]\sin\omega_V t \\
&-\frac{\lambda}{2}\left[\lambda\bar{\alpha}_0+2\bar{\alpha}_{1S}-k_V\left(\left(\frac{1-2a}{2}\right)\bar{\alpha}_{1C}+\bar{h}_{1C}\right)\right]\cos 2\omega_V t \\
&+\frac{\lambda}{2}\left[2\bar{\alpha}_{1C}+k_V\left(\left(\frac{1-2a}{2}\right)\bar{\alpha}_{1S}+\bar{h}_{1S}\right)\right]\sin 2\omega_V t \\
&-\frac{\lambda^2}{4}\bar{\alpha}_{1S}\sin 3\omega_V t-\frac{\lambda^2}{4}\bar{\alpha}_{1C}\cos 3\omega_V t
\end{aligned} \tag{2.23}$$

Even from this simple result, it can be seen that the lift response includes a $3/rev$ component because of the multiplication of the trigonometric functions. When the compression and stretching of the shed wake is taken into account, then the vorticity in the shed wake does not have a sinusoidal form anymore but more of a kind of Fourier series of harmonics. The conclusion is that there will also be a series of harmonics in the lift and moment response that is not predicted by quasisteady assumptions. Additionally, if the airfoil is set at a constant angle of attack and has no pitch or plunge motion, both Theodorsen's theory and quasisteady theory lead to the same circulatory lift since no lift deficiency function is in effect. Thus, the use of quasisteady theory or Theodorsen's theory in an unsteady freestream velocity is questionable, in general.

Despite this, the quasisteady theory is a reasonable simplification for small reduced frequencies, but it is unclear whether this statement holds also for large flow oscillation amplitudes λ, even when the reduced frequency is small. This will be clarified using results from more complex theories.

An example for the combination of Theodorsen's theory and quasisteady theory is given in Fig. 2.6 for a pure sinusoidal oscillation in angle of attack. Basically one obtains a very similar result as for a constant freestream where the lift deficiency function of Theodorsen leads to a phase lag as well as to an amplitude modification to the lift (and lift coefficient). The freestream amplitude, even at values very close to one, does not change the sinusoidal form of the lift coefficent.

2.2 Isaacs' Theory

2.2.1 Constant Angle of Attack

Starting from the model given in Fig. 2.7, the freestream velocity consists of a constant and a sinusoidal part, i.e.,

$$V(t) = V_0(1 + \lambda \sin \omega_V t) \qquad |\lambda| < 1 \tag{2.24}$$

and the angle of attack is constant with respect to time

$$\alpha = \alpha_0 \tag{2.25}$$

The normal velocity along the airfoil chord is given as

$$v_n(x,t) = \alpha_0 V(t) + v_{n,w}(x,t) \tag{2.26}$$

The second part of Eq. 2.26 is the contribution of the shed wake. It is important to note here that the velocity of the unsteady freestream is not thought of as to produce a different normal velocity at different airfoil chordwise positions; instead it is considered as constant along chord. This is true only in case of *pure fore-aft motion* of the airfoil, but not in the case of unsteady

freestream with a gradient in normal velocity along chord. Therefore, it is clear that the results may not agree well with results obtained for the physically different environment of an unsteady freestream velocity, especially at higher reduced frequencies.

Now an integral relationship between the varying velocity at the airfoil and the circulation of the airfoil can be derived. Without showing all the steps, this problem can be solved in form of a Fourier series and the result is made nondimensional by dividing through by the lift at the mean velocity, V_0,

$$L_0 = \frac{\rho}{2} V_0^2 c 2\pi\alpha_0 \tag{2.27}$$

This gives for the noncirculatory and circulatory parts of the lift

$$\begin{aligned} \frac{L_{nc}}{L_0} &= \lambda \frac{k_V}{2} \cos\omega_V t \\ \frac{L_c}{L_0} &= \left(1 + \frac{\lambda^2}{2}\right)(1 + \lambda \sin\omega_V t) + \lambda \sum_{m=1}^{\infty} (l_m \cos m\omega_V t + l'_m \sin m\omega_V t) \end{aligned} \tag{2.28}$$

where k_V is the reduced frequency of the freestream velocity oscillations

$$k_V = \frac{\omega_V c}{2V_0} \tag{2.29}$$

It must be noted that there are no additional simplifications or assumptions included, so this is the mathematically exact result. This result contains the steady case of constant angle of attack in a constant freestream (L_0, the "1" in the first term of Eq. 2.28), a term of noncirculatory origin, $(\lambda k_V/2)\cos\omega_V t$, and the rest of the terms are of circulatory origin including the unsteady wake effect in the coefficients l_m and l'_m. The coefficients of the Fourier series are

given by

$$l_m + il'_m = -\frac{m}{i^m}\sum_{n=1}^{\infty}\{F_n[J_{n+m}(n\lambda) - J_{n-m}(n\lambda)] + iG_n\,[J_{n+m}(n\lambda) + J_{n-m}(n\lambda)]\} \tag{2.30}$$

and herein

$$\left.\begin{matrix} F_n \\ G_n \end{matrix}\right\} = \frac{J_{n+1}(n\lambda) - J_{n-1}(n\lambda)}{n^2}\left\{\begin{matrix} F(nk_V) \\ G(nk_V) \end{matrix}\right. \tag{2.31}$$

It is interesting to examine this result in the case of very small reduced frequencies, say $k_V \to 0$, so $F(k_V) = 1$ and $G(k_V) = 0$. Then

$$l_m + il'_m = -\frac{m}{i^m}\sum_{n=1}^{\infty}\frac{J_{n+1}(n\lambda) - J_{n-1}(n\lambda)}{n^2}\,[J_{n+m}(n\lambda) - J_{n-m}(n\lambda)] \tag{2.32}$$

It can be seen, that even the quasisteady case contains an infinite number of harmonics. Now, when $\lambda \to 0$, the sum over m in Eq. 2.28 disappears and we get the same result as in quasisteady theory.

Comparing to the result of quasisteady theory (from Eq. 2.23),

$$\frac{L_{c,qs}}{L_0} = \left(1 + \frac{\lambda^2}{2}\right) + 2\lambda\sin\omega_V t - \frac{\lambda^2}{2}\cos 2\omega_V t \tag{2.33}$$

The mean values obtained by the quasisteady and unsteady theory are the same for the case of constant angle of attack, but the quasisteady theory does not give harmonics above the second, while the unsteady theory includes harmonics up to infinity.

A closer look at Isaacs' result Eq. 2.28 indicates certain limitations in its application since there are two nested summations involved.

1. The first sum (over m) represents the harmonic content of the lift response. If the interest is mainly in the rotor performance, one can

neglect the higher harmonics and will obtain sufficiently accurate results with the first few harmonics alone.

2. The second sum (over n) has to be calculated for every item in the first sum. Since here Bessel functions of the first kind and n-th integer order are involved, as well as the computation of the Theodorsen function, this part requires enormous computational time when it is necessary to calculate higher harmonics. One has to keep in mind that the Theodorsen function also consists of Bessel functions of the first and second kind. This series, therefore, has to be terminated after computing a sufficient number of elements in order to reduce computational time.

For the special case (thought to be typical for helicopters in 1945) of a reduced frequency $k_V = 0.0424$ and a freestream oscillation amplitude of $\lambda = 0.4$, Isaacs gave a numerical example for the total lift ratio L/L_0 and compared it to the quasisteady theory leading to the result:

"...so that for this case the effects herein considered[1] *are not large."*

This sentence often seems to be in mind when it comes to justifying the flow oscillation effect. Since it is based only on this special case of moderate flow amplitude (nowadays helicopters encounter much greater values of λ, even larger than unity) it is not to be taken as the general case. Only a systematic study with a variety of parametric variations including all reduced frequencies of interest, as well as all flow oscillation amplitudes, will be required to justify the necessity of including these effects.

Since the calculation of Bessel functions was not easy in 1945, it is ques-

[1] Unsteady freestream effects are meant here

	A_0	A_{1C}	A_{1S}	A_{2C}	A_{2S}
(1)	1.08	-0.0376	0.770	-0.0790	-0.00697
(2)	1.08	-0.0381595	0.770396	-0.079016	-0.0061575
		A_{3C}	A_{3S}	A_{4C}	A_{4S}
(1)		-0.00061	-0.0050	-0.00003	0.000042
(2)		-0.00061028	-0.00037179	-0.000074784	0.000047096
(1): Isaacs (2): Recalculation $k = 0.0424$ $\lambda = 0.4$ $\alpha = \alpha_0$					

Table 2.7: Coefficients of lift response given by Isaacs in comparison to the recalculation

tionable if the coefficients in the numerical example were calculated correctly. Therefore the author recalculated these coefficients for up to the $30th$ element in the sum of the Bessel functions by using the IMSL subroutines in double precision. The result is shown in Table 2.7 and indicates some differences to Isaacs' results as assumed.

An expression for the pitching moment was not given in [6], but it can be derived from Isaacs' work including periodic variations in angle of attack [7] by setting the harmonic components of angle of attack to zero. The pitching moment is nondimensionalized by the steady moment about the midchord position, M_0,

$$M_0 = L_0 \frac{c}{2} = \frac{\rho}{4} V_0^2 c^2 2\pi\alpha_0 \tag{2.34}$$

and split into circulatory and noncirculatory parts, i.e.,

$$\frac{M_{nc}}{M_0} = 0$$

$$\frac{M_c}{M_0} = \left(1+\frac{\lambda^2}{2}\right) + 2\lambda \sin\omega_V t - \frac{\lambda^2}{2}\cos 2\omega_V t + \\ +\lambda \sum_{m=1}^{\infty} (t_m \cos m\omega_V t + t'_m \sin m\omega_V t) \tag{2.35}$$

Here the coefficients t_m and t'_m are calculated in the same mannor as l_m and l'_m for the lift, except that $F(nk_V)$ must be replaced by $F(nk_V) - 1$. There is no noncirculatory moment, since the reference point for the moment is the midchord and no pitch oscillations are involved.

2.2.2 Oscillating Angle of Attack about Midchord

In Isaacs' first publication [6], he did not give a solution for the aerodynamic pitching moment, yet this was given in his second paper [7] that also includes a $1/rev$ variation in angle of attack with the same frequency. This was thought to be representative for rotorcraft aerodynamics, i.e.,

$$\alpha = \alpha_0(\bar{\alpha}_0 + \bar{\alpha}_{1S}\sin\omega_V t + \bar{\alpha}_{1C}\cos\omega_V t) \tag{2.36}$$

In this case, the derivation becomes more complicated but the result can again be expressed in the form of a Fourier series. However, the constraint here is that *the derivation is made for a rotational axis at midchord* without a parameter accounting for another position of the center of rotation. In rotorcraft this is usually the quarterchord point. Again, the result is decomposed into its noncirculatory and circulatory parts, i.e.,

$$\frac{L_{nc}}{L_0} = \frac{k_V}{2}\Big[(\lambda\bar{\alpha}_0 + \bar{\alpha}_{1S})\cos\omega_V t - \bar{\alpha}_{1C}\sin\omega_V t \\ + \lambda(\bar{\alpha}_{1C}\cos 2\omega_V t + \bar{\alpha}_{1S}\sin 2\omega_V t)\Big]$$

$$\frac{L_c}{L_0} = \left[\bar{\alpha}_0\left(1+\frac{\lambda^2}{2}\right)+\lambda\left(\bar{\alpha}_{1S}-\frac{k_V}{4}\bar{\alpha}_{1C}\right)\right](1+\lambda\sin\omega_V t) + \sum_{m=1}^{\infty}(l_m\cos m\omega_V t + l'_m \sin m\omega_V t) \quad (2.37)$$

with the coefficients looking very similar to the case of constant angle of attack Eq. 2.28, i.e.,

$$l_m + il'_m = -2\frac{m}{i^m}\sum_{n=1}^{\infty}\left\{F_n[J_{n+m}(n\lambda)-J_{n-m}(n\lambda)] + iG_n[J_{n+m}(n\lambda)+J_{n-m}(n\lambda)]\right\} \quad (2.38)$$

Here

$$F_n + iG_n = [F(nk_V)+iG(nk_V)]\frac{H_n+iH'_n}{n^2} \quad (2.39)$$

with

$$H_n = \frac{J_{n+1}(n\lambda)-J_{n-1}(n\lambda)}{2}\left(\lambda\bar{\alpha}_0-\bar{\alpha}_{1S}-\frac{k_V}{2}\bar{\alpha}_{1C}\right)-\frac{2J_n(n\lambda)}{n\lambda}\bar{\alpha}_{1S}$$
$$H'_n = \frac{J_{n+1}(n\lambda)-J_{n-1}(n\lambda)}{n}\bar{\alpha}_{1C}+\frac{J_n(n\lambda)}{\lambda}\left[\bar{\alpha}_{1C}(1-\lambda^2)-\frac{k_V}{2}\bar{\alpha}_{1S}\right] \quad (2.40)$$

On first examination, the result in Eq. 2.37 looks different from the earlier equation presented (Eq. 2.28), but setting $\bar{\alpha}_{1S} = \bar{\alpha}_{1C} = 0$ and $\bar{\alpha}_0 = 1$ one obtains the identical expression as in Eq. 2.28. The quasisteady formulation yields for $a = 0$ (rotation about midchord)

$$\frac{L_{c,qs}}{L_0} = \bar{\alpha}_0\left(1+\frac{\lambda^2}{2}\right)+\lambda\left(\bar{\alpha}_{1S}-\frac{k_V}{4}\bar{\alpha}_{1C}\right) + \left[\bar{\alpha}_{1C}\left(1+\frac{\lambda^2}{4}\right)+\frac{k_V}{2}\bar{\alpha}_{1S}\right]\cos\omega_V t + \left[2\lambda\bar{\alpha}_0+\bar{\alpha}_{1S}\left(1+\frac{3\lambda^2}{4}\right)-\frac{k_V}{2}\bar{\alpha}_{1C}\right]\sin\omega_V t$$

$$
\begin{aligned}
&-\frac{\lambda}{2}\left(\lambda\bar{\alpha}_0 + 2\bar{\alpha}_{1S} - \frac{k_V}{2}\bar{\alpha}_{1C}\right)\cos 2\omega_V t \\
&+\frac{\lambda}{2}\left(\qquad 2\bar{\alpha}_{1C} + \frac{k_V}{2}\bar{\alpha}_{1S}\right)\sin 2\omega_V t \\
&-\frac{\lambda^2}{4}\bar{\alpha}_{1C}\cos 3\omega_V t - \frac{\lambda^2}{4}\bar{\alpha}_{1S}\sin 3\omega_V t
\end{aligned} \tag{2.41}
$$

Comparing the two expressions (the quasisteady result Eq. 2.41 and the unsteady result Eq. 2.37), one can see that the mean values again are the same in both cases as they were in case of constant angle of attack. The dynamic part, however, is different since it includes the lift deficiency function for dynamic pitch in oscillating flow. This consists of the Theodorsen function for the pitch oscillation as well as of Bessel functions for the unsteady flow effect.

In addition to the lift, there is a similar result for the pitching moment,

$$
\begin{aligned}
\frac{M}{M_0} \;=\;& \bar{\alpha}_0\left(1+\frac{\lambda^2}{2}\right) + \lambda\bar{\alpha}_{1S} + \frac{k_V^2}{8}(\bar{\alpha}_{1C}\cos\omega_V t + \bar{\alpha}_{1S}\sin\omega_V t) \\
&+\bar{\alpha}_{1C}\left(1+\frac{\lambda^2}{4}\right)\cos\omega_V t + \left[2\lambda\bar{\alpha}_0 + \bar{\alpha}_{1S}\left(1+\frac{3}{4}\lambda^2\right)\right]\sin\omega_V t \\
&-\lambda\left(\frac{\lambda}{2}+\bar{\alpha}_{1S}\right)\cos 2\omega_V t + \lambda\bar{\alpha}_{1C}\sin 2\omega_V t - \frac{\lambda^2}{4}\bar{\alpha}_{1C}\cos 3\omega_V t \\
&-\frac{\lambda^2}{4}\bar{\alpha}_{1S}\sin 3\omega_V t + \sum_{m=1}^{\infty}(t_m\cos m\omega_V t + t'_m\sin m\omega_V t)
\end{aligned} \tag{2.42}
$$

Herein, the coefficients t_m and t'_m are calculated in the same manner as l_m and l'_m for the lift in Eq. 2.38 except that $F(nk_V)$ must be replaced by $F(nk_V)-1$. The only contribution to the noncirculatory part originates from an acceleration in angle of attack ($\ddot{\alpha}$) about the axis of rotation at midchord (the term with $k_V^2/8$ in Eq. 2.42). There is no $\dot{V}\alpha$ term included, since this produces a lift acting at midchord, and therefore does not lead to a moment

about that point. Surprisingly, there is no term from $V\dot{\alpha}$. It will be shown later that this term is included in the t_m and t'_m terms.

It is interesting whether or not the well known result from Theodorsen for pure angle of attack oscillation about the midchord axis in a steady freestream can be extracted by setting $\lambda = 0$. From the behavior of the Bessel functions, with the argument $\to 0$ one will only get a value for the zero order function $J_0(0) = 1$, while all others are zero, $J_n(0) = 0$. Additionally,

$$\begin{aligned} \lim_{x\to 0} \frac{J_1(x)}{x} &= 0.5 \\ \lim_{x\to 0} \frac{J_n(x)}{x} &= 0 \qquad (n > 1) \end{aligned} \tag{2.43}$$

so that the sum over all m reduces to only the first element, and the same is in effect for the sum over n. The result for the lift is finally

$$\begin{aligned} \frac{L_{nc}}{L_0} &= \frac{k_V}{2}(\bar{\alpha}_{1S}\cos\omega_V t - \bar{\alpha}_{1C}\sin\omega_V t) \\ \frac{L_c}{L_0} &= \bar{\alpha}_0 + l_1\cos\omega_V t + l'_1\sin\omega_V t \end{aligned} \tag{2.44}$$

where $k \equiv k_V$ and

$$\begin{aligned} l_1 &= F(k_V)\left(\bar{\alpha}_{1C} + \bar{\alpha}_{1S}\frac{k_V}{2}\right) + G(k_V)\left(\bar{\alpha}_{1S} - \bar{\alpha}_{1C}\frac{k_V}{2}\right) \\ l'_1 &= F(k_V)\left(\bar{\alpha}_{1S} - \bar{\alpha}_{1C}\frac{k_V}{2}\right) - G(k_V)\left(\bar{\alpha}_{1C} + \bar{\alpha}_{1S}\frac{k_V}{2}\right) \end{aligned} \tag{2.45}$$

and it can easily be seen that it is identical to Theodorsen's result, leading to

$$\frac{L_c}{L_0} = \bar{\alpha}_0 + \left[\bar{\alpha}_{1S}\sin\omega_V t + \bar{\alpha}_{1C}\cos\omega_V t + \frac{k_V}{2}(\bar{\alpha}_{1S}\cos\omega_V t - \bar{\alpha}_{1C}\sin\omega_V t)\right]C(k_V) \tag{2.46}$$

Additionally, one obtains for the noncirculatory and circulatory moment about the midchord

$$\frac{M}{M_0} = \frac{L_c}{L_0} + \frac{k_V^2}{8}(\bar{\alpha}_{1C}\cos\omega_V t + \bar{\alpha}_{1S}\sin\omega_V t) - \frac{k_V}{2}(\bar{\alpha}_{1S}\cos\omega_V t - \bar{\alpha}_{1C}\sin\omega_V t) \tag{2.47}$$

The additional noncirculatory contribution of $V\dot{\alpha}$ was hidden in the coefficients t_m and t'_m by replacing $F(nk_V)$ by $F(nk_V) - 1$. Also, the pitching moment coefficient is identical to Theodorsen's result. Therefore, Isaacs' theory of combined periodic flow and angle of attack oscillations with arbitrary phase angle between both of these motions can be considered as the best available theory for attached flow. However, when it comes to practical application, the tremendous amount of computational effort involved with the repeated evaluation of Bessel functions places many limitations on this theory.

2.3 Generalisation of Isaacs' Theory

Since Isaacs' derivation [7] was made for a fixed pitch axis at midchord, the results are not very useful because in helicopter applications the pitch axis is usually the quarter chord point. In other applications, it may be even another axis, so that a more general formulation is required where the position of the pitch axis is a free parameter, just like in the result given by Theodorsen for unsteady airfoil motion in a constant freestream flow.

Additionally, Isaacs' theory does not include the effect of plunge motion although this degree of freedom is a very important one in helicopter aerodynamics. The subject of this section is to derive results including all degrees

of freedom in two dimensions:

- Pitch motion (including higher harmonics) about an arbitrary location of pitch axis on the chord.
- Fore-aft motion ($1/rev$) with velocity amplitudes smaller than the velocity of the freestream itself.
- Plunge motion (including higher harmonics).

This extension of Isaacs' theory was never given before, and therefore it will be made here for the first time. The complete derivation is very lengthy and is not shown here, but is included in Appendix B. The general procedure follows very closely to the derivation of Isaacs given in [6, 7].

The configuration is shown in Fig. 2.8, where the pitch axis has an arbitrary offset of $ac/2$ from the midchord, positive aft. From this, the normal velocity across the chord is defined as

$$v_n(x,t) = \alpha(t)V(t) + \left(x - a\frac{c}{2}\right)\dot{\alpha}(t) + \dot{h}(t) + v_{n,w}(x,t) \qquad (2.48)$$

where the wake velocity $v_{n,w}$ is produced by the shed vorticity $-\Gamma'(\tau)d\tau$. Since the circulation of the airfoil Γ is a function of its own time history, shed into the wake, one gets an integral equation to be solved.

For the special case of harmonically varying fore-aft motion, angle of attack and plunge motion like

$$\begin{aligned} V(t) &= V_0(1 + \lambda \sin \omega t) \qquad |\lambda| < 1 \\ \alpha(t) &= \alpha_0 \left(\bar{\alpha}_0 + \sum_{n=1}^{\infty} \bar{\alpha}_{nS} \sin n\omega t + \bar{\alpha}_{nC} \cos n\omega t\right) \end{aligned}$$

$$h(t) = \alpha_0 \frac{c}{2} \sum_{n=1}^{\infty} (\bar{h}_{nS} \sin n\omega t + \bar{h}_{nC} \cos n\omega t) \tag{2.49}$$

the integral equation can be solved (the method is shown in Appendix B) and one gets the following result for the lift

$$\begin{aligned}
\frac{L_{nc}}{L_0} = \frac{k}{2} \Bigg\{ & \left[\lambda\bar{\alpha}_0 + \bar{\alpha}_{1S} + k(a\bar{\alpha}_{1C} - \bar{h}_{1C}) - \frac{\lambda}{2}\bar{\alpha}_{2C} \right] \cos\psi \\
& + \left[-\bar{\alpha}_{1C} + k(a\bar{\alpha}_{1S} - \bar{h}_{1S}) - \frac{\lambda}{2}\bar{\alpha}_{2S} \right] \sin\psi \\
& + \sum_{n=2}^{\infty} n \left[\bar{\alpha}_{nS} + nk(a\bar{\alpha}_{nC} - \bar{h}_{nC}) + \frac{\lambda}{2}\left(\bar{\alpha}_{(n-1)C} - \bar{\alpha}_{(n+1)C}\right) \right] \cos n\psi \\
& + \sum_{n=2}^{\infty} n \left[-\bar{\alpha}_{nC} + nk(a\bar{\alpha}_{nS} - \bar{h}_{nS}) + \frac{\lambda}{2}\left(\bar{\alpha}_{(n-1)S} - \bar{\alpha}_{(n+1)S}\right) \right] \sin n\psi \Bigg\}
\end{aligned} \tag{2.50}$$

$$\begin{aligned}
\frac{L_c}{L_0} = & \left\{ \left(1 + \frac{\lambda^2}{2}\right)\bar{\alpha}_0 + \lambda \left[\bar{\alpha}_{1S} - \frac{k}{2}\left(\left(\frac{1-2a}{2} \right) \bar{\alpha}_{1C} + \bar{h}_{1C} \right) - \frac{\lambda}{4}\bar{\alpha}_{2C} \right] \right\} \\
& \times (1 + \lambda \sin\psi) \\
& + \sum_{m=1}^{\infty} (l_m \cos m\psi + l'_m \sin m\psi)
\end{aligned} \tag{2.51}$$

with $\psi = \omega_V t$. The coefficients l_m, l'_m are built up in the same way as in Eq. 2.38 and Eq. 2.39, but the values of H_n and H'_n include the position of axis of rotation a, as well as the amplitude of plunge motion $\bar{h}_{nC}$ and $\bar{h}_{nS}$, and those of pitch in $\bar{\alpha}_{nC}, \bar{\alpha}_{nS}$. In the case of pure $1/rev$ and steady components, the coefficients H_n and H'_n can be written in a form very similar to Isaacs.

$$H_n = \frac{J_{n+1} - J_{n-1}}{2} \left[\lambda\bar{\alpha}_0 - \bar{\alpha}_{1S} - k\left(\left(\frac{1-2a}{2} \right) \bar{\alpha}_{1C} + \bar{h}_{1C} \right) \right] - \frac{2J_n}{n\lambda}\bar{\alpha}_{1S} \tag{2.52}$$

$$H'_n = \frac{J_{n+1} - J_{n-1}}{n}\bar{\alpha}_{1C} + \frac{J_n}{\lambda} \left[\bar{\alpha}_{1C}(1 - \lambda^2) - k\left(\left(\frac{1-2a}{2} \right) \bar{\alpha}_{1S} + \bar{h}_{1S} \right) \right] \tag{2.53}$$

This will be used later to show the effect of another pitch axis location on the lift development.

2.4 Greenberg's Theory

2.4.1 General Theory

Like Theodorsen, Greenberg worked at NACA and he extended Theodorsen's theory of harmonic airfoil motion in a constant freestream flow to the case of an additional periodically varying freestream flow conditions [8]. However, Greenberg also defines the freestream velocity as constant over the chord, and this really means an unsteady fore-aft motion of the airfoil and not a varying freestream. As shown previously, the real case will lead to a velocity gradient over the chord. This is indicated in an appendix to [8], where Greenberg explaines the assumptions about the wake form: *"Consider an airfoil moving back and forth..."*. Despite this, everywhere else Greenberg refers to flow oscillations. However, for the positioning of the wake relative to the airfoil there indeed is no difference whether the airfoil is fixed in a varying freestream or it is moving back and forth in a constant freestream velocity. A fundamental difference can only be seen in the velocity distribution on the chord, and will result in different noncirculatory as well as circulatory aerodynamic forces.

Therefore, Greenberg's derivation includes the third degree of freedom of the airfoil, and the procedure is basically the same as that used by Theodorsen. Greenberg started with a velocity potential function, and solved the equation of motion for the unsteady flow by the small disturbance assumption, including the Kutta condition at the trailing edge, i.e.,

The velocity changes and pitch and plunge motion are considered of gen-

eral harmonic type with a different frequency:

$$\begin{aligned} V &= V_0\left[1+\lambda e^{i\omega_V t}\right] \\ \alpha &= \alpha_0\left[\bar{\alpha}_0+\bar{\alpha}e^{i(\omega_\alpha t+\psi_\alpha)}\right] \\ h &= h_0 e^{i(\omega_h t+\psi_h)} \end{aligned} \tag{2.54}$$

where the phase angles ψ_α and ψ_h allow for different phase with respect to the velocity oscillation as the reference, and the amplitudes λ, $\bar{\alpha}$ and h_0 are of a general complex type. Of course, the restriction that $|\lambda| < 1$ is made in order to have the wake complete behind the airfoil, and not to overlap the vorticity sheets with each other and the airfoil itself. In addition, Greenberg places some assumptions on the form of the wake. These are, first that the effects of mean value and sinusoidal part can be handled separately and that the sinusoidal part may be considered as an airfoil in a constant stream undergoing *fore-aft* motions. The second assumption considers the wake vorticity to be distributed sinusoidally, and this is derived by the final value of infinite frequency of fluctuations in the inplane motion. This assumption is questionable, since the theory is built up on the basic assumption of small disturbances and therefore of small frequencies in airfoil motion as well as freestream fluctuations. However, the sinusoidal wake form leads to key simplifications in evaluating the wake integrals in order to obtain a closed form solution of Theodorsen's type. This solution is presented here in its noncirculatory and circulatory components for lift and moment about the axis of rotation a of the airfoil

$$L_{nc} = \pi\rho\frac{c^2}{4}[\ddot{h}+V\dot{\alpha}+\dot{V}\alpha-a\frac{c}{2}\ddot{\alpha}]$$

$$
\begin{aligned}
L_c &= 2\pi\frac{\rho}{2}Vc\Big\{V_0\alpha_0\left[1+\lambda e^{i\omega_V t}C(k_V)+\lambda e^{i\omega_V t}\bar{\alpha}e^{i\omega_\alpha t}C(k_V+k_\alpha)\right] \\
&\quad +ik_h\bar{h}e^{i\omega_h t}C(k_h)+\bar{\alpha}\left[1+ik_\alpha\frac{1-2a}{2}\right]e^{i\omega_\alpha t}C(k_\alpha)\Big\} \\
M_{nc} &= -\pi\rho\frac{c^3}{8}\left[V\frac{1-2a}{2}\dot{\alpha}-\dot{V}a\alpha-a\ddot{h}+\frac{c}{2}\left(\frac{1}{8}+a^2\right)\ddot{\alpha}\right] \\
M_c &= \frac{c}{2}\frac{1+2a}{2}L_c
\end{aligned}
\tag{2.55}
$$

It can be seen from these equations, that they are very similar to Theodorsen's results and in case of setting $\lambda = 0$ they are identical to those of Theodorsen. It is noteworthy that the pulsating wake has no influence in the plunge motion results since there is no term like $C(k_V + k_h)$ involved. This type of coupling is only related to the unsteady parts of the freestream and angle of attack variations.

The reason for this is found in the small angle assumption, because the angle of attack resulting from plunge motion is $\alpha = \tan^{-1}(\dot{h}/V) \approx \dot{h}/V$. Then the normal velocity at 3/4 chord is the product of velocity and angle of attack $w = V\alpha \approx \dot{h}$, and therefore there is no influence of the oncoming velocity. Nevertheless, this remains questionable since the flow oscillation produces a periodic stretching and compression of the wake also under pure plunge motion, and this should have an effect on the resulting lift and moment development similar to the case of pure angle of attack oscillations.

2.4.2 Transformation of the Results into a Real Fourier Series

Now it remains to rewrite these equations Eq. 2.55 in the form of a real Fourier series. This is required for any application, and in order to make comparisons with Isaacs' theory possible. This form of the results was not

given by Greenberg, and therefore the derivation was made here in this thesis. One has to define the complex amplitudes as follows (the form of V was used by Greenberg to compare the case of constant angle of attack with Isaacs' theory)

$$\begin{aligned} V &= V_0 \Re\left[1 - i\lambda e^{i\omega_V t}\right] = V_0(1 + \lambda \sin\omega_V t) \\ \alpha &= \alpha_0 \Re\left[\bar{\alpha}_0 + (\bar{\alpha}_{1C} - i\bar{\alpha}_{1S})e^{i\omega_\alpha t}\right] = \alpha_0(\bar{\alpha}_0 + \bar{\alpha}_{1C}\cos\omega_V t + \bar{\alpha}_{1S}\sin\omega_\alpha t) \\ h &= \alpha_0 \frac{c}{2} \Re\left[(\bar{h}_{1C} - i\bar{h}_{1S})e^{i\omega_h t}\right] = \alpha_0 \frac{c}{2}(\bar{h}_{1C}\cos\omega_h t + \bar{h}_{1S}\sin\omega_h t) \end{aligned} \tag{2.56}$$

Herein, the phase angles ψ_α and ψ_h are expressed by the cosine and sine amplitude components. Again, the lift will be nondimensionalized by the lift of mean velocity and mean angle of attack, L_0. One has to be very careful in applying the specific functions for velocity, angle of attack and plunge motion. The Theodorsen function is applied to the angle of attack motion, and reduces to an effective angle of attack. Therefore we obtain

$$\begin{aligned} \frac{L_c}{L_0} &= \Re\left[1 - i\lambda e^{i\omega_V t}\right] \Re\Big\{ \bar{\alpha}_0 - i\lambda\bar{\alpha}_0 e^{i\omega_V t}[F(k_V) + iG(k_V)] \\ &\quad + (\bar{\alpha}_{1C} - i\bar{\alpha}_{1S})\left(1 + ik_V\frac{1-2a}{2}\right)e^{i\omega_\alpha t}[F(k_\alpha) + iG(k_\alpha)] \\ &\quad + (\bar{h}_{1C} - i\bar{h}_{1S})ik_h e^{i\omega_h t}[F(k_h) + iG(k_h)] \\ &\quad - i\lambda(\bar{\alpha}_{1C} - i\bar{\alpha}_{1S})e^{i\omega_V t}e^{i\omega_\alpha t}[F(k_V + k_\alpha) + iG(k_V + k_\alpha)]\Big\} \end{aligned} \tag{2.57}$$

Care must be taken for the evaluation of the last term. Using the Euler formula for trigonometric functions

$$e^{i\omega t} = \cos\omega t + i\sin\omega t \tag{2.58}$$

one ends up with the multiplication of trigonometric functions with different frequencies in their argument. These lead to the following expressions

$$\begin{aligned} \sin ax \sin bx &= \frac{1}{2}[\cos(a-b)x - \cos(a+b)x] \\ \sin ax \cos bx &= \frac{1}{2}[\sin(a-b)x + \sin(a+b)x] \end{aligned} \tag{2.59}$$

Then the Theodorsen function $C(a+b)$ is applied to the term with frequency $a+b$, and of course $C(a-b)$ to the term with frequency $a-b$. The latter term does not immediately appear in the complex exponential notation, but the physics of unsteady aerodynamics lead always to the Theodorsen function with the frequency of the oscillation as argument. Now, we are interested in the case of $k_V = k_h = k_\alpha$, and therefore $a = b$. This leads to $C(a-b) = 1$ and

$$\begin{aligned} \sin ax \sin bx C(a+b) &= \frac{1}{2}[\cos(a-b)xC(a-b) - \cos(a+b)xC(a+b)] \\ &\overset{a\equiv b}{=} \frac{1}{2}[1 - \cos 2axC(2a)] \\ \sin ax \cos bx C(a+b) &= \frac{1}{2}[\sin(a-b)xC(a-b) + \sin(a+b)xC(a+b)] \\ &\overset{a\equiv b}{=} \frac{\sin 2ax}{2}C(2a) \end{aligned} \tag{2.60}$$

Thus, after extracting the real part on the right side of Eq. 2.57 we end up with

$$\begin{aligned} \frac{L_c}{L_0} = (1+\sin\omega_V t)\Big\{ & \bar{\alpha}_0 + \frac{\lambda}{2}\bar{\alpha}_{1S} + [\lambda\bar{\alpha}_0 G(k_V) + f_{1C}]\cos\omega_V t \\ & + [\lambda\bar{\alpha}_0 F(k_V) + f_{1S}]\sin\omega_V t \\ & - \frac{\lambda}{2}f_{2S}\cos 2\omega_V t + \frac{\lambda}{2}f_{2C}\sin 2\omega_V t \Big\} \end{aligned} \tag{2.61}$$

where the coefficients f_{1S} and f_{1C} are the same as defined before, while

$$f_{2S} = F(2k_V)\bar{\alpha}_{1S} - G(2k_V)\bar{\alpha}_{1C}$$

$$f_{2C} = F(2k_V)\bar{\alpha}_{1C} + G(2k_V)\bar{\alpha}_{1S} \tag{2.62}$$

Multiplication and sorting of terms finally yields

$$\begin{aligned}
\frac{L_{nc}}{L_0} &= \frac{k_V}{2}\left\{\left[\lambda\bar{\alpha}_0 + \bar{\alpha}_{1S} + k_V(a\bar{\alpha}_{1C} - \bar{h}_{1C})\right]\cos\omega_V t + \lambda\bar{\alpha}_{1C}\cos 2\omega_V t\right. \\
&\qquad \left. + \left[-\bar{\alpha}_{1C} + k_V(a\bar{\alpha}_{1S} - \bar{h}_{1S})\right]\sin\omega_V t + \lambda\bar{\alpha}_{1S}\sin 2\omega_V t\right\} \\
\frac{L_c}{L_0} &= \bar{\alpha}_0\left[1 + \frac{\lambda^2}{2}F(k_V)\right] + \frac{\lambda}{2}\left[f_{1S} + \bar{\alpha}_{1S}\right] \\
&\quad + \left[\lambda\bar{\alpha}_0 G(k_V) \quad + f_{1C} + \frac{\lambda^2}{4}f_{2C}\right]\cos\omega_V t \\
&\quad + \left[\lambda\bar{\alpha}_0[1 + F(k_V)] + f_{1S} + \frac{\lambda^2}{4}f_{2S} + \frac{\lambda^2}{2}\bar{\alpha}_{1S}\right]\sin\omega_V t \\
&\quad - \frac{\lambda}{2}\left[\lambda\bar{\alpha}_0 F(k_V) + f_{1S} + f_{2S}\right]\cos 2\omega_V t \\
&\quad + \frac{\lambda}{2}\left[\lambda\bar{\alpha}_0 G(k_V) + f_{1C} + f_{2C}\right]\sin 2\omega_V t \\
&\quad - \frac{\lambda^2}{4}f_{2C}\cos 3\omega_V t - \frac{\lambda^2}{4}f_{2S}\sin 3\omega_V t \\
\frac{M_{nc}}{M_0} &= k_V\left\{\frac{\lambda}{4}\bar{\alpha}_{1C} + \left[\frac{1-2a}{2}\bar{\alpha}_{1C} + k_V\left(\left[\frac{1}{8} + a^2\right]\bar{\alpha}_{1S} - a\bar{h}_{1S}\right)\right]\sin\omega_V t\right. \\
&\quad - \left[\frac{1-2a}{2}\bar{\alpha}_{1S} - \lambda a\bar{\alpha}_0 - k_V\left(\left[\frac{1}{8} + a^2\right]\bar{\alpha}_{1C} - a\bar{h}_{1C}\right)\right]\cos\omega_V t \\
&\quad \left. - \lambda\left(\frac{1}{4} - a\right)\left(\bar{\alpha}_{1S}\sin 2\omega_V t + \bar{\alpha}_{1C}\cos 2\omega_V t\right)\right\} \\
\frac{M_c}{M_0} &= (1 + 2a)\frac{L_c}{L_0}
\end{aligned} \tag{2.63}$$

2.5 Kottapalli's Theory

2.5.1 General Theory

Like in the theories presented before, Kottapalli [15] also assumed the instantaneous velocity distribution along the chord as a constant, but his publication in 1979 [16] was titled with "...Fluctuating Free Stream". In another paper in 1985 [17], however he explicitly states that the velocity fluctuation

is only due to inplane motion of the airfoil in a constant freestream. The additional restriction of small oscillation amplitudes of this lead-lag motion limits the applicability of his theory to the case of a hovering rotor, or one at low advance ratios in forward flight. Consequently, he acknowledges that the primary use of this derivation should be the stability analysis of a hovering rotor.

For the derivation, Kottapalli uses the singularity method and prescribes simple harmonic motion for the airfoil. For the wake vorticity a sum of exponential functions is used, and the coefficients are identified by satisfying the Kutta condition at the trailing edge, applying the assumption of small amplitudes in velocity oscillation, and therewith dropping all terms of order λ^2, λ^3 and higher order. The final results for the lift and moment coefficients (the latter taken about the axis of rotation a), both referenced to the dynamic pressure of the mean velocity, are

$$\begin{aligned} \frac{C_l}{2\pi\alpha_0} &= \frac{L}{L_0} = c_0 + c_1 e^{i\omega t} + c_2 e^{i2\omega t} \\ \frac{C_m}{\pi\alpha_0/2} &= \frac{M}{M_0} = d_0 + d_1 e^{i\omega t} + d_2 e^{i2\omega t} \end{aligned} \tag{2.64}$$

with the following coefficients

$$\begin{aligned} c_0 &= \bar{\alpha}_0 \\ c_1 &= \lambda\bar{\alpha}_0 + \left\{\bar{\alpha} + \lambda\bar{\alpha}_0 + ik\left[\frac{1-2a}{2}\bar{\alpha} + \bar{h}\right]\right\} C(k) \\ &\quad + \frac{k}{2}[i(\bar{\alpha} + \lambda\bar{\alpha}_0) + k(a\bar{\alpha} - \bar{h})] \\ c_2 &= 2\lambda\left\{\bar{\alpha} + ik\left[\frac{1-2a}{2}\bar{\alpha} + \bar{h}\right]\right\} C(k) \\ &\quad - ik\lambda\left(\frac{1-2a}{2}\bar{\alpha} + \bar{h}\right) C(2k) \\ &\quad + ik\lambda\bar{\alpha} \end{aligned}$$

$$
\begin{aligned}
d_0 &= (1+2a)\bar{\alpha}_0 \\
d_1 &= (1+2a)\left\{\lambda\bar{\alpha}_0 + \left[\bar{\alpha} + \lambda\bar{\alpha}_0 + ik\left(\frac{1-2a}{2}\bar{\alpha} + \bar{h}\right)\right] C(k)\right\} \\
&\quad -ik\left(\frac{1-2a}{2}\bar{\alpha} - a\lambda\bar{\alpha}_0\right) + k^2\left[\left(\frac{1}{8} + a^2\right)\bar{\alpha} - a\bar{h}\right] \\
d_2 &= 2\lambda(1+2a)\left[\bar{\alpha} + ik\left(\frac{1-2a}{2}\bar{\alpha} + \bar{h}\right)\right] C(k) \\
&\quad -ik\lambda(1+2a)\left(\frac{1-2a}{2}\bar{\alpha} + \bar{h}\right) C(2k) \\
&\quad -ik\lambda\bar{\alpha}\frac{1-4a}{2}
\end{aligned}
\tag{2.65}
$$

Here, the parts containing the Theodorsen function indicate the circulatory contribution, while the coefficients c_1, c_2, d_1, d_2 also contain the noncirculatory part (always the last term). Setting $\lambda = 0$, one obtains the Theodorsen result, as required for airfoil oscillations in constant freestream velocity. In case of pure velocity oscillations for an airfoil of constant pitch, the following result can be extracted (setting $\bar{h} = \bar{\alpha} = 0$)

$$
\begin{aligned}
\frac{L}{L_0} &= \bar{\alpha}_0\left\{1 + \lambda\left[1 + C(k) + \frac{ik}{2}\right] e^{i\omega t}\right\} \\
\frac{M}{M_0} &= \bar{\alpha}_0\left\{(1+2a)\left\{1 + \lambda[1 + C(k)]e^{i\omega t}\right\} + ika\lambda e^{i\omega t}\right\}
\end{aligned}
\tag{2.66}
$$

If the moment is taken about the quarterchord ($a = -0.5$) there will be no circulatory contribution, and the pitching moment is only produced by the noncirculatory part.

2.5.2 Transformation of the Results into a Real Fourier Series

The above given results are given in complex notation, however they can be transformed into a real Fourier series like Greenberg's results. Since the noncirculatory part is the same as in Isaacs' or Greenberg's result, it is not

considered here. For the circulatory lift, one applies the same formalism used in transforming Greenberg's results into a real Fourier series. Therefore, we substitute λ by $-i\lambda$, $\bar{\alpha}$ by $\bar{\alpha}_{1C} - i\bar{\alpha}_{1S}$ and $\bar{h}$ by $\bar{h}_{1C} - i\bar{h}_{1S}$. Also, care must be taken where two dynamic parts are multiplied by each other. These lead to a constant contribution and, again, here the Theodorsen function has the argument $\omega \pm \omega$, leading to $C(0) = 1$ and to $C(2k_V)$. It is interesting to note, that in this mixed term of Eq. 2.64 the Theodorsen function also appears with only $1k_V$ as the argument; Kottapalli made no comment to this in [17], where these formulas were published. The final result is

$$\begin{aligned}\frac{L_c}{L_0} = \; & \bar{\alpha}_0 + \lambda\left[\bar{\alpha}_{1S} - \frac{k_V}{2}\left(\frac{1-2a}{2}\bar{\alpha}_{1C} + \bar{h}_{1C}\right)\right] \\ & + [\lambda\bar{\alpha}_0 G(k_V) + f_{1C}]\cos\omega t + [\lambda\bar{\alpha}_0(1 + F(k_V)) + f_{1S}]\sin\omega t \\ & -\lambda\left[\frac{k_V}{2}f_{3C} + f_{1S}\right]\cos 2\omega t - \lambda\left[\frac{k_V}{2}f_{3S} - f_{1C}\right]\sin 2\omega t\end{aligned} \tag{2.67}$$

with the coefficients f_{1S}, f_{1C} like defined before and

$$\begin{aligned} f_{3S} &= F(2k_V)\left(\frac{1-2a}{2}\bar{\alpha}_{1S} + \bar{h}_{1S}\right) - G(2k_V)\left(\frac{1-2a}{2}\bar{\alpha}_{1C} + \bar{h}_{1C}\right) \\ f_{3C} &= F(2k_V)\left(\frac{1-2a}{2}\bar{\alpha}_{1C} + \bar{h}_{1C}\right) + G(2k_V)\left(\frac{1-2a}{2}\bar{\alpha}_{1S} + \bar{h}_{1S}\right) \end{aligned} \tag{2.68}$$

Immediately one sees that Kottapalli's derivation includes only two harmonics in contrast to three harmonics even in quasisteady theory. Here, the assumption of small flow oscillation amplitudes is responsible since all terms of higher order in λ are missing and the $3/rev$ was multiplied with λ^2 in the quasisteady, Theodorsen's and Greenberg's theories.

2.6 Arbitrary Motion Theory in an Unsteady Freestream

After investigating the various thin airfoil theories that are all set up for oscillating motion of the airfoil or the freestream, it is of utmost interest, whether or not the theory of arbitrary motion will lead to the same results as the exact theory in the case of an unsteady freestream. The methodology is the same as has been used in the Section 2.1.4, except that now the freestream velocity is no longer constant. Therefore, additional deficiency functions occur, as will be shown. This method is based on the superposition principal and the use of Duhamel's integral in combination with the indicial response of lift (or moment) due to a sudden change in any of the degrees of freedom.

In incompressible flow the circulatory lift is determined from the normal velocity at 3/4 chord of the airfoil, while the noncirculatory lift is the result of the instantaneous local accelerations. Thus, the total lift is

$$\begin{aligned} L = \; & \pi\rho\frac{c^2}{4}\left[\ddot{h}(t) + V(t)\dot{\alpha}(t) + \dot{V}(t)\alpha(t) - a\frac{c}{2}\ddot{\alpha}(t)\right] \\ & +2\pi\rho V(t)\frac{c}{2}\left[w_{3/4}(0)\phi(s) + \int_0^s \frac{\partial w_{3/4}(\sigma)}{\partial\sigma}\phi(s-\sigma)d\sigma\right] \end{aligned} \tag{2.69}$$

where $\phi(s)$ is Wagner's deficiency function for the lift [11], s the distance travelled by the airfoil (in half chords) and $w_{3/4}(t)$ the instantaneous value of normal velocities at the three quarter chord point. The normal velocity depends on the angle of attack $\alpha(t)$, the flap or plunge motion $h(t)$, the position of the pitch axis $ac/2$, and the time-dependent velocity $V(t)$. This velocity may originate from freestream variations or lead-lag motion of the airfoil or a combination of both. However, it is assumed here to depend on

time only, so the velocity distribution along the chord is the same everywhere. As explained earlier in Section 2.1.1, this is realistic for the lead-lag motion, but is somewhat unrealistic for a freestream velocity variation. An unsteady freestream velocity should be handled in general as a type of propagating gust, and therefore must lead to a gradient in velocity along chord. However, in order to compare results of arbitrary motion theory with those of the other theories analysed so far, the velocity is considered to be constant across chord. Thus, the normal velocity at three quarter chord is

$$w_{3/4}(t) = V(t)\alpha(t) + \dot{h}(t) + \frac{c}{2}\left(\frac{1-2a}{2}\right)\dot{\alpha}(t) \tag{2.70}$$

There are two approaches that can be taken. First, for a given forcing function one can analytically integrate to obtain a closed form solution; second, one can let the type of motion be unknown and apply a finite difference method. Both cases will be handled in the following sections.

2.6.1 Analytical Solution for Periodic Motion

In order to compare the arbitrary motion theory with the others, some specific function for angle of attack, plunge and velocity must be assumed. These are, as before,

$$\begin{aligned} V(t) &= V_0\left(1 + \lambda \sin \omega_V t\right) \\ \alpha(t) &= \alpha_0\left(\bar{\alpha}_0 + \bar{\alpha}_{1S} \sin \omega_V t + \bar{\alpha}_{1C} \cos \omega_V t\right) \\ h(t) &= \alpha_0 \frac{c}{2}\left(\bar{h}_{1S} \sin \omega_V t + \bar{h}_{1C} \cos \omega_V t\right) \end{aligned} \tag{2.71}$$

with the same frequency for velocity and pitch and plunge. The product of time t and frequency of oscillation ω can be expressed in terms of the reduced

frequency k_V and the *mean value of the distance travelled by the airfoil* $\bar{s}$

$$\omega_V t = \frac{\omega_V c}{2V_0}\frac{tV_0}{c/2} = k_V \bar{s} \tag{2.72}$$

while the *actual distance travelled by the airfoil* s results from the integral over the velocity and therefore is

$$\begin{aligned} s &= \frac{1}{c/2}\int_0^t V(t)dt \\ &= \frac{V_0}{c/2}t - \frac{\lambda}{k_V}\cos\omega_V t \\ &= \bar{s} - \frac{\lambda}{k_V}(\cos k_V \bar{s} - 1) + C_I \end{aligned} \tag{2.73}$$

The integration constant C_I is identified through the requirement that the mean distance travelled in one period has to be $\bar{s}$. Therefore, one finds $C_I = -\lambda/k_V$. It is important to note that this value of s forms the upper limit of the integral and therefore the final response will have functions of the following type

$$\sin k_V s = \sin(k_V \bar{s} - \lambda \cos k_V \bar{s}) \tag{2.74}$$

This is a periodic function, and therefore can be replaced by a Fourier series with an infinite number of harmonics.

To obtain the final result, the derivative of the normal velocity must be calculated and included in the integral. The indicial response function ϕ is the Wagner function, but since this is a very difficult function, (it is expressed in terms of Bessel functions), it is much more convenient to replace ϕ by one of its common approximations. These can be written in form of a series of exponential functions

$$\phi(s) = \sum_{i=1}^{N} A_i e^{b_i s} \tag{2.75}$$

and usually this series is cancelled after the second or third term, because the degree of accuracy achieved is sufficiently high. The following steps to evaluate a final result are straight forward, but somewhat lengthy and complicated, since Bessel functions are involved. Therefore they are not shown here, but are included in Appendix C. From that, the final result is,

$$\begin{aligned}\frac{L_c}{L_0} &= D_0 - \lambda\Im(D_1) \\ &\quad + [2\Re(D_1) - \lambda\Im(D_2)]\cos\omega_V t + [\lambda\,[D_0 - \Re(D_2)] - 2\Im(D_1)]\sin\omega_V t \\ &\quad + \sum_{m=2}^{\infty}\Big\{[2\Re(D_m) + \lambda\,(\Im(D_{m-1} - D_{m+1})]\cos m\omega_V t \\ &\qquad + [-2\Im(D_m) + \lambda\Re\,(D_{m-1}) - D_{m+1})]\sin m\omega_V t\Big\} \qquad (2.76)\end{aligned}$$

with the following coefficients

$$D_m = \sum_{n=-2}^{2} C_n i^{(n-m)} J_{n-m}(-n\lambda) \qquad (2.77)$$

including the complex amplitudes

$$\begin{aligned}C_0 &= c_0 A_1 \\ C_1 &= \frac{1}{2}\left[\hat{F}(k_V)c_{1C} + \hat{G}(k_V)c_{1S} - i\left(\hat{F}(k_V)c_{1S} - \hat{G}(k_V)c_{1C}\right)\right] = \bar{C}_{-1} \\ C_2 &= \frac{1}{2}\left[\hat{F}(2k_V)c_{2C} + \hat{G}(2k_V)c_{2S} - i\left(\hat{F}(2k_V)c_{2S} - \hat{G}(2k_V)c_{2C}\right)\right] = \bar{C}_{-2}\end{aligned} \qquad (2.78)$$

and therein

$$\begin{aligned}c_0 &= \bar{\alpha}_0 + \frac{\lambda}{2}\bar{\alpha}_{1S} \\ c_{1C} &= \bar{\alpha}_{1C} + k_V\left(\left(\frac{1-2a}{2}\right)\bar{\alpha}_{1S} + \bar{h}_{1S}\right) \\ c_{1S} &= \lambda\bar{\alpha}_0 + \bar{\alpha}_{1S} - k_V\left(\left(\frac{1-2a}{2}\right)\bar{\alpha}_{1C} + \bar{h}_{1C}\right)\end{aligned}$$

$$
\begin{aligned}
c_{2C} &= -\frac{\lambda}{2}\bar{\alpha}_{1S} \\
c_{2S} &= \frac{\lambda}{2}\bar{\alpha}_{1C}
\end{aligned}
\tag{2.79}
$$

Note that the real and imaginary part of Theodorsen's function, $\hat{F}$ and $\hat{G}$, here are represented by the coefficients of the approximation of the Wagner function by an exponential series and therefore are denoted by $\hat{F}$ and $\hat{G}$, instead of F and G.

The noncirculatory part of the lift leads to the same results as in the thin airfoil theories, and therefore is omitted. The case of $\lambda = 0$ reduces exactly to the case of Theodorsen's theory in a constant freestream, as required. Yet, one difference to the exact theory of Isaacs is immediately obvious. Isaacs' theory includes the Theodorsen function of all harmonics up to infinity, and here only the first two harmonics are included, like in Greenberg's theory.

2.6.2 Solution with the Method of Finite Differences

Another possibility to come to a solution for the case of arbitrary motion is to assume the airfoil motion as unknown. Then Duhamel's integral yields for the circulatory part of the lift like above

$$
\begin{aligned}
L_c &= 2\pi\frac{\rho}{2}V(t)c\left[w_{3/4}(0)\phi(s) + \int_0^s \frac{\partial w_{3/4}(\sigma)}{\partial\sigma}\phi(s-\sigma)d\sigma\right] \\
&= 2\pi\frac{\rho}{2}V(t)c\, w_{3/4,eff}
\end{aligned}
\tag{2.80}
$$

and again the normal velocity at 3/4 chord is written as

$$
w_{3/4}(t) = V(t)\alpha(t) + \dot{h}(t) + \frac{c}{2}\left(\frac{1-2a}{2}\right)\dot{\alpha}(t) \tag{2.81}
$$

Now the derivative $\partial w_{3/4}(\sigma)/\partial\sigma$ is generally

$$\frac{\partial w_{3/4}(\sigma)}{\partial\sigma} = \frac{\partial V(\sigma)}{\partial\sigma}\alpha(\sigma) + V(\sigma)\frac{\partial\alpha(\sigma)}{\partial\sigma} + \frac{\partial\dot{h}(\sigma)}{\partial\sigma} + \frac{c}{2}\left(\frac{1-2a}{2}\right)\frac{\partial\dot{\alpha}(\sigma)}{\partial\sigma} \quad (2.82)$$

The method of finite differences introduces the calculation at different time steps with a stepwidth being rather small relative to the highest frequency encountered. Therefore, normally about 45 to 60 steps are made within one cycle. However, this implies the use of some mechanism to describe the state between the time steps, and this is usually done by a zero order hold. By this a finite difference approximation can be made for the integrals, when using one of the common exponential sereis approximations for the Wagner function.

$$\phi(s) = \sum_{k=1}^{N} A_k e^{b_k s} \quad (2.83)$$

Then, for the sample with index n being the current sample, the expression in the brackets in Eq. 2.80 for the effective normal velocity at 3/4 chord becomes $w_{3/4,eff} = w_{3/4,n}$.

$$w_{3/4,n} = \sum_{i=0}^{n}\left[V_i\Delta\alpha_i + \alpha_i\Delta V_i + \frac{c}{2}\left(\frac{1-2a}{2}\right)\Delta\dot{\alpha}_i + \Delta\dot{h}_i\right] - \sum_{j=1}^{4}\sum_{k=2}^{N} X_{n,k}^{(j)} \quad (2.84)$$

Herein, the X are called deficiency functions and contain the information of the time history of the different degrees of freedom. They are [33]

$$X_{n,k}^{(j)} = X_{n-1,k}^{(j)} e^{b_k\Delta s} + A_k\Delta^{(j)} e^{b_k\Delta s/2} \quad (2.85)$$

The values A_k and b_k are those of the usual approximation to the Wagner function; for example Jones approximation ([34], see Table 2.4). If a higher order approximation is used, such as that of Peterson and Crawley ([35], see Table 2.5), than additional deficiency functions are added, as indicated by

the upper limit N. This is not usually desirable, since more terms lead to additional computational effort without leading to any significant gains in the accuracy of the results. One has to note that $4N$ deficiency functions have to be computed, and therefore one must keep N as small as possible. The values denoted by $\Delta^{(j)}$ are the differential changes of the four derivatives in the current sample [33], i.e.,

$$\begin{aligned} \Delta^{(1)} &= V_n \Delta\alpha_n & \qquad \Delta^{(2)} &= \Delta V_n \alpha_n \\ \Delta^{(3)} &= \frac{c}{2}\left(\frac{1-2a}{2}\right)\Delta\dot{\alpha}_n & \qquad \Delta^{(4)} &= \Delta\dot{h}_n \end{aligned} \tag{2.86}$$

and the increment in the distance travelled by the airfoil Δs is

$$\Delta s = \frac{2}{c}\int_t^{t+\Delta t} V(t)\, dt = \frac{V_n + V_{n-1}}{c}\Delta t \tag{2.87}$$

The total response of lift due to arbitrary motion of the airfoil can be calculated by updating the deficiency functions at each sample.

$$\frac{L_{c,n}}{L_0} = \frac{V_n}{V_0}\frac{w_{3/4,n}}{V_0\alpha_0} \tag{2.88}$$

When this formalism is applied to a constant freestream, Theodorsen's result is represented to an accuracy depending on the coefficients of the indicial function ϕ. In this case $\lambda = 0$ and

$$\Delta s = \frac{2V}{c}\Delta t = \frac{\Delta\psi}{k_V} \tag{2.89}$$

with $\psi = \omega_V t = k_V \bar{s}$ being the rotor azimuth.

This formalism now can be applied to any type of airfoil motion, for example harmonic motion like that of Eq. 2.71. This will now be the subject of investigation. In all the cases presented, the number of steps in one cycle

was set to 64. This is somewhat high, and therefore is on the conservative side. So here space steps are used instead of time steps, and therefore no difficulties occur when it comes to high frequencies where a time spacing leads to fewer steps within one cycle than at lower frequencies.

2.6.3 Introduction of Compressibility Effects

In general a helicopter rotor has a relatively high tip speed, normally with a tip Mach number of about $M = 0.64$ in hover. In fast forward flight the local Mach number approaches $M = 1$ on the advancing side, while it is reduced on the retreating side. So a rotor blade is in a most complicated situation with periodic motion in an unsteady freestream environment, also with changing Mach numbers and changing Reynolds numbers. Both Reynolds and Mach numbers have a significant influence on the airfoil behavior, however in all theories shown before, the flow is considered to be incompressible and with infinite Reynolds number. Now, the arbitrary motion theory has the important advantage that the deficiency functions can be adapted to compressible flow and various comparisons [33, 37] have shown the validity of doing so in a constant freestream. The modified deficiency function includes the Glauert compressibility factor $\beta = \sqrt{1 - M^2}$.

$$\phi(s) = \sum_{i=1}^{N} A_i e^{b_i \beta^2 s} \tag{2.90}$$

and the lift curve slope changes its gradient by

$$C_{L\alpha} = \frac{C_{L\alpha,inc.}}{\beta} = \frac{2\pi}{\beta} \tag{2.91}$$

Of course in the case of a helicopter, the Mach number is a function varying periodically with time and radius and therefore has to be calculated contin-

uously. It must be kept in mind, that this modification is only valid up to Mach numbers of about $M = 0.8$, depending on the airfoil shape. The lift curve slope at subsonic Mach numbers closer to one drops significantly and this is not included in this compressibility correction factor. In the finite difference method presented in the section before, the deficiency functions now are

$$X_{n,k}^{(j)} = X_{n-1,k}^{(j)} e^{b_k \beta^2 \Delta s} + A_k \Delta^{(j)} e^{b_k \beta^2 \Delta s/2} \tag{2.92}$$

$$L_{c,n} = \frac{2\pi}{\beta} \rho V(t) \frac{c}{2} w_{3/4,eff} \tag{2.93}$$

Thus, with a minimal amount of additional work, but with somewhat more computational effort a possibility to include the compressibility effects is given. However, there are no experimental data of oscillating airfoils in oscillating freestream available, where the mean velocity has a Mach number of 0.6 or even near that. All experiments were made in essentially incompressible flow at Mach numbers of about 0.05 or less, so there are only negligible compressibility effects included. Also, no exact theory exists for unsteady airfoil motion in a subsonic varying freestream and therefore no theoretical data exist as a basis for comparison.

Furthermore, the noncirculatory parts of the lift no longer depend only on the instantaneous motion, unlike in the incompressible case. Therefore, they are much more difficult to calculate since like the circulatory terms they also have a time history effect. This introduces additional deficiency functions; for more detail see [37].

Chapter 3

Results and Discussion

3.1 Isaacs' Theory

3.1.1 Lift Transfer Function for Constant Pitch

The formulas in Eq. 2.28 are not very expressive for a physical understanding of the problem, since there will be a response with a whole range of frequencies to the input of only one frequency in $V(t)$. Since the lift is proportional to the square of the velocity, the input consists of steady, $1/rev$ and $2/rev$ parts, and the output will mainly consist of these harmonics, including some phase lag effects. The circulatory lift coefficient, based on the instantaneous dynamic pressure, is far from uniform, as predicted by quasisteady theory, and this is shown in Fig. 3.1 for a reduced frequency of $k_V = 0.05$ and 0.2.

These results were calculated by including terms up to the $15th$ harmonic, and for each harmonic up to the $25th$ order in the reduced frequency and in the freestream oscillation amplitude λ. This is required to include as many terms as necessary to show the correct solution. The higher order terms become smaller and approach zero because of the factor n^2 in the

denominator of Eq. 2.31, and because of the behavior of the Bessel functions for large arguments. Nevertheless, a calculation with fewer terms has shown that for high freestream amplitudes, say $\lambda = 0.8$, the peak in lift coefficient at the minimum velocity ($\omega_V t = 270^o$) has not yet converged, so one has to take all these terms into account. Of course, this results in a huge amount of computational time and this again makes this theory very impractical for rotorcraft applications. However, there are no restrictions made with respect to the flow oscillation amplitude, except that λ has to be less than one. Therefore, this theory is a kind of "best theory available", with which the other theories with more rigorous assumptions can be compared.

These results show the typical effects of unsteady aerodynamics already known from constant freestream theory. First, there is a phase lag resulting in a lag in the lift buildup with respect to the change in velocity. Second, there is an effect on the circulatory lift amplitude resulting in a smaller value of maximum lift (where the velocity is at maximum) and more lift in the regime where the velocity is a minimum. It must be noted here, that both effects strongly depend on the reduced frequency, and for high reduced frequencies, the phase lag reduces to zero and the reduction in lift amplitude approaches a final value that will be determined later. This behavior was not unexpected, since the solution contains the Theodorsen function.

The steady part of the lift transfer function is the same as in quasisteady theory, and therefore not shown here. More interesting is the dynamic part, since Isaacs' theory produces a Fourier series with an infinite number of harmonics as the system response, even at constant angle of attack. The first four harmonics of the response are shown in Fig. 3.2. One can see the

typical behavior of the Theodorsen function in the $1/rev$ and $2/rev$ of the lift response. With increasing flow oscillation amplitudes, the amplification also increases, but the phases angles remain the same except for high values of λ. Interesting forms of the transfer function can be found in the $3/rev$ and $4/rev$ components; here loop-type transfer functions are encountered. This means a change in phase angle of 180^o from zero frequency to very high reduced frequencies in the $3/rev$-part and a change of 270^o in the $4/rev$-part of the lift transfer function. Also, the amplification starts with zero for zero reduced frequenc, obtains its maximum at reduced frequencies of about 0.2, and becomes smaller again for high reduced frequencies with a final value of zero for infinite frequency.

It must be noted here, that for the $1/rev$ and $2/rev$-parts terms up to the $25th$ in k_V and λ are sufficiently enough and for values of $\lambda \leq 0.8$ this holds also for the $3/rev$ and $4/rev$-part. However, for the high flow amplitudes one needs much more terms to obtain a converged solution, that is, for $\lambda = 0.9$ one must include up to the $50th$ multiple of k_V and λ. For $\lambda = 0.999999$ one has to include up to the $200th$ multiple. Therefore, the computational effort increases tremendously with λ becoming close to unity.

Now the results of combining flow oscillations with periodic airfoil pitch changes will be presented and discussed. Unfortunately, with increasing degrees of freedom the number of parameters to be varied are increase significantly, therefore one has to reduce these variations to a few examples showing the most important combinations. First, this will be a pure sinusoidal motion in pitch, than the pure cosine, and then the so called helicopter case of combined steady and sinusoidally oscillating angle of attack where the motion of

angle of attack is in counterphase to the velocity changes.

3.1.2 Lift Transfer Function for Sinusoidal Pitch Oscillations

The angle of attack is assumed to consist only of its sinusoidal part, say $\bar{\alpha}_0 = \bar{\alpha}_{1C} = 0$ and $\bar{\alpha}_{1S} = 1$. The lift response is shown in the time domain in Fig. 3.3 for two reduced frequencies of $k_V = 0.05$ and 0.2. In both cases, the quasisteady theory result as well as the result of Theodorsen's theory also plotted for comparison.

At low reduced frequencies, two interesting observations can be made

1. At the maximum velocity ($\omega_V t = 90^o$), the unsteady lift for high freestream amplitudes is very close to the quasisteady value, with a small phase lag. The lift amplitude reduction is not as much as Theodorsen's theory would predict.

2. At the minimum velocity ($\omega_V t = 270^o$), the unsteady lift for high freestream amplitudes is closer to zero, as in the quasisteady case or in Theodorsen's theory. This can be seen very clearly in the lift coefficient, for example at $\lambda = 0.8$.

The reason for this surprising behavior is due to the effect of stretching and compressing the shed wake vorticity, respectively. The stretching leads to a smaller effective reduced frequency, while the compression leads to larger effective reduced frequencies with a more significant reduction of circulatory lift. This observation is in agreement with Johnson's results [3]. For the higher reduced frequency of $k = 0.2$, these effects become more dramatic

especially in the low velocity region. Here, the lift deficiency function drops very rapidly. With increasing freestream amplitude, the circulatory lift even becomes positive, although the angle of attack has its maximum negative value here. Since the lift itself is very small because of the very small dynamic pressure, this can be seen most clearly in the lift coefficient.

The frequency domain presentation of lift response gives the amplitude and phase, and is given in Fig. 3.4 for the constant part and in Fig. 3.5 for the first four harmonics. The constant part of lift response due to the $\bar{\alpha}_{1S}$ term in Isaacs' theory (Eq. 2.37) is identical to the quasisteady theory result ($\lambda\bar{\alpha}_{1S}$), but Theodorsen's theory (see Eq. 2.21) includes the Theodorsen function ($\lambda\bar{\alpha}_{1S}[F(k_V) - k_V G(k_V)(1-2a)/4]$). Therefore, the mean value of lift is significantly underpredicted with increasing reduced frequencies. This is important even for the small fundamental reduced frequencies encountered by a rotor blade. For small flow oscillation amplitudes Theodorsen's theory can be used, but for higher frequencies this theory is not applicable.

There are significant differences in the $1/rev$-part of the lift response, see Fig. 3.5 for the first four harmonics of the dynamic part of the lift transfer function. In Isaacs' theory, the transfer function for $\lambda = 0$ is only shifted to the right with increasing freestream amplitude, and does not change its shape. The combination of Theodorsen's theory with the unsteady freestream leads to rather different results, since the reduction in amplitude is larger and the phases angles are larger for high values of λ. Only minor differences can be found in the $2/rev$-part; here both theories lead to very similar results. It is interesting to note, that the transfer function of the $2/rev$-part simply looks like a transfer function of the $1/rev$ at $\lambda = 0$, but rotated by a phase angle of

90^o. The $3/rev$-part also shows very similar results for both theories, but the final values for high reduced frequency here is not infinite but zero for the cosine part, and a finite number for the sine part. Most interesting now, is the $4/rev$-part of the lift response since there are no harmonic contributions of more than $3/rev$ either in the quasisteady result or the combined Theodorsen - unsteady freestream theory. Therefore one cannot expect a form of transfer function like that of pitch oscillation in a constant flow. Here a loop-type transfer function can be observed, changing its phase by 180^o from zero to very high reduced frequencies.

3.1.3 Lift Transfer Function for Cosine Pitch Oscillations

Now $\bar{\alpha}_0 = \bar{\alpha}_{1S} = 0$ and $\bar{\alpha}_{1C} = 1$. Again, the effect of freestream velocity oscillations will be shown in the time domain as well as in frequency domain. Fig. 3.6 shows the lift development for reduced frequencies of $k_V = 0.05$ and 0.2 for pure cosine angle of atttack motion in a sinusoidally varying freestream; that is the pitch variation is 90^o out of phase with the freestream variation. Again, Isaacs' results are compared to Theodorsen's theory combined with the unsteady freestream and with quasisteady theory results.

From the time domain response, the following can be observed:

1. As for sinusoidal motion, the unsteady lift response is closer to the quasisteady result than the results obtained with Theodorsen's theory. This is because the stretching of the shed wake vorticity leads to a smaller effective reduced frequency, where the velocity is a maximum.

2. In the region with lowest velocity, a lift overshoot occurs. This is in contrast to the sinusoidal pitch motion where the lift deficiency function shows a reduction in lift. It is evident, that the combination of Theodorsen's theory with an unsteady freestream cannot be used to predict the lift coefficient. However, since the total velocity is small here, the difference in lift is not too significant.

The constant (mean) part of the lift transfer function is shown in Fig. 3.7. It can be seen that Theodorsen's theory leads to an increase in this mean value of the total circulatory lift for small reduced frequencies. This is due to the $-G(k_V)$-term in Eq. 2.21. For the range of reduced frequencies a helicopter blade encounters, this leads to completely incorrect trends; however the magnitude of this mean part of the lift is small and therefore the absolute differences are not so severe.

The frequency response in Fig. 3.8 looks very similar to that for sinusoidal pitch motion, although it seems to be rotated by 90^o. A closer look reveals some differences that appear in the scaling of the axis. Again, the $1/rev$ of Isaacs' theory shows smaller phase lags than Theodorsen's theory when the reduced frequency is smaller than about unity, especially when the freestream amplitude is high. There are also higher harmonics present in Isaacs theory that cannot be predicted by quasisteady theory, or the combination of Theodorsen's theory with the unsteady freestream.

3.1.4 The Helicopter Case

Here there is a collective pitch represented by $\bar{\alpha}_0$ and the longitudinal cyclic pitch by $\bar{\alpha}_{1S}$. For a helicopter, one has to alleviate the rolling and pitching

moments produced by nonsymmetric aerodynamic environment in forward flight. Therefore a $1/rev$ cyclic pitch control setting is introduced. Basically this periodic angle of attack is such as to reduce the lift where the dynamic pressure is high (advancing side), and to increase the lift where the dynamic pressure is minimum (retreating side). The phase between the velocity and the angle of attack will be about 180^o, as mentioned before.

To cover the range of reduced frequencies encountered, one calculation is performed at a reduced frequency of $k = 0.05$, and another at $k = 0.2$. The results are shown in Fig. 3.9. For comparison the result of the quasisteady theory and Theodorsen's theory are also plotted. The following characteristics of unsteady combined motion can be observed:

1. This case, which should be more relevant to a rotor environment, leads to more lift in the first quadrant of the disk due to the phase lag of angle of attack motion. It is interesting that smaller lift is obtained in the third quadrant at small values of λ, compared to the quasisteady case. There is about the same lift at $\lambda \approx 0.5$, and more lift for higher λ. Again, the lift coefficient develops a strong peak at $\psi = 270^o$ while the quasisteady formulation does not show any changes for this low reduced frequency of 0.05. In contrast to Theodorsen's theory, the lift coefficient amplitude increases in comparison to the quasisteady values when the flow oscillation amplitude is non-zero. It is also of interest, that due to the unsteady shed wake vorticity the lift coefficient develops a phase lead in the area from $300^o < \psi < 30^o$, when the flow amplitude is high.

2. b) With increasing frequency, one obtains a similar result, including a larger phase lag and a stronger reduction in lift amplitude. This leads to more lift on the advancing blade in the first quadrant, compared to quasisteady lift. The obtained of higher lift around $\psi = 270^o$ now starts for $\lambda = 0.6$, while it was obtained at $\lambda = 0.5$ in case of the smaller reduced frequency. There was only a slight increase in the peak of the lift coefficient with increasing reduced frequency.

All these results generally show that the unsteady freestream effects are not small, and should be included, especially when the relative amplitude of the freestream oscillations exceeds values of about $\lambda = 0.2$.

3.2 Greenberg's Theory

3.2.1 Numerical Comparison with Isaacs' results

In order to compare Greenberg's results (Eq. 2.63) with those of Isaacs, the case of constant angle of attack in a pulsating freestream velocity was chosen by Greenberg. This was done at a relatively small reduced frequency of $k_V = 0.0424$ and for a medium flow oscillation amplitudes of $\lambda = 0.4$. These values were considered representative for current helicopter operations at that time. Assuming a representative radial station of $y = r/R = 0.75$, these values correspond to a ratio of $c/R = 0.0636$ and an advance ratio of $\mu = 0.3$. Todays helicopters, however, exceed these values, for example the world speed record set by a Westland Lynx obtained an advance ratio of $\mu \approx 0.5$.

From Eq. 2.63, one gets for the case of $\bar{\alpha}_{1S} = \bar{\alpha}_{1C} = \bar{h}_{1S} = \bar{h}_{1C} = 0$

$$\begin{aligned}
\frac{L_{nc}}{L_0} &= \bar{\alpha}_0 \lambda \frac{k_V}{2} \cos \omega_V t \\
\frac{L_c}{L_0} &= \bar{\alpha}_0 \left\{ 1 + \frac{\lambda^2}{2} F(k_V) + \right. \\
&\quad + \lambda [G(k_V) \cos \omega_V t + [1 + F(k_V)] \sin \omega_V t] - \\
&\quad \left. - \frac{\lambda^2}{2} [F(k_V) \cos 2\omega_V t - G(k_V) \sin 2\omega_V t] \right\}
\end{aligned} \tag{3.1}$$

In contrast to Isaacs' result which has an infinite series of harmonics (see Eq. 2.28), here only a $1/rev$ and $2/rev$ component exist (Eq. 2.63). Additionally the pure sinusoidal shed wake vorticity leads only to the Theodorsen function of the reduced frequency itself, but not to any multiples of k_V like in Isaacs' theory; not even a $C(2k_V)$-term is included. The noncirculatory parts are identical, since they result only from the instantaneous motion of the airfoil and freestream, and therefore must be independent of any theory.

A comparison of the numerical values of the coefficients was made, and only small differences were found. Additionally, it was stated in [8] that this agreement with Isaacs' results holds for relatively large values of λ at relatively small values of reduced frequency. With respect to the assumptions made in the form of the wake, even better agreement should be expected at high reduced frequencies, citing Greenberg [8]. Putting the total lift (noncirculatory and circulatory parts) into the form of a Fourier series

$$\frac{L}{L_0} = A_0 + A_{1C} \cos \omega_V t + A_{1S} \sin \omega_V t + A_{2C} \cos 2\omega_V t + \ldots \tag{3.2}$$

the coefficients can be compared. The coefficients given by Greenberg are listed in Table 3.1. It should be noted, that the coefficient A_0 of Isaacs theory

	A_0	A_{1C}	A_{1S}	A_{2C}	A_{2S}	A_{3C}	A_{3S}
(1)	1.079	-0.0376	0.770	-0.079	-0.00697	-0.00061	-0.005
(2)	1.074	-0.0395	0.768	-0.074	-0.00960	-	-
(1): Isaacs (2): Greenberg $k = 0.0424$ $\lambda = 0.4$ $\bar{\alpha}_0 = 1$							

Table 3.1: Coefficients of lift resp onse given by Greenberg in comparison to the result of Isaacs

(given by Greenberg) is not identical to that given by Isaacs in [6], since A_0 should have been exactly 1.08 (as can be easily proved). It is unclear how this error could have occured. All harmonic coefficients were the same as given by Isaacs. Indeed, the differences seem to be small in this special case, but an analysis with a wider spectrum of reduced frequencies and flow oscillation amplitudes give a better basis for comparison. Also, it is questionable how accurately the Bessel functions could be calculated in 1946. Therefore, a recalculation using the IMSL-subroutines in double precision was made, using up to the 30th multiple in k. There are some differences even in the third decimal digit, and this is somewhat surprising. A recalculation of the coefficients was done here using up to the 200th multiple in reduced freauency and in λ, and is given in Table 3.2. This comparison covers the same configurations as were used by Isaacs in [6] to show the effect of unsteady freestream effect on lift development.

In the following sections, the lift transfer functions obtained from Greenberg's results are compared to Isaacs' results. First, the case of constant angle of attack will be shown for different reduced frequencies, then the combined motion of velocity and angle of attack. The lift transfer function for

	A_0	A_{1C}	A_{1S}	A_{2C}	A_{2S}
(1)	1.080000	-0.0381595	0.770396	-0.079016	-0.0061575
(2)	1.073792	-0.0394386	0.768958	-0.073792	-0.0095837
		A_{3C}	A_{3S}	A_{4C}	A_{4S}
(1)		-0.00061028	-0.00037179	-0.000074784	0.000047096
(2)		-	-	-	-
(1): Isaacs (2): Greenberg $k = 0.0424$ $\lambda = 0.4$ $\bar{\alpha}_0 = 1$					

Table 3.2: Coefficients of lift response of Greenberg's and Isaacs' solution, recalculated

the combined motion will finally show the differences in lift amplitude and phase angle. It must be kept in mind that the comparison is made for the same frequency in pitch and velocity oscillations, since Isaacs' results cannot account for different frequencies, unlike those given by Greenberg.

3.2.2 Lift Transfer Function for Constant Pitch

In case of a constant pitch setting, it can be seen from Fig. 3.10 that Greenberg's theory significantly underpredicts the peak of lift in the area of high velocity. Also, in the area of smallest velocity the lift calculated by Greenberg's theory is smaller than that obtained by Isaacs. On the left side of Fig. 3.10 the circulatory lift and circulatory lift coefficients are plotted for a reduced frequency of $k_V = 0.05$, while on the right the reduced frequency is $k_V = 0.2$.

The differences between the theories increase with both the flow oscillation amplitude as well as with the reduced frequency. These differences can be seen more clearly in the lift coefficient development, while for small values

of $\lambda \leq 0.2$ both theories lead to almost the same results. The significant peak in lift coefficient for higher values of λ as shown by Isaacs' results, reduces to about half of the magnitude in Greenberg's theory. This is due to the simplifications made in the wake model of Greenberg's theory, and this leads to smaller lift coefficients for higher λ nearly everywhere, especially in the region of small dynamic pressure (retreating side of the disk). Except in the region of decelerating flow around $135^o < \omega t < 200^o$, the lift coefficient is always slightly smaller. Good agreement between both theories were obtained for freestream amplitudes of up to $\lambda \approx 0.4$; the higher the reduced frequency, the smaller the values of λ have to be for good agreement. The reason for this behavior can be seen in the assumptions made for the wake, leading to different solutions especially in the constant part of the circulatory lift, but also in the harmonic parts.

Looking at the total circulatory lift in Fig. 3.10, however, the discrepancies in the region of high dynamic pressure are more significant than those in the low dynamic pressure region. Here, the absolute differences in lift coefficient are small, but in terms of total lift they are very large. Again, it becomes obvious that under time varying freestream flow conditions the lift coefficient looses its importance since the physically active parameter is the lift force and not the lift coefficient. Thus, a definition of a force coefficient, nondimensionalized by a constant velocity (for example V_0), seems to be a physically more meaningful approach than using the classical lift coefficient, that depends on the local velocity.

The lift transfer function is given in Fig. 3.11 and Fig. 3.12 for the constant and dynamic parts of the lift response. Especially for the constant part,

there are significant differences to be seen. This is somewhat surprising, since normally the dynamic parts are more difficult to determine than the steady ones. While Isaacs' theory shows an independence of the constant part with respect to reduced frequency, Greenberg's theory leads to a dependency on the Theodorsen function (see Eq. 2.63). This is of importance even for small flow oscillation amplitudes and small reduced frequencies. Therefore, the mean value of the lift is significantly underpredicted by Greenberg's theory. Looking to the right half of Fig. 3.11, where only the range of reduced frequencies encountered by a helicopter blade is shown, one can see, that the numerical comparison made by Greenberg in [8] is not very representative. At $k_V = 0.0424$ and $\lambda = 0.4$ indeed the differences are not very large, but with higher reduced frequencies the differences between both theories increase significantly, even for small values of λ, see Fig. 3.11. This is contrary to Greenberg's statement [8] that the agreement for high reduced frequencies will be better than at low ones because of the high frequency assumption made for the wake.

More differences are revealed by the dynamic part of the lift transfer function, see Fig. 3.12. For values of $\lambda < 0.4$, the agreement with Isaacs' theory is very good for the $1/rev$ component, but for higher flow amplitudes the phase angles predicted by Greenberg's theory are larger than those of Isaacs. Furthermore, the final values for infinite reduced frequencies are not the same; Greenberg's theory underpredicts them significantly, especially for high λ. The $2/rev$-part shows good agreement with Isaacs' result. However, there are no higher harmonic response components in Greenberg's theory, while Isaacs' theory still has contributions for all harmonics allthough they

are smaller with each higher harmonic. Typically, these higher harmonics start at zero for small reduced frequencies, and produce to a change in phase of 180^o at high reduced frequencies in the $3/rev$-part, and 270^o in the $4/rev$-part. The sum of all these harmonics leads to important effects on the total lift response.

The next comparison covers the simultaneous oscillation of inplane velocity and angle of attack, both with the same frequency, but with two different phases. First the in-phase condition with sinusoidally pitch changes will be considered, and then the case of cosine motion in pitch. Both have been investigated in the previous section, and will be compared to Isaacs' theory.

3.2.3 Lift Transfer Function for Sinusoidal Pitch Oscillations

For a reduced frequency of $k_V = 0.05$ and 0.2, Greenberg's results are compared with Isaacs' results in Fig. 3.13. Here only $\bar{\alpha}_{1S} = 1$ while all other amplitudes are set to zero. The following differences can be seen:

1. In the region of high velocity the lift is significantly underpredicted by Greenberg's theory. This means that the effective reduced frequency is too high here, leading to a lift deficiency that is too large.

2. In the region of smallest velocity, the additional loss in lift is not completely predicted by Greenberg's theory, so here the effective reduced frequency is too small, leading to more lift than predicted by the exact theory of Isaacs. In the total lift, this will hardly be noticed since the dynamic pressure is very small, but if the issue of interest is the lift

coefficient, this will be very important. This is especially true, if the lift coefficient is operating near stall conditions like on the retreating side of the disk.

Both effects can be seen as a sequence of the wake approximation Greenberg made in his derivation. In general the effects of "stretching and compressing" the shed wake vorticity described before, and by Johnson in [3], are represented by Greenberg's theory in the correct trend. However the magnitude is not completely correct. More information can be obtained from the lift transfer function, which is shown in Fig. 3.14 for the constant part of the lift, and in Fig. 3.15 for the first four harmonics. Even from the constant part of the lift, it can be seen that the statement made by Greenberg of "good agreement with Isaacs' theory" in [8] does not hold. While in Isaacs' theory the constant part of the lift is directly proportional to $\lambda\bar{\alpha}_{1S}$, in Greenberg's formulation the constant part of the lift depends on the Theodorsen function and is proportional to $0.5\lambda\bar{\alpha}_{1S}[1 + F(k_V) - 0.5k_V G(k_V)]$, see Eq. 2.63. Therefore, the final value for high reduced frequencies is only 0.75 of that of Isaacs theory. Thus the constant part of lift response is significantly underpredicted by Greenberg's theory. Even the case of small reduced frequency ($k_V = 0.0424$) and a moderate flow oscillation amplitude of ($\lambda = 0.4$) reveals large differences, and it seems that the assumption made for the wake in Greenberg's derivation is not justified. Greenberg's theory leads to good agreement with Isaacs' theory only for small and medium freestream amplitudes and small reduced frequencies.

Looking to the dynamic parts of the lift response, the most significant differences can be seen in the $1/rev$-part. Here, for reduced frequencies greater

than about 0.15, the phase lags are overpredicted and the final values for high reduced frequency are smaller in the sine-components. Good agreement can be found in the second and third harmonics, but there is no higher harmonic lift response calculated by Greenberg's formulas. this is in contrast to Isaacs results as shown before.

3.2.4 Lift Transfer Function for Cosine Pitch Oscillations

It is interesting to examine how the lift transfer function of Greenberg's theory behaves for the case of out of phase pitch motion, say $\bar{\alpha}_{1C} = 1$, for which all other amplitudes are zero. The lift development is shown in Fig. 3.16 for a reduced frequency of $k_V = 0.05$ and 0.2. It can be seen that the overall agreement with Isaacs' theory is good for this case, and the lift overshoot in the decellerating flow region is also predicted by Greenberg's theory in the correct trend, but not in magnitude. The lift is slightly overpredicted at the begining of the period for high flow oscillation amplitudes ($0 < \omega_V t < 90^o$).

The transfer function for this case is given in Fig. 3.17 and Fig. 3.18 for the constant and dynamic part, respectively. The biggest differences are to be found in the constant part, which is proportional to $-0.5\lambda\bar{\alpha}_{1C}[G(k_V) + 0.5F(k_V)k_V]$ in Greenberg's formulation, while Isaacs only gives a linear proportionality to $-\lambda k_V\bar{\alpha}_{1C}/4$. However, for helicopter rotors the interesting range of reduced frequencies in freestream oscillations (right half of Fig. 3.17) is smaller. In this range the magnitude of the constant part of lift response is small and the differences might not be as severe compared to the harmonic content in Fig. 3.18. Indeed, rather good agreement is found especially in

the second and third harmonic. Only for the first harmonic the phase lag is overpredicted for small reduced frequencies with increasing flow amplitude, and the final values for high reduced frequencies are not the same for both theories. Again, Greenberg's theory does not give higher harmonics than the third, so all harmonic content of the lift response beyond that is missing.

Overall, Greenberg's theory appears useful as long as only small reduced frequencies and small to medium flow oscillation amplitudes are concerned. In the helicopter case, where mainly a sinusoidally change in angle of attack is introduced by control inputs, Greenberg's theory leads to erraneous results. That is the lift in the high velocity region is significantly underpredicted, and in the low velocity range it leads to a smaller lift loss than predicted by Isaacs' exact theory.

3.3 Kottapalli's Theory

3.3.1 Lift Transfer Function for Constant Pitch

An example for the lift development predicted by Kottapalli's theory is shown in Fig. 3.19 for reduced frequencies of $k_V = 0.05$ and 0.2, and a constant angle of attack. This also demonstrates the limits in applicability to helicopter problems. It can be seen that the agreement with Isaacs' theory is good only for very small freestream amplitudes; for higher amplitudes the theory is invalid. In Kottapalli's theory, the lift is only described by a $1/rev$ component, and therefore the lift coefficient shows a somewhat strange behavior for values of λ beyond the permitted limits. The constant part of the lift is only proportional to $\bar{\alpha}_0$, and therefore is constant. The dynamic content

of the circulatory lift is proportional to $\lambda\bar{\alpha}_0 G(k_V)$ in the cosine part and $\lambda\bar{\alpha}_0[1 + F(k_V)]$ in the sine part (see Eq. 2.67). Therefore, this is identical to the expression of Greenberg for the $1/rev$ in Eq. 2.63 and the transfer function is not shown here; the differences are the same as can be seen in Fig. 3.12. Of course, here no $2/rev$ part is included.

3.3.2 Lift Transfer Function for Sinusoidal Pitch Oscillations

The lift development for harmonic in-phase motion of the angle of attack is shown in Fig. 3.20. Here, much better agreement is found between Kottapalli's and Isaacs' theory in the range of flow oscillation amplitudes up to $\lambda = 0.2$. It can be seen that the additional lift loss in the small velocity region is overpredicted by Kottapalli's theory, but the lift in the high velocity region is underpredicted with increasing λ. The mean value, however, is the same as for Isaacs' theory, since it is proportional to $\lambda\bar{\alpha}_{1S}$ and does not depend on the reduced frequency (unlike Greenberg's result). From these results, again, the observation can be made that Kottapalli's theory is useful only for small values of λ.

From the formulas of Kottapalli, see Eq. 2.67, one can see immediately that the $1/rev$ response due to $\bar{\alpha}_{1S}$ is not a function of λ, and therefore cannot predict the amplitude and phase correctly. This becomes obvious in the transfer function of the dynamic parts of lift response, see Fig. 3.21. For all values of λ, the $1/rev$ remains the same, leading to larger phase lags and to smaller lift amplitudes for higher flow oscillation amplitudes. The $2/rev$ part, however, shows good agreement with Isaacs' theory, but all harmonics

beyond the $2/rev$ are missing in Kottapalli's theory, leading to erroneous results for $\lambda > 0.2$ in this case.

3.3.3 Lift Transfer Function for Cosine Pitch Oscillations

Now only $\bar{\alpha}_{1C}$ is considered, and the results arecompared to Isaacs' theory again. For the lift development at $k_V = 0.05$ and 0.2, as shown in Fig. 3.22, the differences between the two theories are small up to values of $\lambda = 0.4$. For higher amplitudes, the lift is increasingly underpredicted in the region of high velocity while it is overpredicted in the smaller velocity region. The differences between the two theories are more obvious in the lift transfer function (Fig. 3.23. The constant part is proportional to $-\lambda k_V \bar{\alpha}_{1C}/4$, and therefore is identical to Isaacs' (as for in the case of sine motion).

The dynamic parts of the lift response are given in Fig. 3.23. As for the case of a sinusoidally varying angle of attack, the $1/rev$-part predicted by Kottapalli's theory is independent of λ, and therefore is only valid for small flow oscillation amplitudes. Again, the $2/rev$-part is in fairly good agreement, and all higher harmonics were omitted by Kottapalli thus restricting the applicability of his theory to small values of λ.

Overall, Kottapalli's theory seems to be of limited use for a helicopter analysis in forward flight; only in hover for aeroelastic analyses it will be of any value and can be viewed as an alternative to Greenberg's theory. The correct representation of the mean value of lift in Kottapalli's theory (in contrast to Greenberg's theory) makes this theory an interesting alternative, and obviously more correct, for these cases.

3.4 Arbitrary Motion Theory in an Unsteady Freestream

3.4.1 Lift Transfer Function for Constant Pitch, Analytic Approach

As a comparison, the case of constant angle of attack in an oscillating freestream will be investigated. This case is shown in Fig. 3.24 and compared to the exact theory of Isaacs. It is easy to see that the results derived in this section are not identical to Isaacs' theory; it is only for $\lambda = 0$. With increasing freestream oscillation amplitudes, the differences become larger and the lift deficiencies are not plausible. Thus, the derivation includes a systematic error although exactly the same formulation works well in a constant freestream.

The fact that there are only the first two harmonics considered in the Theodorsen function leads to an interesting experiment. Although in the derived formulas Bessel functions are involved, they seem to be related to the results of Greenberg. The experiment now is to replace s in the upper boundary of the integral for the lift by its mean value $\bar{s}$, and therefore immediately one eliminates the Bessel functions. Mathematically this means the distance travelled by the airfoil does not depend on the flow oscillation amplitude, or that the flow oscillation amplitude is zero. Consideration of the distance travelled, s, gives

$$s = \bar{s} - \frac{\lambda}{k_V} \cos k_V \bar{s} \tag{3.3}$$

and it is clear that for very small λ this equation reduces to $s = \bar{s}$. The result is surprisingly exactly the same as that of Greenberg's derivation in Eq. 2.63,

but obtained with a different method. However, here an the approximation to the Wagner function is involved, and so there are small differences between the exact values for $C(k_V)$ and $\hat{C}(k_V)$. A figure is not included for this case, because the result of the analytical derivation with $s = \bar{s}$ is almost the same, as can be seen in Figs. 3.10 to 3.18. Very small differences are due to the fact, that the Theodorsen function now is represented by the approximation to the Wagner function. This result leads to the following observation:

Greenberg's high frequency assumption for the wake integral really means a small amplitude approximation for the flow oscillation amplitude λ for parts of the derivation (not all parts since there are other terms with λ^2 retained). This clarifies why Greenberg's theory works not as well for medium and high freestream amplitudes and places certain restrictions to the application of this theory, since in the helicopter case the assumption of small λ is not applicable.

A possibility for the afore mentioned systematic error when deriving an analytic solution for the periodic motion may be an incorrect solution for the derivative $\partial w_{3/4}(\sigma)/\partial\sigma$. In the integral of Eq. 2.69, σ is a dummy variable for s and since in steady flow conditions $s = \bar{s}$ there also $\sigma = \bar{\sigma}$ is valid (in steady flow the actual distance travelled is identical to the mean distance travelled). Now the normal velocity $w_{3/4}$ is only a function of $\bar{s}$, not of s, as can be seen from Eq. 2.71. With σ being the dummy variable of s, say $\sigma = \bar{\sigma} - (\lambda/k_V)\cos k_V\bar{\sigma}$, therefore $\partial\sigma = [1 + \lambda \sin k_V\bar{\sigma}]\partial\bar{\sigma}$. Thus, the derivative may be written as

$$\frac{\partial w_{3/4}(\bar{\sigma})}{\partial\sigma} = \left(\frac{1}{1 + \lambda \sin k_V\bar{\sigma}}\right) \frac{\partial w_{3/4}(\bar{\sigma})}{\partial\bar{\sigma}} \tag{3.4}$$

and the variable of integration is $\bar{\sigma}$. So the integral may more correctly be written as

$$\int_0^s \left(\frac{1}{1+\lambda \sin k_V \bar{\sigma}}\right) \frac{\partial w_{3/4}(\bar{\sigma})}{\partial \bar{\sigma}} \phi(s-\sigma) d\bar{\sigma} \qquad |\lambda| < 1 \qquad (3.5)$$

The fraction $1/(1+\lambda \sin k_V \bar{\sigma})$ is periodic, and in general can be expressed in form of an infinite Fourier series whose coefficients, because of the trigonometric function, will consist of Bessel functions with nk_V as the argument. From this, as in Isaacs' theory, an infinite series over all multiples of the reduced frequency will be introduced, in addition to that over all multiples of the freestream oscillation amplitude. However, a Fourier series expansion of this fraction could not be found in the mathematical literature and therefore it is not possible to give the proof of the correctness of this assumption here. This will be a subject of future research. However, it seems to be the right step in order to obtain an analytical result close to the derivation of Isaacs.

3.4.2 Lift Transfer Function for Constant Pitch, Finite Difference Approach

To perform the calculation, the numerical algorithm of arbitrary motion theory requires several cycles in order to eliminate all transients. The number of cycles has been set to 10, and it was found that this is enough for all the reduced frequencies investigated here. In the case of constant angle of attack, the results obtained by Isaacs Eq. 2.28 and the arbitrary motion theory are almost identical, so there is no result presented here; the form of the lift response was already shown in Fig. 3.1. Small differences are due to the approximation of the Wagner function by a truncated exponential series. For the same reason the constant part of the lift transfer function is not shown

here. There excellent agreement was found for all reduced frequencies (up to $k_V = 2.0$ as plotted in Fig. 3.2) and all values of λ. The dynamic part of the lift transfer function is given in Fig. 3.25. It can be seen in Fig. 3.25, that for all harmonics we find nearly perfect agreement with the exact theory of Isaacs, with certain small differences, which are mainly related to the use of an approximation to the Theodorsen function instead of using the Bessel functions.

This result can be used as proof that:

The arbitrary motion theory is able to calculate the aerodynamic loads for a constant angle of attack in an unsteady flow environment to a precision that is dependant only on the accuracy of the approximation made for the Wagner function.

3.4.3 Lift Transfer Function for Sinusoidal Pitch Oscillations

In addition to the case of constant angle of attack, the case of pure sinusoidally motion is presented in Fig. 3.26 for the lift development at two reduced frequencies, $k_V = 0.05$ and 0.2. It can be seen that the arbitrary motion theory represents the unsteady lift behavior in an almost perfect manner. The only differences to be seen are at higher reduced frequencies, where the magnitude of lift is slightly underpredicted. Also, the behavior of the lift coefficient in the region of smallest velocity is correct in the trend, but not completely correct in magnitude.

In Fig. 3.27 and Fig. 3.28, the lift transfer function for this case is given for the constant and dynamic part of the lift transfer functions, respectively.

From the constant part of the transfer function, it can be seen that the arbitrary motion theory leads to an underprediction of lift with increasing reduced frequency, but in the range of k_V encountered of a rotor blade the differences are not as severe. However, this behavior of the arbitrary motion theory cannot be explained with the approximation of the Wagner function. To clarify this behavior, additional research is necessary.

The dynamic parts of the lift transfer function (Fig. 3.28) show differences in the $1/rev$ component for $k_V > 0.2$. These differences are increasing with increasing freestream amplitude. All other harmonics are in excellent agreement with Isaacs' theory and differences are mainly related to the approximation of the Wagner function by a truncated series of exponential functions.

3.4.4 Lift Transfer Function for Cosine Pitch Oscillations

For pure cosine motion, the results are presented in Fig. 3.29. No significant differences can be seen in the lift development for either reduced frequencies. This excellent agreement can also be found in the lift transfer function, see Fig. 3.30 for the constant part and Fig. 3.31 for the dynamic part. In all these cases, it can be seen that the arbitrary motion theory produces results almost identical to the exact theory of Isaacs. The small differences remaining can be explained by the inaccuracy of the approximation made to the Wagner function by a finite number of exponential functions instead of an infinite number as required to make $C(k) = \hat{C}(k)$.

In general, the results obtained for constant, as well as for oscillating,

angle of attack show excellent agreement with Isaacs' theory. This is the proof that

> *The arbitrary motion theory is able to calculate the unsteady aerodynamic loads, even in an unsteady freestream flow environment, if all the appropriate deficiency functions involved are retained.*

However, it must be kept in mind that the excellent agreement is found only in the case of a constant and oscillating angle of attack 90° out-of-phase. In the in-phase (sinusoidal pitch) motion the constant part of circulatory lift and the $1/rev$-part show some differences that can not be explained with the approximation to the Wagner function alone.

3.4.5 Reduced Algorithm

Very often, because of computational effort, only a reduced algorithm can be applied. This means a reduction in the number of deficiency functions involved, and the functions regularly neglected are those related to the changes in velocity. Then the velocity at 3/4 chord is simply

$$w_{3/4,n} = \sum_{i=0}^{n} \left[V_i \Delta\alpha_i + \frac{c}{2} \left(\frac{1-2a}{2} \right) \Delta\dot{\alpha}_i + \Delta\dot{h}_i \right] - \sum_{j=1}^{3} \sum_{k=2}^{N} X_{n,k}^{(j)} \qquad (3.6)$$

Herein $\Delta V_i \alpha_i$ is eliminated, and the philosophy behind this step is that the changes in flow oscillation are assumed to be of relatively low frequency in relation to that of plunge or pitch motion. This is a quasisteady assumption made only for the velocity (and thereby for the fore-aft motion) while all other degrees of freedom are considered as unsteady.

The results for constant angle of attack case are not shown, since it is easy to see from the equations that in this case the quasisteady theory is exactly reproduced. Therefore, the reduced algorithm is not able to calculate the characteristic lift overshoot where the velocity is lowest. More interesting, is the case of sinusoidally varying angle of attack, for in-phase and 90^o out-of-phase motion relative to the velocity oscillation. The results for reduced frequencies of $k_V = 0.05$ and 0.2 are given in Fig. 3.32 and Fig. 3.33, respectively. For the in-phase motion, good agreement with the exact theory is apparent only for the total lift, while the lift coefficent is inaccurately predicted over larger parts in the second half of the period, especially for high flow oscillation amplitudes. However, this is hard to see in the lift itself because the dynamic pressure is very small over most of this range. Similar agreement was found for the cosine motion of angle of attack. The lift is slightly overpredicted nearly over the entire period, and the characteristic lift coefficient overshoot in the second half is not predicted by the reduced algorithm. Therefore the following statement can be made:

The reduced algorithm of arbitrary motion theory, assuming the oscillations in velocity to be quasisteady, is not appropriate for calculating lift coefficients when the flow oscillation amplitude exceeds the value of $\lambda \approx 0.2$.

It must be noted that the reduced algorithm can also be applied to the analytic derivation, omitting the derivative $\partial V(\sigma)/\partial\sigma$. The approach of handling the freestream oscillation in a quasisteady manner was also used in the combination of Theodorsen's theory with unsteady freestream. Therefore, a relation must exist between Theodorsen's theory and the reduced algorithm of arbitrary motion theory. By the same procedure that was

done with the full algorithm in the analytic approach by setting $s = \bar{s}$ instead of $s = \bar{s} - (\lambda/k_V)\cos k_V \bar{s}$, this relation is obtained. Then one gets a result identical to Theodorsen, see Eq. 2.21, only that the Theodorsen function $C(k_V) = F(k_V) + iG(k_V)$ is replaced by its approximation $\hat{C}(k_V) = \hat{F}(k_V) + i\hat{G}(k_V)$ where the real and imaginary part are built up from the coefficients of the exponential series approximation to the Wagner function. Additional results are not shown for this case; the accuracy of the approximation is as good as in the comparison with Greenberg's theory using the full algorithm and the same substitution.

3.5 Influence of the Position of Pitch Axis

Until now only a pitch motion about the midchord has been investigated. Normally, for a helicopter rotor this is not the case because the feathering axis is very close to the aerodynamic center. In incompressible flow, this is the quarter chord point, and helicopter manufacturers take a great effort to bring the elastic axis (as well as the center of gravity) and the feathering axis to the 1/4 chord point. The derivation in Appendix B gives the influence of pitch axis on lift development, which was not given by the theory of Isaacs. Therefore, since also Greenberg's, Kottapalli's and the combination of Theodorsen's theory with unsteady freestream include this parameter, its influence can now be studied and compared. As could be seen in Theodorsen's theory in a constant freestream (see Fig. 2.3 and Fig. 2.4), the pitch axis position (represented by the parameter a) has a significant influence on the lift transfer function.

In general, if $a = 0.5$, then the axis of rotation is at 3/4 chord, where in

incompressible flow the reference point for the normal velocity is considered. In that case, $\dot{\alpha}$ does not contribute to the circulatory lift. This is expressed by the factor $(1-2a)/2$ in Eq. 2.51 and Eq. 2.53. In the following figures, this parameter is first set to $a = 0.5$ (pitch axis at 3/4 chord), and then to $a = -0.5$ which is the helicopter case, where the pitch axis is at quarter chord. Generally a does not appear in the constant part of the lift transfer function, and so that part is not shown here. Only the dynamic parts are affected.

3.5.1 Effect of a on the Lift Transfer Function for $\bar{\alpha}_{1S}$

The first case of $a = 0.5$ is shown in Fig. 3.34, and it is compared with results for $a = -0.5$ in Fig. 3.35. Because the multiplier at the $\dot{\alpha}$-term is $(1-2a)/2 = 0$ in the first case, this eliminates the terms proportional to the reduced frequency, and therefore the transfer functions of the different harmonics do not asymptote to infinity. They results basically follow the Theodorsen function, with different scalings. This is for all except the $4th$ harmonic, which is built up only from the Bessel functions. However, since the coefficients H'_n and H_n in Appendix B depend on a, the $4/rev$-part changes its shape slightly. In addition to the result of Isaacs, the result of Greenberg's, Kottapalli's and the combination of Theodorsen's theory with unsteady freestream are plotted in Fig. 3.34 ($a = 0.5$) and Fig. 3.35 ($a = -0.5$). All of these results show the same behavior, and have good agreement in the second and third harmonic. The main differences are in the first harmonic, and are more significant than in the case of $a = 0$.

In order to make a direct comparison, the scaling is kept the same in

Fig. 3.34 and Fig. 3.35. So for $a = -0.5$ the multiplier becomes $(1-2a)/2 = 1$. This is very important now, because it leads to infinite amplification of the lift, as can be seen in Fig. 3.35 for the first and second harmonic where this factor appears. It is interesting to note that in all of Greenberg's, Kottapalli's and Theodorsen's theory, the third harmonic is independent of a, while in Isaacs' theory a appears in the sum over all reduced frequencies in every harmonic, and therefore changes the lift transfer function in every harmonic. This can be seen in the maximum value (cosine part) and in its final value for high reduced frequency. The differences between the other theories become more apparent in the $2/rev$ and remain in the $1/rev$.

3.5.2 Effect of a on the Lift Transfer Function for $\bar{\alpha}_{1C}$

Again, this is demonstrated for $a = 0.5$ in Fig. 3.36 and for $a = -0.5$ in Fig. 3.37. Basically we find the same behavior and changes that were observed in case of the sinusoidal motion. Especially noteworthy is the large difference between Isaacs' theory and the other theories in the $1/rev$ component, where Greenberg's and Theodorsen's theory predict much larger phase lags. The $2/rev$-parts are in good agreement, while in the $3/rev$-parts of Greenberg's, Kottapalli's and Theodorsen's theory do not show any dependency on a. However, this is the case in Isaacs' theory, and leads to a change in amplification of the lift and in the final values for high reduced frequencies.

Over all, the parameter a leads to important changes in the $1/rev$ and $2/rev$ components of the lift response, while in steady flow only the $1/rev$ is influenced. For the $3/rev$ and all higher harmonics, only Isaacs' theory is able to show a dependency on the pitch axis location. However the differences

obtained by changing from a pitch axis at midchord to one at quarter chord are not severe even there.

Chapter 4

Summary and Conclusions

In this study five theories handling the effect of unsteady freestream have been analysed. These are:

- Isaacs' theory
- Greenberg's theory
- Theodorsen's theory combined with unsteady freestream
- Kottapalli's theory
- Arbitrary motion theory

It was found, that *all* of these theories handle the case of a fore-aft moving airfoil instead of an unsteady freestream. This latter case should be more correcly viewed as a system of horizontally propagating gusts. A helicopter rotor blade section in forward flight encounters both unsteady freestream (the superposistion of rotation and forward flight velocity components) and fore-aft motion (through lead-lag). It was found, that both phenomena are physically different, but in the range of reduced frequencies encountered by

a helicopter blade the results will be very similar. Thus, the interpretation of unsteady freestream as an equivalent to fore-aft motion can be viewed as a good approximation in the helicopter case.

All of the theories cited above lead to the same noncirculatory expressions, and all of them reduce to Theodorsen's theory when the freestream oscillation amplitude becomes zero. The general effect of an oscillating freestream is a "stretching and compressing" of the shed wake vorticity behind the airfoil.

From the analysis and comparisons of Chapter 2 and 3 the following conclusions can be made:

1. Isaacs' Theory:

   This is the only theory for the case of an unsteady freestream that gives an analytic solution without additional simplifications, and therefore can be seen as the only "exact theory". The lift for oscillating freestream flow conditions is represented as an infinite Fourier series. The induced phase lags and amplifications depend on the type of motion of the airfoil. Therefore, at constant angle of attack there is a significant lift coefficient overshoot, where the velocity is smallest, but in case of sinusoidally varying angle of attack (in-phase motion) an additional lift deficiency occurs. A cosine motion (90^o out-of-phase) also leads to lift coefficient overshoots, but they are not as significant as in the case of constant angle of attack.

2. Greenberg's Theory:

   This theory is similar to Theodorsen's theory, but includes the unsteady freestream as additional degree of freedom and the result for the lift

contains up to three harmonics. To obtain a simple closed form solution, an additional simplification to the form of the wake was made. That was that an infinite frequency assumption makes the wake vorticity sinusoidal again. It was shown with an analytical derivation via arbitrary motion theory, that this is equivalent to neglecting the flow oscillation amplitude for the induced velocities. Therefore Greenberg's high frequency assumption physically is an assumption of quasisteady convection velocity for the shed wake. This makes Greenberg's theory questionable for high freestream oscillation amplitudes, and it was found that the differences with the exact theory of Isaacs are significant above $\lambda \approx 0.4$. For constant or oscillating angle of attack the basic behavior was correctly represented, but the magnitudes and phase angles were not well represented in the important constant and $1/rev$ parts of lift response.

3. Kottapalli's Theory:

   From the beginning, an assumption for small freestream amplitudes was made reducing this theory for the cases of aeroelastic investigations in hover, or very small forward flight conditions. The agreement with Isaacs' theory for that range of freestream oscillations was found to be slightly better than that of Greenberg's results. Because of the assumption made here, only up to the second harmonics describe the lift response.

4. Theodorsen's Theory Combined with Unsteady Freestream:

Here the changes in velocity are viewed as quasisteady and the Theodorsen function is only applied to angle of attack and plunge motion. The characteristic lift coefficient overshoots cannot be predicted by this method. It was proved that with an analytical derivation via arbitrary motion theory from the reduced algorithm (omitting the deficiency functions for the changes in velocity), that this is equivalent to neglecting the flow oscillation amplitude for the induced velocities.

5. Arbitrary Motion Theory:

   The finite difference approach using the superposition principle and Duhamel's integral leads nearly exatly to the same results as for Isaacs' theory, when the angle of attack is constant or oscillating 90^o out-of-phase. For sinusoidal angle of attack motion (in-phase) there are increasing differences with increasing reduced frequencies for the constant and $1/rev$-part of the lift response. In the range of reduced frequencies encountered by a rotor blade, this seems not to be a severe limitation. In all cases the dynamic lift response is represented correctly, depending on the approximation used for the Wagner function. This is proof that the arbitrary motion theory can accurately calculate the lift even in unsteady freestream conditions. The often used "reduced algorithm", considering the freestream variations as quasisteady, leads to good results for the lift, but the characteristic overshoots in the lift coefficient related to the compression of the shed wake vorticity (at the retreating side of the rotor), are not represented.

The conclusion is, that when the lift coefficient is the subject of investigation, Isaacs' theory or the arbitrary motion theory with all the appropriate

deficiency functions are necessary to calculate the correct lift coefficient overshoots or deficiencies. If the lift itself is the subject, then for small freestream amplitudes all theories are useful, for medium amplitudes Isaacs, Greenberg's and arbitrary motion theory are valid, and for high oscillation amplitudes Isaacs' or arbitrary motion theory with all deficiency functions are necessary to accurately calculate the lift response.

As an additional contribution to the analytical side of the problem, Isaacs' theory (that was derived for $1/rev$ oscillations in angle of attack only about midchord) has been generalized to the case of an infinite Fourier series in angle of attack about an arbitrary axis, including also an infinite Fourier series for plunge motion. As a recommendation for future research, this derivation can be used for a general unsteady aerodynamic theory, featuring infinite Fourier series in all types of motion (also fore-aft motion) and with different fundamental frequencies for pitch, plunge and freestream oscillations.

For the application of unsteady freestream aerodynamic theory to rotorcraft problems, the arbitrary motion theory appears to be the most promosing approach since the coefficients of the exponential series representing the Wagner function can be modified to represent compressibility effects. However, it is very difficult to justify whether the compressibility corrections of these coefficients, that have prooved to be correct in unsteady aerodynamics in a constant freestream, are also correct in an unsteady freestream. To validate this, experimental measurements in compressible flow are necessary. However to achieve high values of freestream oscillation amplitudes at the reduced frequencies of a rotor blade section seems to be an unsolvable problem for todays wind tunnels.

A final comment in this thesis must be made regarding the experimental aspect. Only very few experiments have been conducted to cases when unsteady freestream variations are involved, compared to the tremendous amount of experiments related to unsteady airfoil motion in pitch, and even in plunge, for example [19, 20]. Naturally the experimental setup is much more difficult, leading to very small mean velocities in order to achieve high velocity amplitudes. In all experimental data available [21] - [30], separated flow conditions even for small angle of attack occur due to very small Reynolds number, and therefore a direct comparison with experimental data cannot be made. A recommendation for future measurements must be the introduction of a means to keep the flow attached to the airfoil, and therefore to artificially prohibit laminar flow separation on the surface of the airfoil.

Bibliography

[1] Johnson, W., "Application of Unsteady Airfoil Theory to Rotary Wings," *Journal of Aircraft*, Vol. 17, No. 4, pp. 285-286, 1980

[2] Kaza, K. R. V., "Application of Unsteady Airfoil Theory to Rotary Wings," *Journal of Aircraft*, Vol. 18, No. 7, pp. 604-605, 1981

[3] Johnson, W., *Helicopter Theory*, Princeton University Press, 1980

[4] Theodorsen, T., "General Theory of Aerodynamic Instability and the Mechanism of Flutter," NACA Rep. No. 496, 1935

[5] Sears, W. R., "Operational Methods in the Theory of Airfoil in Non-Uniform Motion," *Journal of the Franklin Institute*, Vol. 230, No. 1, pp. 95-111, 1940

[6] Isaacs, R., "Airfoil Theory for Flows of Variable Velocity," *Journal of the Aeronautical Sciences*, Vol. 12, No. 1, pp. 113-117, 1945

[7] Isaacs, R., "Airfoil Theory for Rotary Wing Aircraft," *Journal of the Aeronautical Sciences*, Vol. 13, No. 4, pp. 218-220, 1946

[8] Greenberg, J. M., "Airfoil in Sinusoidal Motion in a Pulsating Stream," NACA TN No. 1326, 1946

[9] Diniavari, M. A. H., Friedmann, P. P., "Application of Time-Domain Unsteady Aerodynamics to Rotary-Wing Aeroelasticity," *AIAA Journal*, Vol. 24, No. 9, pp. 1424-1432, 1986

[10] Ashley, H., Dugundji, J., Neilson, D. O., "Two Methods for Predicting Air Loads on a Wing in Accelerated Motion," *Journal of the Aeronautical Sciences*, Vol. 19, No. 8, pp. 543-552, 1952

[11] Wagner, H., "Über die Entstehung des dynamischen Auftriebs von Tragflügeln," *Zeitschrift für angewandte Mathematik und Mechanik*, Band 5, pp. 17-35, 1925

[12] Drischler, J. A., Diederich, F. W., "Lift and Moment Responses to Penetration of Sharp-Edged Travelling Gusts, with Application to Penetration of Weak Blast Waves," NACA TN No. 3956, 1957

[13] Küssner, H. G., "Zusammenfassender Bericht über den instationären Auftrieb von Flügeln," *Luftfahrtforschung*, Band 13, Nr. 12, pp. 410-424, 1936

[14] Strand, T., "Angle of Attack Increase of an Airfoil in Decelerating Flow," *Journal of Aircraft*, Vol. 9, No. 7, pp. 506-507, 1972

[15] Kottapalli, S. B. R., *Drag on an Oscillating Airfoil in a Fluctuating Free Stream*, Ph.D. Thesis, Georgia Institute of Technology, 1977

[16] Kottapalli, S. B. R., Pierce, G. A., "Drag on an Oscillating Airfoil in a Fluctuating Free Stream," Transactions of the ASME, *Jounal of Fluids Engineering*, Vol. 101, No. 3, pp. 391-399, 1979

[17] Kottapalli, S. B. R., "Unsteady Aerodynamics of Oscillating Airfoils with Inplane Motions," *Journal of the American Helicopter Society*, Vol. 30, No. 1, pp. 62-63, 1985

[18] Ando, S., Ichikawa, A., "Effect of Forward Acceleration on Aerodynamic Characteristics of Wings," *AIAA Journal*, Vol. 17, No. 6, pp. 653-655, 1979

[19] Liiva, J., Davenport, F. J., Gray, L., Walton, I. C., "Two-Dimensional Tests of Airfoils Oscillating Near Stall," US-AAVLABS TR-68-13, 1968

[20] Dadone, L. U., "Two-Dimensional Wind Tunnel Test of an Oscillating Rotor Airfoil," NASA CR 2914 and 2915, 1977

[21] Saxena, L. S., Fejer, A. A., Morkovin, M. V., "Features of Unsteady Flow over Airfoils," AGARD-CP-227: *Proceedings of the AGARD-FDP Meeting of Unsteady Aerodynamics*, Ottawa, Ontario, Canada, 1977

[22] Fejer, A. A., "Visual Study of Oscillating Flow over a Stationary Airfoil," In: *Turbulence in Internal Flows: Turbomachinery and other Engineering Applications, Proceedings of the SQUID Workshop*, Washington, D. C., USA, 1977

[23] Fejer, A. A., Hajek, T. J., "A New Approach to Rotor Blade Stall Analyses," *4th European Rotorcraft and Powered Lift Aircraft Forum*, Stresa, Italy, 1978

[24] Saxena, L. S., Fejer, A. A., Morkovin, M. V., "Effects of Periodic Changes in Free Stream Velocity on Flows over Airfoils near Stall," In:

Nonsteady Fluid Dynamics: Proceedings of the Winter Annual Meeting, San Francisco, California, USA, 1978

[25] Pierce, G. A., Kunz, D. L., Malone, J. B., "The Effect of Varying Free-stream Velocity on Airfoil Dynamic Stall Characteristics," *32nd Annual Forum of the American Helicopter Society*, Washington, D. C., USA, 1976, also: *Journal of the American Helicopter Society*, Vol. 23, No. 2, pp. 27-33, 1978

[26] Maresca, C. A., Favier, D. J., Rebont, J. M., "Unsteady Aerodynamics of an Aerofoil at High Angle of Incidence Performing Various Linear Oscillations in a Uniform Stream," *5th European Rotorcraft and Powered Lift Aircraft Forum*, Amsterdam, Netherlands, 1979, also: *Journal of the American Helicopter Society*, Vol. 26, No. 2, pp. 40-45, 1981

[27] Maresca, C. A., Favier, D. J., Rebont, J. M., "Experiments on an Aerofoil at High Angle of Incidence in Longitudinal Oscillations," *Journal of Fluid Mechanics*, Vol. 92, No. 4, pp. 671-690, 1979

[28] Maresca, C. A., Favier, D. J., Rebont, J. M., "Large-Amplitude Fluctuations of Velocity and Incidence on an Oscillating Airfoil," *AIAA Journal*, Vol. 17, No. 11, pp. 1265-1267, 1979

[29] Maresca, C. A., Favier, D. J., Rebont, J. M., "Dynamic Stall due to Fluctuations of Velocity and Incidence," *AIAA Journal*, Vol. 20, No. 7, pp. 865-871, 1982

[30] Favier, D. J., Agnes, A., Barbi, C., Maresca, C. A., "Combined Translation/Pitch Motion: A New Airfoil Dynamic Stall Simulation," *Journal of Aircraft*, Vol. 25, No. 9, pp. 805-814, 1988

[31] Beddoes, T. S., "Practical Computation of Unsteady Lift," *5th European Rotorcraft an Powered Lift Aircraft Forum*, Aix-en-Provence, France, 1982

[32] Beddoes, T. S., "Representation of Airfoil Behaviour," *Vertica*, Vol. 7, No. 2, pp. 183-197, 1983

[33] Leishman, J. G., Beddoes, T. S., "A Generalised Model for Airfoil Unsteady Aerodynamic Behaviour and Dynamic Stall Using the Indicial Method," *42nd Annual Forum of the American Helicopter Society*, Washington, D. C., 1986

[34] Jones, R. T., "The Unsteady Lift of a Wing of Finite Aspect Ratio," NACA Rep. 681, 1940

[35] Peterson, L. D., Crawley, E. F., "Improved Exponential Time Series Approximation of Unsteady Aerodynamic Operators," *Journal of Aircraft*, Vol. 25, No. 2, pp. 121-127, 1988

[36] Eversmann, W. Tewari, A., "Modified Exponential Series Approximation for the Theodorsen Function," *Journal of Aircraft*, Vol. 28, No. 9, pp. 553-557, 1991

[37] Leishman, J. G., "Validation of Approximate Indicial Aerodynamic Functions for Two-Dimensional Subsonic Flow," *Journal of Aircraft*, Vol. 25, No. 10, 1988

[38] *Handbook of Tables for Mathematics*, 3rd Edition, The Chemical Rubber Co., Cleveland, Ohio, USA, 1967

[39] Nielsen, N. W., *Handbuch der Theorie der Cylinderfunktionen*, Teubner Verlag, Leipzig, 1904

[40] Jahnke, E., Emde, F., *Tables of Functions with Formulae and Curves*, Dover Publications, New York, 4th Ed., 1945

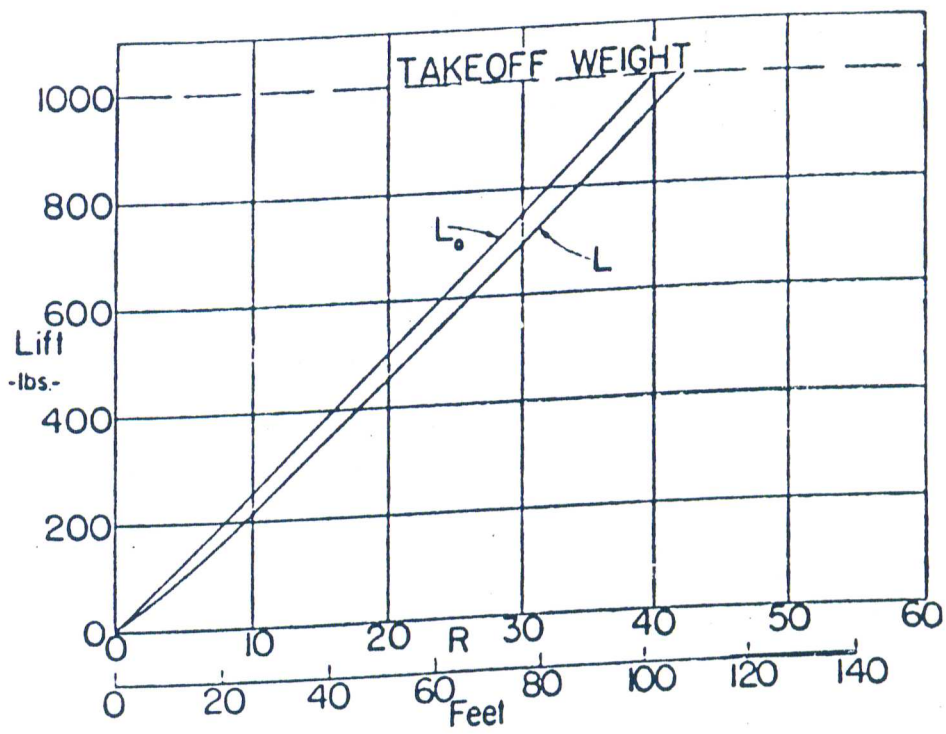

Figure 1.1: Actual and quasi-steady-state lift forces L and L_0 plotted vs. distance for Helioplane take-off in calm air. From [10].

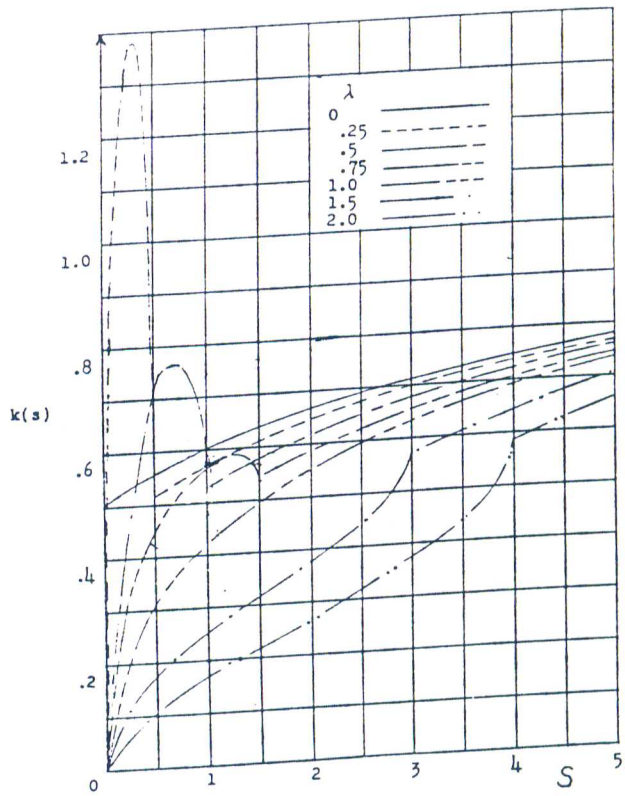

Figure 1.2: Indicial-lift functions for a wing in incompressible two-dimensional flow when penetrating travelling sharp-edged gusts for several values of the parameter $\lambda = V_{horiz.}/(V_{horiz.}+V_{vert.})$. From [12].

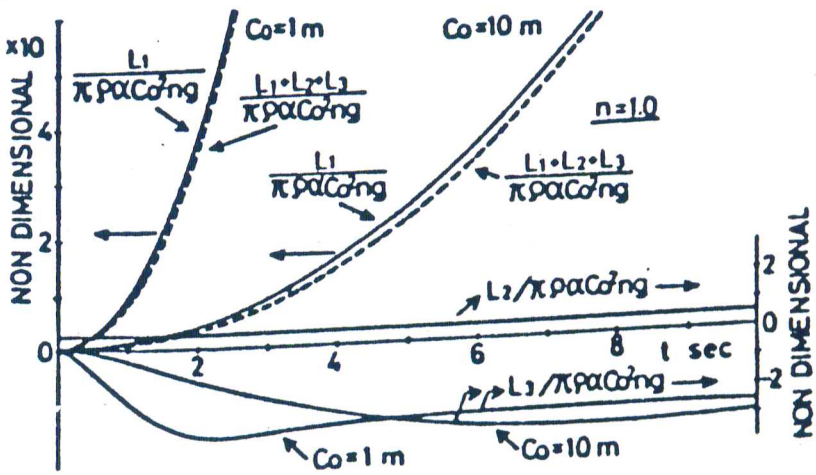

Figure 1.3: Lift of flat two-dimensional airfoils flying with constant acceleration from rest, calculations. From [18].

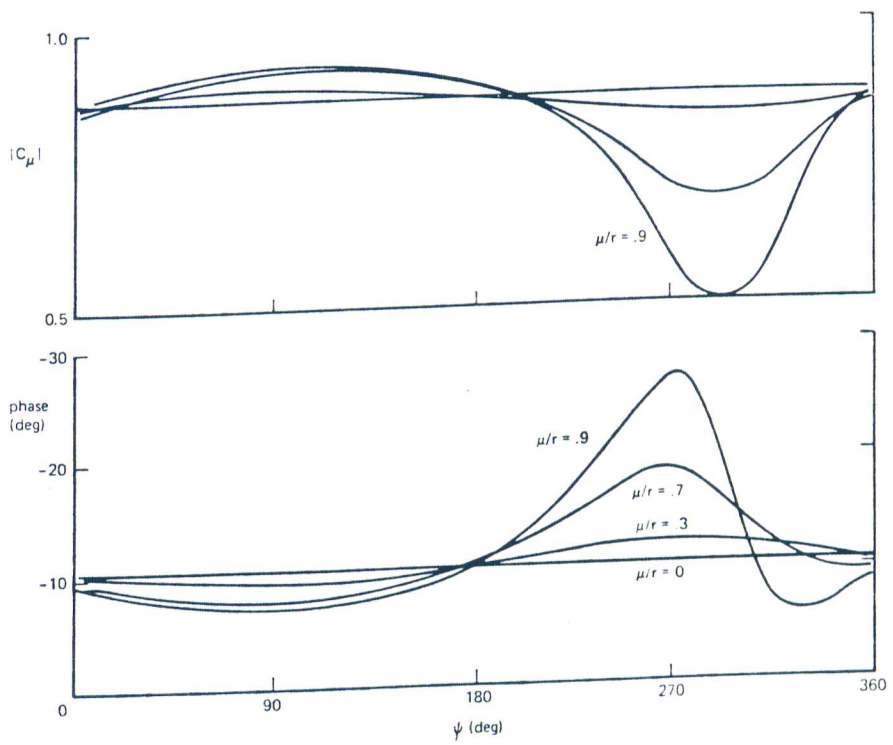

Figure 1.4: Lift deficiency function with a time-varying free stream, for the second harmonic ($n = 2$) and $k = 0.04$. From [3].

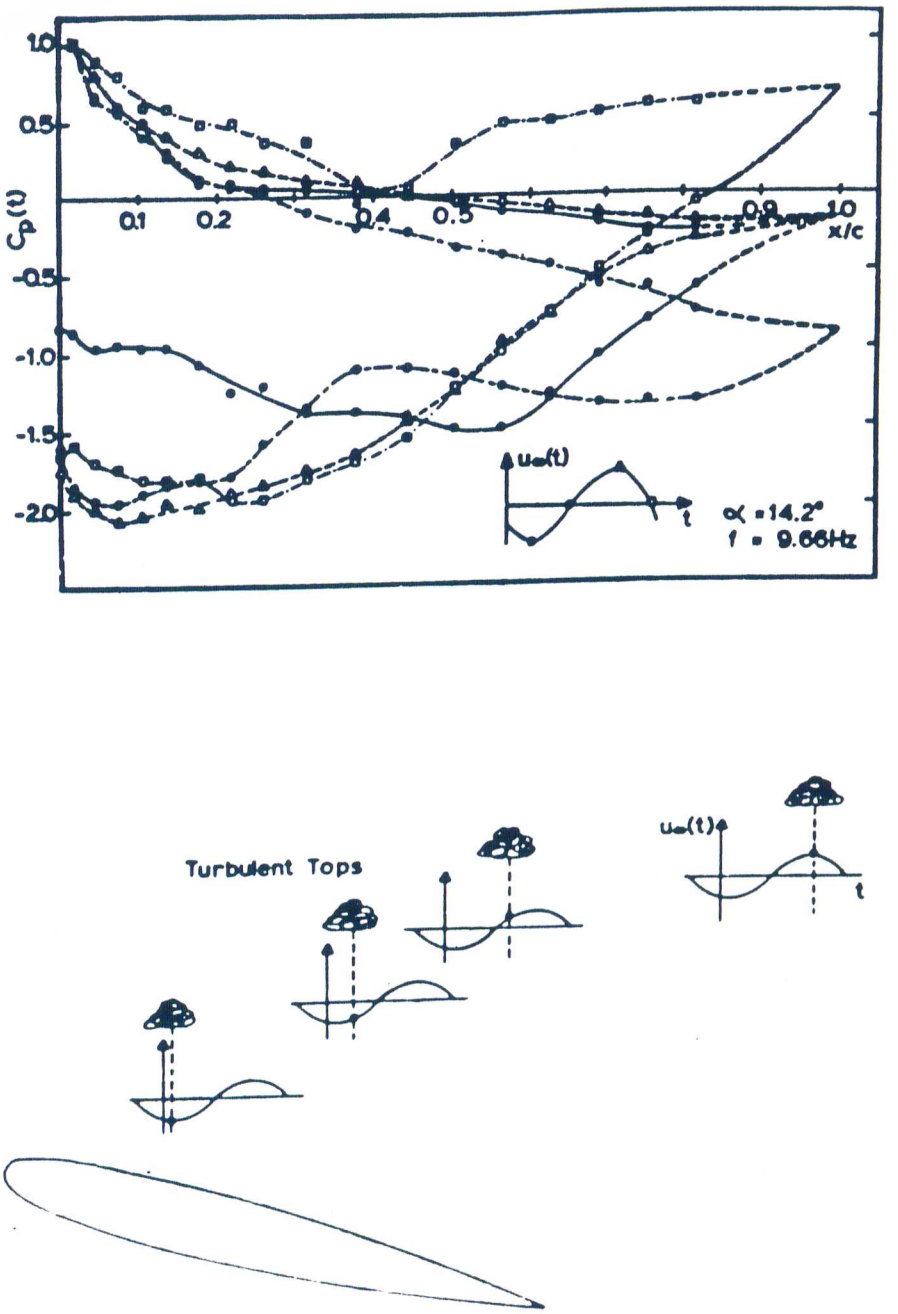

Figure 1.5: Pressure distribution and separated flow region at const. angle of attack. From [21].

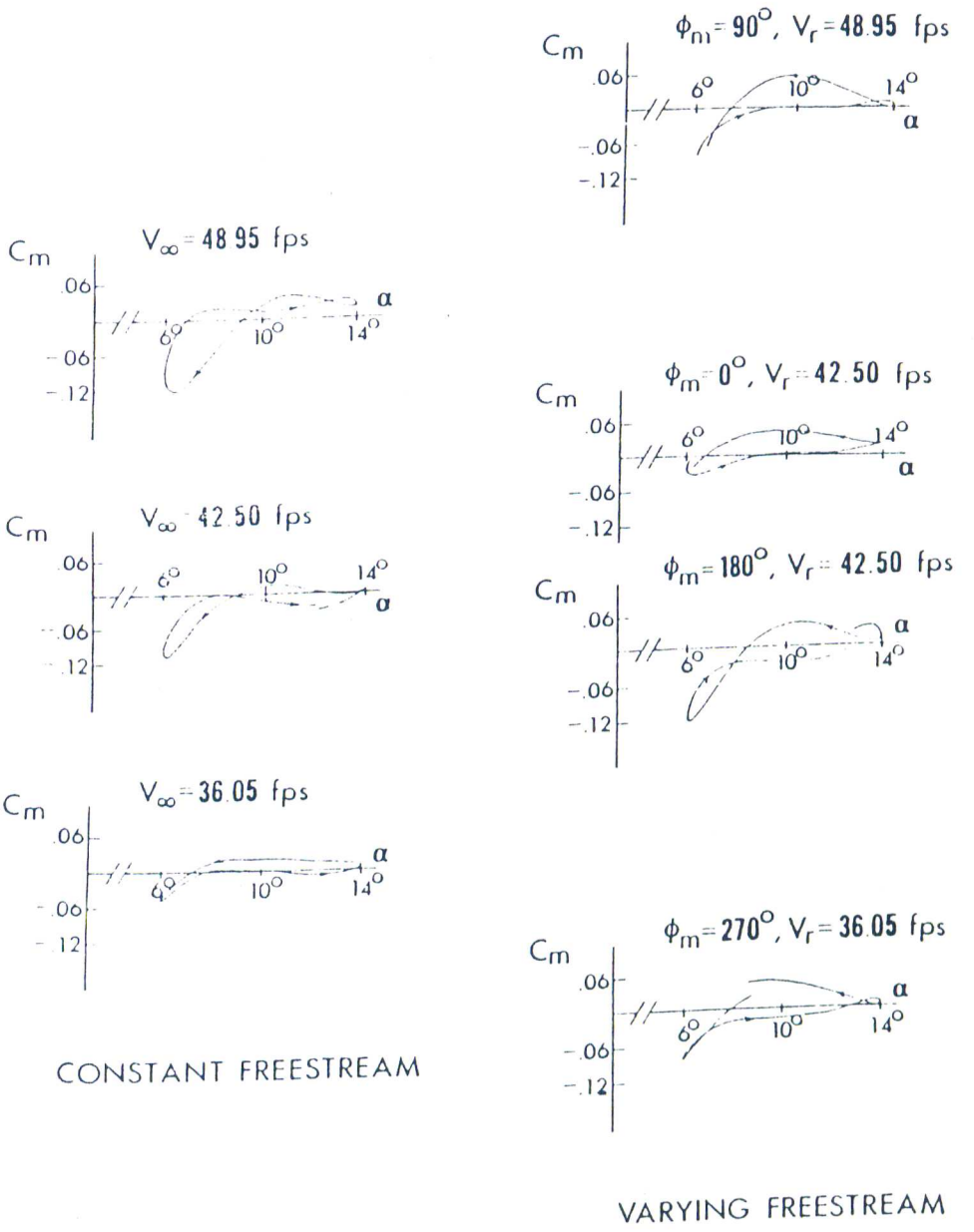

Figure 1.6: C_m vs. α for oscillations about 10^o at $6Hz$ in constant and $1Hz$ freestreams. From [25].

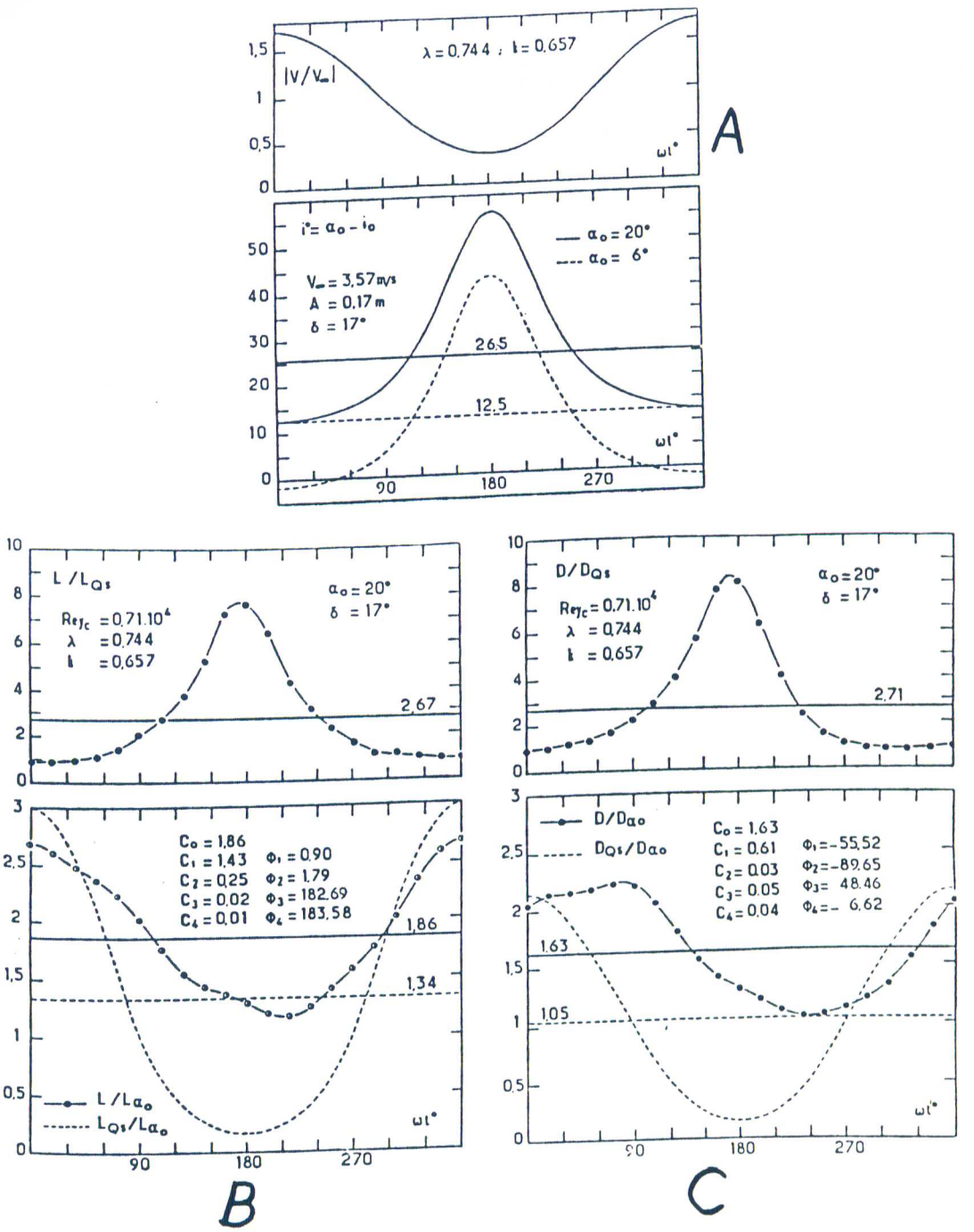

Figure 1.7: Variation of velocity and incidence with time in combined motion (A), Unsteady and quasi-steady lift in combined motion (B), Unsteady and quasisteady drag in combined motion (C). From [26].

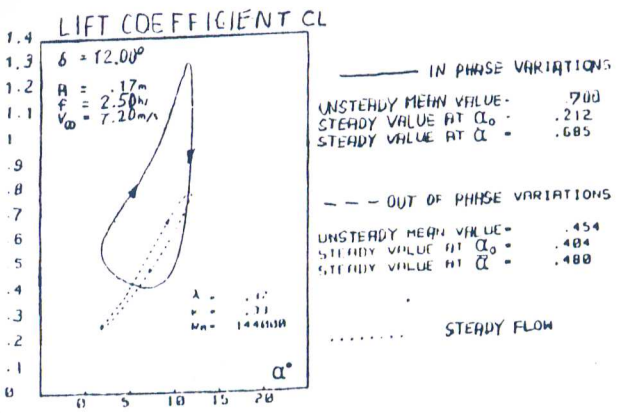

C_L variations below stall.

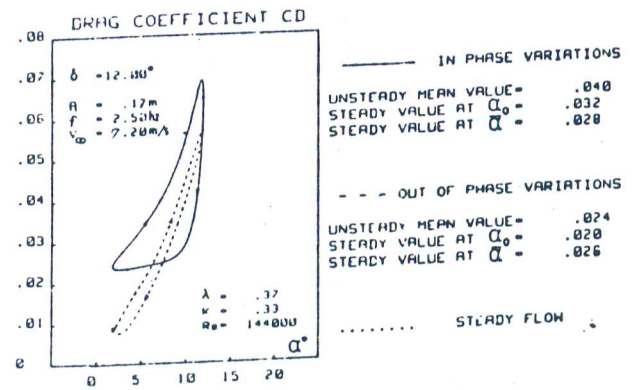

C_D variations below stall.

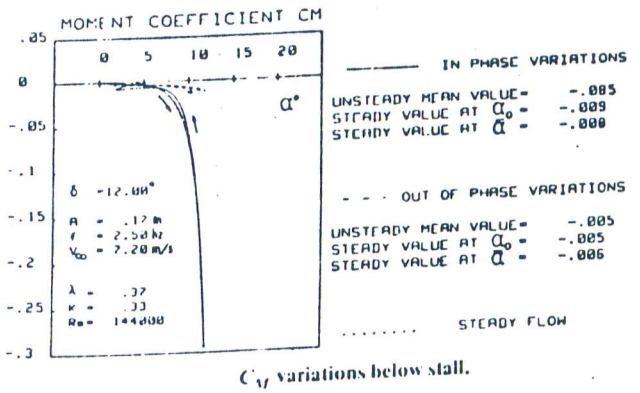

C_M variations below stall.

Figure 1.8: Results from [29]

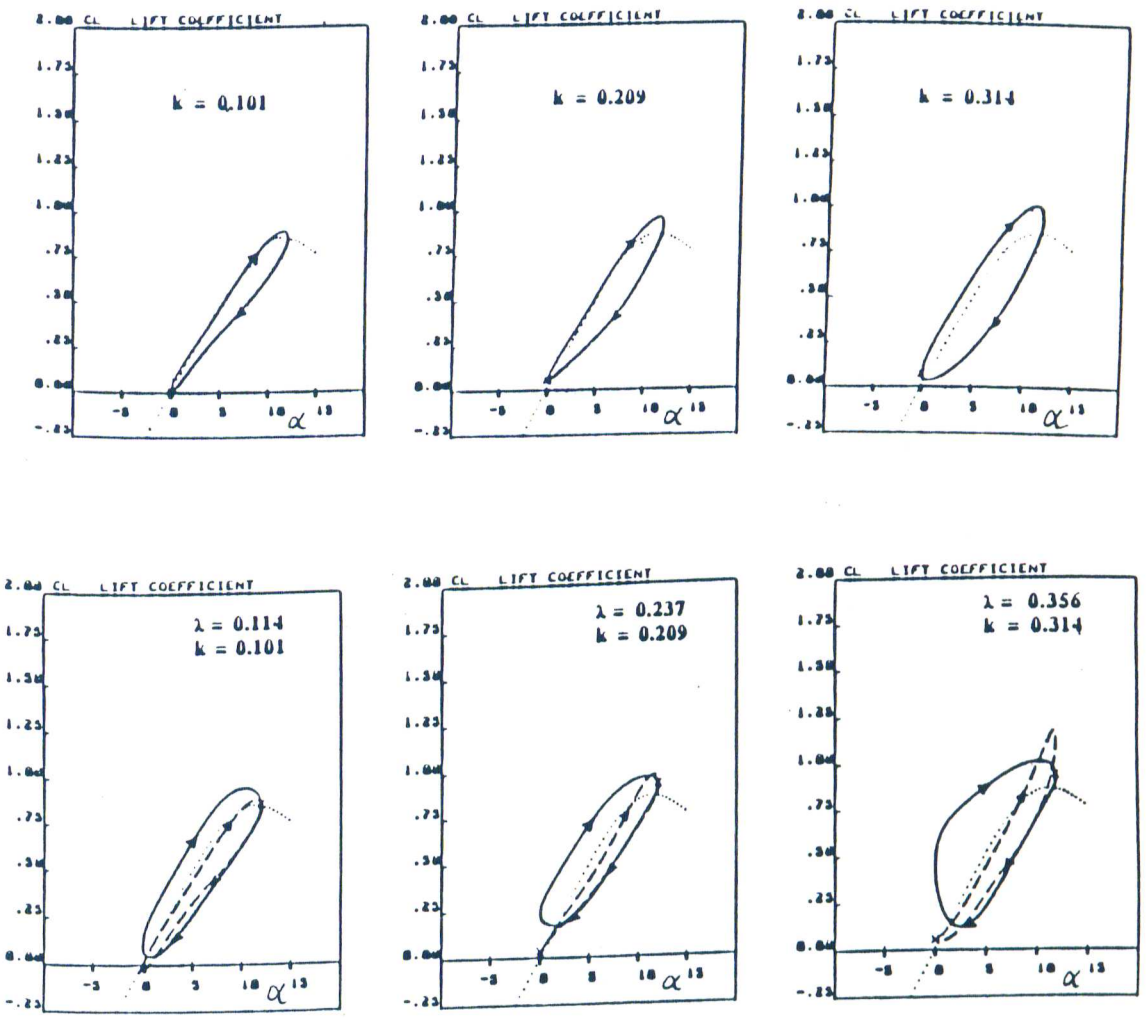

Figure 1.9: Lift coefficient C_L as a function of α for $\alpha_0 = 6^o$, $\Delta\alpha = 6^o$. Without inplane motion (top) and with inplane motion (bottom), $--\ \Phi = 0^o$, $--\ \Phi = 180^o$. From [30].

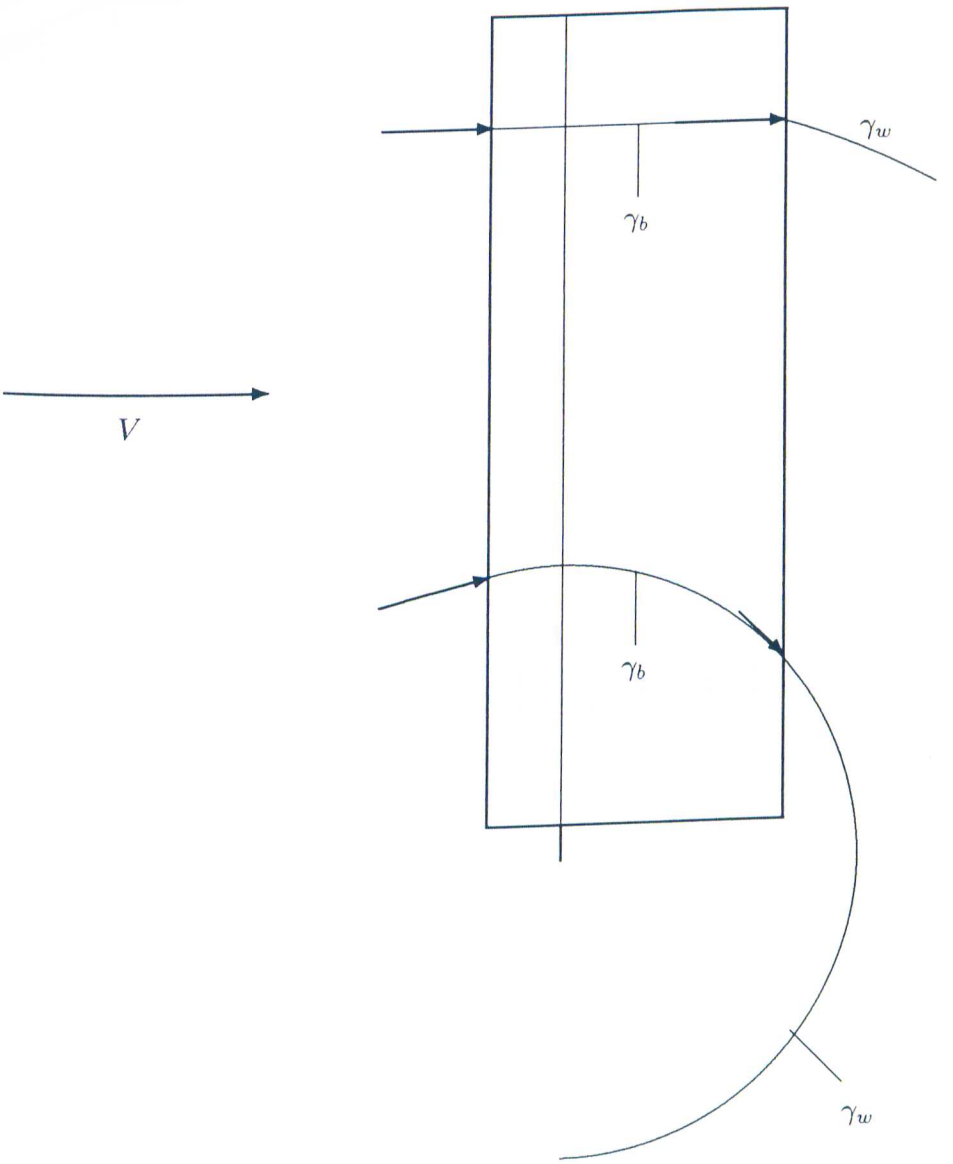

Figure 2.1: Flow environment of a rotating blade

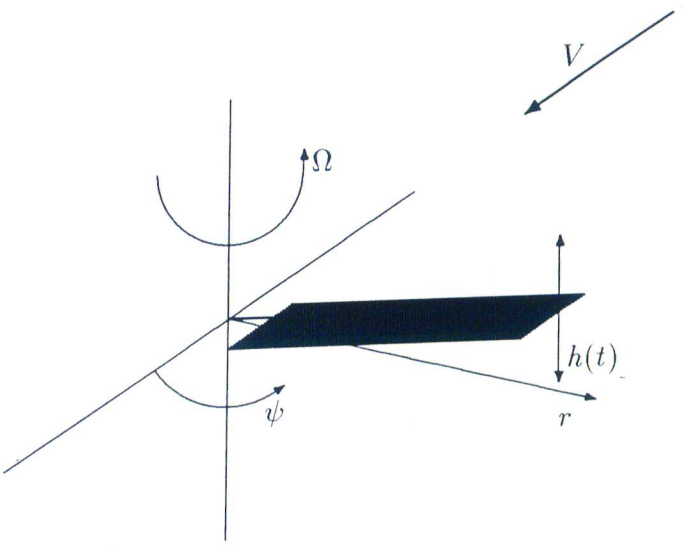

Figure 2.2: Flapping hinged blade

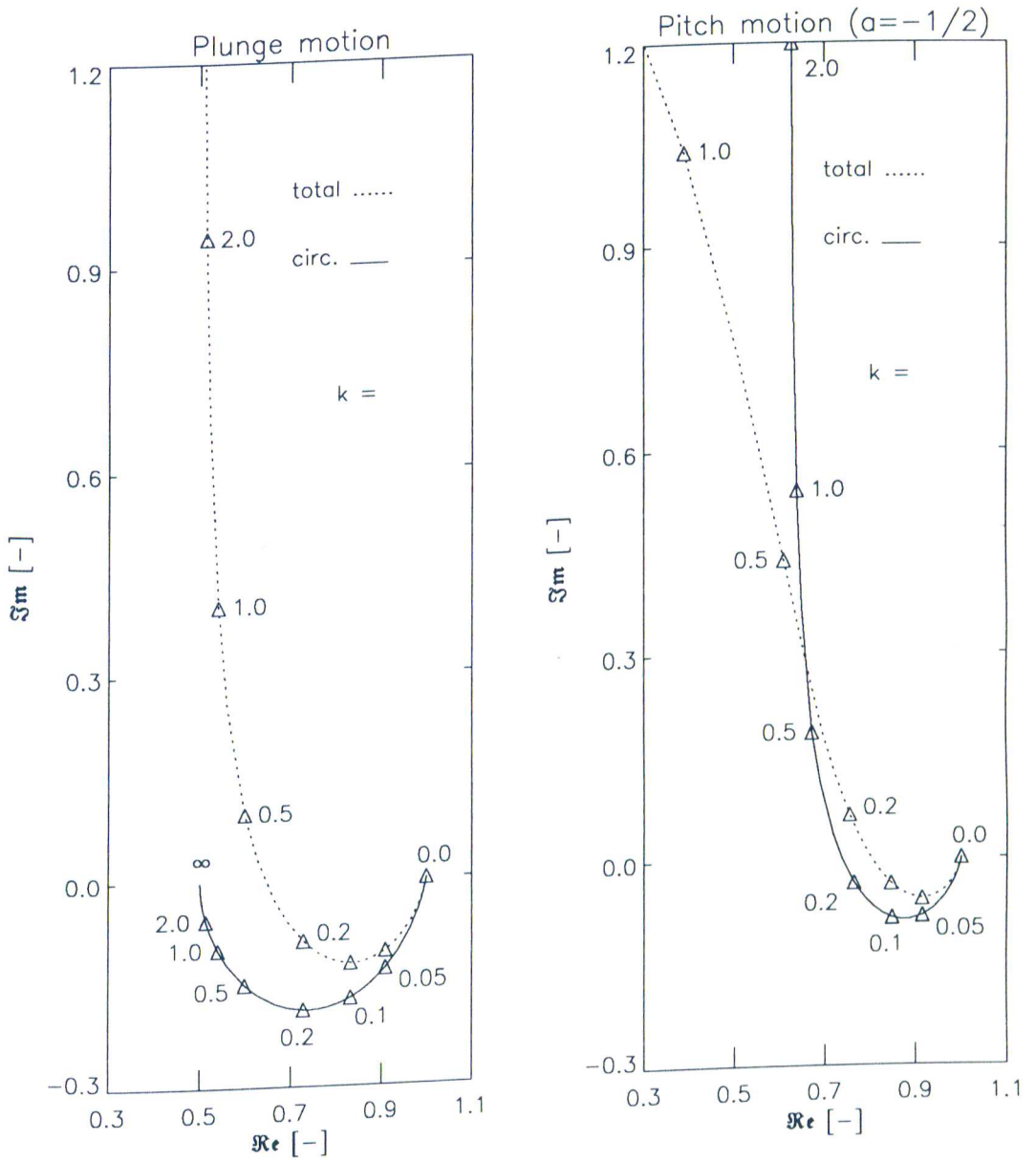

Figure 2.3: Lift transfer function of plunge and pitch oscillation, Theodorsen's theory

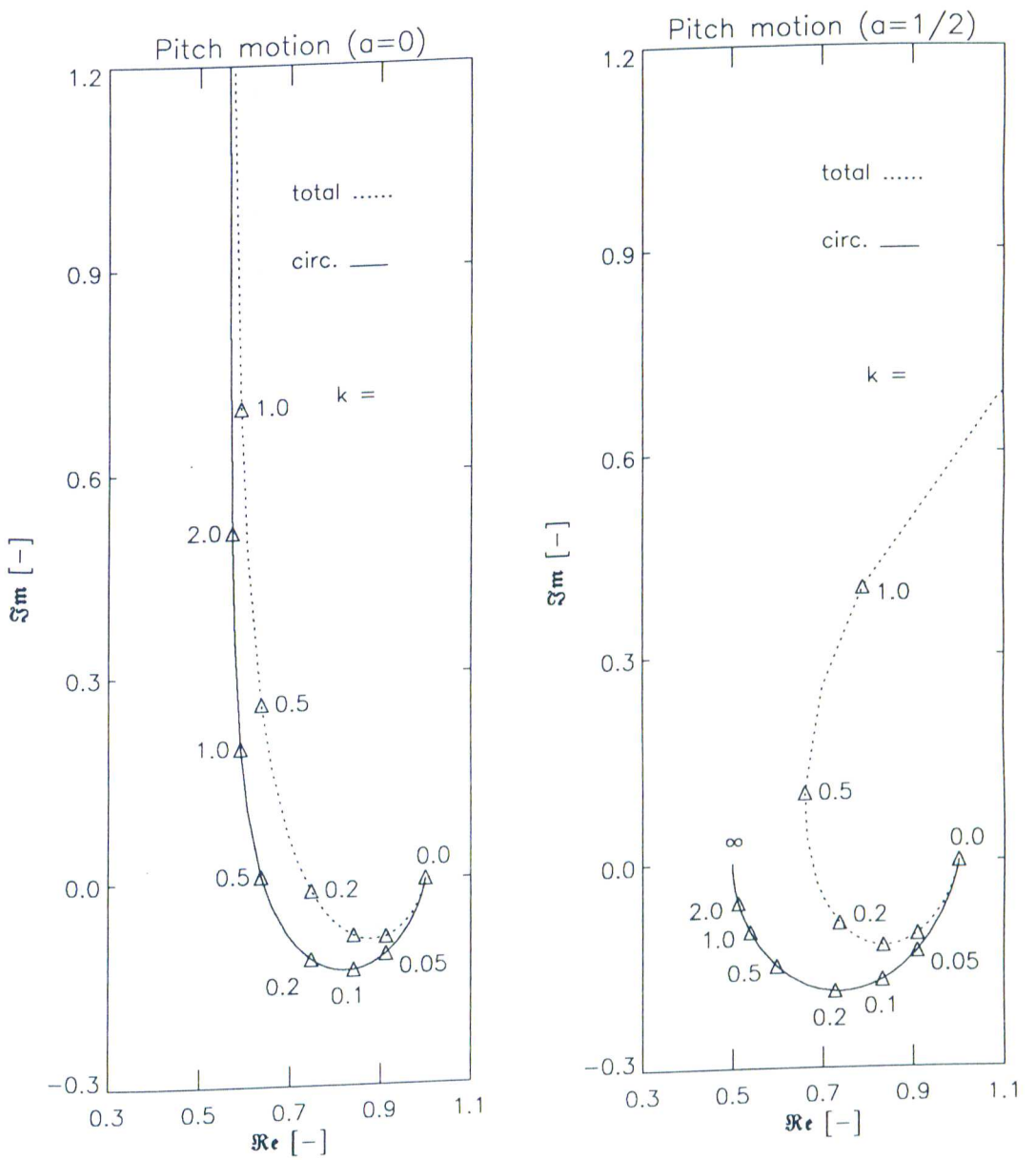

Figure 2.4: Lift transfer function of pitch oscillation about different positions of axis of rotation

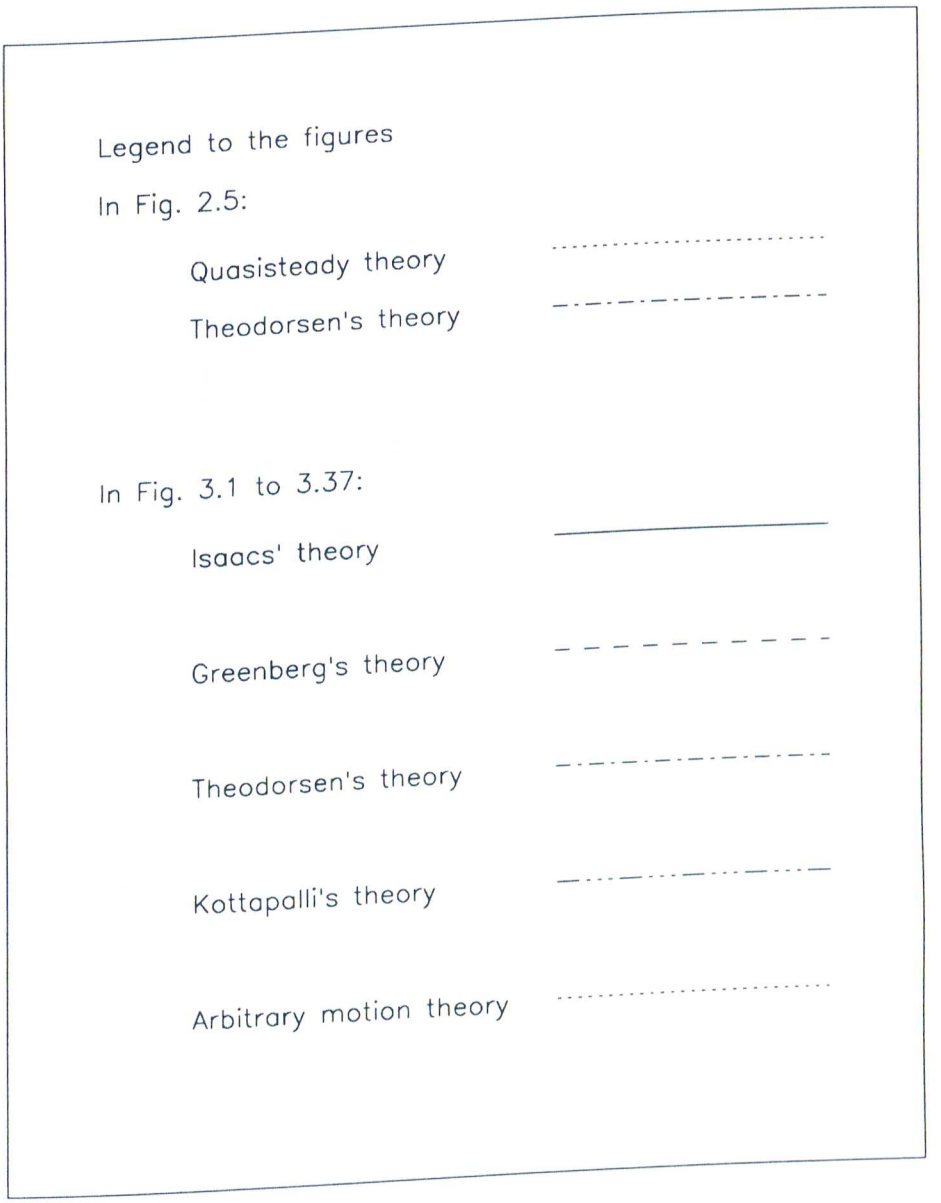

Figure 2.5: Legend for the following figures

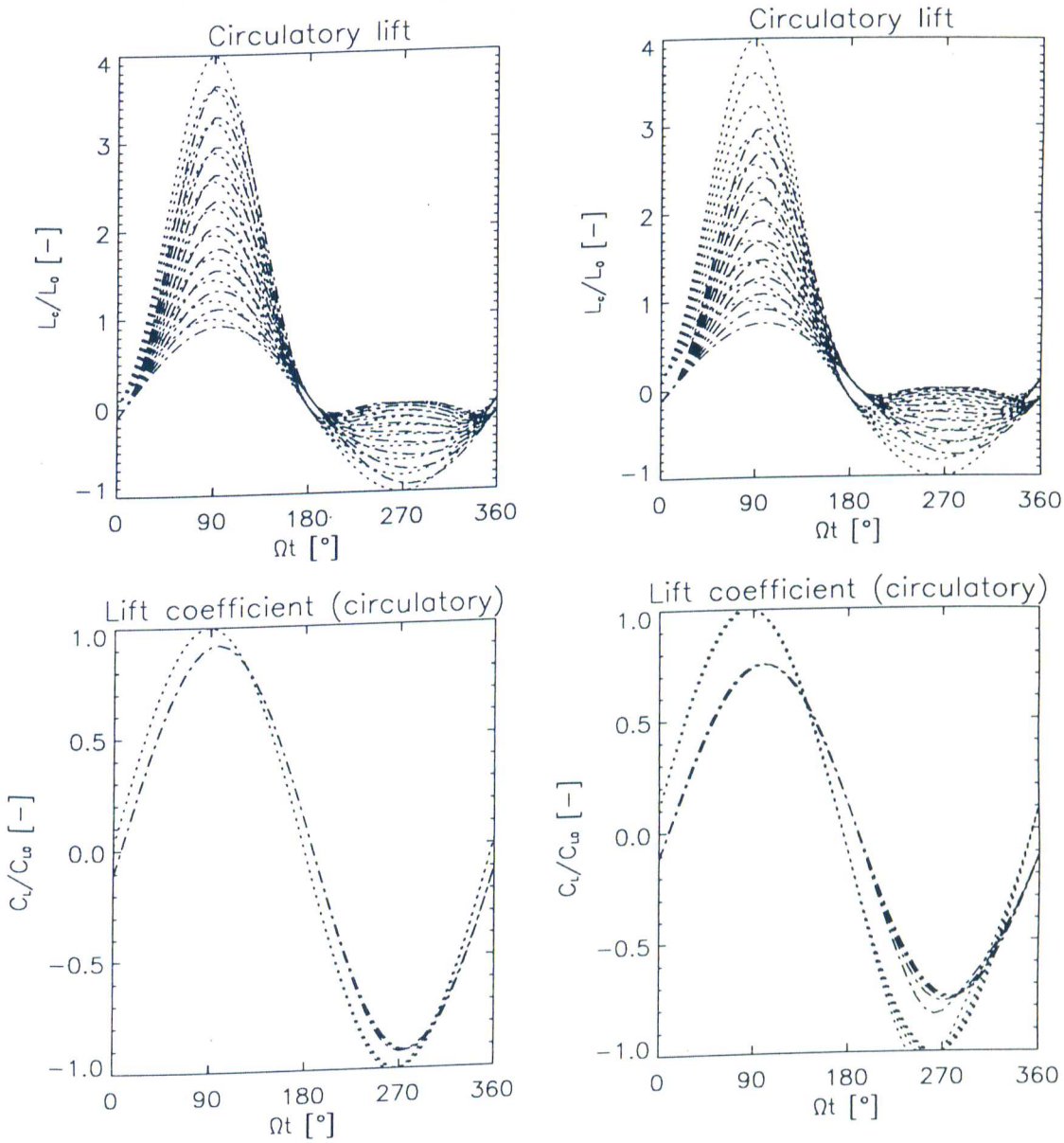

Figure 2.6: Unsteady lift development for sinusoidally varying angle of attack in an oscillating flow, $k_V = 0.05$ (left) and 0.2 (right), $a = 0$, Theodorsen's theory combined with unsteady freestream compared with quasisteady theory

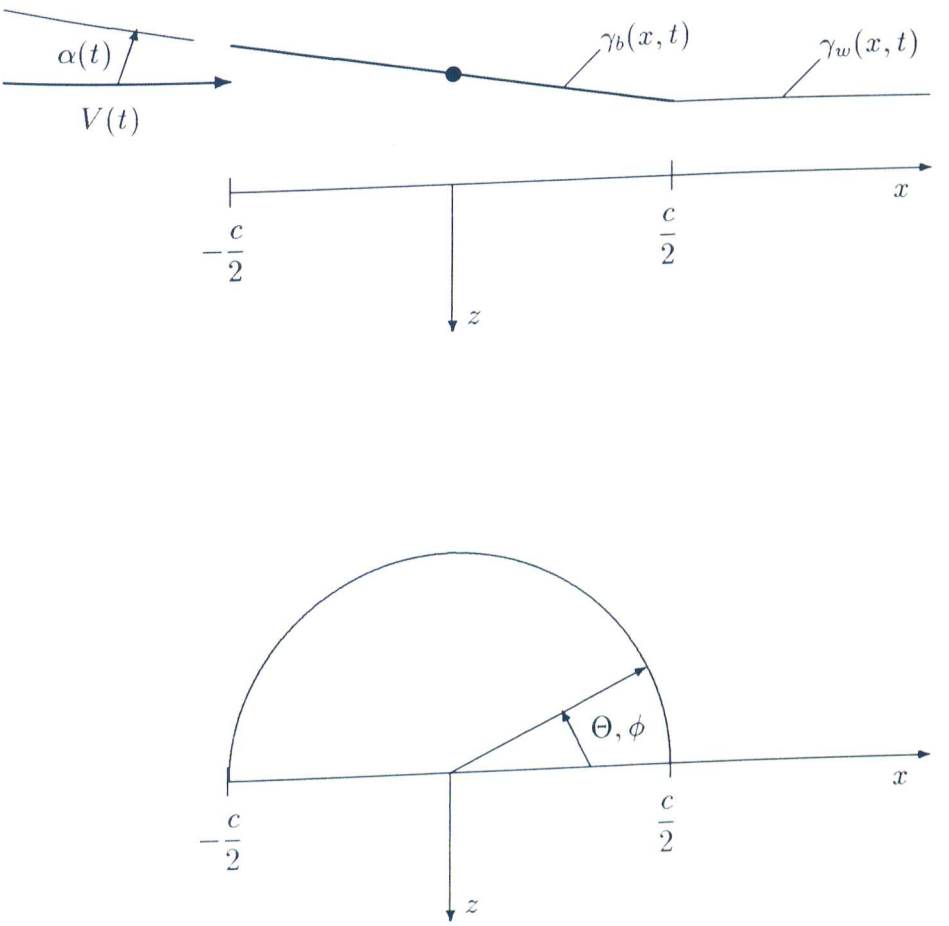

$$x = \frac{c}{2}\cos\Theta$$

Figure 2.7: Airfoil in an unsteady freestream

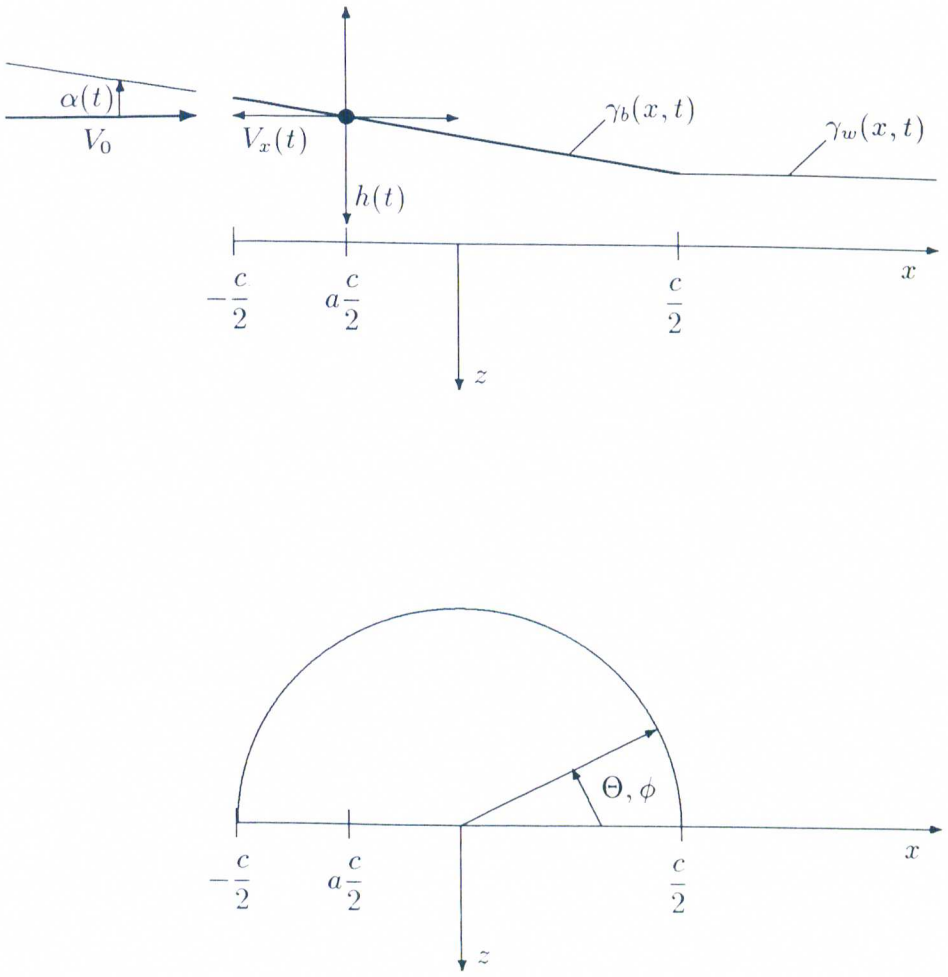

$$x = \frac{c}{2}\cos\Theta$$

Figure 2.8: Airfoil pitching about arbitrary axis in oscillating fore-aft motion

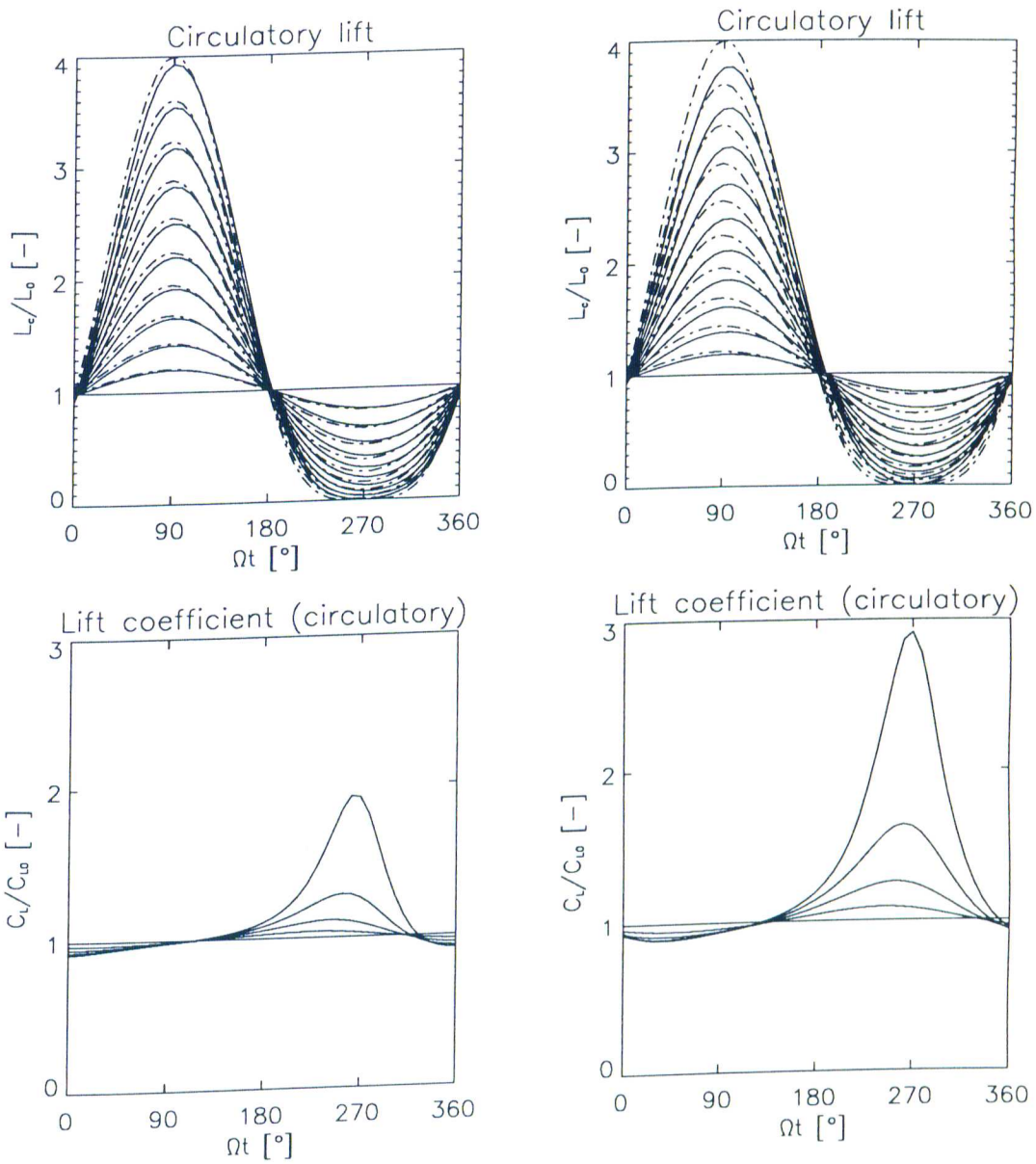

Figure 3.1: Unsteady lift development for constant angle of attack in an oscillating flow, $k_V = 0.05$ (left) and 0.2 (right), Isaacs' theory compared to Theodorsen's theory

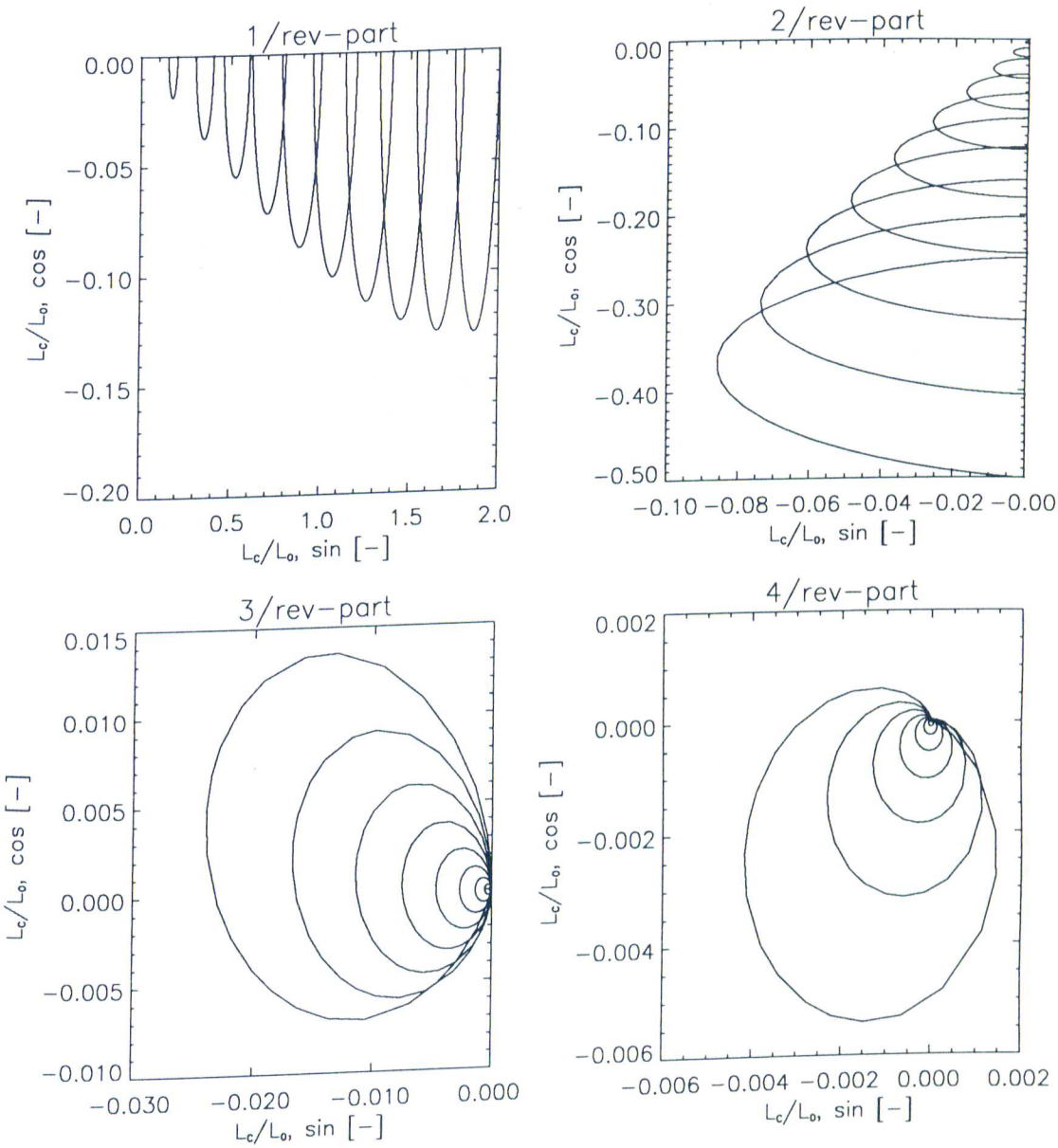

Figure 3.2: Lift transfer function for constant angle of attack in an oscillating flow, Isaacs' theory compared to Theodorsen's theory

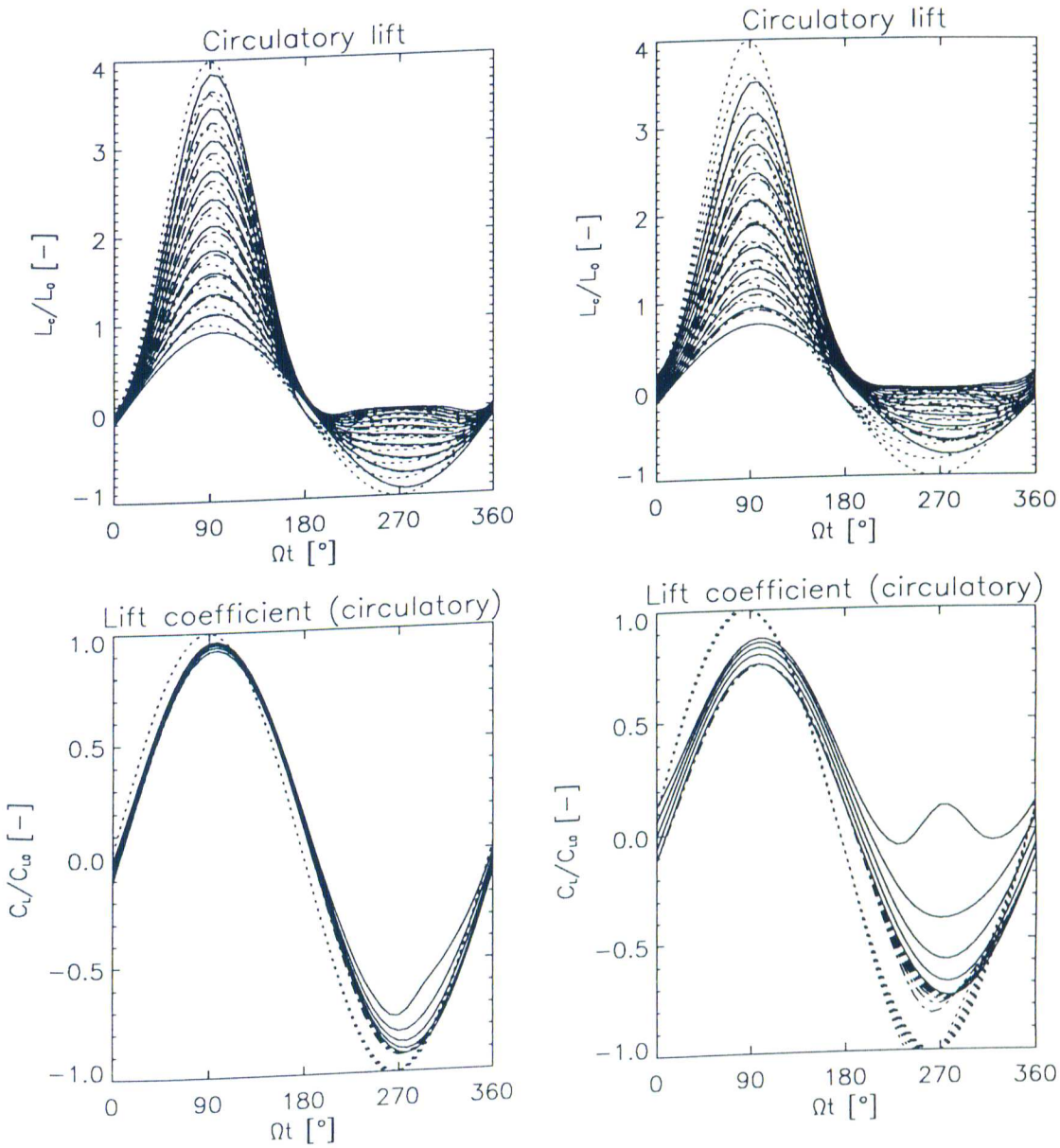

Figure 3.3: Unsteady lift development for sinusoidally varying angle of attack in an oscillating flow, $k_V = 0.05$ (left) and 0.2 (right), $a = 0$, Isaacs' theory compared to Theodorsen's theory and quasisteady theory

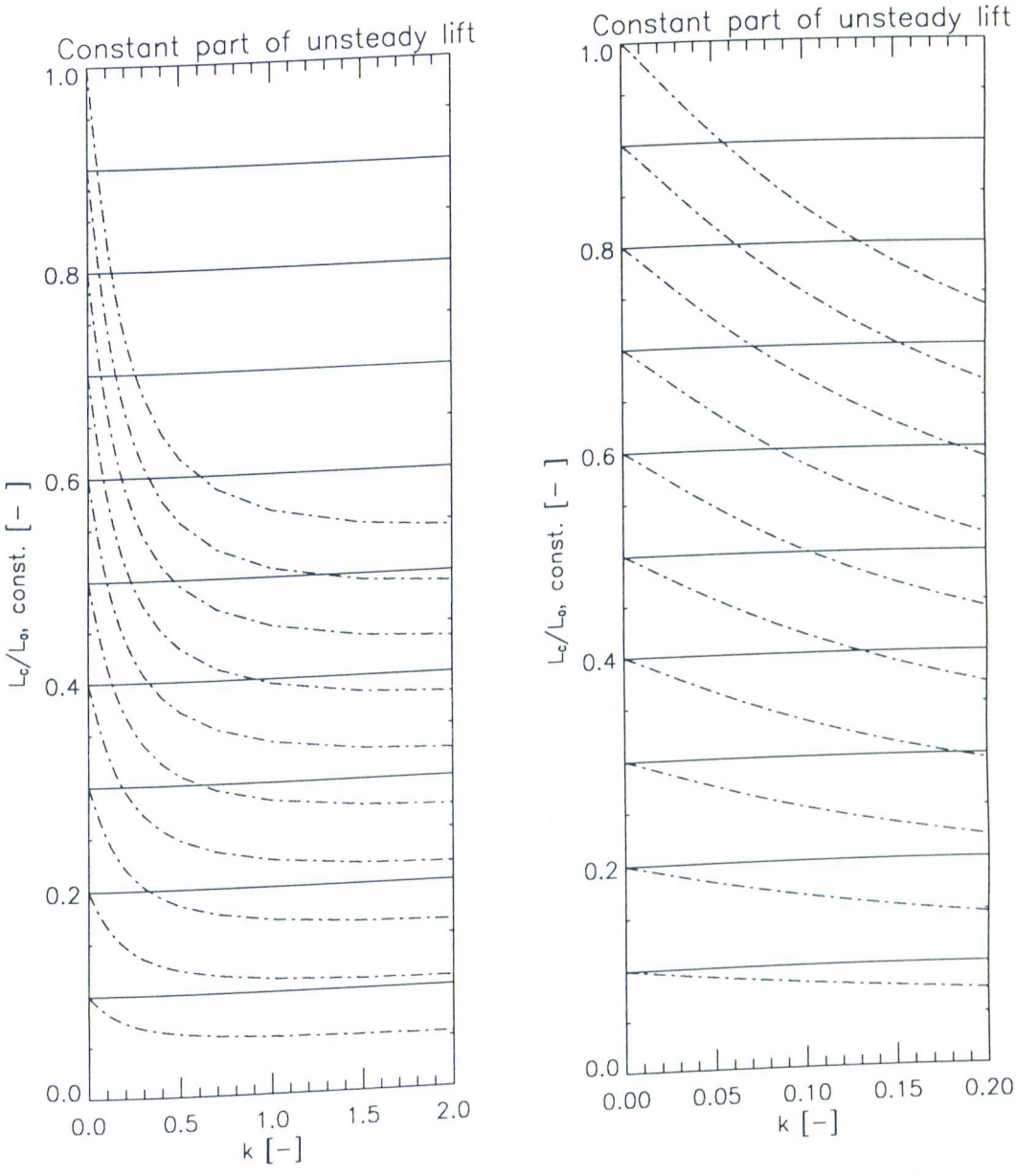

Figure 3.4: Lift transfer function for sinusoidally varying angle of attack in an oscillating flow, $a = 0$, Isaacs' theory compared with Theodorsen's theory

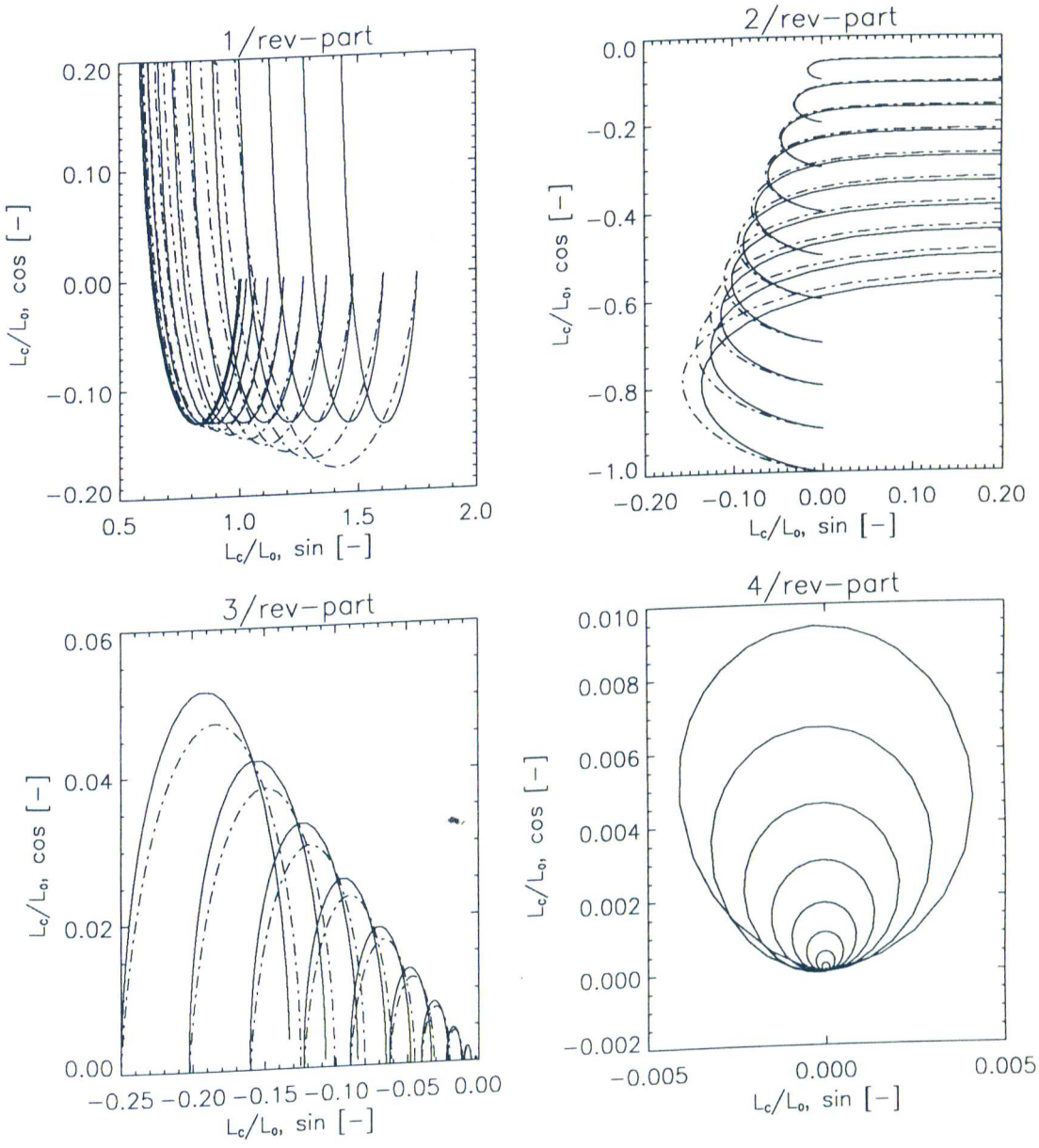

Figure 3.5: Lift transfer function for sinusoidally varying angle of attack in an oscillating flow, $a = 0$, Isaacs' theory compared with Theodorsen's theory

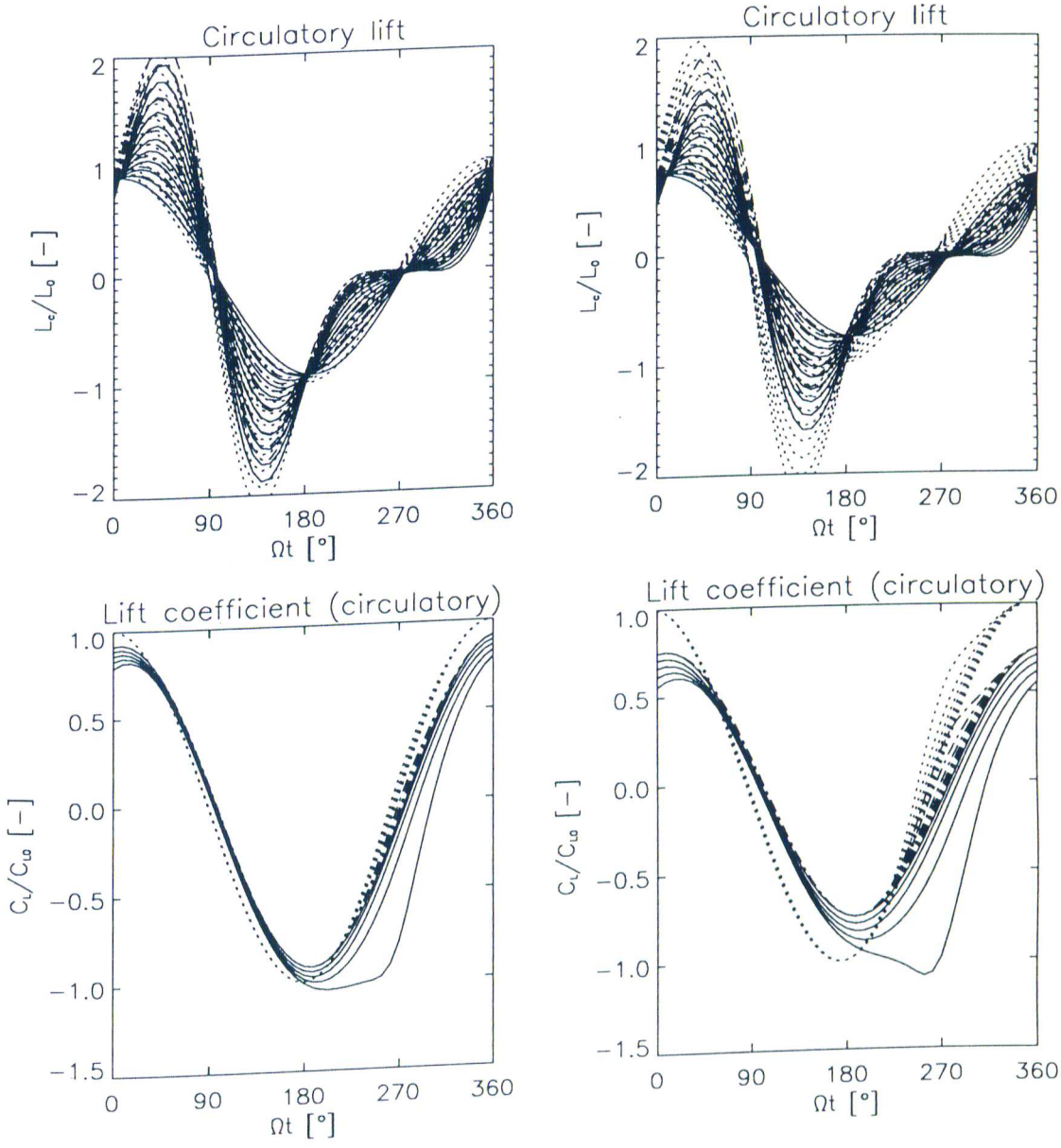

Figure 3.6: Unsteady lift development for sinusoidally varying angle of attack 90^o out-of-phase in an oscillating flow, $k_V = 0.05$ (left) and 0.2 (right), $a = 0$, Isaacs' theory compared to Theodorsen's theory and quasisteady theory

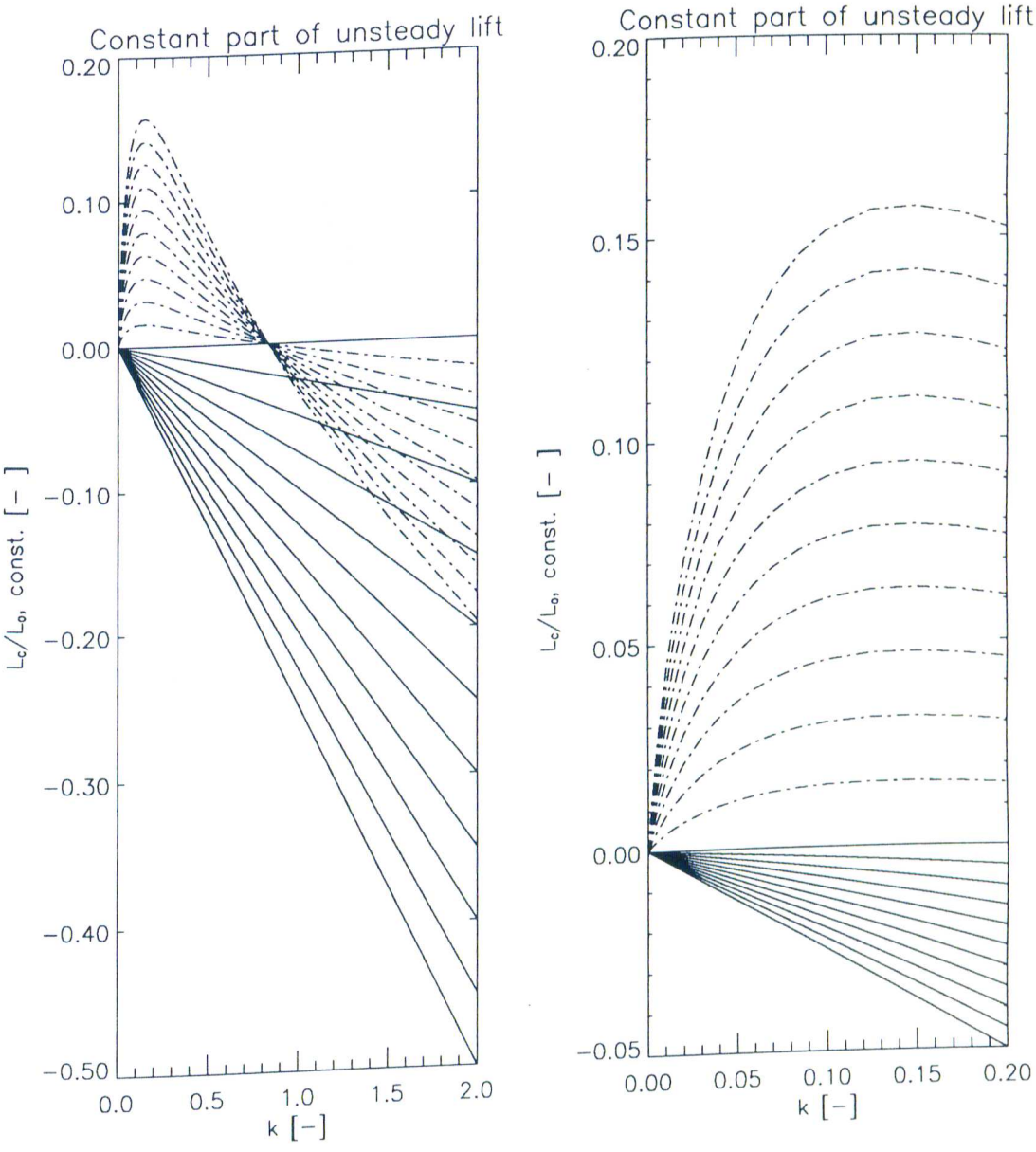

Figure 3.7: Lift transfer function for sinusoidally varying angle of attack 90° out-of-phase in an oscillating flow, $a = 0$, Isaacs' theory compared with Theodorsen's theory

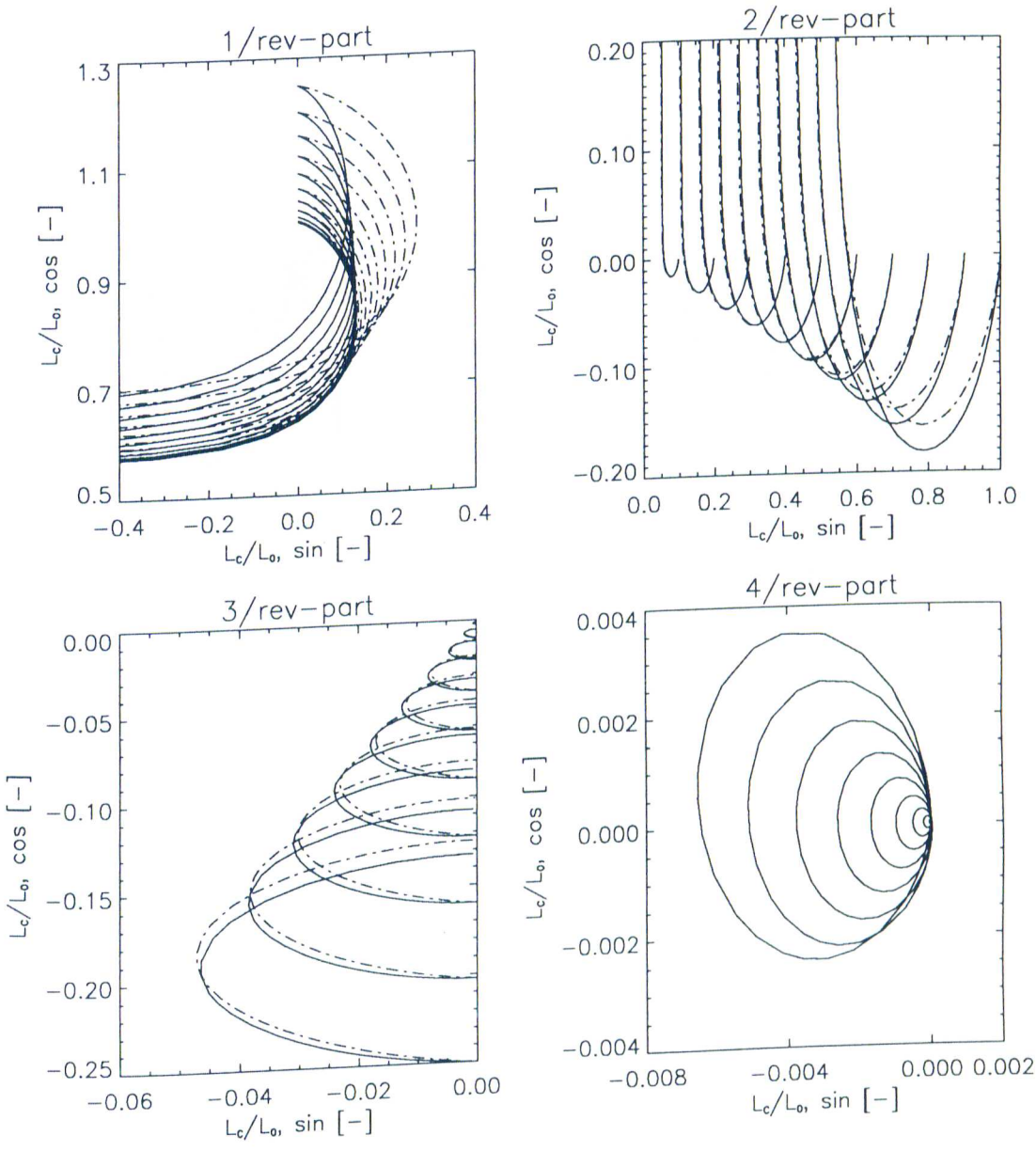

Figure 3.8: Lift transfer function for sinusoidally varying angle of attack 90° out-of-phase in an oscillating flow, $a = 0$, Isaacs' theory compared with Theodorsen's theory

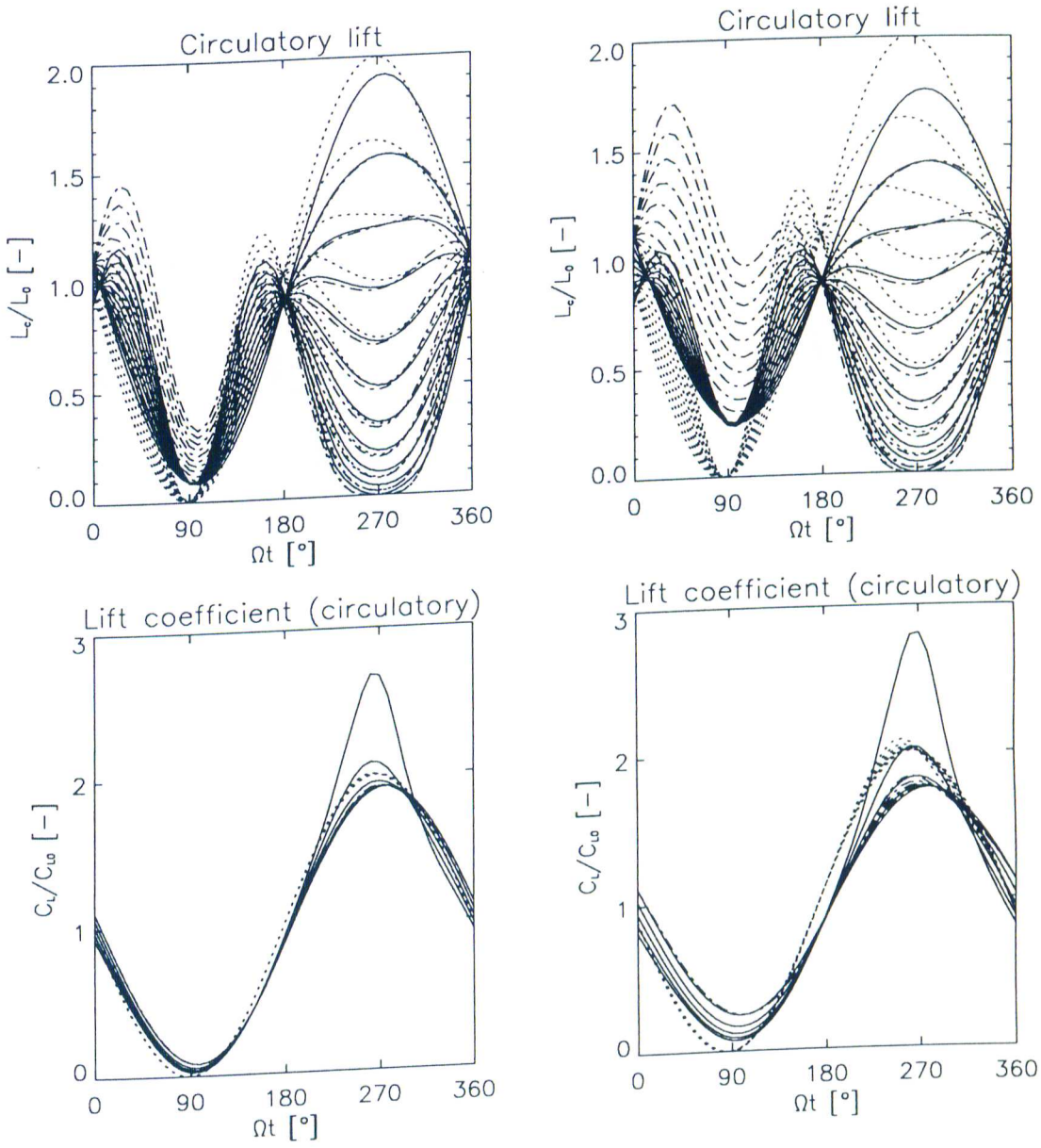

Figure 3.9: Unsteady lift development for the helicopter case, $k_V = 0.05$ (left) and 0.2 (right), $a = 0$, Isaacs' theory compared with Theodorsen's theory and quasisteady theory

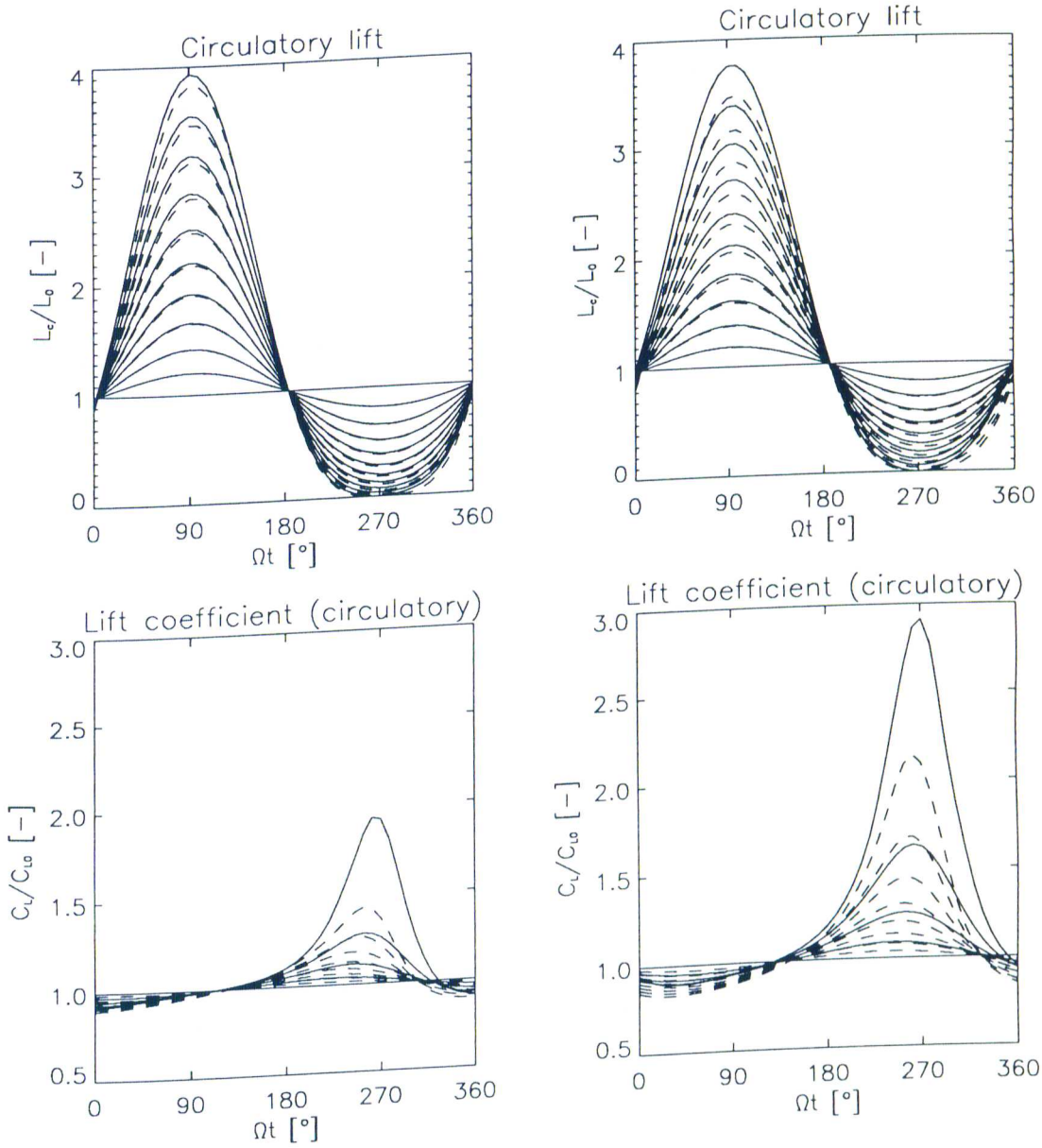

Figure 3.10: Unsteady lift development for constant angle of attack in an oscillating flow, $k_V = 0.05$ (left) and 0.2 (right), Greenberg's theory compared with Isaacs' theory

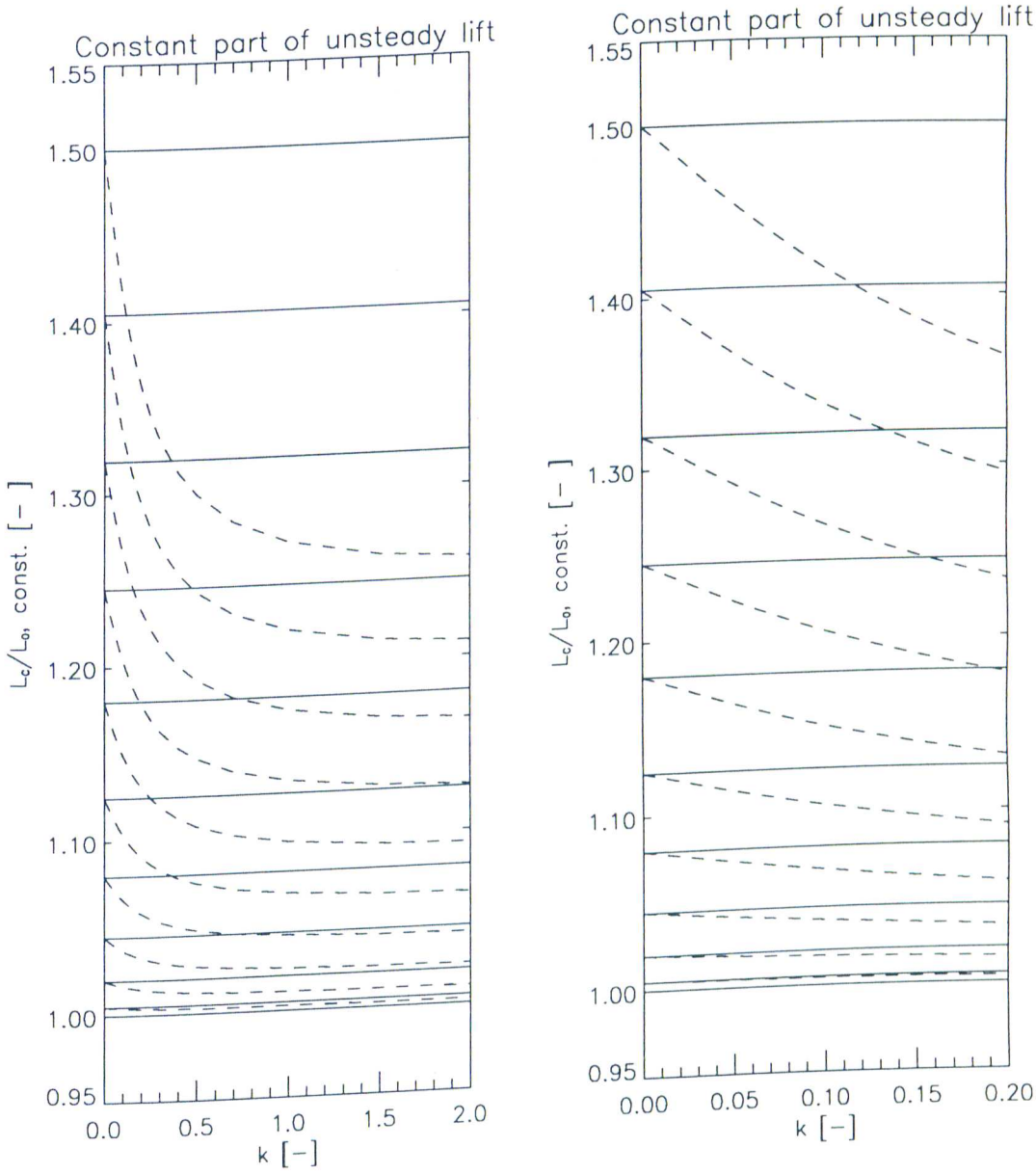

Figure 3.11: Lift transfer function for constant angle of attack in an oscillating flow, Greenberg's theory compared with Isaacs' theory

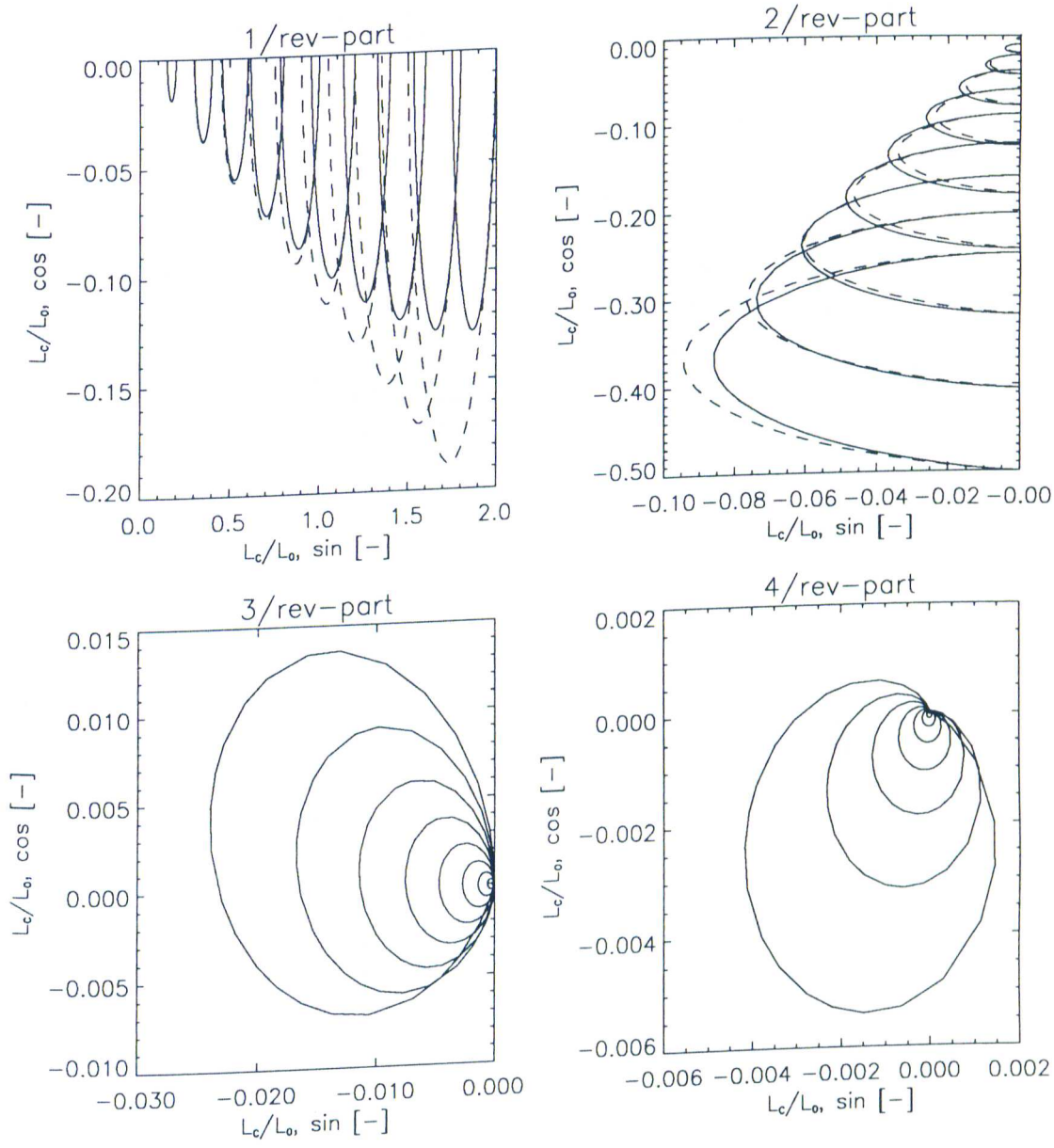

Figure 3.12: Lift transfer function for constant angle of attack in an oscillating flow (dynamic part), Greenberg's theory compared with Isaacs' theory

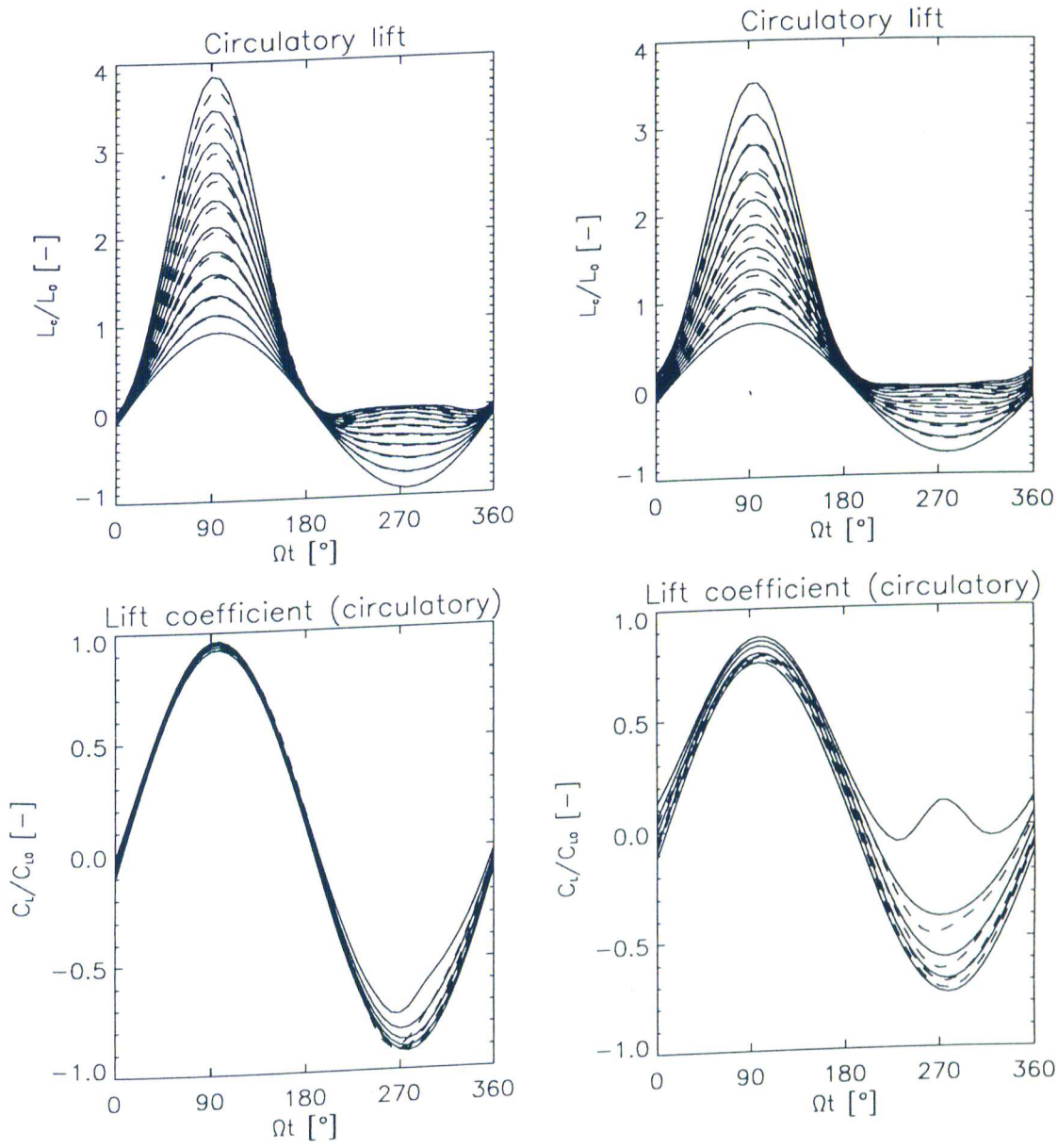

Figure 3.13: Unsteady lift development for sinusoidally varying angle of attack in an oscillating flow, $k_V = 0.05$ (left) and 0.2 (right), $a = 0$, Greenberg's theory compared with Isaacs' theory

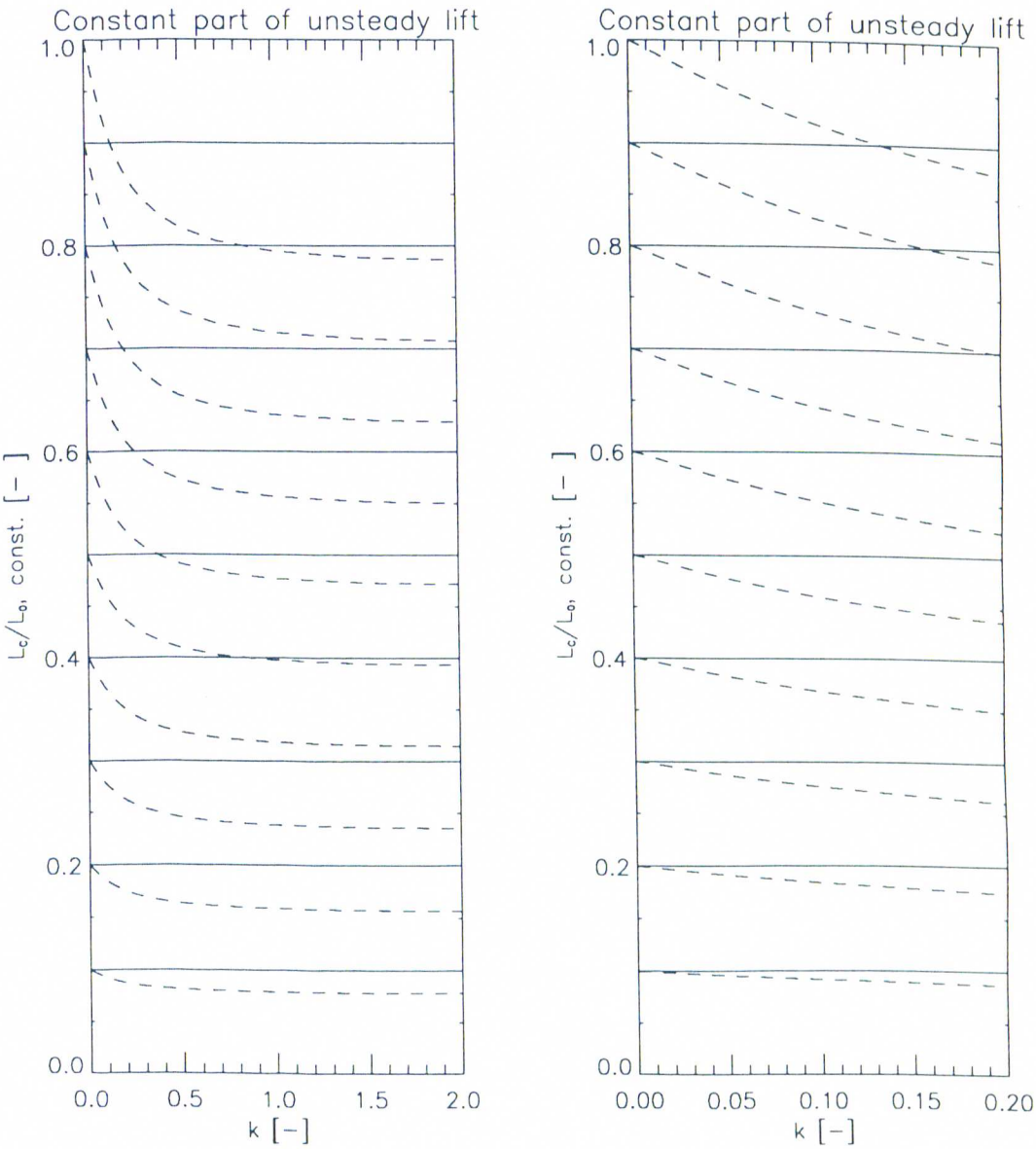

Figure 3.14: Lift transfer function for sinusoidally varying angle of attack in an oscillating flow, $a = 0$, Greenberg's theory compared with Isaacs' theory

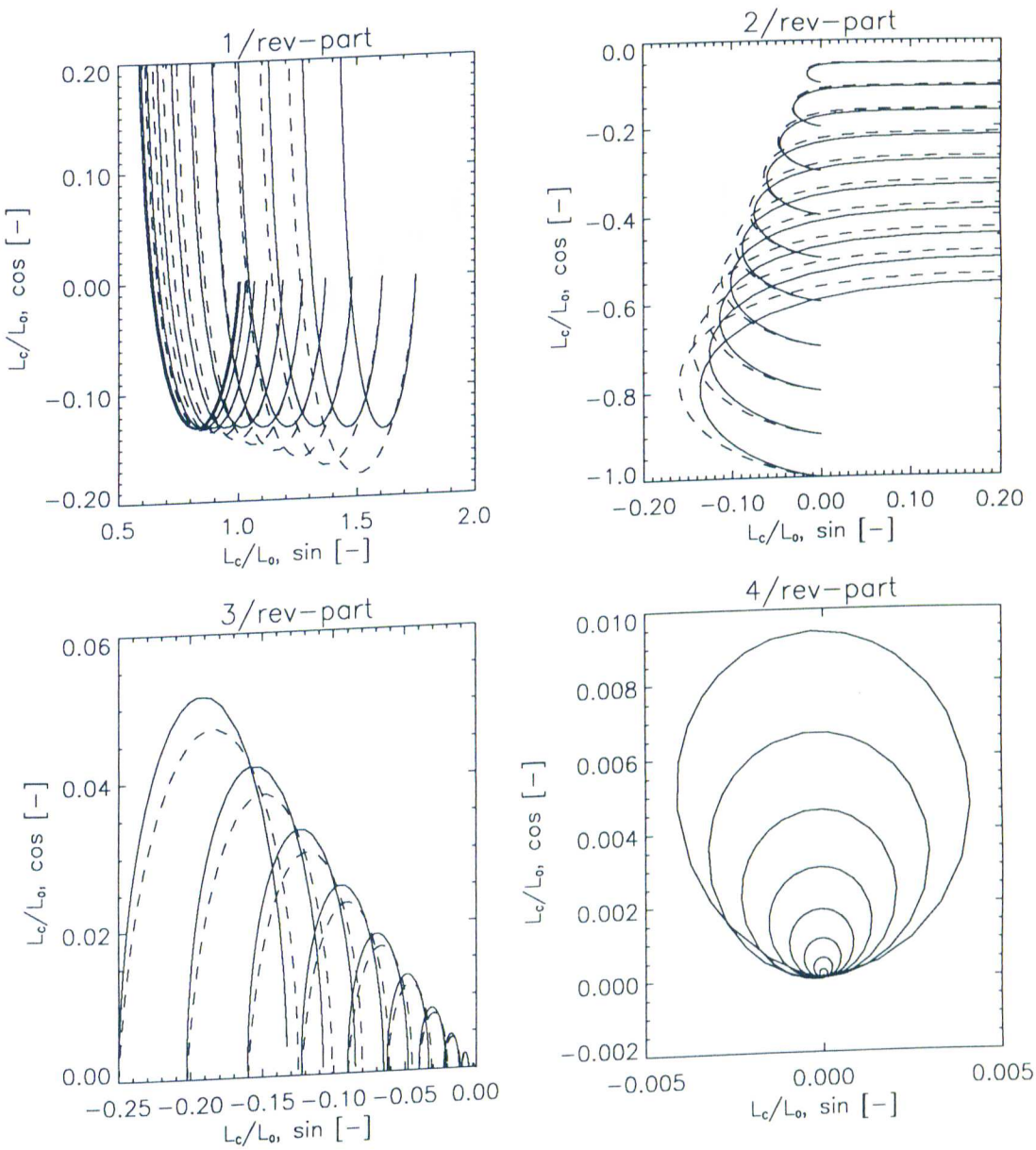

Figure 3.15: Lift transfer function for sinusoidally varying angle of attack in an oscillating flow, $a = 0$, Greenberg's theory compared with Isaacs' theory

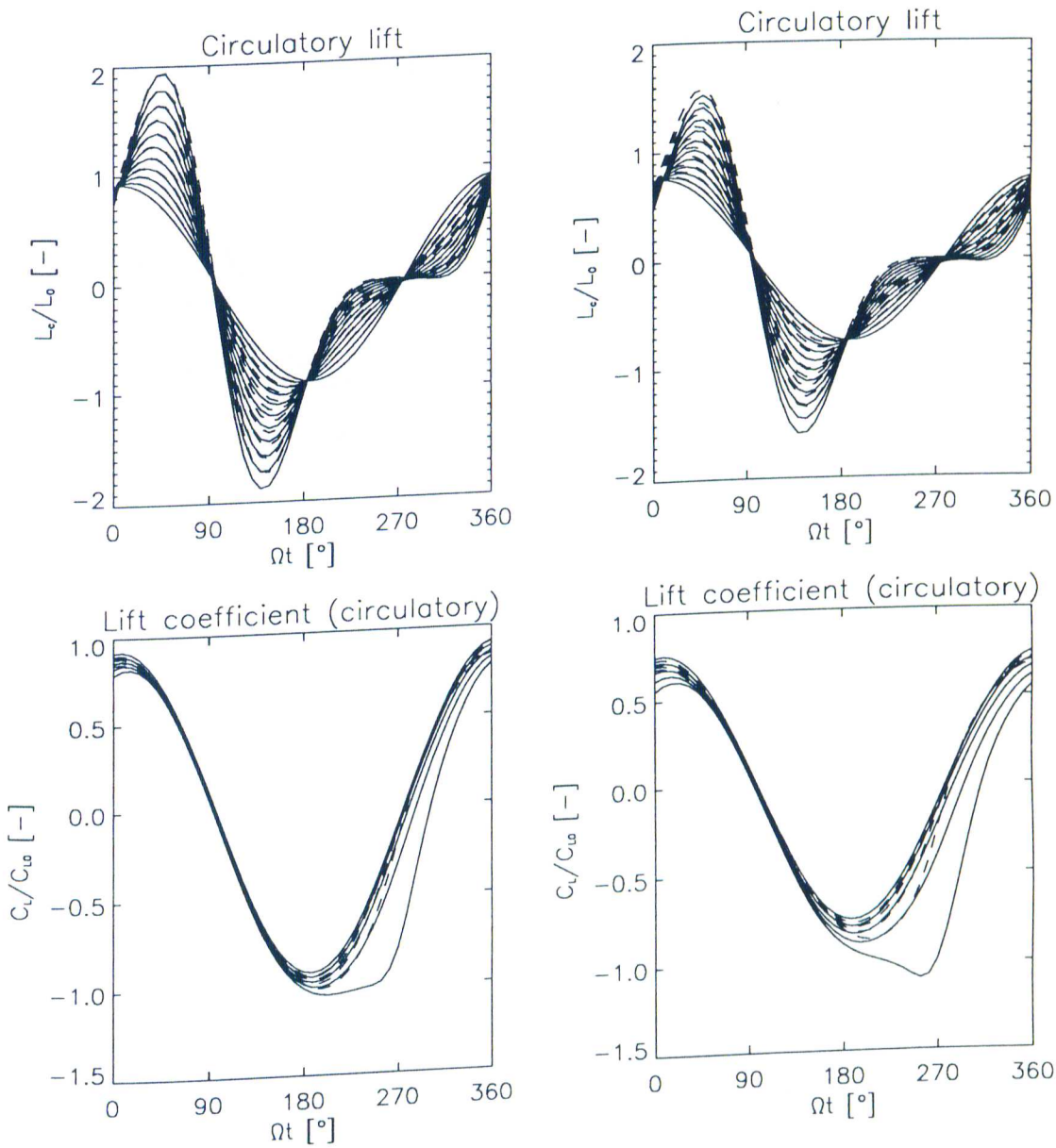

Figure 3.16: Unsteady lift development for sinusoidally varying angle of attack 90^o out-of-phase in an oscillating flow, $k_V = 0.05$ (left) and 0.2 (right), $a = 0$, Greenberg's theory compared with Isaacs' theory

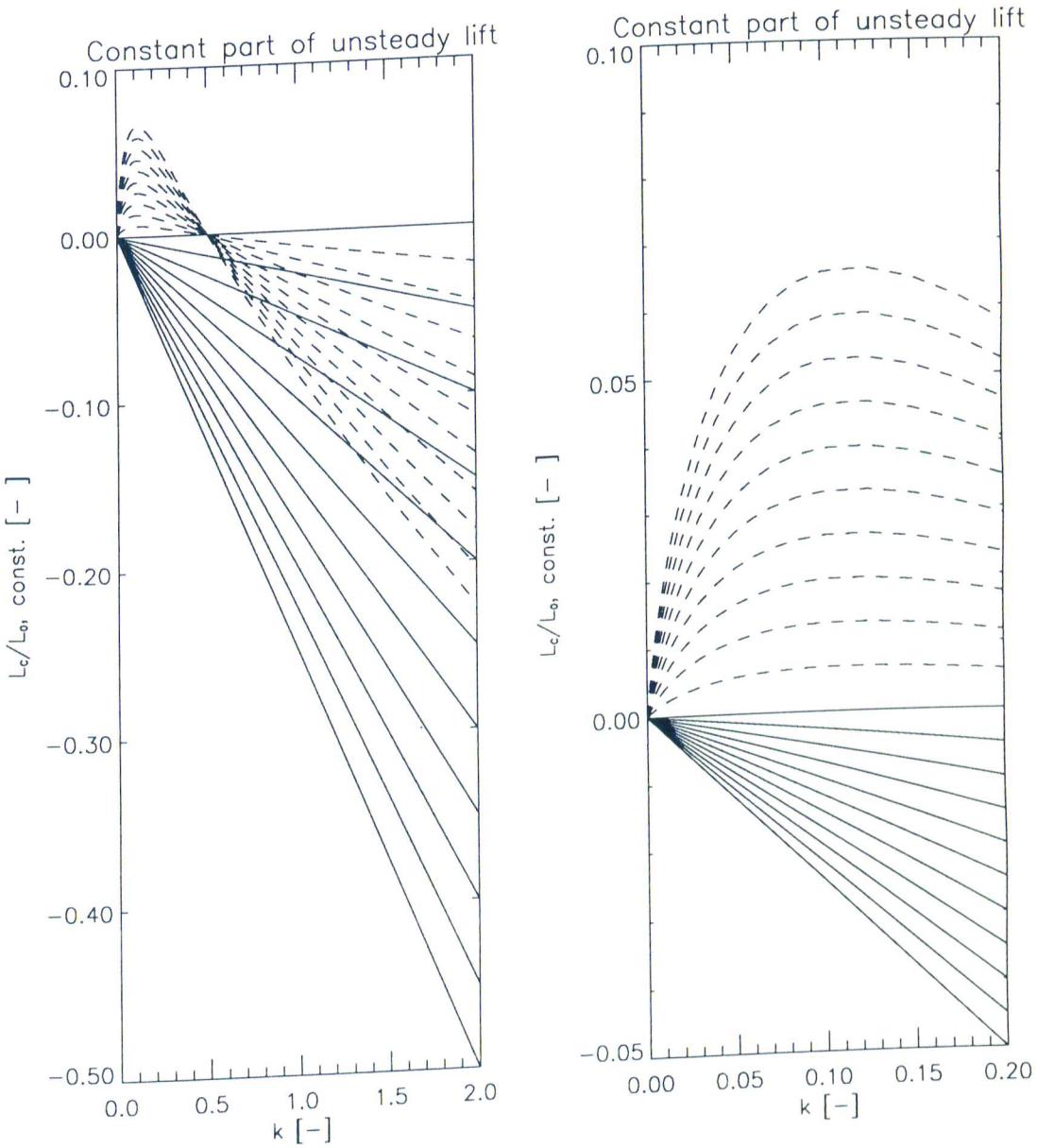

Figure 3.17: Lift transfer function for sinusoidally varying angle of attack 90^o out-of-phase in an oscillating flow, $a = 0$, Greenberg's theory compared with Isaacs' theory

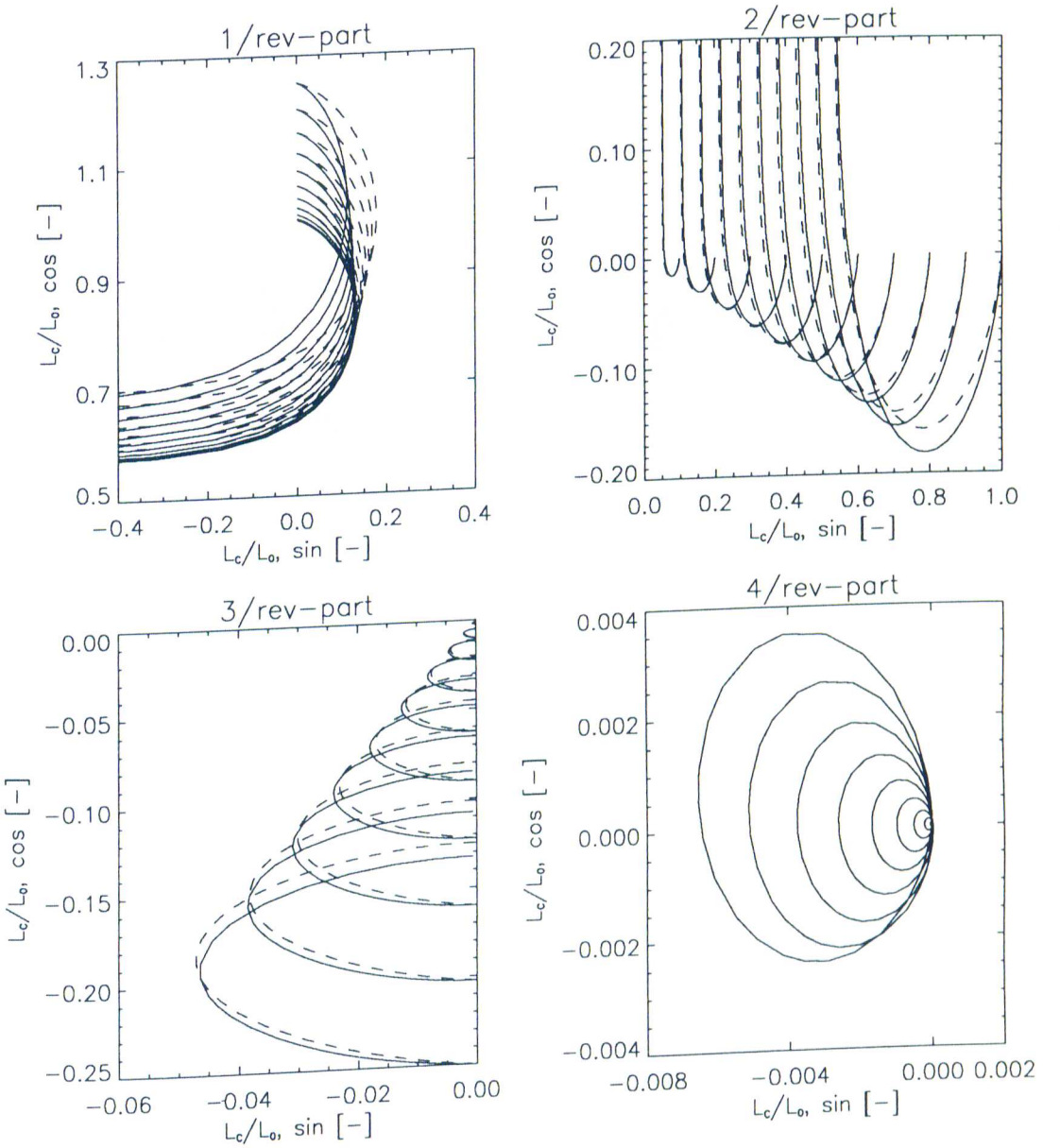

Figure 3.18: Lift transfer function for sinusoidally varying angle of attack 90° out-of-phase in an oscillating flow, $a = 0$, Greenberg's theory compared with Isaacs' theory

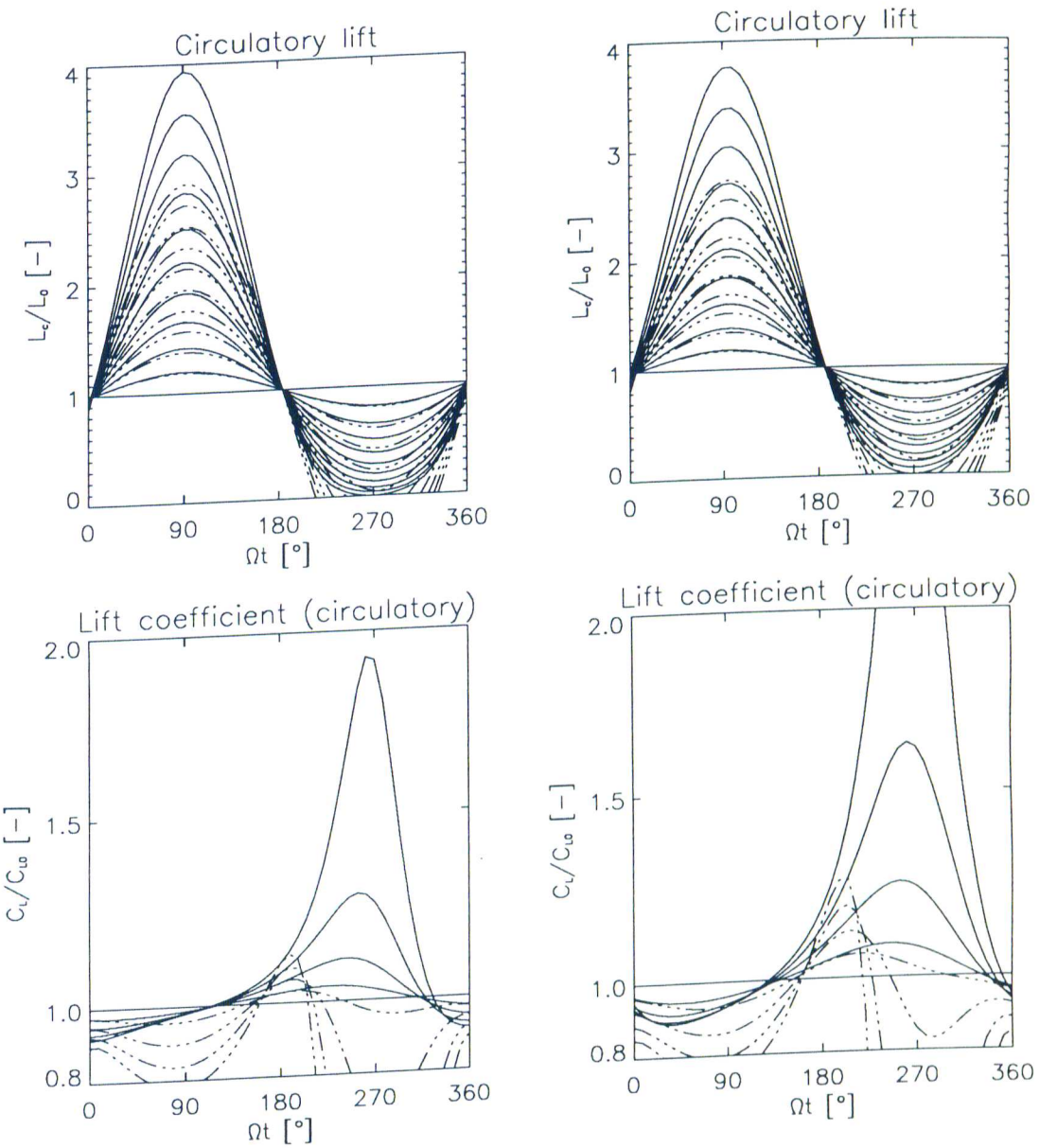

Figure 3.19: Unsteady lift development for constant angle of attack in an oscillating flow, $k_V = 0.05$ (left) and 0.2 (right), Kottapalli's theory compared with Isaacs' theory

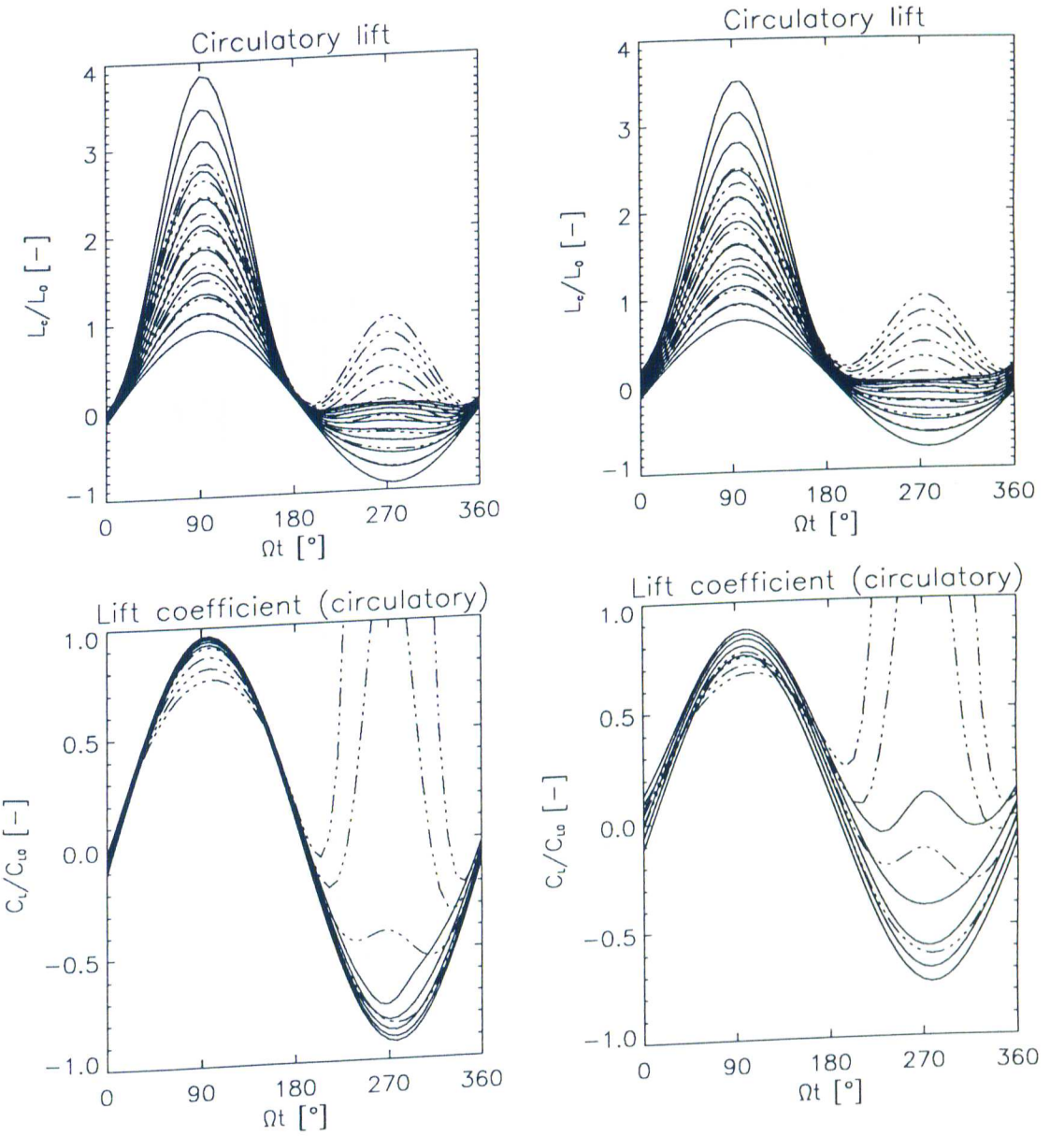

Figure 3.20: Unsteady lift development for sinusoidally varying angle of attack in an oscillating flow, $k_V = 0.05$ (left) and 0.2 (right), $a = 0$, Kottapalli's theory compared with Isaacs' theory

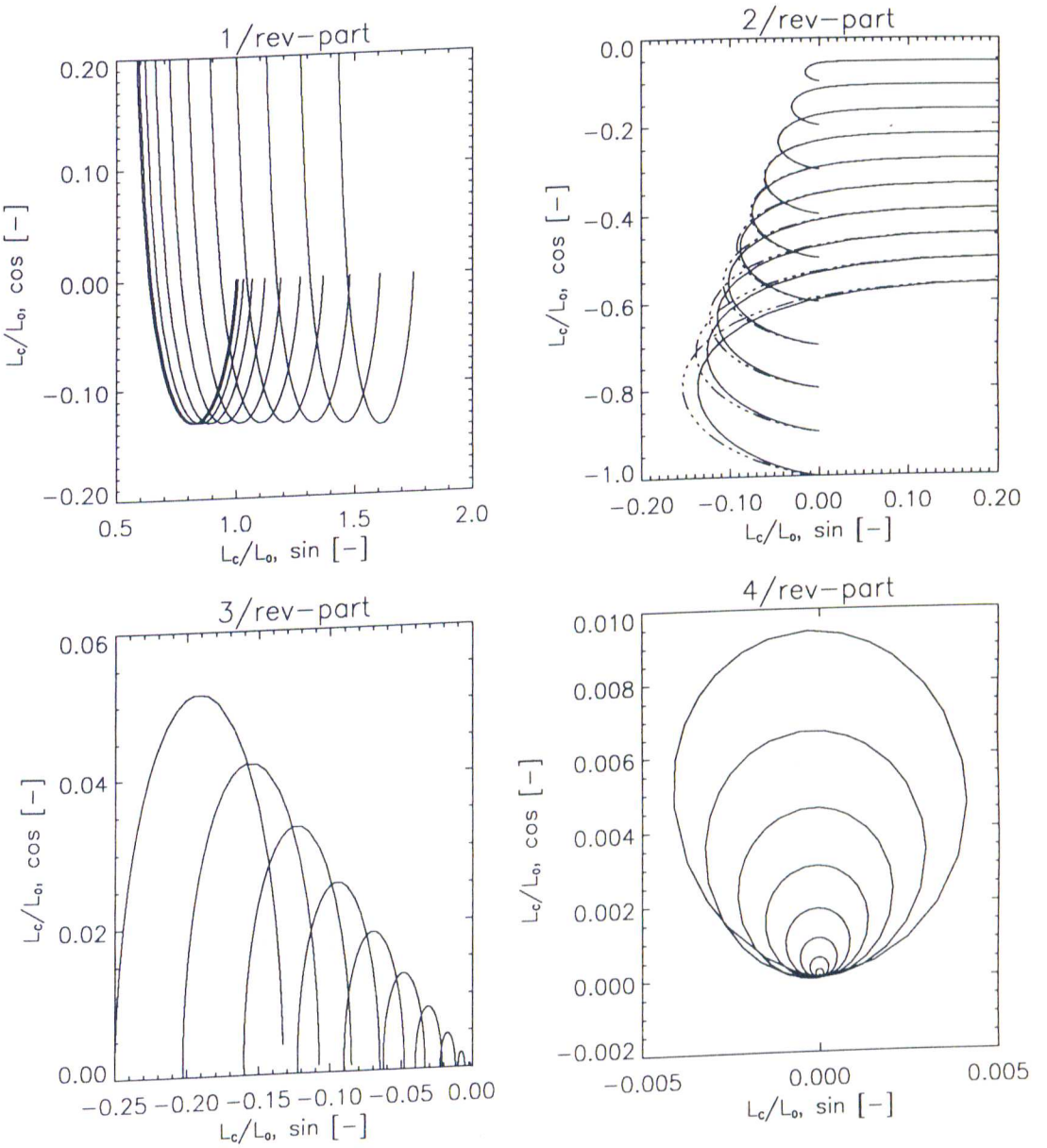

Figure 3.21: Lift transfer function for sinusoidally varying angle of attack in an oscillating flow, $a = 0$, Kottapalli's theory compared with Isaacs' theory

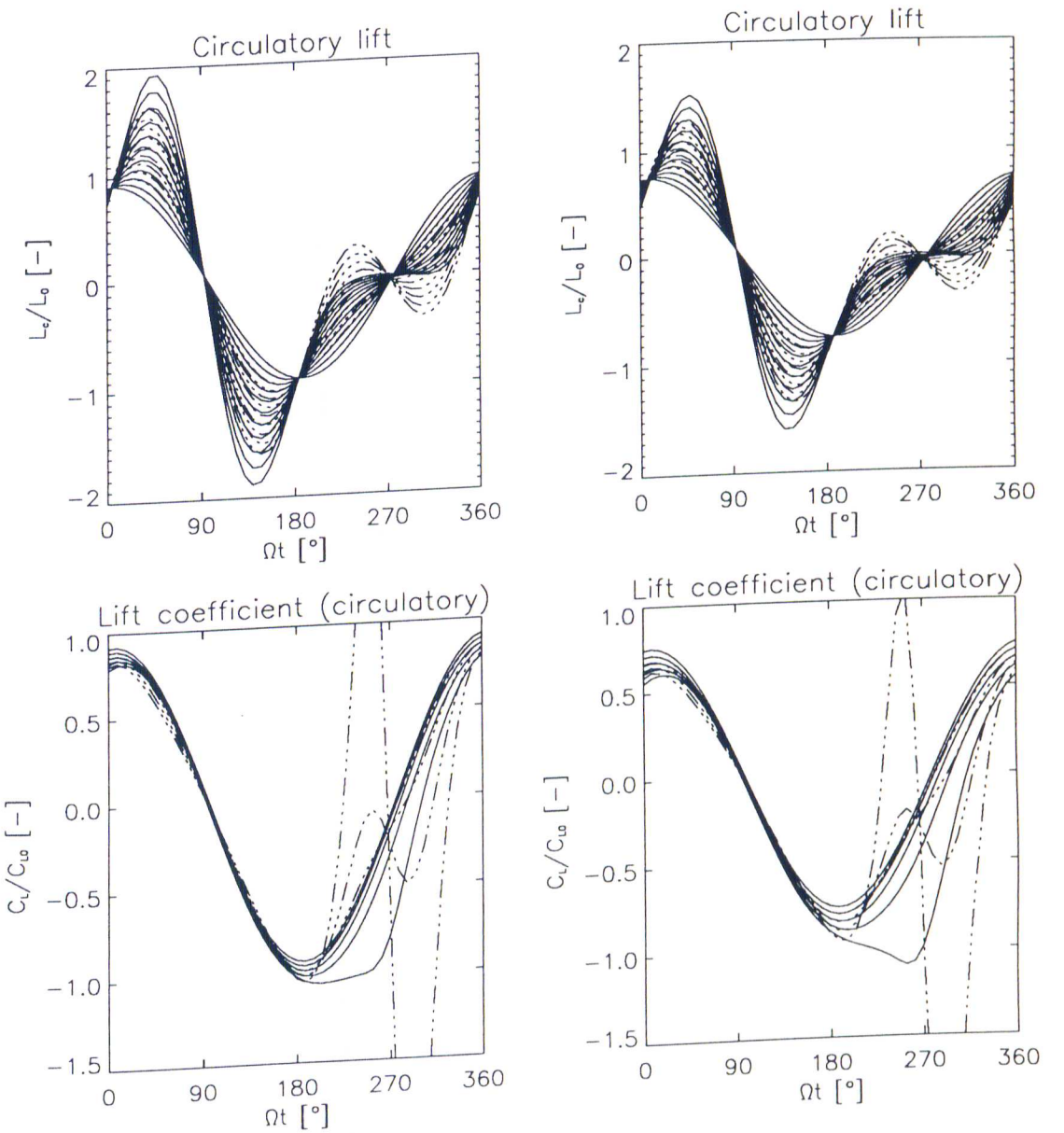

Figure 3.22: Unsteady lift development for sinusoidally varying angle of attack 90° out-of-phase in an oscillating flow, $k_V = 0.05$ (left) and 0.2 (right), $a = 0$, Kottapalli's theory compared with Isaacs' theory

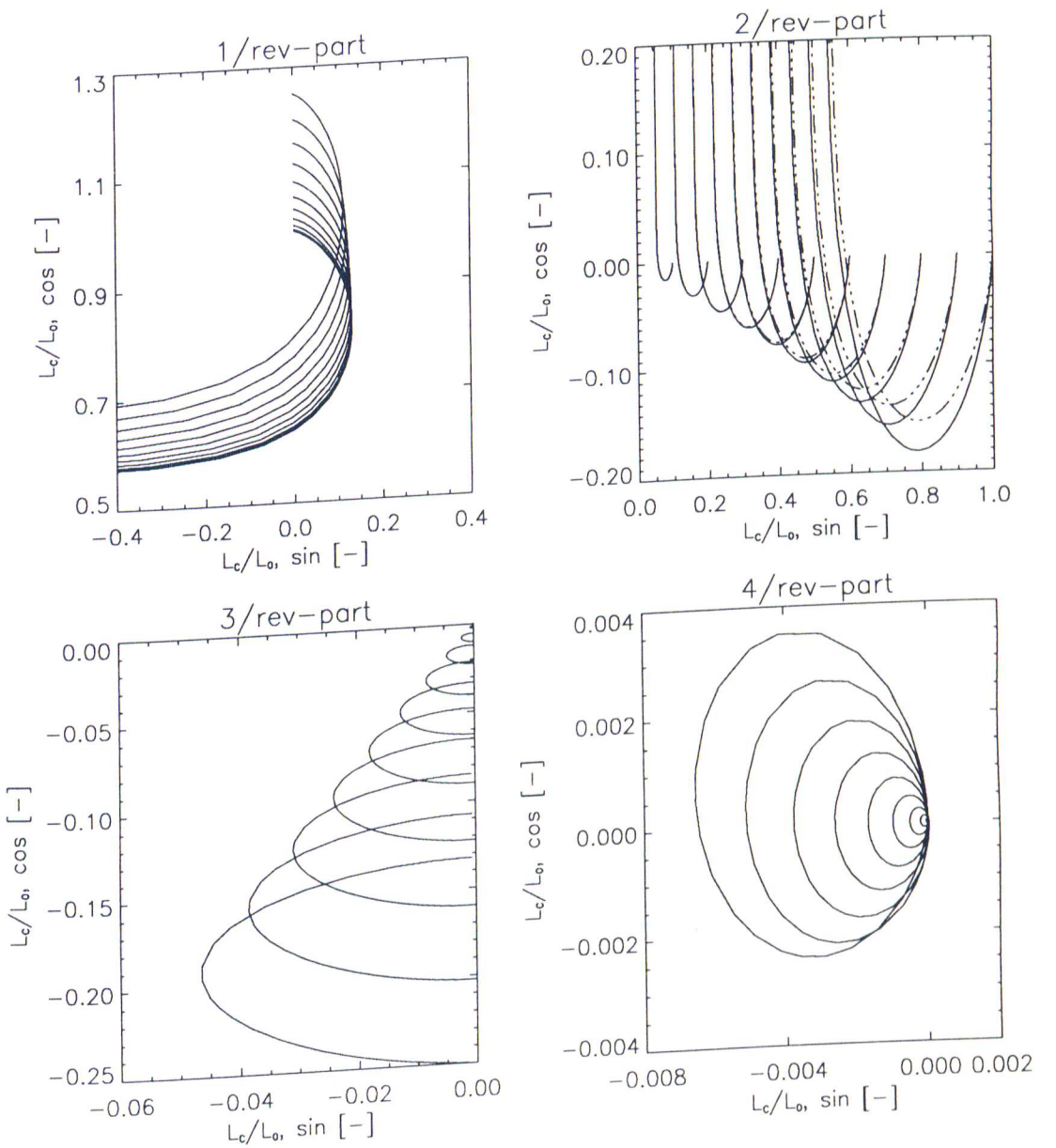

Figure 3.23: Lift transfer function for sinusoidally varying angle of attack 90^o out-of-phase in an oscillating flow, $a = 0$, Kottapalli's theory compared with Isaacs' theory

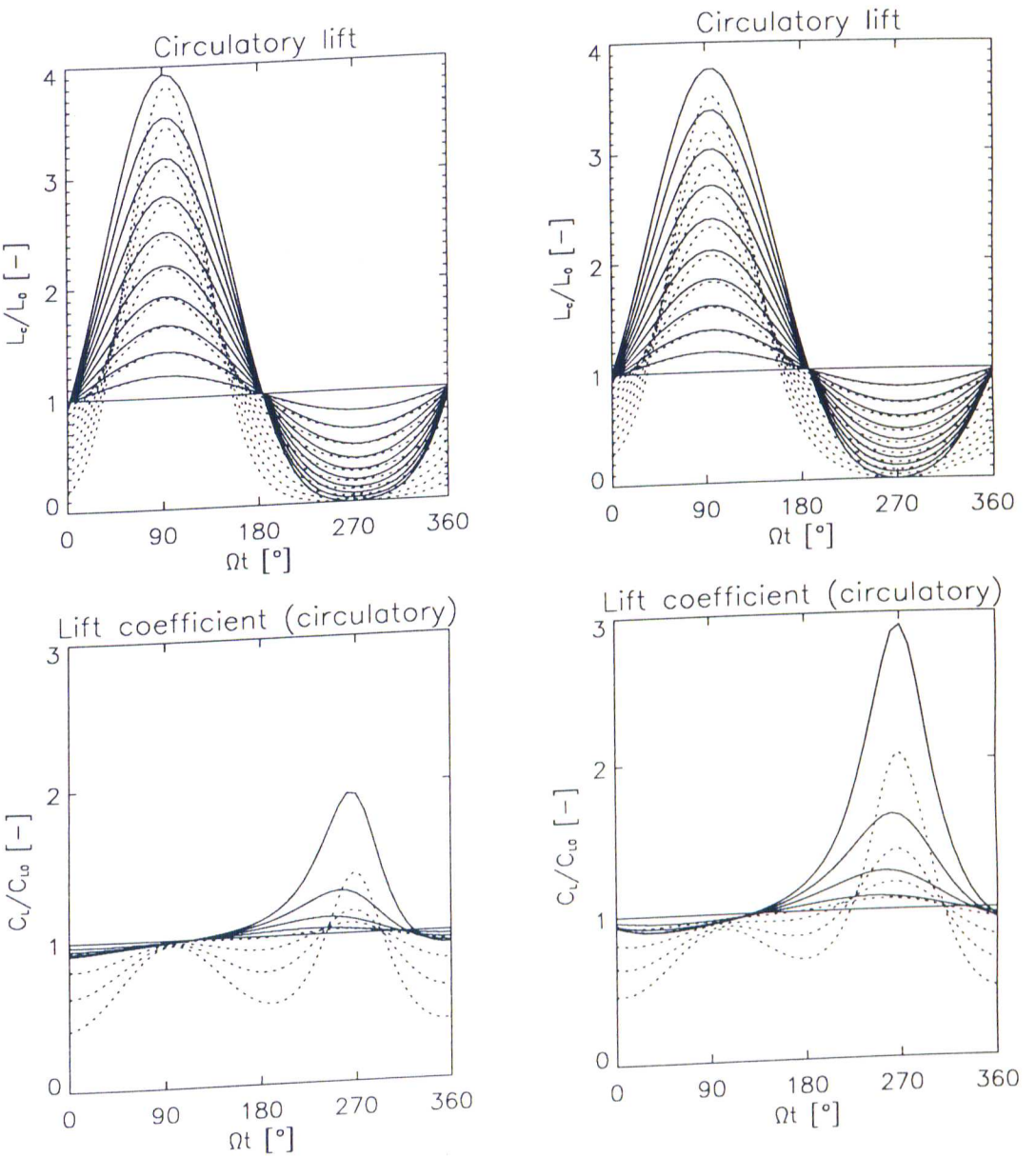

Figure 3.24: Unsteady lift development for constant angle of attack in an oscillating flow, $k_V = 0.05$ (left) and 0.2 (right), arbitrary motion theory (analytic result) compared with Isaacs' theory

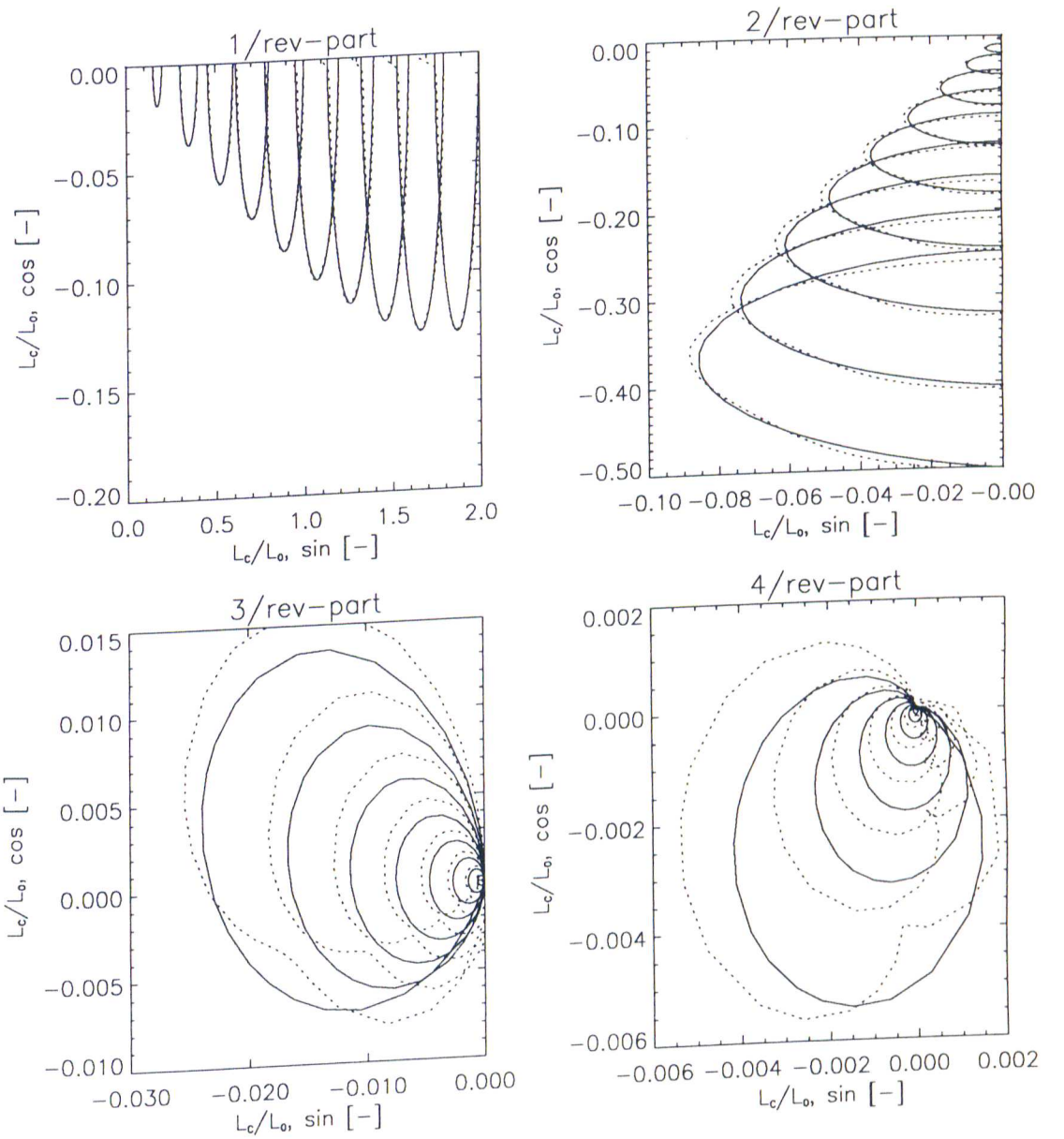

Figure 3.25: Lift transfer function for constant angle of attack in an oscillating flow (dynamic part), arbitrary motion theory (finite differences) compared with Isaacs' theory

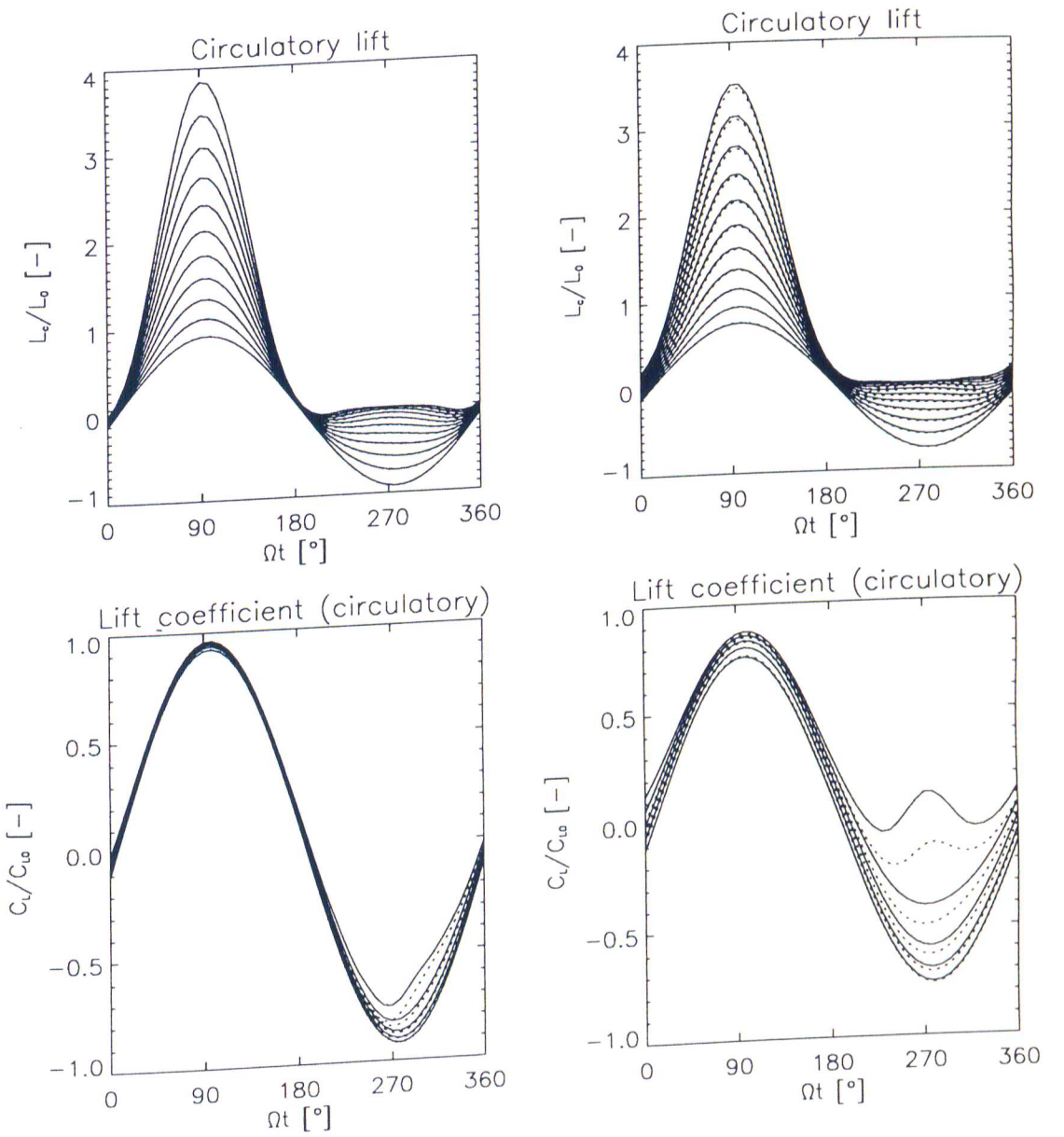

Figure 3.26: Unsteady lift development for sinusoidally varying angle of attack in an oscillating flow, $k_V = 0.05$ (left) and 0.2 (right), $a = 0$, arbitrary motion theory (finite differences) compared with Isaacs' theory

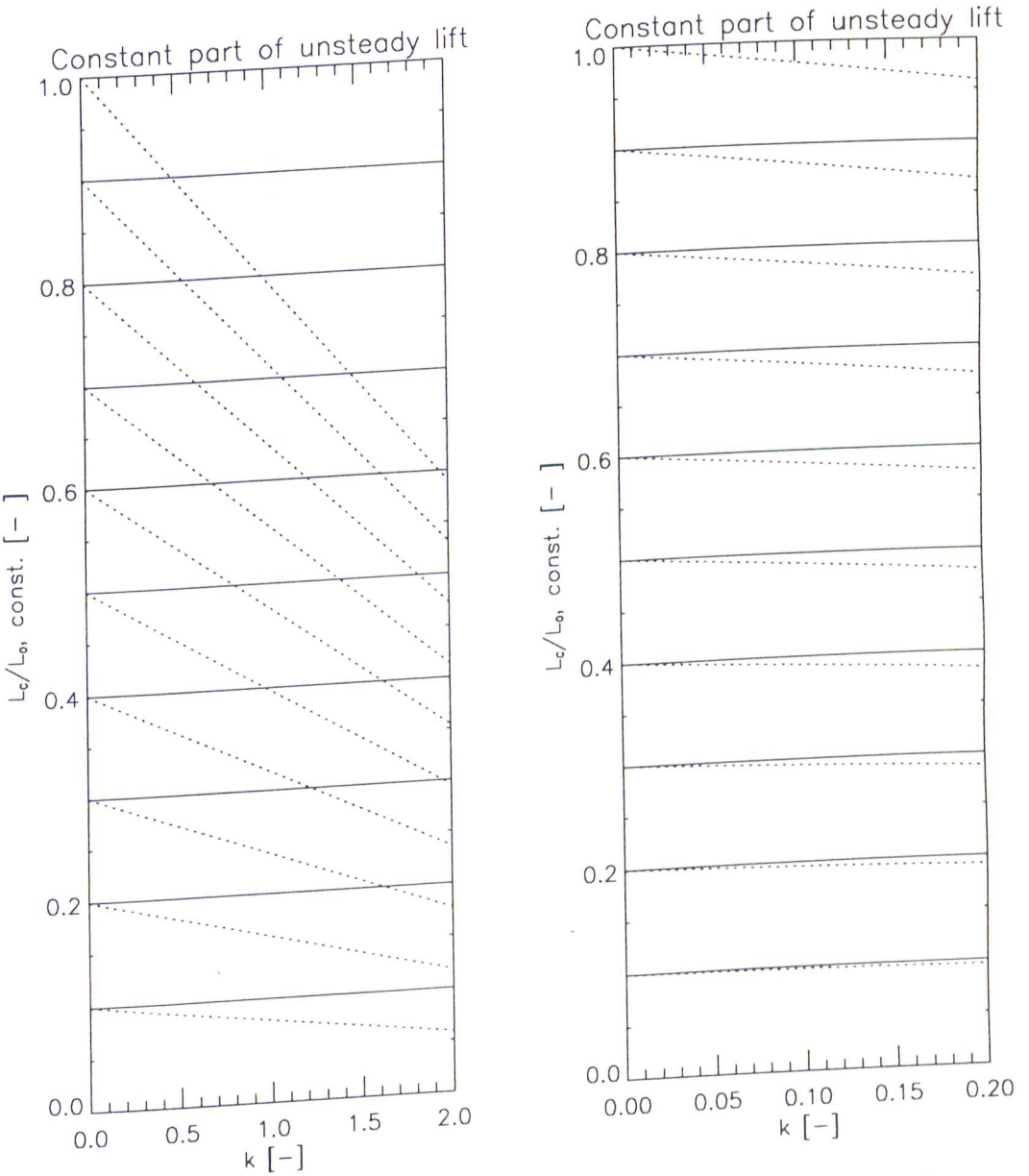

Figure 3.27: Lift transfer function for sinusoidally varying angle of attack in an oscillating flow, $a = 0$, arbitrary motion theory (finite differences) compared with Isaacs' theory

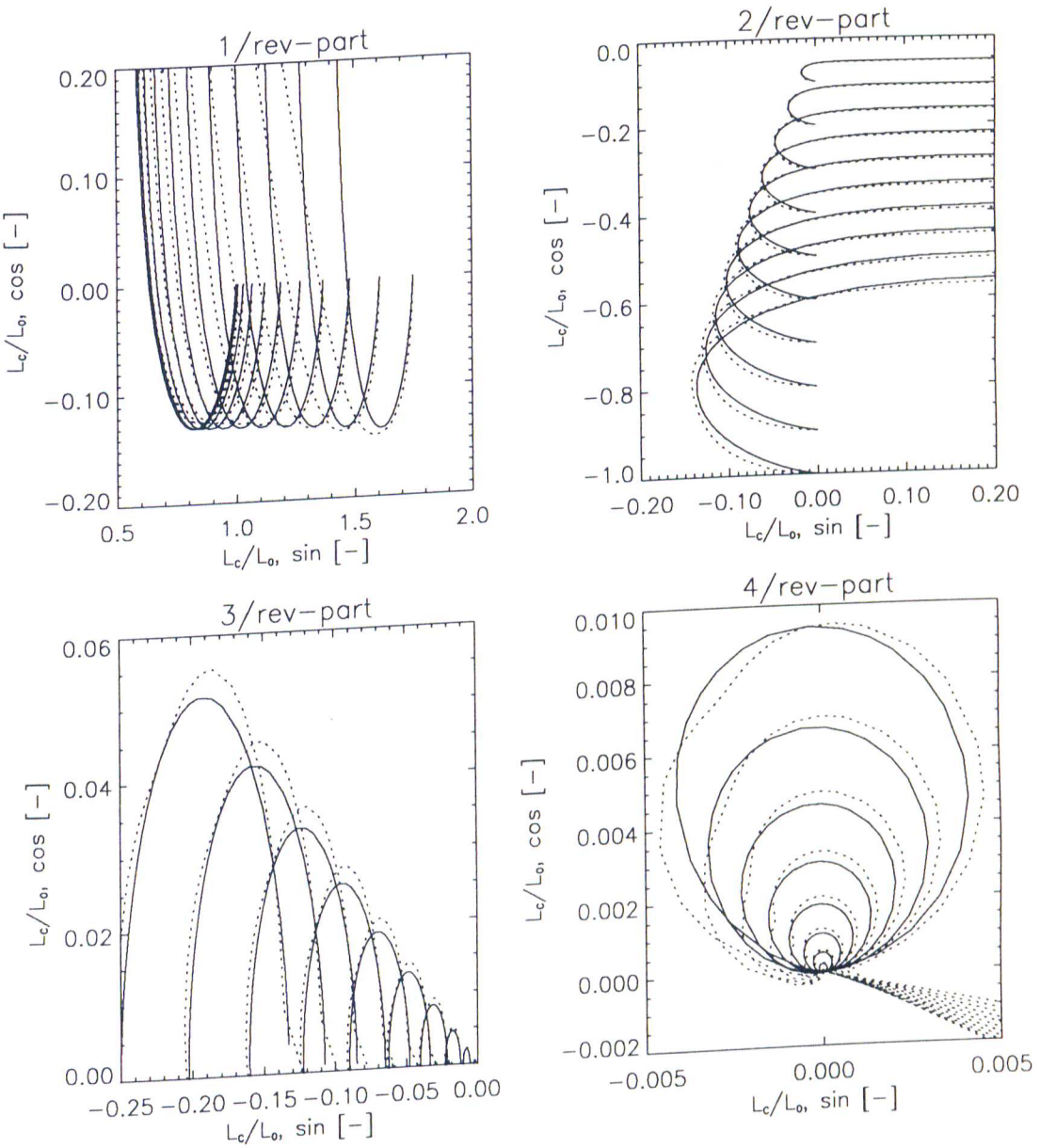

Figure 3.28: Lift transfer function for sinusoidally varying angle of attack in an oscillating flow, $a = 0$, arbitrary motion theory (finite differences) compared with Isaacs' theory

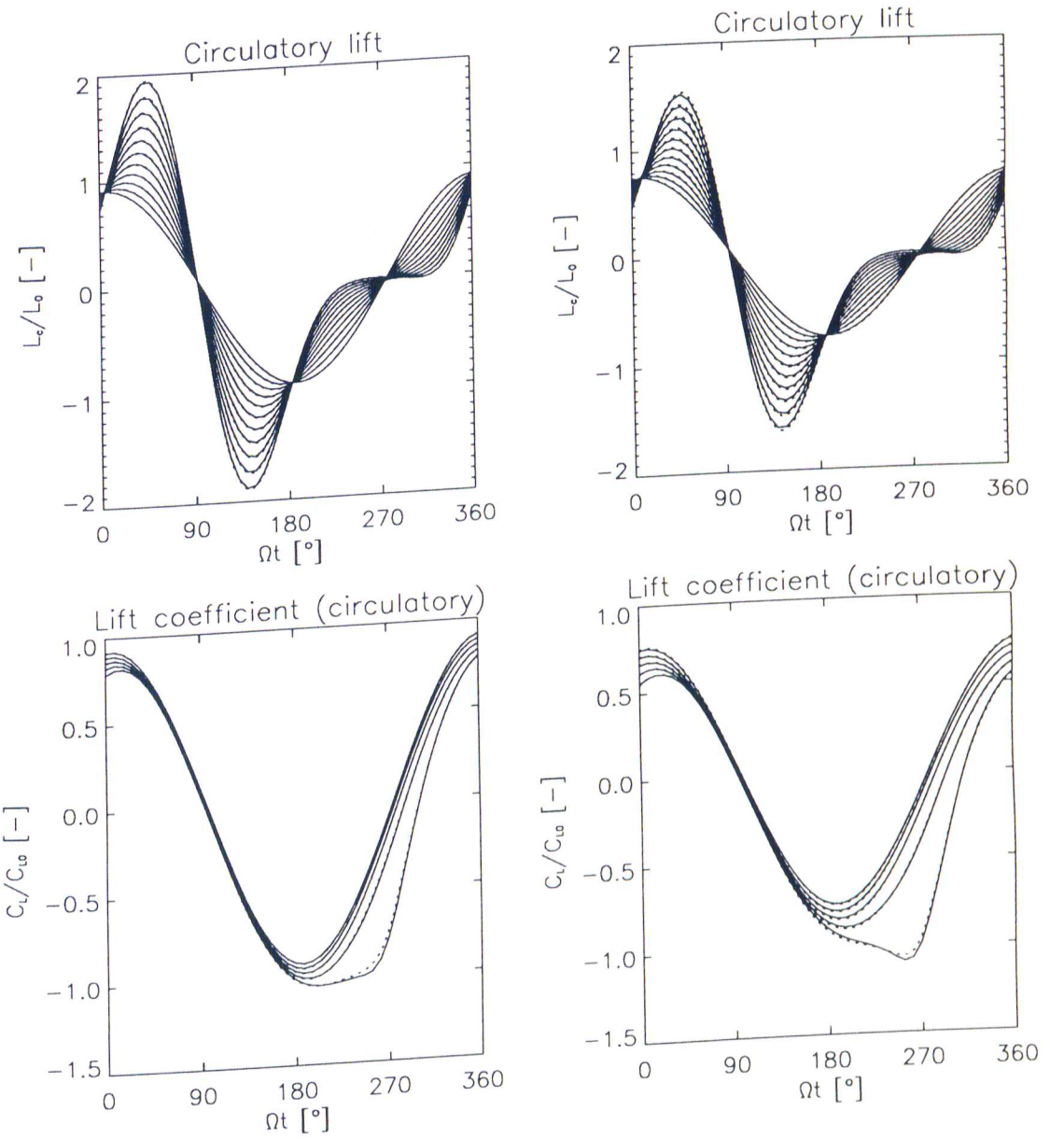

Figure 3.29: Unsteady lift development for sinusoidally varying angle of attack 90^o out-of-phase in an oscillating flow, $kv = 0.05$ (left) and 0.2 (right), $a = 0$, arbitrary motion theory (finite differences) compared with Isaacs' theory

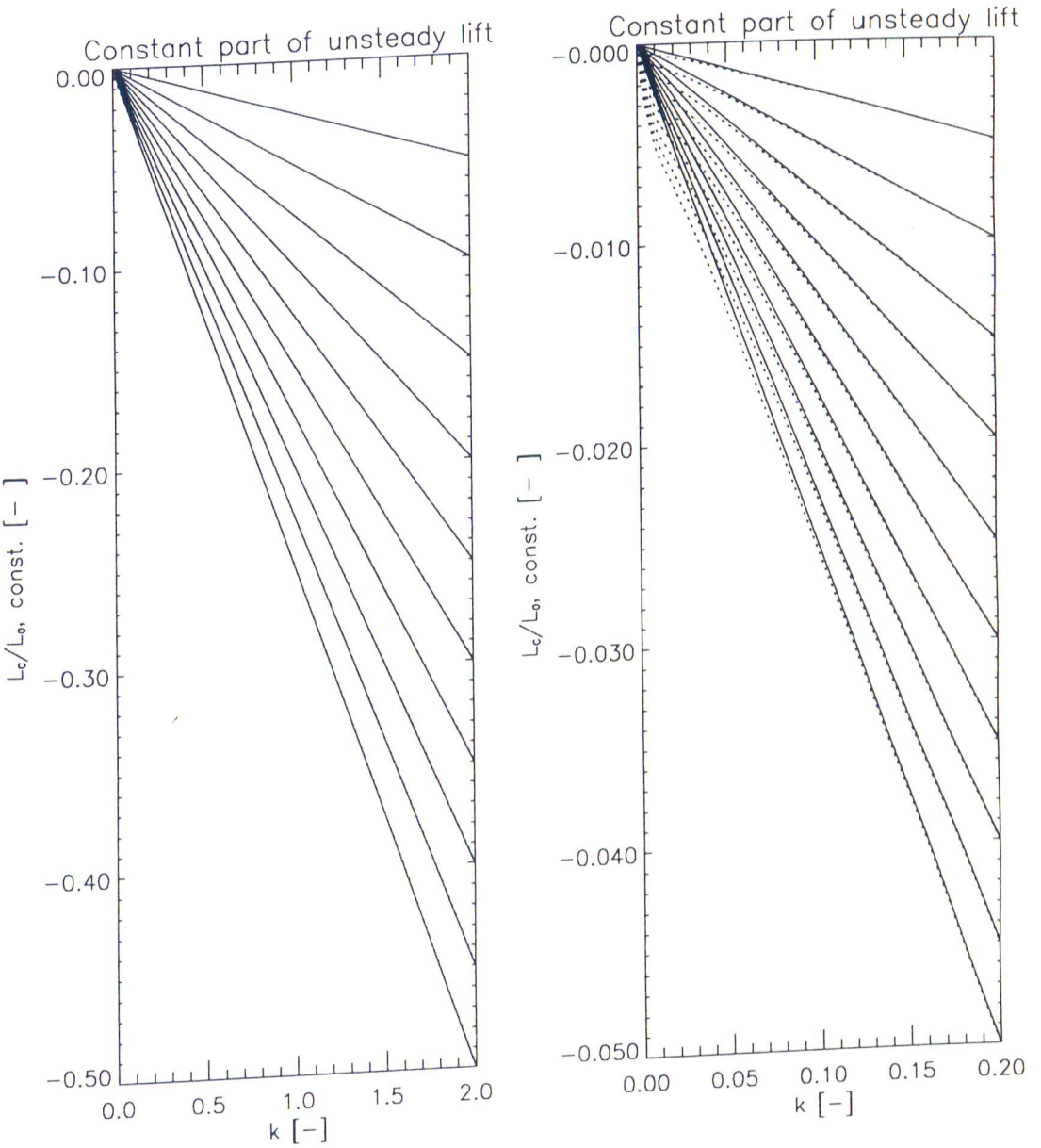

Figure 3.30: Lift transfer function for sinusoidally varying angle of attack 90^o out-of-phase in an oscillating flow, $a = 0$, arbitrary motion theory (finite differences) compared with Isaacs' theory

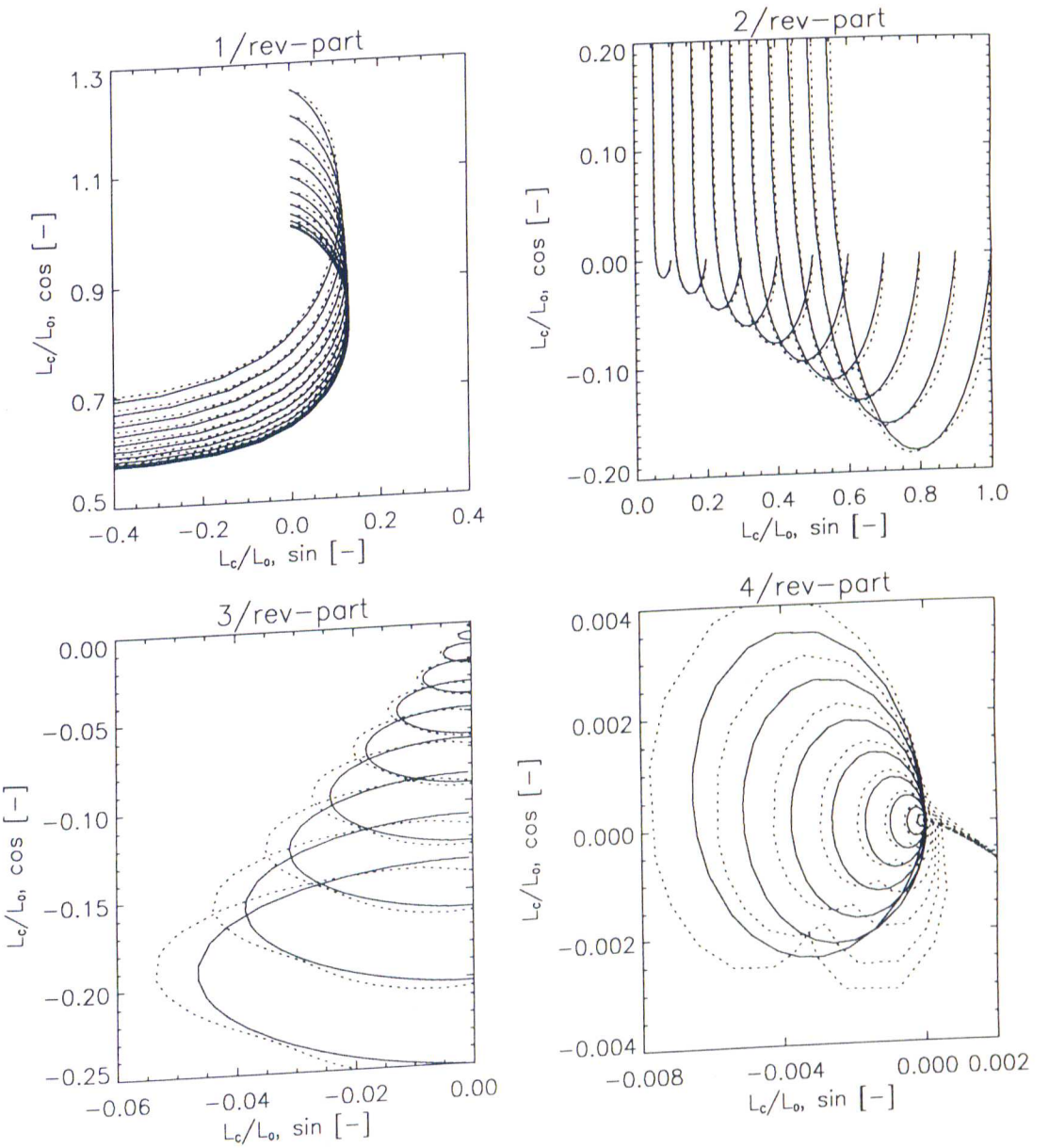

Figure 3.31: Lift transfer function for sinusoidally varying angle of attack 90° out-of-phase in an oscillating flow, $a = 0$, arbitrary motion theory (finite differences) compared with Isaacs' theory

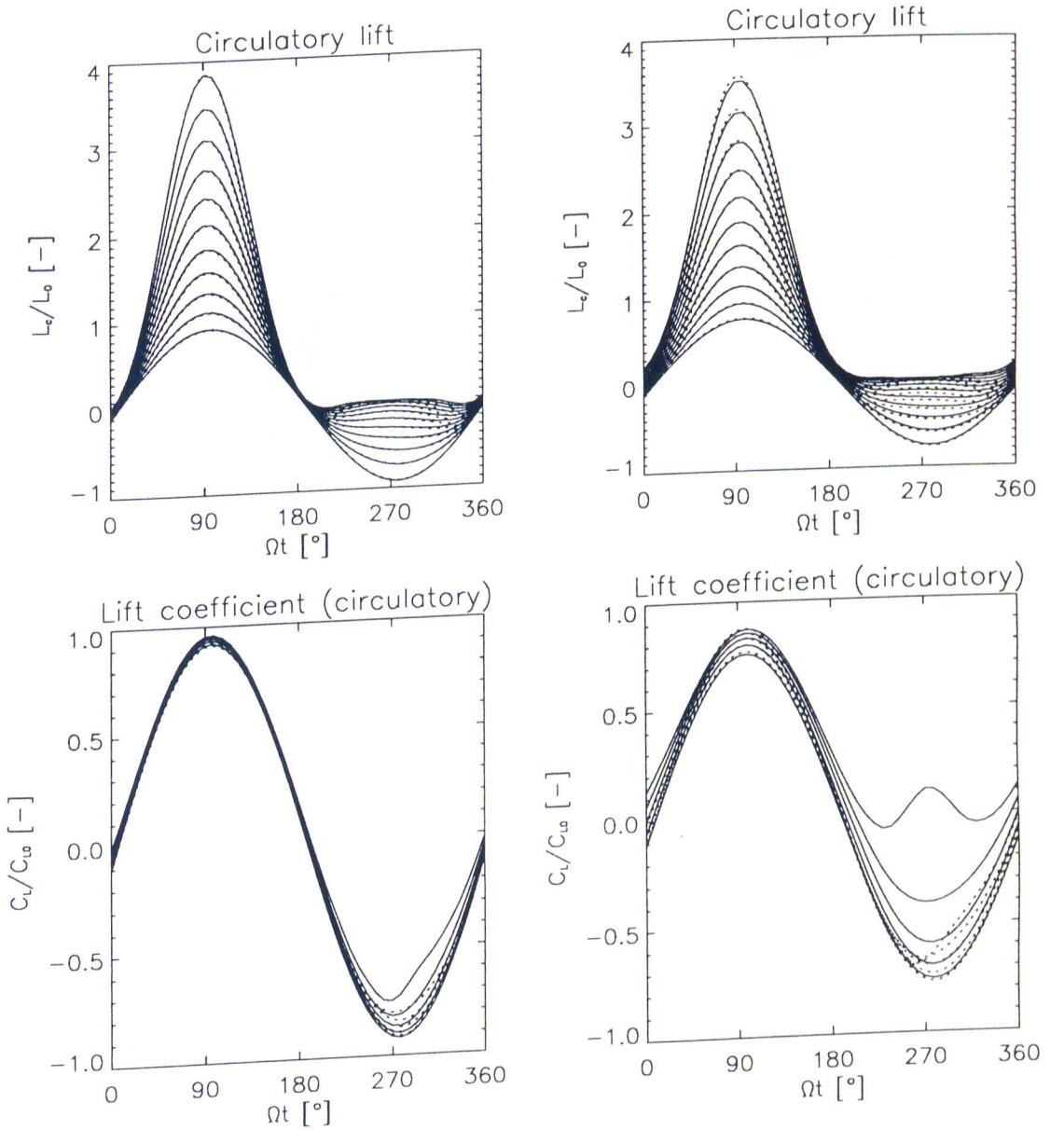

Figure 3.32: Unsteady lift development for sinusoidally varying angle of attack in an oscillating flow, $k_V = 0.05$ (left) and 0.2 (right), $a = 0$, arbitrary motion theory (finite differences, reduced algorithm) compared with Isaacs' theory

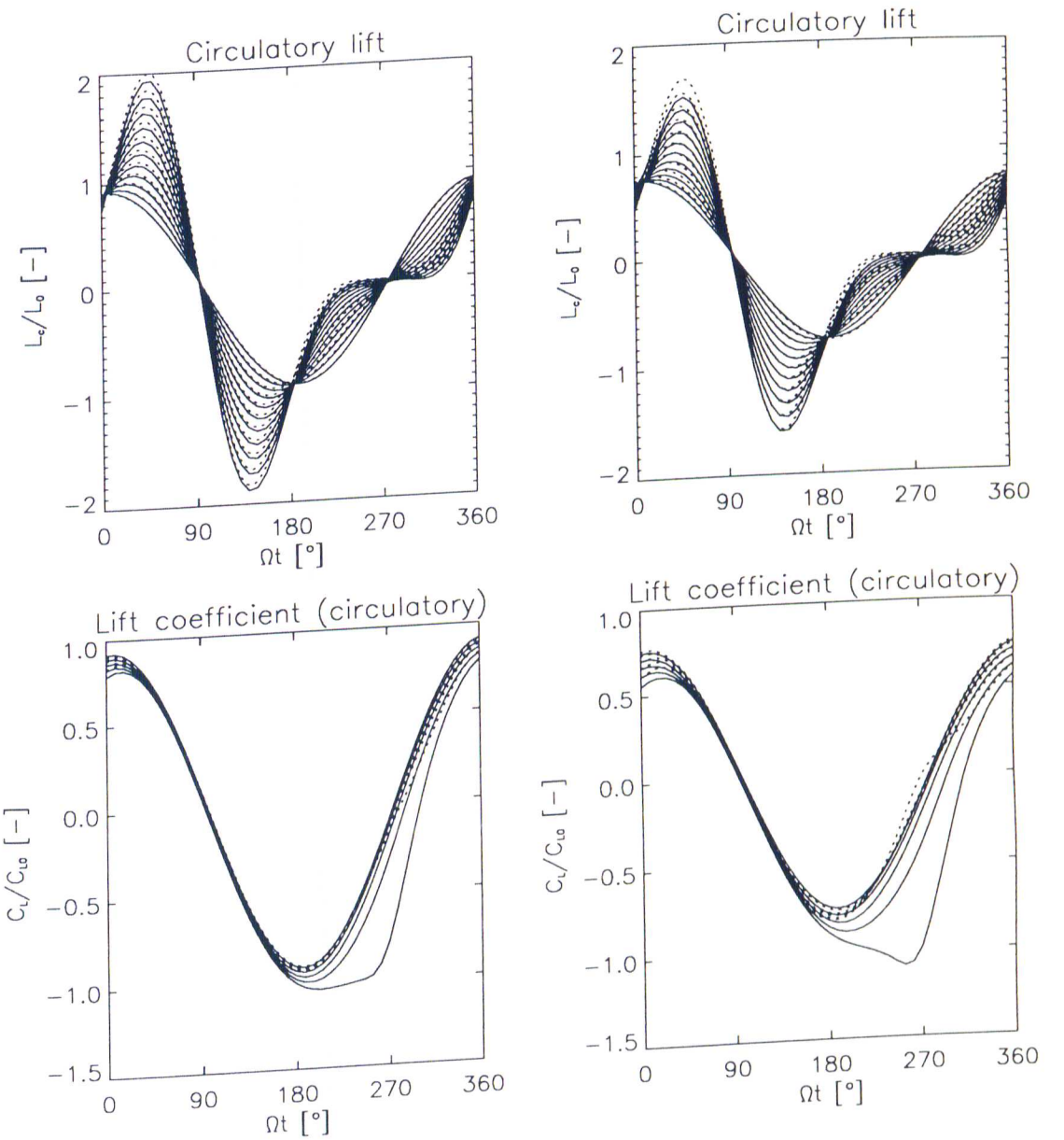

Figure 3.33: Unsteady lift development for sinusoidally varying angle of attack 90^o out-of-phase in an oscillating flow, $kv = 0.05$ (left) and 0.2 (right), $a = 0$, arbitrary motion theory (finite differences, reduced algorithm) compared with Isaacs' theory

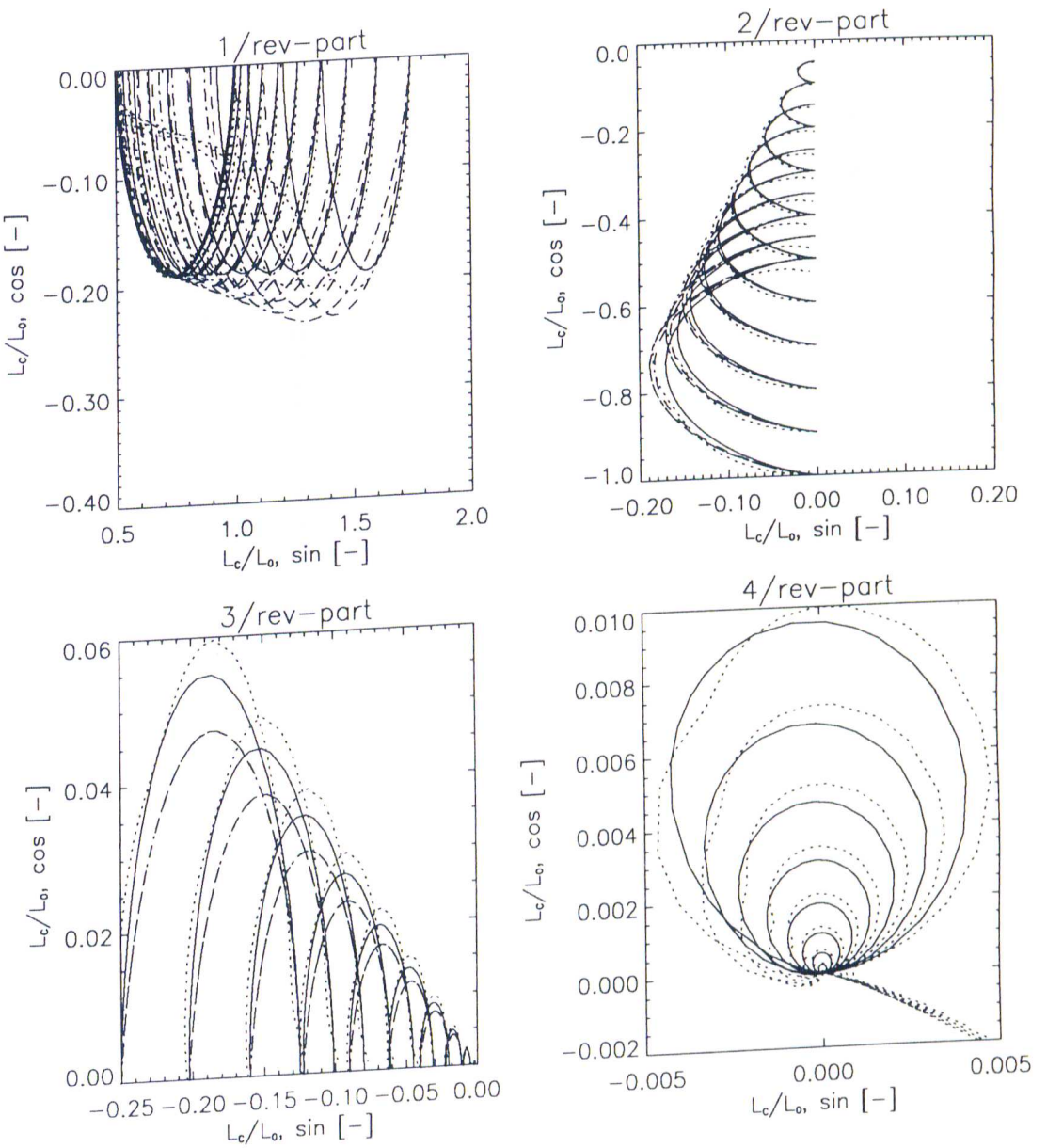

Figure 3.34: Lift transfer function for sinusoidally varying angle of attack about 3/4 chord in an oscillating flow, Isaacs' theory compared with Greenberg's, Kottapalli's and Theodorsen's theory

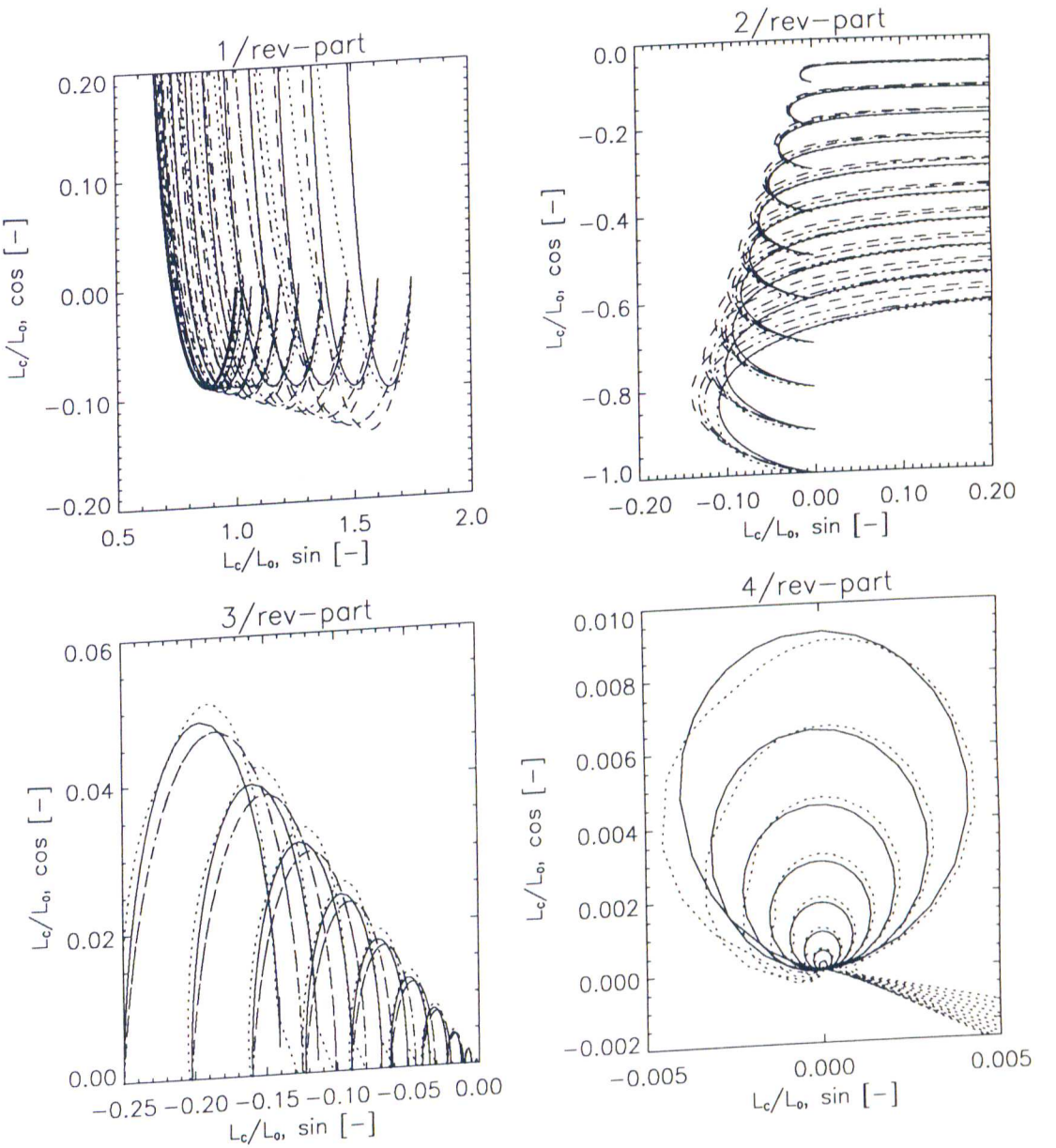

Figure 3.35: Lift transfer function for sinusoidally varying angle of attack about 1/4 chord in an oscillating flow, Isaacs' theory compared with Greenberg's, Kottapalli's and Theodorsen's theory

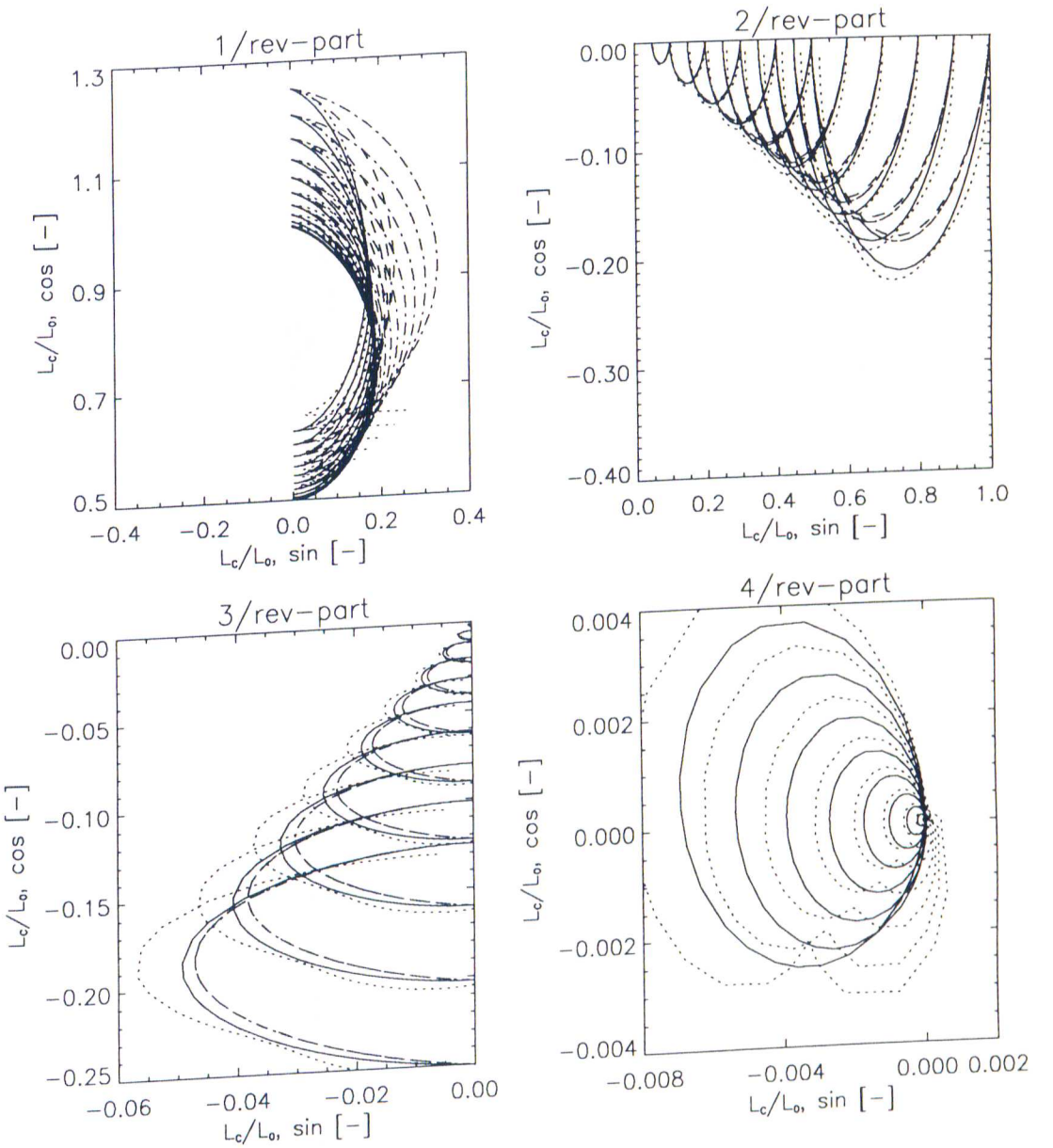

Figure 3.36: Lift transfer function for sinusoidally varying angle of attack 90^o out-of-phase about 3/4 chord in an oscillating flow, Isaacs' theory compared with Greenberg's, Kottapalli's and Theodorsen's theory

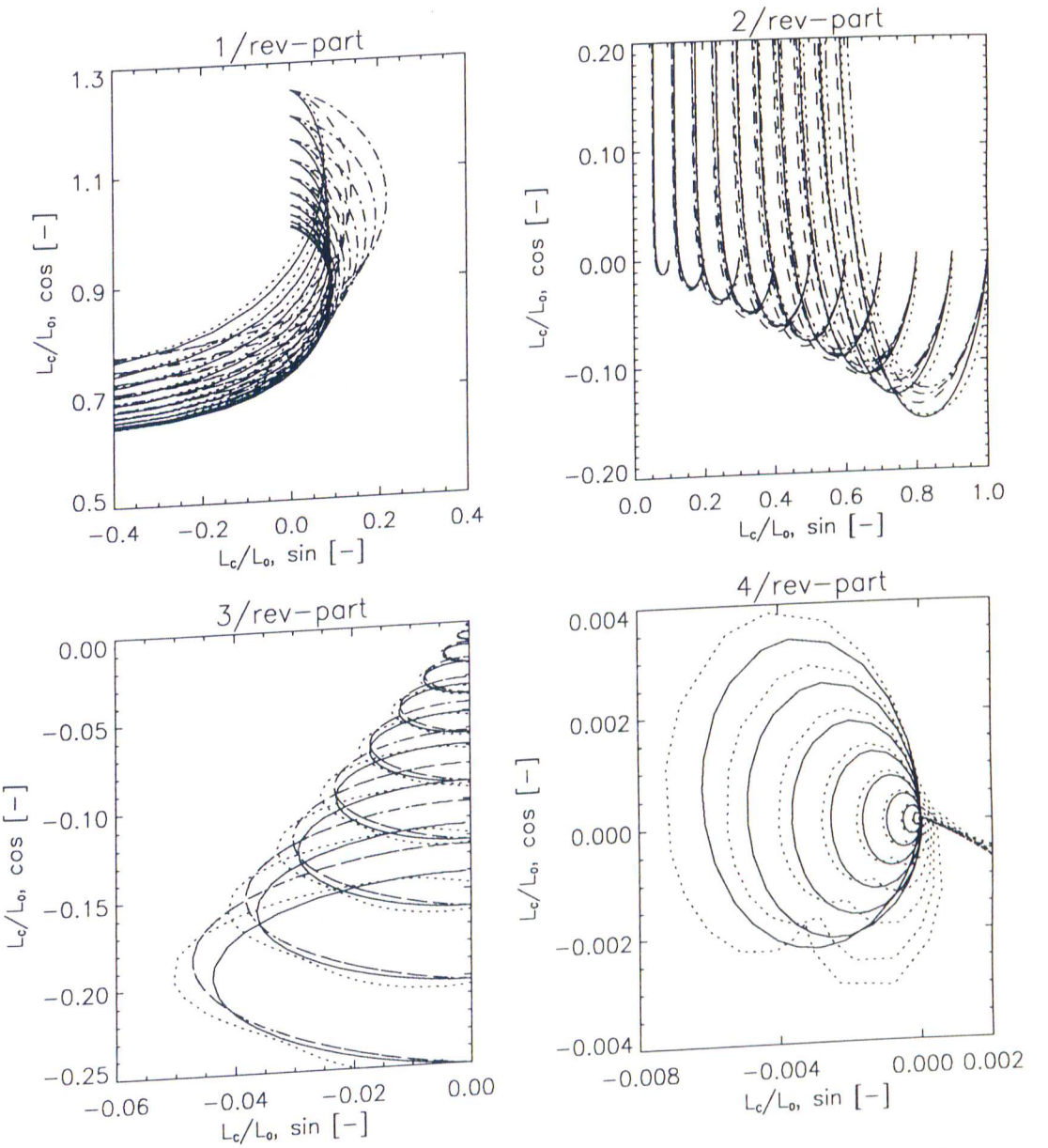

Figure 3.37: Lift transfer function for sinusoidally varying angle of attack 90° out-of-phase about 1/4 chord in an oscillating flow, Isaacs' theory compared with Greenberg's, Kottapalli's and Theodorsen's theory

Appendix A

Arbitrary Airfoil Motion in a Constant Freestream

Starting from the indicial function for a step change in angle of attack, the so called Wagner function

$$\phi\left(\frac{2V}{c}t\right) = \phi(s) = \sum_{i=1}^{N} A_i e^{b_i s} \tag{A.1}$$

and the Duhamel integral for superposition of steps to an arbitrary motion

$$L = \pi\rho\frac{c^2}{4}[\ddot{h} + V\dot{\alpha} - ba\ddot{\alpha}] + 2\pi\frac{\rho}{2}Vc\left[w_{3/4}(0)\phi(s) + \int_0^s \frac{\partial w_{3/4}}{\partial\sigma}\phi(s-\sigma)d\sigma\right] \tag{A.2}$$

one can obtain a closed form solution for harmonic motion in angle of attack and plunge.

$$\begin{aligned} \alpha &= \alpha_0[\bar{\alpha}_0 + \bar{\alpha}_{1S}\sin ks + \bar{\alpha}_{1C}\cos ks] \\ h &= \alpha_0\frac{c}{2}[\bar{h}_{1S}\sin ks + \bar{h}_{1C}\cos ks] \end{aligned} \tag{A.3}$$

The velocity at 3/4 chord is build up by vertical motion of the airfoil and the instantaneous angle of attack as well as its time derivative

$$w_{3/4} = V\alpha + \dot{h} + \frac{c}{2}\frac{1-2a}{2}\dot{\alpha} \tag{A.4}$$

The derivatives needed are

$$\begin{aligned}
\frac{\partial \alpha}{\partial \sigma} &= \alpha_0 k[\bar{\alpha}_{1S}\cos k\sigma - \bar{\alpha}_{1C}\sin k\sigma] \\
\frac{\partial \dot{\alpha}}{\partial \sigma} &= -\alpha_0 \frac{2V}{c} k^2[\bar{\alpha}_{1S}\sin k\sigma + \bar{\alpha}_{1C}\cos k\sigma] \\
\frac{\partial \dot{h}}{\partial \sigma} &= -\alpha_0 V k^2[\bar{h}_{1S}\sin k\sigma + \bar{h}_{1C}\cos k\sigma]
\end{aligned} \tag{A.5}$$

So the integral in the circulatory part of the lift becomes

$$\begin{aligned}
\int_0^s \frac{\partial w_{3/4}}{\partial \sigma}\phi(s-\sigma)d\sigma = \alpha_0 V \sum_{i=1}^{N} kA_i \int_0^s e^{b_i(s-\sigma)} \\
\times \left\{\left[\bar{\alpha}_{1S} - k\left(\tfrac{1-2a}{2}\bar{\alpha}_{1C} + \bar{h}_{1C}\right)\right]\cos k\sigma \right. \\
\left. - \left[\bar{\alpha}_{1C} + k\left(\tfrac{1-2a}{2}\bar{\alpha}_{1S} + \bar{h}_{1S}\right)\right]\sin k\sigma\right\} d\sigma
\end{aligned} \tag{A.6}$$

Now the integral can be evaluated by means of (for example [38], p. 566, No. 407 and 412)

$$\begin{aligned}
\int e^{-b_i\sigma}\cos k\sigma d\sigma &= \frac{e^{-b_i\sigma}}{b_i^2+k^2}(-b_i\cos k\sigma + k\sin k\sigma) \\
\int e^{-b_i\sigma}\sin k\sigma d\sigma &= \frac{e^{-b_i\sigma}}{b_i^2+k^2}(-b_i\sin k\sigma - k\cos k\sigma)
\end{aligned} \tag{A.7}$$

to get finally

$$\int_0^s \frac{\partial w_{3/4}}{\partial \sigma}\phi(s-\sigma)d\sigma = \alpha_0 V \sum_{i=1}^{N} B_{1i}\cos ks + B_{2i}\sin ks \tag{A.8}$$

with the coefficients

$$\begin{aligned}
B_{1i} &= \frac{A_i k}{b_i^2+k^2}(b_i C_1 + kC_2) \\
B_{2i} &= \frac{A_i k}{b_i^2+k^2}(kC_1 - b_i C_2) \\
C_1 &= \bar{\alpha}_{1S} - k\left(\frac{1-2a}{2}\bar{\alpha}_{1C} + \bar{h}_{1C}\right) \\
C_2 &= \bar{\alpha}_{1C} + k\left(\frac{1-2a}{2}\bar{\alpha}_{1S} + \bar{h}_{1S}\right)
\end{aligned} \tag{A.9}$$

Thus, one finally gets

$$
\begin{aligned}
L \;=\; & \pi\rho\frac{c^2}{4}[\ddot{h} + V\dot{\alpha} - ba\ddot{\alpha}] + 2\pi\frac{\rho}{2}V^2 c\alpha_0 \left\{ \bar{\alpha}_0 \right. \\
& + \left[\left(\bar{w}_{1S} + \bar{\alpha}_{1S} - k\frac{1-2a}{2}\bar{\alpha}_{1C} \right) \sin\omega t \right. \\
& \left. + \left(\bar{w}_{1C} + \bar{\alpha}_{1C} + k\frac{1-2a}{2}\bar{\alpha}_{1S} \right) \cos\omega t \right] \sum_{i=1}^{N} \frac{A_i k^2}{b_i^2 + k^2} \\
& + \left[\left(\bar{w}_{1S} + \bar{\alpha}_{1S} - k\frac{1-2a}{2}\bar{\alpha}_{1C} \right) \cos\omega t \right. \\
& \left. \left. - \left(\bar{w}_{1C} + \bar{\alpha}_{1C} + k\frac{1-2a}{2}\bar{\alpha}_{1S} \right) \sin\omega t \right] \sum_{i=1}^{N} \frac{A_i k b_i}{b_i^2 + k^2} \right.
\end{aligned}
\tag{A.10}
$$

Appendix B

Extension of Isaacs Theory

B.1 General Theory for an Airfoil Pitching about an Arbitrary Axis with Inplane and Plunging Motion

Ths derivation is made following that of Isaacs for constant and varying angle of attack about midchord [6, 7]. The purpose is to include the following extensions:

- The location of pitch axis on the airfoil chord now is arbitrary.
- Plunge motion is added as additional degree of freedom.
- Pitch and plunge are thought to be a Fourier series including higher harmonics.

Therefore the result is the general oscillating airfoil theory for incompressible inviscid flows while Theodorsens theory is restricted to a constant flow without inplane motion and Isaacs theory excludes the above given degrees of

freedom. In order to identify where the additional degrees of freedom change expressions, Isaacs theory has to rederived carefully.

Fig. 2.8 shows an airfoil pitching and undergoing fore-aft motion in a constant freestream of velocity V_0. We have the following equation for the normal velocity distribution along chord (small angles assumed)

$$v_n(x,t) = \alpha(t)V(t) + \left(x - a\frac{c}{2}\right)\dot{\alpha}(t) + \dot{h}(t) + v_{n,w}(x,t) \qquad \text{(B.1)}$$

Here the velocity $V(t)$ includes the freestream velocity V_0 and the velocity imposed by the fore-aft motion. The terms $-a(c/2)\dot{\alpha}(t) + \dot{h}(t)$ have been added to the expression given by Isaacs in [7]. Eq. B.1 is a function of all variables like time, coordinate, frequency and amplitudes of motion. In order to simplify it, the variables have to be separated and the first variable to be eliminated is the coordinate x.

B.1.1 Eliminating the Coordinate x

The induced velocity of the wake (index w) behind the airfoil $v_{n,w}(x,t)$, containing the shed vorticity, varies across the chord. At time τ the shed wake vorticity has a strength that is given by the time derivative of the bound vorticity $-\Gamma'(\tau)d\tau$, so that in incompressible flow the induced velocity can be calculated using

$$v_{n,w}(x,t) = -\frac{1}{2\pi}\int_{-\infty}^{t} \frac{\Gamma'(\tau)}{(c/2 - x) + [W(t) - W(\tau)]}d\tau \qquad \text{(B.2)}$$

Here $W(t)$ is the distance travelled by the airfoil, so that $dW(t)/dt = W'(t) = V(t)$. To simplify the derivation, one can use a coordinate transformation from x to an angular coordinate Θ, i.e.

$$x = \frac{c}{2}\cos\Theta \qquad \text{(B.3)}$$

In addition, the denominator of Eq. B.1 can be nondimensionalised by dividing by the airfoil semichord, $c/2$, as a reference length and separated into a part depending on the new coordinate Θ and another term containing a constant and time dependent part , i.e.,

$$v_{n,w}(\Theta,t) = -\frac{1}{\pi c}\int_{-\infty}^{t} \frac{\Gamma'(\tau)}{1+\frac{W(t)-W(\tau)}{c/2}-\cos\Theta}d\tau \tag{B.4}$$

Defining the variable $a_1(t,\tau)$ as

$$a_1(t,\tau) = 1 + \frac{W(t)-W(\tau)}{c/2} \geq 1 \tag{B.5}$$

the induced velocity is

$$v_{n,w}(\Theta,t) = -\frac{1}{\pi c}\int_{-\infty}^{t} \frac{\Gamma'(\tau)}{a_1(t,\tau)-\cos\Theta}d\tau \tag{B.6}$$

Expanding this into a Fourier series one obtains

$$\frac{1}{a_1(t,\tau)-\cos\Theta} = \frac{\gamma_0(t,\tau)}{2} + \sum_{n=1}^{\infty}\gamma_n(t,\tau)\cos n\Theta \tag{B.7}$$

The Fourier coefficients are obtained from an integral evaluation:

$$\frac{2}{\pi}\int_0^{\pi}\frac{\cos n\Theta}{a_1-\cos\Theta}d\Theta = \begin{cases} 2\dfrac{\left[a_1-\sqrt{a_1^2-1}\right]^n}{\sqrt{a_1^2-1}} & \text{if} \quad a_1 > 1 \\ -2\sin n\Theta/\sin\Theta & \text{if} \quad -1 < a_1 < 1 \end{cases} \tag{B.8}$$

Therefore, from B.8 the coefficients in Eq. B.7 are

$$\gamma_n(t,\tau) = 2\frac{\left[a_1(t,\tau)-\sqrt{a_1^2(t,\tau)-1}\right]^n}{\sqrt{a_1^2(t,\tau)-1}} \tag{B.9}$$

The induced velocity distribution can be replaced by a Fourier series

$$v_{n,w}(\Theta,t) = \frac{b_0(t)}{2} + \sum_{n=1}^{\infty} b_n(t)\cos n\Theta \tag{B.10}$$

and the coefficients of this series are found by comparison with Eq. B.6 to be

$$\begin{aligned} b_n(t) &= -\frac{1}{\pi c}\int_{-\infty}^{t} \Gamma'(\tau)\gamma_n(t,\tau)d\tau \\ &= -\frac{2}{\pi c}\int_{-\infty}^{t} \Gamma'(\tau)\frac{\left[a_1(t,\tau)-\sqrt{a_1^2(t,\tau)-1}\,\right]^n}{\sqrt{a_1^2(t,\tau)-1}}d\tau \end{aligned} \qquad \text{(B.11)}$$

The airfoil is considered as a bound vortex sheet (index b) with unknown strength $\gamma_b(\Theta,t)$. The self-induced normal velocity is given by

$$v_{n,b}(\Theta,t) = \frac{1}{2\pi}\int_0^{\pi} \frac{\gamma_b(\phi,t)\sin\phi}{\cos\Theta-\cos\phi}d\phi \qquad \text{(B.12)}$$

The nominator of Eq. B.12, as well as the self-induced velocity, can be written as a Fourier series

$$\begin{aligned} v_{n,b}(\Theta,t) &= \frac{1}{2\pi}\int_0^{\pi} \frac{c_0(t)+\sum_{n=1}^{\infty} c_n(t)\cos n\phi}{\cos\Theta-\cos\phi}d\phi \\ &= \frac{c_0(t)}{2\pi}\int_0^{\pi}\frac{1}{\cos\Theta-\cos\phi}d\phi + \sum_{n=1}^{\infty}\frac{c_n(t)}{2\pi}\int_0^{\pi}\frac{\cos n\phi}{\cos\Theta-\cos\phi}d\phi \\ &= \frac{d_0(t)}{2}+\sum_{n=1}^{\infty} d_n(t)\cos n\Theta \end{aligned} \qquad \text{(B.13)}$$

Using the integral relation in Eq. B.8 for the calculation of the coefficients and a sequence of trigonometrical relationships, the relationship between the bound vorticity and the induced normal velocity coefficients are found to be

$$c_n(t) = d_{n+1}(t) - d_{n-1}(t) \qquad n>0 \qquad \text{(B.14)}$$

It is necessary to satisfy the requirement of flow tangency on the surface of the airfoil. This means that the self-induced normal velocity equals the other contributions so that the net velocity normal to the airfoil surface is zero,

i.e.,

$$0 = \alpha(t)V(t) + \left(x - a\frac{c}{2}\right)\dot{\alpha}(t) + \dot{h}(t) + v_{n,w}(x,t) - v_{n,b}(x,t) \qquad \text{(B.15)}$$

Putting into the Fourier series for the wake-induced velocity (Eq. B.10) and self-induced velocity (Eq. B.13), one obtains

$$\begin{aligned} 0 = \alpha(t)V(t) + \frac{c}{2}(\cos\Theta - a)\dot{\alpha}(t) + \dot{h}(t) + \frac{b_0(t) - d_0(t)}{2} \\ + \sum_{n=1}^{\infty}[b_n(t) - d_n(t)]\cos n\Theta \end{aligned} \qquad \text{(B.16)}$$

A comparison of the coefficients of Eq. B.10 and Eq. B.14 gives

$$c_0(t) = b_1(t) + b_0(t) + 2\alpha(t)V(t) + \frac{c}{2}(1 - 2a)\dot{\alpha}(t) + 2\dot{h}(t) \qquad \text{(B.17)}$$

$$c_1(t) = b_2(t) - b_0(t) - 2\alpha(t)V(t) + ac\dot{\alpha}(t) - 2\dot{h}(t) \qquad \text{(B.18)}$$

$$c_2(t) = b_3(t) - b_1(t) - \frac{c}{2}\dot{\alpha}(t) \qquad \text{(B.19)}$$

$$c_n(t) = b_{n+1}(t) - b_{n-1}(t) \qquad n > 2 \qquad \text{(B.20)}$$

All terms with $a\dot{\alpha}$ and $\dot{h}$ have been added to the expressions given by Isaacs [7]. The coefficient c_0 is found by invoking the Kutta condition at the trailing edge where the bound vorticity $\gamma_b(c/2, t) = 0$. This and the fact that the Fourier coefficients $b_n \to 0$ for $n \to \infty$, implies that

$$c_0(t) = -\sum_{n=1}^{\infty} c_n(t) \qquad \text{(B.21)}$$

and gives the result in Eq. B.17. The total circulation about the airfoil is the integral of the bound vorticity over the surface. In the following, the change of variable in Eq. B.3 is used, as well as a change in limits of integration

$$\Gamma(t) = \int_{-c/2}^{c/2} \gamma_b(x,t)\, dx$$

$$
\begin{aligned}
&= -\int_{\pi}^{0} \gamma_b(\Theta,t)\frac{c}{2}\sin\Theta\, d\Theta \\
&= \frac{c}{2}\int_{0}^{\pi} \gamma_b(\Theta,t)\sin\Theta\, d\Theta \\
&= \frac{c}{2}\int_{0}^{\pi} \left[c_0(t) + \sum_{n=1}^{\infty} c_n(t)\cos n\Theta\right] d\Theta \\
&= \frac{\pi c}{2} c_0(t)
\end{aligned}
\tag{B.22}
$$

Setting the previous expression for $c_0(t)$ in Eq. B.17 into Eq. B.22 and using the coefficients $b_0(t)$ and $b_1(t)$ given by Eq. B.11, the expression for the circulation becomes

$$
\begin{aligned}
\Gamma(t) = \; & \frac{\pi c}{2}[2\alpha(t)V(t) + \frac{c}{2}(1-2a)\dot{\alpha}(t) + 2\dot{h}(t)] \\
& -\int_{-\infty}^{t} \Gamma'(\tau)\frac{1 + a_1(t,\tau) - \sqrt{a_1^2(t,\tau)-1}}{\sqrt{a_1^2(t,\tau)-1}} d\tau
\end{aligned}
\tag{B.23}
$$

and the local coordinate x has been eliminated from the aerodynamic problem. It remains an equation for the circulation as a function of itself to be solved.

B.1.2 The Integral Equation for the Circulation

Rearranging Eq. B.23 and resubstituting $a_1(t,\tau)$ from Eq. B.5 leads to

$$
\frac{\pi c}{2}[2\alpha(t)V(t) + \frac{c}{2}(1-2a)\dot{\alpha}(t) + 2\dot{h}(t)] = \Gamma(t) + \int_{-\infty}^{t} \Gamma'(\tau)\left[\sqrt{\frac{a_1(t,\tau)+1}{a_1(t,\tau)-1}} - 1\right] d\tau
\tag{B.24}
$$

For brevity, the left side of Eq. B.24 may be denoted as a time varying function $g(t)$.

$$
g(t) = \Gamma(t) + \int_{-\infty}^{t} \Gamma'(\tau)\left[\sqrt{\frac{1 + \frac{W(t)-W(\tau)}{c/2} + 1}{1 + \frac{W(t)-W(\tau)}{c/2} - 1}} - 1\right] d\tau
$$

$$= \Gamma(t) + \int_{-\infty}^{t} \Gamma'(\tau) \left[\sqrt{\frac{c}{W(t) - W(\tau)} + 1} - 1 \right] d\tau \qquad \text{(B.25)}$$

With the substitution $T = t - \tau$, $dT = -d\tau$ the limits of integration change from $\tau = t$ to $T = 0$ and from $\tau = -\infty$ to $T = t + \infty = \infty$.

$$\begin{aligned} g(t) &= \Gamma(t) - \int_{\infty}^{0} \Gamma'(t-T) \left[\sqrt{\frac{c}{W(t) - W(t-T)} + 1} - 1 \right] dT \\ &= \Gamma(t) + \int_{0}^{\infty} \Gamma'(t-T) \left[\sqrt{\frac{c}{W(t) - W(t-T)} + 1} - 1 \right] dT \end{aligned} \qquad \text{(B.26)}$$

A second transformation brings this into a more managable form. Denoting $W(t)$ as an independent variable instead of time t, and therefore setting $\Gamma(t) = Q(W(t))$ and $\Gamma(t-T) = Q(W(t-T)) = Q(X)$ with $X = W(t-T)$ gives

$$g(t) = Q(W(t)) + \int_{-\infty}^{W(t)} Q'(X) \left[\sqrt{\frac{c}{W(t) - X} + 1} - 1 \right] dX \qquad \text{(B.27)}$$

Now a third transformation is made, using $\Lambda = W(t) - X$, and again changing the limits of integration yields finally

$$g(t) = Q(W(t)) + \int_{0}^{\infty} Q'(W(t) - \Lambda) \left[\sqrt{\frac{c}{\Lambda} + 1} - 1 \right] d\Lambda \qquad \text{(B.28)}$$

This is the sought after relationship between velocity, angle of attack and circulation. If the circulation Q is given, then Eq. B.28 is a differential equation for W and α. If the latter are given, then Eq. B.28 is an integral equation for the circulation Q. By integration of the velocity, the distance travelled W is known, and may be inverted to give t as a function of W. This can be substituted in $g(t)$ so that the left side of Eq. B.28 also becomes a function of W.

By the same transformations one finds for the Fourier coefficients of the wake-induced velocity

$$b_n(t) = -\frac{2}{\pi c}\int_0^\infty Q'(W(t)-\Lambda)\frac{\left[a_2(\Lambda)-\sqrt{a_2^2(\Lambda)-1}\,\right]^n}{\sqrt{a_2^2(\Lambda)-1}}d\Lambda \qquad \text{(B.29)}$$

where $a_2(\Lambda) = 1 + 2\Lambda/c$.

B.2 Periodic Fore-aft Motion

Until now, no use has been made of a specific function for the velocity $V(t)$ or the angle of attack variations $\alpha(t)$, or the plunge motion $h(t)$. In rotary wing aircraft problems all the V, α, and h are periodic in time with a basic frequency ω. In general the total velocity, consisting of a constant freestream velocity V_0 and a fore-aft motion V_x, can be written as

$$V_x(t) = \bar{V}_x \sin\omega t \qquad \text{(B.30)}$$

$$V(t) = V_0(1 + \lambda \sin\omega t) \qquad \text{(B.31)}$$

where $\lambda = \bar{V}_x/V_0$ is the nondimensional amplitude of fore-aft velocity. Therefore the distance travelled by the airfoil through the flow is

$$W(t) = \int V(t)dt = V_0\left(t - \frac{\lambda}{\omega}\cos\omega t\right) \qquad \text{(B.32)}$$

and using the abbreviation in Eq. B.5, $a_1(t,\tau)$ becomes

$$a_1(t,\tau) = 1 + \frac{2V_0}{c}\left[t - \tau - \frac{\lambda}{\omega}(\cos\omega t - cos\omega\tau)\right] \geq 1 \qquad \text{(B.33)}$$

The left side of Eq. B.28 will also be periodic in time, and can be written, in general, as

$$g(t) = \sum_{n=-\infty}^{\infty} g_n e^{in\omega t} = \sum_{n=-\infty}^{\infty} g_n e^{in\psi} \qquad \text{(B.34)}$$

with the nondimensional time variable ψ that can be interpreted as the rotor azimuth. The circulation must also be periodic and therefore Q can be written as

$$Q(W(t)) = \sum_{n=-\infty}^{\infty} a_n e^{in(\omega/V_0)W(t)} \tag{B.35}$$

Because Q has to be real, the coefficients will be $a_{(-n)} = \bar{a}_n$. Also

$$\frac{dQ(W(t)-\Lambda)}{dW(t)} = Q'(W(t)-\Lambda) = \sum_{n=-\infty}^{\infty} a_n in \frac{\omega}{V_0} e^{in(\omega/V_0)(W(t)-\Lambda)} \tag{B.36}$$

B.2.1 Separating the Reduced Frequency Effect and the Freestream Amplitude Effect

As known from Theodorsen's theory the reduced frequency appears in Bessel functions as the argument. The same can be expected here for the reduced frequency k as well as for the freestream amplitude λ. Inserting the series for the circulation into the integral equation of Eq. B.28 gives

$$\sum_{n=-\infty}^{\infty} g_n e^{in\psi} = \sum_{n=-\infty}^{\infty} a_n e^{in(\omega/V_0)W(t)} \left\{1 + in\frac{\omega}{V_0}\int_0^{\infty} e^{-in(\omega/V_0)\Lambda}\left[\sqrt{\frac{c}{\Lambda}+1}-1\right]d\Lambda\right\} \tag{B.37}$$

or

$$\sum_{n=-\infty}^{\infty} g_n e^{in\psi} = \sum_{n=-\infty}^{\infty} A_n e^{in(\omega/V_0)W(t)} \tag{B.38}$$

with

$$\begin{aligned} A_n &= a_n\left\{1 + in\frac{\omega}{V_0}\int_0^{\infty} e^{-in(\omega/V_0)\Lambda}\left[\sqrt{\frac{c}{\Lambda}+1}-1\right]d\Lambda\right\} \\ &= a_n R_n \end{aligned} \tag{B.39}$$

By defining the reduced frequency as

$$k = \frac{\omega c}{2V_0} \tag{B.40}$$

Eq. B.39 becomes

$$A_n = a_n \left\{ 1 + ink\frac{c}{2} \int_0^\infty e^{-ink(2\Lambda/c)} \left[\sqrt{\frac{c}{\Lambda} + 1} - 1 \right] d\Lambda \right\} \tag{B.41}$$

From a comparison of the coefficients, it follows that

$$\begin{aligned} R_0 &= 1 \\ R_n &= \Psi\left(n\frac{\omega c}{2V_0}\right) = \Psi(nk) \\ R_{(-n)} &= \bar{R}_n \end{aligned} \tag{B.42}$$

where Eq. B.42 results from the fact Eq. B.38 is real. The function Ψ is a function of multiples of the reduced frequency. Here the transformation $\bar{\Lambda} = n(\omega/V_0)\Lambda$ with $d\lambda = d\bar{\Lambda}/[n(\omega/V_0)]$ is applied, thus

$$\Psi(nk) = 1 + i \int_0^\infty e^{-i\bar{\Lambda}} \left[\sqrt{\frac{2nk}{\bar{\Lambda}} + 1} - 1 \right] d\bar{\Lambda} \tag{B.43}$$

The coefficients A_n are obtained by multiplying both sides of Eq. B.38 by $(1 + \lambda \sin\psi)e^{-im(\psi - \lambda\cos\psi)}$ and integrating from 0 to 2π. The advantage is to use the following relationship in which we substitute $\kappa = \psi - \lambda\cos\psi$ with $d\psi = d\kappa/(1 + \lambda\sin\psi)$

$$\int_0^{2\pi} (1 + \lambda\sin\psi) e^{i(n-m)(\psi - \lambda\cos\psi)} d\psi = \int_{-\lambda}^{2\pi - \lambda} e^{i(n-m)\kappa} d\kappa = \begin{cases} 0 & m = n \\ 2\pi & m \neq n \end{cases} \tag{B.44}$$

Therefore,

$$\begin{aligned} A_n &= \frac{1}{2\pi} \sum_{m=-\infty}^{\infty} g_m \int_0^{2\pi} (1 + \lambda\sin\psi) e^{i(m-n)\psi} e^{in\lambda\cos\psi} d\psi \\ &= \frac{i^n}{n} \sum_{m=-\infty}^{\infty} \frac{m}{i^m} g_m J_{n-m}(n\lambda) \qquad n \neq 0 \end{aligned} \tag{B.45}$$

$$A_0 = g_0 - \frac{\lambda}{2i}(g_1 - \bar{g}_1) \tag{B.46}$$

The J_{n-m} are the well known Bessel functions, here with multiples of the nondimensional amplitude of the fore-aft motion, λ, as the argument. By this procedure the variables reduced frequency and freestream amplitude have been separated in form of the functions $R_n(nk)$ and $J_{n-m}(n\lambda)$.

B.2.2 Periodic Angle of Attack and Plunge Motion

Now the expression for the angle of attack as well as for plunge motion has to be introduced. Here, both are assumed to be a Fourier series; later only the $1/rev$ component will be used.

$$\alpha(t) = \alpha_0 \left[\bar{\alpha}_0 + \sum_{n=1}^{\infty} (\bar{\alpha}_{nS} \sin n\psi + \bar{\alpha}_{nC} \cos n\psi) \right] \tag{B.47}$$

$$h(t) = \frac{c}{2} \alpha_0 \sum_{n=1}^{\infty} (\bar{h}_{nS} \sin n\psi + \bar{h}_{nC} \cos n\psi) \tag{B.48}$$

The expression for the velocity was given in Eq. B.31 so that $g(t)$ in Eq. B.25 takes the form

$$\begin{aligned} g(\psi) = \frac{\pi c}{2} \Bigg\{ & 2\alpha_0 V_0 \left[\bar{\alpha}_0 + \sum_{n=1}^{\infty} (\bar{\alpha}_{nS} \sin n\psi + \bar{\alpha}_{nC} \cos n\psi) \right] (1 + \lambda \sin \psi) \\ & + 2\alpha_0 V_0 k \sum_{n=1}^{\infty} n (\bar{h}_{nS} \cos n\psi - \bar{h}_{nC} \sin n\psi) \\ & + \alpha_0 \frac{\omega c}{2} (1 - 2a) \sum_{n=1}^{\infty} n (\bar{\alpha}_{nS} \cos n\psi - \bar{\alpha}_{nC} \sin n\psi) \Bigg\} \end{aligned} \tag{B.49}$$

A rearrangement leads to

$$
\begin{aligned}
g(\psi) = hV_0 \Bigg\{ & \bar{\alpha}_0 + \frac{\lambda}{2}\bar{\alpha}_{1S} \\
& + \left[\bar{\alpha}_{1C} + k\left(\frac{1-2a}{2}\bar{\alpha}_{1S} + \bar{h}_{1S}\right) + \frac{\lambda}{2}\bar{\alpha}_{2S} \right] \cos\psi \\
& + \left[\lambda\bar{\alpha}0 + \bar{\alpha}_{1S} - k\left(\frac{1-2a}{2}\bar{\alpha}_{1C} + \bar{h}_{1C}\right) - \frac{\lambda}{2}\bar{\alpha}_{2C} \right] \sin\psi \\
& + \sum_{n=2}^{\infty} \left[\bar{\alpha}_{nC} + nk\left(\frac{1-2a}{2}\bar{\alpha}_{nS} + \bar{h}_{nS}\right) + \frac{\lambda}{2}\left(\bar{\alpha}_{(n+1)S} - \bar{\alpha}_{(n-1)S}\right) \right] \cos n\psi \\
& + \sum_{n=2}^{\infty} \left[\bar{\alpha}_{nS} - nk\left(\frac{1-2a}{2}\bar{\alpha}_{nC} + \bar{h}_{nC}\right) - \frac{\lambda}{2}\left(\bar{\alpha}_{(n+1)C} - \bar{\alpha}_{(n-1)C}\right) \right] \sin n\psi \Bigg\}
\end{aligned}
\tag{B.50}
$$

where h stands for $h = \pi c\alpha_0$. The extension to arbitrary pitch axis location and plunge motion is to be seen in the terms with a, $\bar{h}_{nS}$ and $\bar{h}_{nC}$, all known from Theodorsen's result. Basically $g(\psi)$ is of the form

$$
g(\psi) = G_0 + \sum_{n=1}^{\infty} [G_{nS} \sin n\psi + G_{nC} \cos n\psi] \tag{B.51}
$$

By comparison of Eq. B.38 with Eq. B.49 and

$$
\left.
\begin{array}{c}
g_n + g_{-n} = G_{nC} \\
i(g_n - g_{-n}) = G_{nS}
\end{array}
\right\} \rightarrow
\left\{
\begin{array}{l}
g_n = (G_{nS} + iG_{nC})/(2i) \\
g_{-n} = (-G_{nS} + iG_{nC})/(2i)
\end{array}
\right. \tag{B.52}
$$

we find the coefficients g_n, $n = -\infty ... + \infty$ to be

$$
g_0 = hV_0 \left[\bar{\alpha}_0 + \frac{\lambda}{2}\bar{\alpha}_{1S} \right] \tag{B.53}
$$

$$
\begin{aligned}
g_1 = \frac{hV_0}{2i} \Bigg\{ & \lambda\bar{\alpha}_0 + \bar{\alpha}_{1S} - k\left(\frac{1-2a}{2}\bar{\alpha}_{1C} + \bar{h}_{1C}\right) - \frac{\lambda}{2}\bar{\alpha}_{2C} \\
& + i\left[\bar{\alpha}_{1C} + k\left(\frac{1-2a}{2}\bar{\alpha}_{1S} + \bar{h}_{1S}\right) + \frac{\lambda}{2}\bar{\alpha}_{2S} \right] \Bigg\} = \bar{g}_{-1}
\end{aligned}
\tag{B.54}
$$

$$
\begin{aligned}
g_n = \frac{hV_0}{2i} \sum_{n=2}^{\infty} \Bigg\{ & \bar{\alpha}_{nS} - nk\left(\frac{1-2a}{2}\bar{\alpha}_{nC} + \bar{h}_{nC}\right) - \frac{\lambda}{2}\left(\bar{\alpha}_{(n+1)C} - \bar{\alpha}_{(n-1)C}\right) \\
& + i\left[\bar{\alpha}_{nC} + nk\left(\frac{1-2a}{2}\bar{\alpha}_{nS} + \bar{h}_{nS}\right) + \frac{\lambda}{2}\left(\bar{\alpha}_{(n+1)S} - \bar{\alpha}_{(n-1)S}\right) \right] \Bigg\}
\end{aligned}
\tag{B.55}
$$

$$
= \bar{g}_{-n}
$$

It should be noted, that in [7] there was a typographical error, since it was stated there $g_1 = -\bar{g}_{-1}$. With this, the coefficients A_0 and A_n can be calculated ($g_1 - \bar{g}_1 = 2i\ Im(g_1)$), i.e.,

$$\begin{aligned} A_0 &= hV_0 \left\{ \bar{\alpha}_0 + \frac{\bar{\alpha}_{1S}\lambda}{2} \right. \\ &\quad \left. -\frac{\lambda}{2i}\left[-i\left(\lambda\bar{\alpha}_0 + \bar{\alpha}_{1S} - \frac{k}{2}(1-2a)\bar{\alpha}_{1C} - k\bar{h}_{1C} - \frac{\lambda}{2}\bar{\alpha}_{2C} \right) \right] \right\} \\ &= hV_0 \left\{ \left(1 + \frac{\lambda^2}{2} \right) \bar{\alpha}_0 \right. \\ &\quad \left. +\lambda\left[\bar{\alpha}_{1S} - \frac{k}{4}(1-2a)\bar{\alpha}_{1C} - \frac{k}{2}\bar{h}_{1C} - \frac{\lambda}{4}\bar{\alpha}_{2C} \right] \right\} \end{aligned} \tag{B.56}$$

$$A_n = \frac{i^n}{n} hV_0 (H_n + iH_n') \tag{B.57}$$

where the coefficients H_n are evaluated from Eq. B.45. In case of only $1/rev$ in angle of attack and plunge motion the sum in Eq. B.45 can be simplified using the well known relationship of the Bessel functions:

$$J_{n+1}(x) + J_{n-1}(x) = \frac{2n}{x} J_n(x) \tag{B.58}$$

Here the sum in Eq. B.45 is only taken for $m = -2$ to $m = 2$ since for larger m the coefficients $g_m = 0$. This is not the case when the input function of angle of attack or plunge contains a series of harmonics.

In order to reduce the number of Bessel functions J to be computed here a short form of the coefficients H_n and H_n' will be derived following Isaacs [7].

$$\begin{aligned} \frac{A_n}{i^n/n} &= \frac{-2}{i^{-2}} g_{-2} J_{n+2} + \frac{-1}{i^{-1}} g_{-1} J_{n+1} + \frac{1}{i^1} g_1 J_{n-1} + \frac{2}{i^2} g_2 J_{n-2} \\ &= 2(g_{-2} J_{n+2} - g_2 J_{n-2}) - i(g_{-1} J_{n+1} + g_1 J_{n-1}) \end{aligned} \tag{B.59}$$

Since the argument of the Bessel functions is always $n\lambda$, it is omitted. For conciseness set $g_1 = hV_0(A - iB)/2$. Therefore $g_{(-1)} = hV_0(A + iB)/2$, as well as $g_2 = -hV_0(C + iD)\lambda/4$, and $g_{(-2)} = hV_0(-C + iD)\lambda/4$. Then

$$\begin{aligned} \frac{A_n}{hV_0 i^n/n} = & \frac{\lambda}{2}C(J_{n-2} - J_{n+2}) + \frac{B}{2}(J_{n+1} - J_{n-1}) \\ & + i\left[\frac{\lambda}{2}D(J_{n+2} + J_{n-2}) - \frac{A}{2}(J_{n+1} + J_{n-1})\right] \end{aligned} \tag{B.60}$$

Now one uses the results

$$J_{n-1} + J_{n+1} = \frac{2}{\lambda}J_n \tag{B.61}$$

$$\begin{aligned} J_{n-2} - J_{n+2} &= \frac{2(n-1)}{n\lambda}J_{n-1} - J_n - \left[\frac{2(n+1)}{n\lambda}J_{n+1} - J_n\right] \\ &= \frac{2}{\lambda}\left[J_{n-1} - J_{n+1} - \frac{1}{n}(J_{n-1} + J_{n+1})\right] \\ &= \frac{2}{\lambda}(J_{n-1} - J_{n+1}) - \frac{4}{\lambda^2 n}J_n \end{aligned} \tag{B.62}$$

$$\begin{aligned} J_{n-2} + J_{n+2} &= \frac{2}{\lambda}\left[J_{n-1} + J_{n+1} + \frac{1}{n}(J_{n+1} - J_{n-1})\right] - 2J_n \\ &= \frac{2}{n\lambda}(J_{n+1} - J_{n-1}) + \left(\frac{4}{\lambda^2} - 2\right)J_n \end{aligned} \tag{B.63}$$

It follows that

$$\begin{aligned} H_n &= -\frac{2J_n}{n\lambda}C + C(J_{n-1} - J_{n+1}) + B\frac{J_{n+1} - J_{n-1}}{2} \\ &= -\frac{2J_n}{n\lambda}C + \frac{J_{n+1} - J_{n-1}}{2}(B - 2C) \end{aligned} \tag{B.64}$$

$$\begin{aligned} H'_n &= D\frac{J_{n+1} - J_{n-1}}{n} + \frac{J_n}{\lambda}(2 - \lambda^2)D - A\frac{J_{n+1} + J_{n-1}}{2} \\ &= D\frac{J_{n+1} - J_{n-1}}{n} + \frac{J_n}{\lambda}[(2 - \lambda^2)D - A] \end{aligned} \tag{B.65}$$

However, this is only useful, when there is only a $1/rev$ in angle of attack and plunge under consideration. In that case the result after substitution of

$A = \lambda\bar{\alpha}_0 + \bar{\alpha}_{1S} - (k/2)(1-2a)\bar{\alpha}_{1C} - k\bar{h}_{1C}$, $B = \bar{\alpha}_{1C} + (k/2)(1-2a)\bar{\alpha}_{1S} + k\bar{h}_{1S}$, $C = \bar{\alpha}_{1S}$ and $D = \bar{\alpha}_{1C}$ is finally

$$H_n = \frac{J_{n+1} - J_{n-1}}{2}\left[\lambda\bar{\alpha}_0 - \bar{\alpha}_{1S} - k\left(\frac{1-2a}{2}\bar{\alpha}_{1C} + \bar{h}_{1C}\right)\right] - \frac{2J_n}{n\lambda}\bar{\alpha}_{1S} \quad \text{(B.66)}$$

$$H'_n = \frac{J_{n+1} - J_{n-1}}{n}\bar{\alpha}_{1C} + \frac{J_n}{\lambda}\left[\bar{\alpha}_{1C}(1-\lambda^2) - k\left(\frac{1-2a}{2}\bar{\alpha}_{1S} + \bar{h}_{1S}\right)\right] \quad \text{(B.67)}$$

Comparing to Isaacs [7] the brackets include more terms now because of the influence of pitch axis location and plunge motion. Now from $a_n = A_n/R_n$ it follows that

$$a_0 = A_0 \quad \text{(B.68)}$$

$$a_n = \frac{A_n}{\Psi(nk)} \quad \text{(B.69)}$$

and from $Q(W)$ the circulation can be calculated. It must be noted, however, that this reduction can take other forms if the angle of attack and plunge motion contains a series of harmonics, like in a dynamic response problem. Then Eq. B.45 has to be written

$$\begin{aligned}
A_n &= \frac{i^n}{n}\sum_{m=-\infty}^{\infty}\frac{m}{i^m}g_m J_{n-m} \\
&= \frac{i^n}{n}\sum_{m=1}^{\infty}\left(\frac{m}{i^m}g_m J_{n-m} - m i^m \bar{g}_m J_{n+m}\right) \\
&= \frac{i^n}{n}\sum_{m=1}^{\infty}\frac{m}{i^m}\left(g_m J_{n-m} - i^{2m}\bar{g}_m J_{n+m}\right) \\
&= \frac{i^n}{n}\sum_{m=1}^{\infty}\frac{m}{i^m}\left(g_m J_{n-m} - (-1)^m \bar{g}_m J_{n+m}\right) \\
&= \frac{i^n}{n}\sum_{m=1}^{\infty}\frac{m}{i^m}\left(\frac{G_{mS} + iG_{mC}}{2i}J_{n-m} - (-1)^m\frac{-G_{mS} + iG_{mC}}{2i}J_{n+m}\right) \\
&= \frac{i^n}{n}\sum_{m=1}^{\infty}\frac{m}{2i^{m+1}}\{G_{mS}\left[J_{n-m} + (-1)^m J_{n+m}\right] + iG_{mC}[J_{n-m} - (-1)^m J_{n+m}]\}
\end{aligned} \quad \text{(B.70)}$$

and the coefficients G_{mS} and G_{mC} are given in Eq. B.50.

The fore-aft motion is restricted to $1/rev$ only since a series of harmonics in $V(t)$ will lead to a series of harmonics in $W(t)$, and this leads to additional complications in solving the integral Eq. B.28.

Using the formulas for the case of plunge motion one must be aware of the small desturbance and small angle assumption. Especially at high amplitudes of fore-aft motion (λ slightly smaller than 1) even a small vertical velocity produces great angles of attack and probably violates the small angle assumption. Therefore one must carefully check the conditions of airfoil motion before applying this theory.

B.3 Calculation of the Lift

The total lift consists of circulatory and noncirculatory parts. Following Isaacs in [6] it is split up into a "Joukowsky" lift L_J and an "impulsive pressure" lift L_I, i.e.,

$$\begin{aligned} L(t) &= L_J(t) + L_I(t) \\ &= \rho V(t)\Gamma(t) + \rho \frac{d}{dt} \int_{-c/2}^{c/2} \gamma_b(x,t) \left(\frac{c}{2} - x \right) dx \\ &= \rho V(t)\Gamma(t) + \rho \frac{d}{dt} I(t) \\ &= \rho V(t) \sum_{n=-\infty}^{\infty} a_n e^{ink(2W(t)/c)} + \rho \frac{d}{dt} I(t) \end{aligned} \tag{B.71}$$

where the integral $I(t)$ is

$$I(t) = \frac{c}{2} \int_{-c/2}^{c/2} \gamma_b(x,t) dx - \int_{-c/2}^{c/2} \gamma_b(x,t) x \, dx$$

$$
\begin{aligned}
&= \frac{c}{2}\Gamma(t) - \frac{c^2}{4}\int_0^{\pi} \gamma_b(\phi,t)\sin\phi\cos\phi\, d\phi \\
&= \frac{c}{2}\Gamma(t) - \frac{c^2}{4}\int_0^{\pi}\left[c_0(t) + \sum_{n=1}^{\infty} c_n(t)\cos n\phi\right]\cos\phi\, d\phi \\
&= \frac{c}{2}\Gamma(t) - \frac{\pi c^2}{8}c_1(t)
\end{aligned}
\tag{B.72}
$$

Using the expression for $c_1(t)$ from Eq. B.18, as well as those for $b_2(t)$ and $b_0(t)$ from Eq. B.11

$$
\begin{aligned}
c_1(t) &= -2\alpha(t)V(t) + ac\dot{\alpha}(t) - 2\dot{h}(t) \\
&\quad -\frac{2}{\pi c}\int_{-\infty}^{t}\Gamma'(\tau)\left[\frac{\left[a_1(t,\tau) - \sqrt{a_1^2(t,\tau)-1}\right]^2}{\sqrt{a_1^2(t,\tau)-1}} - \frac{1}{\sqrt{a_1^2(t,\tau)-1}}\right]d\tau \\
&= -2\alpha(t)V(t) + ac\dot{\alpha}(t) - 2\dot{h}(t) \\
&\quad -\frac{4}{\pi c}\int_{-\infty}^{t}\Gamma'(\tau)\frac{a_1^2(t,\tau) - 1 - a_1(t,\tau)\sqrt{a_1^2(t,\tau)-1}}{\sqrt{a_1^2(t,\tau)-1}}d\tau \\
&= -2\alpha(t)V(t) + ac\dot{\alpha}(t) - 2\dot{h}(t) \\
&\quad +\frac{4}{\pi c}\int_{-\infty}^{t}\Gamma'(\tau)\left[a_1(t,\tau) - \sqrt{a_1^2(t,\tau)-1}\right]d\tau
\end{aligned}
\tag{B.73}
$$

Resubstituting $a_1(t,\tau)$ from Eq. B.5 gives

$$
\begin{aligned}
I(t) = \frac{c}{2}\Gamma(t) + \frac{\pi c^2}{4}\alpha(t)V(t) - a\frac{\pi c^3}{8}\dot{\alpha}(t) + \frac{\pi c^2}{4}\dot{h}(t) \\
-\frac{c}{2}\int_{-\infty}^{t}\Gamma'(\tau)\left[1 + \frac{W(t)-W(\tau)}{c/2} - \sqrt{\left[1 + \frac{W(t)-W(\tau)}{c/2}\right]^2 - 1}\right]d\tau
\end{aligned}
\tag{B.74}
$$

Now the same transformation is made as in passing from Eq. B.25 to Eq. B.28. Here, $\Lambda = W(t) - W(\tau)$ with $Q'(W(\tau)) = Q'(W(t) - \Lambda)$, and this results in

$$
\begin{aligned}
I(t) = \frac{\pi c^2}{4}\left[\alpha(t)V(t) - a\frac{c}{2}\dot{\alpha}(t) + \dot{h}(t)\right] + \frac{c}{2}Q(W(t)) - \\
-\frac{c}{2}\int_0^{\infty} Q'(W(t)-\Lambda)\left[1 + \frac{2\Lambda}{c} - \sqrt{\left[1 + \frac{2\Lambda}{c}\right]^2 - 1}\right]d\Lambda
\end{aligned}
\tag{B.75}
$$

By use of the series expansion for the circulation in Eq. B.35 it follows that

$$I(t) = \frac{\pi c^2}{4}\left[\alpha(t)V(t) - a\frac{c}{2}\dot{\alpha}(t) + \dot{h}(t)\right] \tag{B.76}$$

$$+\frac{c}{2}\sum_{n=-\infty}^{\infty} a_n e^{ink(2W(t)/c)} \times\left\{1 - in\frac{\omega}{V_0}\int_0^{\infty} e^{-in(\omega/V_0)\Lambda}\left[1 + \frac{2\Lambda}{c} - \sqrt{\left[1+\frac{2\Lambda}{c}\right]^2 - 1}\right] d\Lambda\right\} \tag{B.77}$$

$$= \frac{\pi c^2}{4}\left[\alpha(t)V(t) - a\frac{c}{2}\dot{\alpha}(t) + \dot{h}(t)\right] + \frac{c}{2}\sum_{n=-\infty}^{\infty} a_n[1 - iS_n(nk)]e^{ink(2W(t)/c)}$$

The S-function in Eq. B.77 is given by

$$S_n = \xi(nk) \qquad n \neq 0$$

$$= \int_0^{\infty} e^{-i\bar{\Lambda}}\left[1 + \frac{\bar{\Lambda}}{nk} - \sqrt{\left(1+\frac{\bar{\Lambda}}{nk}\right)^2 - 1}\right] d\bar{\Lambda} \tag{B.78}$$

$$S_0 = 0 \tag{B.79}$$

Replacing the distance travelled by Eq. B.32 and making the derivation with respect to time, i.e.,

$$\frac{d}{dt}\left[e^{ink(2W(t)/c)}\right] = in\omega e^{ink(2W(t)/c)}(1 + \lambda\sin\psi) \tag{B.80}$$

the lift contribution L_I becomes

$$L_I(t) = \rho\frac{\pi c^2}{4}\left[\dot{\alpha}(t)V(t) + \alpha(t)\dot{V}(t) - a\frac{c}{2}\ddot{\alpha}(t) + \ddot{h}(t)\right] + \rho\frac{c}{2}\sum_{n=-\infty}^{\infty} a_n in\omega[1 - iS_n]e^{ink(2W(t)/c)}(1 + \lambda\sin\psi)$$

$$= \rho\frac{\pi c^2}{4}\left[\dot{\alpha}(t)V(t) + \alpha(t)\dot{V}(t) - a\frac{c}{2}\ddot{\alpha}(t) + \ddot{h}(t)\right] + \rho V(t)\sum_{n=-\infty}^{\infty} a_n ink[1 - iS_n]e^{ink(2W(t)/c)} \tag{B.81}$$

Now the total lift becomes

$$\begin{aligned} L(t) = \; & \rho\pi\frac{c^2}{4}\left[\dot{\alpha}(t)V(t) + \alpha(t)\dot{V}(t) - a\frac{c}{2}\ddot{\alpha}(t) + \ddot{h}(t)\right] \\ & +\rho V(t)\sum_{n=-\infty}^{\infty} a_n[1 + nk(S_n + i)]e^{ink(2W(t)/c)} \end{aligned} \tag{B.82}$$

Here a_n has to be replaced by A_n/R_n, and the following function is encountered,

$$\frac{1 + nk[S_n(nk) + i]}{R_n(nk)} = \begin{cases} 1 & n = 0 \\ C(nk) & n > 0 \end{cases} \tag{B.83}$$

$C(nk)$ is the well known Theodorsen function with multiples of the reduced frequency as the argument, i.e.,

$$\begin{aligned} C(nk) &= \frac{1 + nk[\xi(nk) + i]}{\Psi(nk)} \\ &= \frac{H_1^{(2)}(nk)}{H_1^{(2)}(nk) + iH_0^{(2)}(nk)} \\ &= \frac{J_1(nk) - iY_1(nk)}{J_1(nk) + Y_0(nk) + i[J_0(nk) - Y_1(nk)]} \\ &= F(nk) + iG(nk) \end{aligned} \tag{B.84}$$

The J-functions are Bessel functions, Y are Weber functions, and H are Hankel's cylinder functions that are built up from Bessel and Weber functions. The lower index gives the order and the upper index the kind of the appropriate function, see for example [39]. Since L has to be real we have $C(-nk) = \bar{C}(nk)$. Thus the lift takes the following form

$$\begin{aligned} L(t) = \; & \rho V(t)\left[A_0 + \sum_{n\neq 0} A_n C(nk)e^{ink(2W(t)/c)}\right] \\ & +\rho\frac{\pi c^2}{4}\left[\dot{\alpha}(t)V(t) + \alpha(t)\dot{V}(t) - a\frac{c}{2}\ddot{\alpha}(t) + \ddot{h}(t)\right] \end{aligned}$$

$$= \rho h V_0^2 \left\{ \left(1+\frac{\lambda^2}{2}\right)\bar{\alpha}_0 + \lambda\left[\bar{\alpha}_{1S} - \frac{k}{2}\left(\frac{1-2a}{2}\bar{\alpha}_{1C} + \bar{h}_{1C}\right) - \frac{\lambda}{4}\bar{\alpha}_{2C}\right]\right\} \times(1+\lambda\sin\psi)$$

$$+\rho\frac{\pi c^2}{4}\omega V_0\alpha_0\left\{\sum_{n=1}^{\infty} n\left[(\bar{\alpha}_{nS}\cos n\psi - \bar{\alpha}_{nC}\sin n\psi)(1+\lambda\sin\psi)\right.\right.$$

$$\left.+ nk\left[a(\bar{\alpha}_{nS}\sin n\psi + \bar{\alpha}_{nC}\cos n\psi) - \bar{h}_{nS}\sin n\psi - \bar{h}_{nC}\cos n\psi\right]\right]$$

$$\left.+\lambda\cos\psi\left(\bar{\alpha}_0 + \sum_{n=1}^{\infty}\bar{\alpha}_{nS}\sin n\psi + \bar{\alpha}_{nC}\cos n\psi\right)\right\}$$

$$+\rho V(t)\sum_{n\neq 0} A_n C(nk) e^{ink(2W(t)/c)} \tag{B.85}$$

Now, the last term in Eq. B.85 can be viewed in terms of a Fourier series

$$\rho V_0(1+\lambda\sin\psi)\sum_{n\neq 0} A_n C(nk) e^{ink(2W(t)/c)} = \rho h V_0^2 \sum_{m=1}^{\infty}(l_m\cos m\psi + l'_m\sin\psi) \tag{B.86}$$

and after defining a steady lift for the mean velocity and the mean value of the angle of attack as

$$L_0 = \frac{\rho}{2}V_0^2 c 2\pi\alpha_0 = \rho h V_0^2 \tag{B.87}$$

the nondimensionalised unsteady lift finally becomes

$$\frac{L_{nc}}{L_0} = \frac{k}{2}\left\{\left[\lambda\bar{\alpha}_0 + \bar{\alpha}_{1S} + k(a\bar{\alpha}_{1C} - \bar{h}_{1C}) - \frac{\lambda}{2}\bar{\alpha}_{2C}\right]\cos\psi\right.$$

$$+\left[-\bar{\alpha}_{1C} + k(a\bar{\alpha}_{1S} - \bar{h}_{1S}) - \frac{\lambda}{2}\bar{\alpha}_{2S}\right]\sin\psi$$

$$+\sum_{n=2}^{\infty} n\left[\bar{\alpha}_{nS} + nk(a\bar{\alpha}_{nC} - \bar{h}_{nC}) + \frac{\lambda}{2}\left(\bar{\alpha}_{(n-1)C} - \bar{\alpha}_{(n+1)C}\right)\right]\cos n\psi$$

$$\left.+\sum_{n=2}^{\infty} n\left[-\bar{\alpha}_{nC} + nk(a\bar{\alpha}_{nS} - \bar{h}_{nS}) + \frac{\lambda}{2}\left(\bar{\alpha}_{(n-1)S} - \bar{\alpha}_{(n+1)S}\right)\right]\sin n\psi\right\} \tag{B.88}$$

$$\frac{L_c}{L_0} = \left\{\left(1+\frac{\lambda^2}{2}\right)\bar{\alpha}_0 + \lambda\left[\bar{\alpha}_{1S} - \frac{k}{2}\left(\frac{1-2a}{2}\bar{\alpha}_{1C} + \bar{h}_{1C}\right) - \frac{\lambda}{4}\bar{\alpha}_{2C}\right]\right\} \times(1+\lambda\sin\psi) \tag{B.89}$$

$$+\sum_{m=1}^{\infty}(l_m\cos m\psi + l'_m\sin m\psi)$$

with $\psi = \omega t$ and

$$l_m + il'_m = -2\frac{m}{i^m}\sum_{n=1}^{\infty}\left\{F_n[J_{n+m}(n\lambda) - J_{n-m}(n\lambda)] + iG_n[J_{n+m}(n\lambda) + J_{n-m}(n\lambda)]\right\} \tag{B.90}$$

and

$$F_n + iG_n = [F(nk) + iG(nk)]\frac{H_n + iH'_n}{n^2} \tag{B.91}$$

with H_n and H'_n defined before in Eq. B.57 and Eq. B.45.

$$H_n + iH'_n = \sum_{l=-\infty}^{\infty}\frac{l}{i^l}\frac{g_l}{hV_0}J_{n-l}(n\lambda) \tag{B.92}$$

As mentioned before, the formula for H_n and H'_n is not valid in case of higher harmonic motion in pitch or plunge. If these are under consideration, Eq. B.57 has to be used instead.

This result is built up similarly to that of Isaacs in [7], but includes several additional terms of noncirculatory and circulatory nature originating from the additional degrees of motion included here. It should be noted that the derivation is given here also for the inclusion of higher harmonics in angle of attack and plunge motion. For the best of my knowledge that was never given before. In the case of only $1/rev$ components in velocity and angle of attack, no plunge motion ($\bar{h}_{nC} = \bar{h}_{nS} = 0$), pitch about midchord($a = 0$) this result reduces to that of Isaacs in [7]. In the case of $\lambda = 0$ it reduces identically to Theodorsen's result as required.

Appendix C

Arbitrary Airfoil Motion in an Unsteady Freestream

In incompressible flow the circulatory lift is determined from the normal velocity at 3/4 chord of the airfoil, while the noncirculatory lift is the result of the instantaneous local accelerations. Thus the total lift is

$$\begin{aligned} L = \; & \pi\rho\frac{c^2}{4}\left[\ddot{h}(t) + V(t)\dot{\alpha}(t) + \dot{V}(t)\alpha(t) - a\frac{c}{2}\ddot{\alpha}(t)\right] \\ & +2\pi\rho V(t)\frac{c}{2}\left[w_{3/4}(0)\phi(s) + \int_0^s \frac{\partial w_{3/4}(\sigma)}{\partial\sigma}\phi(s-\sigma)d\sigma\right] \end{aligned} \tag{C.1}$$

where $\phi(s)$ is the lift deficiency function for the lift, s the way travelled by the airfoil (in half chords as unit) and $w_{3/4}(t)$ the instantaneous value of normal velocities at the three quarter chord point. The indicial response function ϕ is exactly the Wagner function, but since this is a very difficult function it is much more conveniant to replace it by one of its common approximations. These can be written in form of a series of exponential functions

$$\phi(s) = \sum_{i=1}^{N} A_i e^{b_i s} \tag{C.2}$$

The following degrees of freedom are encountered by the airfoil:

$$\begin{aligned} V(t) &= V_0\,(1+\lambda\sin\omega t) \\ \alpha(t) &= \alpha_0\,(\bar{\alpha}_0+\bar{\alpha}_{1S}\sin\omega t+\bar{\alpha}_{1C}\cos\omega t) \\ h(t) &= \alpha_0\frac{c}{2}\left(\bar{h}_{1S}\sin\omega t+\bar{h}_{1C}\cos\omega t\right) \end{aligned} \tag{C.3}$$

The normal velocity at 3/4 chord can be obtained from Fig. 2.8

$$\begin{aligned} w_{3/4}(t) &= V(t)\alpha(t)+\dot{h}(t)+\frac{c}{2}\frac{1-2a}{2}\dot{\alpha}(t) \\ &= \alpha_0 V_0\left\{\bar{\alpha}_0+\frac{\lambda}{2}\bar{\alpha}_{1S}+\left[\bar{\alpha}_{1C}+k_V\left(\frac{1-2a}{2}\bar{\alpha}_{1S}+\bar{h}_{1S}\right)\right]\cos\omega t\right. \\ &\qquad +\left[\lambda\bar{\alpha}_0+\bar{\alpha}_{1S}-k_V\left(\frac{1-2a}{2}\bar{\alpha}_{1C}+\bar{h}_{1C}\right)\right]\sin\omega t \\ &\qquad \left.-\frac{\lambda}{2}\bar{\alpha}_{1S}\cos 2\omega t+\frac{\lambda}{2}\bar{\alpha}_{1C}\sin 2\omega t\right\} \\ &= \alpha_0 V_0\,(c_0+c_{1C}\cos\omega t+c_{1S}\sin\omega t+c_{2C}\cos 2\omega t+c_{2S}\sin 2\omega t) \end{aligned} \tag{C.4}$$

and therefore the derivative $\partial w_{3/4}(\sigma)/\partial\sigma$ with $\omega t = k_V\sigma$ becomes

$$\begin{aligned} \frac{\partial w_{3/4}(\sigma)}{\partial\sigma} &= \alpha_0 V_0 k_V\,(c_{1S}\cos k_V\sigma-c_{1C}\sin k_V\sigma \\ &\qquad +2c_{2S}\cos 2k_V\sigma-2c_{2C}\sin 2k_V\sigma) \end{aligned} \tag{C.5}$$

Now the integral is

$$\begin{aligned} \int_0^s \frac{\partial w_{3/4}(\sigma)}{\partial\sigma}\phi(s-\sigma)d\sigma = \alpha_0 V_0 k_V \sum_{i=1}^{N} A_i e^{b_i s}\int_0^s & (c_{1S}\cos k_V\sigma-c_{1C}\sin k_V\sigma \\ & +2c_{2S}\cos 2k_V\sigma \\ & -2c_{2C}\sin 2k_V\sigma)\,e^{-b_i\sigma}d\sigma \end{aligned} \tag{C.6}$$

and the kernel integrals are already given in Appendix A. After setting in the upper and lower limits of the integral one finds

$$\int_0^s (c_{1S}\cos k_V\sigma-c_{1C}\sin k_V\sigma+2c_{2S}\cos 2k_V\sigma-2c_{2C}\sin 2k_V\sigma)\,e^{-b_i\sigma}d\sigma$$

$$= \frac{e^{-b_i s}}{b_i^2 + k_V^2}\left[(k_V c_{1C} - b_i c_{1S})\cos k_V s + (k_V c_{1S} + b_i c_{1C})\sin k_V s\right]$$
$$+2\frac{e^{-b_i s}}{b_i^2 + (2k_V)^2}\left[(2k_V c_{2C} - b_i c_{2S})\cos 2k_V s + (2k_V c_{2S} + b_i c_{2C})\sin 2k_V s\right]$$
$$-\frac{1}{b_i^2 + k_V^2}(k_V c_{1C} - b_i c_{1S}) - \frac{2}{b_i^2 + (2k_V)^2}(2k_V c_{2C} - b_i c_{2S}) \qquad (C.7)$$

Also, the product of normal velocity at time zero with the indicial response function $\phi(s)$ has to be evaluated.

$$w_{3/4}(0)\phi(s) = \alpha_0 V_0 (c_0 + c_{1C} + c_{2C}) \sum_{i=1}^{N} A_i e^{b_i s} \qquad (C.8)$$

Now one introduces the actual values of the approximation of the indicial response function to take advantage of their characteristics. The values for the commonly used approximation by Jones are listed in Table 2.4. All the values of b_i are negative except $b_1 = 0$. Therefore, as time takes very big values, the exponential function approaches zero for all $i > 1$ and this means that all initial transient processes have died out. That is the case we are interested in and therefore the bracket in the governing equation for the lift becomes

$$\left[w_{3/4}(0)\phi(s) + \int_0^s \frac{\partial w_{3/4}(\sigma)}{\partial \sigma}\phi(s-\sigma)d\sigma\right]$$

$$= \alpha_0 V_0 c_0 A_1$$
$$+\alpha_0 V_0 \sum_{i=1}^{N} \frac{A_i k_V}{b_i^2 + k_V^2}\left[(k_V c_{1C} - b_i c_{1S})\cos k_V s + (k_V c_{1S} + b_i c_{1C})\sin k_V s\right]$$
$$+\alpha_0 V_0 \sum_{i=1}^{N} \frac{A_i 2k_V}{b_i^2 + (2k_V)^2}\left[(2k_V c_{2C} - b_i c_{2S})\cos 2k_V s + (2k_V c_{2S} + b_i c_{2C})\sin 2k_V s\right] \qquad (C.9)$$

Herein the way travelled by the airfoil s is

$$s = \frac{1}{c/2}\int_0^t V(t)dt = \bar{s} - \frac{\lambda}{k_V}\cos k_V \bar{s} \tag{C.10}$$

with $\bar{s}$ as the mean value, given by $tV_0/(c/2)$. As is easy to see, there apeares a trigonometric function inside another trigonometric function and this is more difficult to handle. Also, this happens only, when the flow oscillation amplitude $\lambda > 0$. When $\lambda = 0$ the case of constant freestream velocity is represented and the results can easily be shown to be identical to Theodorsen's results, when using the identity $C(k) = F(k) + iG(k)$ with

$$\begin{aligned} F(nk_V) &= \sum_{i=1}^{\infty} \frac{A_i(nk_V)^2}{b_i^2 + (nk_V)^2} \\ G(nk_V) &= -\sum_{i=1}^{\infty} \frac{A_i(nk_V)b_i}{b_i^2 + (nk_V)^2} \end{aligned} \tag{C.11}$$

Normally the sum is cancelled after the first few terms and therefore small inaccuracies are implicitly build in. Then it is better to differentiate between the exact values of the Theodorsen function and those obtained by a finite series approximation, denoted by a $\hat{}$ here.

$$\begin{aligned} \hat{F}(nk_V) &= \sum_{i=1}^{N} \frac{A_i(nk_V)^2}{b_i^2 + (nk_V)^2} \approx F(nk_V) \\ \hat{G}(nk_V) &= -\sum_{i=1}^{N} \frac{A_i(nk_V)b_i}{b_i^2 + (nk_V)^2} \approx G(nk_V) \end{aligned} \tag{C.12}$$

The expression for the circulatory lift (made nondimensional by the lift of mean velocity and mean angle of attack) becomes

$$\begin{aligned} \frac{L_c}{L_0} = (1 + \sin k_V \bar{s}) \Big[& c_0 A_1 + \left(\hat{F}(k_V)c_{1C} + \hat{G}(k_V)c_{1S}\right)\cos k_V s \\ & + \left(\hat{F}(k_V)c_{1S} - \hat{G}(k_V)c_{1C}\right)\sin k_V s \end{aligned}$$

$$
\begin{aligned}
&+\left(\hat{F}(2k_V)c_{2C}+\hat{G}(2k_V)c_{2S}\right)\cos 2k_V s \\
&+\left(\hat{F}(2k_V)c_{2S}-\hat{G}(2k_V)c_{2C}\right)\sin 2k_V s\Big] \\
= \;& (1+\sin k_V\bar{s})\sum_{n=-2}^{2} C_n e^{ink_V s}
\end{aligned}
\tag{C.13}
$$

with the complex amplitudes

$$
\begin{aligned}
C_0 &= c_0 A_1 \\
C_1 &= \frac{1}{2}\left[\hat{F}(k_V)c_{1C}+\hat{G}(k_V)c_{1S}-i\left(\hat{F}(k_V)c_{1S}-\hat{G}(k_V)c_{1C}\right)\right]=\bar{C}_{-1} \\
C_2 &= \frac{1}{2}\left[\hat{F}(2k_V)c_{2C}+\hat{G}(2k_V)c_{2S}-i\left(\hat{F}(2k_V)c_{2S}-\hat{G}(2k_V)c_{2C}\right)\right]=\bar{C}_{-2}
\end{aligned}
\tag{C.14}
$$

Now, since $\cos nk_V s$ and $\sin nk_V s$ are periodic functions with period 2π, but with a periodic argument $nk_V s$, they can more conveniantly be written in form of a Fourier series with an infinite number of harmonics, having the argument $mk_V\bar{s}$. The difficulty is to identify the coefficients of these Fourier series because they contain Bessel functions, as will be shown. In general, the complex Fourier series will be of the following kind

$$
\sum_{n=-2}^{2} C_n e^{ink_V s}=\sum_{n=-2}^{2} C_n e^{ink_V\bar{s}}e^{-in\lambda\cos k_V\bar{s}}=\sum_{m=-\infty}^{\infty} D_m e^{imk_V\bar{s}} \tag{C.15}
$$

and the coefficients D_m are calculated by multiplying both sides with $e^{-imk_V\bar{s}}$ and integrating over the period of 2π. The variable of integration is $\psi=k_V\bar{s}$.

$$
D_m=\sum_{n=-2}^{2} C_n\frac{1}{2\pi}\int_0^{2\pi} e^{i(n-m)\psi}e^{-in\lambda\cos\psi}d\psi \tag{C.16}
$$

By use of the integral form for the Bessel functions

$$
J_n(x)=\frac{i^{-n}}{2\pi}\int_0^{2\pi} e^{in\psi}e^{ix\cos\psi}d\psi \tag{C.17}
$$

that can be found in [40] on page 149, we find

$$D_m = \sum_{n=-2}^{2} C_n i^{(n-m)} J_{n-m}(-n\lambda) \tag{C.18}$$

Rearranging, this is

$$\begin{aligned} D_0 &= C_0 + 2\left[\Im(C_1)J_1(\lambda) - \Re(C_2)J_2(\lambda)\right] \\ D_m &= i^m \left\{ i\left[C_{-1}J_{m+1}(\lambda) + (-1)^m C_1 J_{m-1}(\lambda)\right]\right. \qquad (C.19) \\ &\quad \left. -C_{-2}J_{m+2}(2\lambda) - (-1)^m C_2 J_{m-2}(2\lambda)\right\} \qquad m > 0 \ (C.20) \end{aligned}$$

Now the circulatory lift becomes

$$\begin{aligned} \frac{L_c}{L_0} &= (1 + \lambda \sin\psi) \sum_{m=-\infty}^{\infty} D_m \left(\cos m\psi + i \sin m\psi\right) \\ &= \sum_{m=-\infty}^{\infty} D_m \left\{ \cos m\psi + \lambda \frac{\sin(1-m)\psi + \sin(1+m)\psi}{2} \right. \\ &\qquad \left. + i\left[\sin m\psi + \lambda \frac{\cos(1-m)\psi - \cos(1+m)\psi}{2}\right]\right\} \qquad (C.21) \end{aligned}$$

Now we can use two properties of complex Fourier series coefficients, that is $D_{-m} = \bar{D}_m$ and $D_0 = real$. With this we can rewrite the expression for the lift

$$\begin{aligned} \frac{L_c}{L_0} &= D_0(1 + \lambda \sin\psi) \\ &\quad + \sum_{m=1}^{\infty} \Re(D_m)\left[2\cos m\psi + \lambda \sin(m+1)\psi - \lambda \sin(m-1)\psi\right] \\ &\quad - \sum_{m=1}^{\infty} \Im(D_m)\left[2\sin m\psi - \lambda \cos(m+1)\psi + \lambda \cos(m-1)\psi\right] \end{aligned} \tag{C.22}$$

A further substitution brings the expression into the sought form. Set $M = m+1 \rightarrow m = M-1$ and $m = 1 \rightarrow M = 2$. Also, set $N = m-1 \rightarrow m = N+1$

and $m = 1 \rightarrow N = 0$. Thus

$$\begin{aligned}
\frac{L_c}{L_0} &= D_0(1 + \lambda \sin\psi) + 2\sum_{m=1}^{\infty} [\Re(D_m)\cos m\psi - \Im(D_m)\sin m\psi] \\
&\quad + \lambda \sum_{M=2}^{\infty} [\Re(D_{M-1})\sin M\psi + \Im(D_{M-1})\cos M\psi] \\
&\quad - \lambda \sum_{N=0}^{\infty} [\Re(D_{N+1})\sin N\psi + \Im(D_{N+1})\cos N\psi] \\
&= D_0 - \lambda\Im(D_1) \\
&\quad + [2\Re(D_1) - \lambda\Im(D_2)]\cos\psi + [\lambda[D_0 - \Re(D_2)] - 2\Im(D_1)]\sin\psi \\
&\quad + \sum_{m=2}^{\infty} \Big\{ [2\Re(D_m) + \lambda(\Im(D_{m-1} - D_{m+1})]\cos m\psi \\
&\qquad + [-2\Im(D_m) + \lambda\Re(D_{m-1}) - D_{m+1})]\sin m\psi \Big\} \qquad \text{(C.23)}
\end{aligned}$$